University of Kentucky

UKnowledge

University of Kentucky Doctoral Dissertations

Graduate School

2005

EFFICIENT INTEGRAL EQUATION METHOD FOR 2.5D MICROWAVE CIRCUITS IN LAYERED MEDIA

Wee-Hua Tang
University of Kentucky, wtang01@engr.uky.edu

Right click to open a feedback form in a new tab to let us know how this document benefits you.

ABSTRACT OF DISSERTATION

Wee-Hua Tang

Graduate School

University of Kentucky

2005

EFFICIENT INTEGRAL EQUATION METHOD FOR 2.5D MICROWAVE CIRCUITS IN LAYERED MEDIA

ABSTRACT OF DISSERATION

A dissertation is submitted in partial fulfillment of the requirements for the degree of Doctor of Philosophy in the college of Engineering at the University of Kentucky

By
Wee-Hua Tang

Director: Dr. Stephen Gedney, Professor of Electrical and Computer Engineering

University of Kentucky, Lexington, KY, 2005

ABSTRACT OF DISSERTATION

EFFICIENT INTEGRAL EQUATION METHOD FOR 2.5D MICROWAVE CIRCUITS IN LAYERED MEDIA

An efficient integral equation method based on a method of moment(MoM) discretization of the Mixed-Potential Integral Equation (MPIE) for the analysis of 2.5D or 3D planar microwave circuits is presented. The robust Discrete Complex Image Method (DCIM) is employed to approximate the Green's functions in layered media for horizontal and vertical sources of fields, where closed-form formulations of the z-integrations are derived in the *spectral* domain. Meanwhile, an efficient and accurate numerical integration technique based on the Khayat-Wilton transform is used to integrate functions with $1/R$ singularities and near singularities. The fast iterative solver — Quadrature Sampled Pre-Corrected Fast Fourier Transform (QSPCFFT) — is associated with the MoM formulation to analyze electrically large, dense and complex microwave circuits.

KEYWORDS: Integral Equation Method, MPIE, Microwave circuits, Layered media Green's function, DCIM, QSPCFFT.

_____

_____

EFFICIENT INTEGRAL EQUATION METHOD FOR 2.5D
MICROWAVE CIRCUITS IN LAYERED MEDIA

By

Wee-Hua Tang

_____

Director of Dissertation

_____

Director of Graduate Studies

_____

RULES FOR THE USE OF DISSERATION

Unpublished dissertations submitted for the Doctor's degree and deposited in the University of Kentucky Library are as a rule open for inspection, but are to be used only with due regard to the rights of the authors. Bibliographical references may be noted, but quotations or summaries of parts may be published only with the permission of the author, and with the usual scholarly acknowledgments.

Extensive copying or publication of the dissertation in whole or in part also requires the consent of the Dean of the Graduate School of the University of Kentucky.

A library that borrows this dissertation for use by its patrons is expected to secure the signature of each user.

<u>Name</u>   <u>Date</u>

_____

_____

_____

_____

_____

_____

_____

_____

_____

_____

_____

DISSERTATION

Wee-Hua Tang

Graduate School

University of Kentucky

2005

EFFICIENT INTEGRAL EQUATION METHOD FOR 2.5D
MICROWAVE CIRCUITS IN LAYERED MEDIA

DISSERTATION

A dissertation is submitted in partial fulfillment of the requirements for
the degree of Doctor of Philosophy in the college of Engineering at the
University of Kentucky

By
Wee-Hua Tang

Director: Dr. Stephen Gedney, Professor of Electrical and Computer
Engineering

University of Kentucky, Lexington, KY, 2005

ACKNOWLEDGEMENTS

I would like to express my deep gratitude to my dissertation advisor Dr. Stephen Gedney for his insightful comments and instructive suggestions throughout my research work. I would like to thank him for his patience, council and guidance enabling me to complete this work   I also would like to acknowledge Dr. Robert J. Adams, Dr. Cai-Cheng Lu, Dr. William T. Smith, Dr. Louis Brock, Dr. Arthur Radun and Dr. Ting-Wen Wu serving on my dissertation committee. I would also like to thank Dr. A.I. Aksun for his valuable comments on the subject of my dissertation.

Finally, I would like to dedicate this dissertation to my family members in Malaysia for their spiritual support and encouragement.

TABLE OF CONTENTS

LIST OF TABLES

LIST OF FIGURES

Chapter One: Introduction

1.1 Background

The boom of high-speed wireless communications and networks has given a rise to the demand for advanced Radio Frequency (RF) and microwave engineering design. Hence many efficient Computer Aid Design tools (CAD) have been developed for the design and analysis of microwave circuits. Many popular Electromagnetic (EM) techniques are used in the CAD tools such as the Finite Different Time Domain (FDTD), Finite Element Method (FEM), Transmission Line Method (TLM) and the Moment of Method (MoM) [1]. For layered media problems the integral equation commonly used in MoM is the Mixed Potential Integral Equation (MPIE) [2-4]. The MPIE is more suitable to analyze multi-layered media problems than other integral equations, such as the Electric Field Integral Equation (EFIE) or the Combined Field Integral Equation (CFIE), because the MPIE does not have to deal with the derivative of the layered Green's function or the hyper-singularity of the kernels. Consequently many researchers have applied the MPIE to solve problems in layered media. For example, Mosig and Gardiol [5, 6] applied the MPIE to solve rectangular microstrip antennas. Johnson [7] used a similar approach to solve the problem of a vertical cylinder penetrating the interface between contiguous half-spaces. Recently, Ling [8] applied the MPIE with high-order basis functions to investigate the photonic band-gap effect of a microstrip filter.

The main concerns that today's CAD tools focus on are efficiency, controllable accuracy of solutions, and computational time of solutions. The fill or setup time required by classical solution technique is $O(N^2)$, while the solve time is of the order $O(N^3)$, where N is the total number of unknowns for the problem. When applying the method to large, complex 3D problems, the computational time can become unreasonably large. The time can further increase when treating more complicated structures with vertical inter-connectors in layered media. Thus, the objective and main challenge of this research is to develop efficient algorithms for analyzing three-dimensional microwave circuits in layered media that are efficient, reduce the computational time, and obtain solutions with controllable accuracy.

1

1.2 Challenges

A principle challenge of the research is to compute the multi-layered media Green's function efficiently, while maintaining high accuracy. In other words, the objective is to significantly reduce the long computation time spent in evaluating the Sommerfeld integration required by the layered Green's function. The Sommerfeld integration is very expensive to evaluate due to the oscillatory nature of the Bessel function in the far-field region. This issue becomes more apparent for problems with vertical components. The reason is that the Sommerfeld integration must be computed as a function of r and $\left(z, z^{'}\right)$. While this is often pre-computed and tabulated, a sufficient density of samples must be computed to accurately treat near field singularities. Likewise, a sufficient density must also be pre-computed to handle the oscillatory nature of the kernel in the far-field. This 2D tabulation of data, at each frequency point, can be extremely expensive.

1.3 Primary focus of dissertation

As mentioned in the previous section, the Sommerfeld integration is computationally expensive to evaluate. To resolve this issue, many approaches have been introduced in the literature to replace the Sommerfeld integral The most effective and robust method is the Discrete Complex Image Method (DCIM) [9-12]. In this dissertation, the vertical reactions of the kernels are expressed in closed form using the DCIM once the integrations in vertical layered media are solved analytically in the *spectral* domain. Subsequently, an efficient 1D windowed-adaptive interpolation scheme is employed to interpolate the value of the Green's function in the spatial domain from a pre-computed 1D rather than a full 2D tabulation. This significantly reduces the overall fill time.

The MPIE formulation has a 1/R singularity in the self-cell and is near-singular in adjacent cells. The traditional method to deal with the 1/R-type singularity is numerical integration based on an extraction method [13], or a cancellation method such as the Duffy transform [14]. In this dissertation, a novel approach employing the adaptive numerical integration based on the Khayat-Wilton transform [15] is used to accelerate the calculation of the impedance matrix and to obtain accurate solutions within a given tolerance. The total computational time to solve arbitrary three-

dimensional microwave circuits is greatly reduced. Also, a new fast solver, referred to as the Quadrature Sample Pre-Corrected Fast Fourier Transform (QSPCFFT) is introduced for the rapid iterative solution of planar circuits in layered media. The solution procedure has a complexity of $O(NlogN)$, as opposed to the direct solver of N^3, and memory of $O(NlogN)$.

1.4 Outline of the dissertation

In Chapter two, a brief discussion of the MPIE and the MoM discretization is presented. In addition a new numerical integration technique based on using the Khayat-Wilton transform to treat the 1/R singularity and near-singularity in the MPIE for self and adjacent cells is also discussed in Chapter two. The Dyadic Green's function for the MPIE in layered media is discussed in Chapter three. The Sommerfeld integration is also presented with a robust DCIM acceleration technique. In the MoM discretization of the MPIE, the analytical formulations for the vertical kernels and basis reactions using the DCIM and computer implementation issues are discussed in Chapter four. In Chapter five, the S-parameters of several examples of planar and 2.5D microwave circuits are extracted and compared with the EM full-wave solver *Zeland-IE3D* [16] for validation. Next, a brief introduction and validation of the fast solution technique — the Quadrature Sample Pre-Corrected Fast Fourier Transform (QSPCFFT) — is presented in Chapter six. The DCIM developed in this dissertation can be further accelerated with QSPCFFT. This is also discussed in Chapter seven. A brief summary and outline for future work is also presented in Chapter seven. Finally, the derivation of the layered media Green's function and analytical closed form expressions for the vertical kernels and basis function reactions are presented in Appendices A and B, respectively.

Chapter Two: Integral Equation Method

When analyzing the electromagnetic scattering of a Perfectly Electrically Conducting (PEC) object situated in a free space, the Electric Field Integral Equation (EFIE) is suitable to derive a solution for the induced current on the PEC. However, if the PEC object is situated in a layered media , the so called mixed-potential form of the EFIE, or the Mixed Potential Integral Equation (MPIE), is preferable because it only requires the vector and scalar potential terms rather than the derivative of a kernel as required by the EFIE. The advantage of the MPIE is that the mixed potentials are only weakly singular. Thus, the MPIE is a more attractive formulation for solving problems in layered media. This property was first recognized by Mosig and Gardiol [17], who applied the MPIE to compute the scattering parameters of planar microstrip structures on a grounded substrate. In addition, the Sommerfeld-type integrals associated with the potential kernels converge more rapidly than other integral equations associated with the field forms. The derivation of a method of moment discretization of the MPIE is discussed in this chapter.

2.1 Mixed Potential Integral Equation (MPIE)

Michalski [18] proposed to use the "horizontal" scalar potential kernel in the MPIE when both vertical and horizontal currents are present. This necessitated a proper "correction" of those elements of the dyadic vector potential kernel associated with vertical currents component in the MPIE. This approach was further developed by Michalski and Zheng [3], who introduced three distinct MPIE formulations (referred to A, B and C) in multi-layered media. In this dissertation, only Formulation C for penetrable objects in the layered media is employed. For formulations A and B, the reader can refer to [3].

   Consider an object situated in a layered media which is to be placed under the influence of a dynamic electromagnetic field. The surface of the object is assumed to be described by a surface S. The derivation of the MPIE is derived by constraining the total electric and magnetic fields $\left(\bar{E}^T, \bar{H}^T \right) = \left(\bar{E}^i + \bar{E}^s, \bar{H}^i + \bar{H}^s \right)$, related to the electric and magnetic surface currents $\left(\bar{J}_s, \bar{M}_s \right)$, on the surface of an object [4]:

4

$$\vec{M}_s = -\hat{n} \times \left(\vec{E}^i + \vec{E}^s \left[\vec{J}_s, \vec{M}_s \right] \right) s_+$$
$$\vec{J}_s = \hat{n} \times \left(\vec{H}^i + \vec{H}^s \left[\vec{J}_s, \vec{M}_s \right] \right) s_+$$

(2.1)

where $\hat{n}$ is the outward unit vector normal to the surface S, and S_+ indicates that the fields are evaluated as the observation point approaches S from the exterior region. The field due to the arbitrary current distributions $\left(\vec{J}, \vec{M} \right)$ may then be expressed as [4]:

$$\vec{E} = \left\langle \overline{\overline{G}}^{EJ}, \vec{J} \right\rangle + \left\langle \overline{\overline{G}}^{EM}, \vec{M} \right\rangle$$
$$\vec{H} = \left\langle \overline{\overline{G}}^{HJ}, \vec{J} \right\rangle + \left\langle \overline{\overline{G}}^{HM}, \vec{M} \right\rangle$$

(2.2)

where $\overline{\overline{G}}^{PQ}\left(r \mid r' \right)$ is the Dyadic Green's function (DGF) relating P-type fields at r and Q-type currents at r', and $\langle \ \rangle$ is the inner-dot-product integral between two vector functions. Consider the case where only the electric current $\vec{J}$ is present. We can express the $\vec{E}$ and $\vec{H}$ fields in (2.2) in terms of vector and scalar potentials, $\vec{A}$ and Φ respectively, as:

$$\boldsymbol{m}_0 \overline{\overline{\boldsymbol{m}}} \cdot \vec{H} = \nabla \times \vec{A}$$
$$\vec{E} = -jw\vec{A} - \nabla \Phi$$

(2.3)

where $\vec{A} = \boldsymbol{m}_0 \left\langle \overline{\overline{G}}^A, \vec{J} \right\rangle$, and Φ is derived via the Lorentz Gauge condition $\nabla \cdot \vec{A} = -jw\boldsymbol{e}\boldsymbol{m}\Phi$. Substituting (2.3) into (2.1) and applying linearity and duality properties, $\vec{E}$ and $\vec{H}$ can be expressed as [4]:

$$\vec{E} = -jw\boldsymbol{m}_0 \left\langle \overline{\overline{G}}^A, \vec{J} \right\rangle + \frac{1}{jw\boldsymbol{e}_0} \nabla \left[\left\langle G_v^\Phi, \nabla' \cdot \vec{J} \right\rangle + \left\langle C_v^\Phi \hat{z}, \vec{J} \right\rangle \right] + \left\langle \overline{\overline{G}}^{EM}, \vec{M} \right\rangle$$
$$\vec{H} = \left\langle \overline{\overline{G}}^{HJ}, \vec{J} \right\rangle - jw\boldsymbol{e}_0 \left\langle \overline{\overline{G}}^F, \vec{M} \right\rangle + \frac{1}{jw\boldsymbol{m}_0} \nabla \left[\left\langle G_v^y, \nabla' \cdot \vec{M} \right\rangle + \left\langle C_v^y \hat{z}, \vec{M} \right\rangle \right]$$

(2.4)

where $\boldsymbol{m}_0$ and $\boldsymbol{e}_0$ denote the free-space permeability and permittivity respectively, and the prime over the nabla operator indicates that the derivative is with respect to the source coordinate. Note that $\nabla \cdot \vec{J}$ and $\nabla \cdot \vec{M}$ are proportional to the electric and magnetic charge densities. Furthermore, $\overline{\overline{G}}^A$ and $\overline{\overline{G}}^F$ are the DGF's for the magnetic

and electric vector potentials respectively, and G_v^Φ and G_v^y are the corresponding scalar potentials for the layered media associated with the horizontal and vertical currents, respectively. C_v^f and C_v^y are the *correction factor* for the electric and magnetic field.

2.2 High-order method

Complex and large structures generally require a large number of unknowns and have slow convergence rates using the MoM with classical low-order elements. Hence high-order numerical techniques have been introduced to reduce the number of unknowns and matrix sizes, and to accelerate the convergence rates in order to obtain accurate solutions [19-21]. A high-order solution can be obtained by employing high-order basis functions and a method of moment like the Galerkin discretization. Typically divergence-conforming basis functions are used for expanding the unknown surface current. Such a basis has the property that normal current continuity is enforced. Also for a pth-order basis, the divergence of the basis completes the polynomial space to order p. A number of divergence conforming bases have been introduced, including the well-known Rao-Wilton-Glisson (RWG) [22]. An alternative high-order method can be realized via the Nyström method, in which the unknown surface currents are represented by their discrete sample points [23-25]. In order to deal with the singularity of the kernels, the Nyström method requires an additional transformation in the regions near the kernel singularity. This is referred to as a Locally Corrected Nyström (LCN) formulation [26]. Overall, both classes of the high-order methods require high-order meshes in order to obtain the desired high-order accuracy in solutions. This dissertation employs the high-order GWP-type basis functions with a Galerkin discretization. This is discussed in Chapter four.

2.3 Discretized MPIE in the MoM

As mentioning in Section 2.1, the DGF $\overline{\overline{G}}^A$ associates with the electric field in (2.4) can be expressed in terms of the vector and scalar potentials $\bar{A}$ and Φ_e in (2.3). Subsequently, the inner product of (2.4) is taken with a known test vector $\bar{T}$. Assuming $\bar{T}$ and $\bar{J}$ are to be expanded with divergence conforming basis functions,

the derivative on Green's function can be transformed to $\bar{T}$ and $\bar{J}$ that leads to the Mixed-Potential Integral Equation (MPIE) [1]:

$$\left\langle f_m, \bar{E}^i \right\rangle = jw\left\langle f_m, \bar{A} \right\rangle + \left\langle f_m, \nabla f_e \right\rangle \tag{2.5}$$

f_m is the surface current represented by M basis function. Finally, the MPIE can be discretized with the Galerkin based point matching basis functions in the MoM [3]:

$$-\iint_s ds\bar{T}(r)\cdot\bar{E}^i(r) = jk_0\boldsymbol{h}_0\iint_s ds\bar{T}(r)\cdot\iint_s ds'\bar{\bar{G}}^A\cdot\bar{J}(r') + \frac{\boldsymbol{h}_0}{jk_0}\iint_s ds\nabla\cdot\bar{T}(r)\iint_{s'}ds'G^V\nabla'\cdot\bar{J}(r') \tag{2.6}$$

where $\bar{E}^i$ is an incident electric field, $\bar{T}$ is a vector test function, $\bar{J}$ is the surface current density, k_0 is the free-space wave number, $\boldsymbol{h}_0$ is the free-space wave impedance and $\bar{\bar{G}}^A$ is the dyadic vector Green's function [2]:

$$\bar{\bar{G}}^A = \begin{bmatrix} G^A_{xx} & 0 & 0 \\ 0 & G^A_{yy} & 0 \\ G^A_{zx} & G^A_{zy} & G^A_{zz} \end{bmatrix} \tag{2.7}$$

that defines in the layered media. The Green's function G^A_{zx} denotes the reaction between the z-directed projection of the field and an x-directed projection of the source. Similar notation is used for the other terms or coefficients. The scalar potential kernel G^V is denoted as:

$$G^V = \begin{cases} G^A_{vz} & for & \bar{J}_z \\ G^A_{vt} & for & \bar{J}_t \end{cases} \tag{2.8}$$

Observe that the scalar potential kernel assumes the current has either purely vertical or horizontal components. Thus the *correction factor* C^Φ for the electric field in (2.4) is zero.

2.4 1/R singularity integration

Many numerical techniques have been developed to integrate a smooth function efficiently and accurately. Among them is the popular numerical integration technique based on the Gauss Quadrature rule [27]. This method is efficient and accurate only when the kernel and basis functions are smooth. However, the kernel

being integrated is singular when the observation point and source point have a vanishing separation. For example, the free-space kernel $e^{-jk|\bar{r}-\bar{r}'|}/|\bar{r}-\bar{r}'|$ has a 1/R singularity at $\bar{r}=\bar{r}'$. Thus, a special numerical algorithm must be employed near the singularity to accurately evaluate the integrals.

This section addresses the treatment of the 1/R-type singularity that occurs in the MPIE. Many integration techniques have been developed to treat the singularity. The earliest technique is the singularity extraction introduced by Wilton for the RWG basis functions [13]. The idea is to integrate the smooth function numerically after the 1/R singular kernel is extracted in the closed form to add the singular kernel back analytically. The main drawback of this approach is not all singular kernels can be expressed in closed forms. Even for the free-space Green's function, this is only a first order extraction of the singularity and numerical integration is still slowly convergent. A more robust numerical technique based on the singularity cancellation is introduced by Duffy using a simple mapping [14].

2.4.1 Duffy Transform

The Duffy Transform [14] is based on a change of variables such that the Jacobian of the transformation cancels the singularity. This approach can only treat self-cell singularities (that's when the source and observation cells are overlapping) at the self-cell term but not for the near singular terms (that's when the separation between the source and observation cells is small). This issue is a concern because most of the effort in filling the impedance matrix in the MPIE sometimes is the evaluation of the near-singular terms of adjacent field and source cells. A more robust technique— the Khayat-Wilton Transform [15] — treats both the singular and near-singular terms effectively that is discussed in detail in the next section.

2.4.2 Khayat-Wilton Transform

A novel numerical integration method introduced by Khayat and Wilton [15] for treating integrals with a 1/R singularity is discussed in this section. Similar to the Duffy Transform, the observation point is projected onto the original quadrilateral patch, and the patch is subdivided into 4 sub-triangles with the common vertex at a singular point as shown in Fig. 2.1.
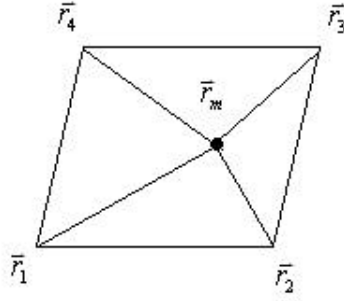
Fig. 2.1 A flat linear quadrilateral is divided into four sub-triangles with a common vertex at the singular point $\vec{r}_m$.

Consider a function $F(R)$ that has a 1/R singularity at the common vertex $\vec{r}_m$. The integral of this function on a quadrilateral patch is the superposition of the integrals over the 4 sub-triangles shown in Fig 2.1. Namely:

$$\bar{I}_n(\vec{r}) = \sum_{k=1}^{4} \bar{I}_n^k(\vec{r}) \quad .$$

(2.9)

For each sub-triangle, the integral of the function has the form:

$$\bar{I}_n^k = \int_{\Delta k} \bar{\Lambda}_n(\vec{r}')F(R)ds_k'$$

(2.10)

where $\bar{\Lambda}_n(\vec{r}')$ is the basis function that is discussed in the next section. Consider a sub-triangle in the local coordinate system (w', v'), illustrated in Fig. 22, where the integrands of the integral (2.10) are defined as [15]:

$$\bar{I}_n^k = \int_{\Delta k} \bar{\Lambda}_n(\vec{r}')F(R)ds_k' = \int_0^{h'} \int_{w_l'(v')}^{w_u'(v')} \bar{\Lambda}_n(\vec{r}')F(R)dw'dv'$$

(2.11)

where

$$\vec{h}' = \left(\frac{2A_\Delta}{|\vec{l}_1|}\right)\left(\frac{\vec{l}_1 \times \hat{n}'}{|\vec{l}_1|}\right) = h\hat{h}'$$

(2.12)

$$\hat{w}' = \hat{h}' \times \hat{n}$$

and

9

$$w_l^{'}\left(v^{'}\right)=\frac{\vec{l_2^{'}}\cdot\vec{l_1^{'}}}{2A_{\Delta}}v^{'}\ ,\ w_u^{'}\left(v^{'}\right)=-\frac{\vec{l_3^{'}}\cdot\vec{l_1^{'}}}{2A_{\Delta}}v^{'}.\tag{2.13}$$

The symbol A_{Δ} is the area of the sub-triangle defines as:

$$A_{\Delta}=\frac{\hat{n}^{'}\cdot\vec{l_1^{'}}\times\vec{l_2^{'}}}{2}\ ,\hat{n}^{'}=\frac{\vec{l_1^{'}}\times\vec{l_2^{'}}}{\left|\vec{l_1^{'}}\times\vec{l_2^{'}}\right|}\tag{2.14}$$

where $\bar{h}^{'}$ is the orthogonal projection for the singular point onto edge $\overline{23}$. This forms the radial $v^{'}$ axis. Thus $\hat{h}^{'}$ is the unit normal vector along $v^{'}$. The transverse coordinate w is chosen to be the direction orthogonal to $\hat{h}^{'}$ and in the plane of the triangle. The bounds of the triangle are then defined to be $v^{'}\in\left(0,h\right)$ and $w^{'}\in\left(w_l^{'},w_u^{'}\right)$, which are defined in (2.13).
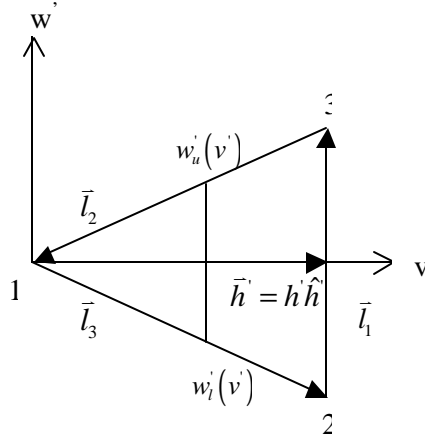
Fig. 2.2 A sub-triangle in a local coordinate system $\left(w_l^{'},w_u^{'}\right)$. Note that vertex 1 is the singular point.

To remove or cancel the 1/R singularity of $F\left(R\right)$, a change of variables is applied:

$$du^{'}=\frac{dw'}{R}=\frac{dw'}{\sqrt{\left(w'\right)^2+\left(v'\right)^2+z^2}}\tag{2.15}$$

where z is the projected distance between the observation point and source patch. From (2.15), u can be expressed as:

10

$$u'\left(w'\right) = \sinh^{-1}\frac{w'}{\sqrt{\left(v'\right)^2 + z^2}} = \frac{1}{2}\ln\left(\frac{R+w'}{R-w'}\right). \tag{2.16}$$

This transformation regularizes the 1/R singularity. Consequently, a Gauss-Legendre Quadrature integration rule with weight and abscissa defined on the local coordinate system can be applied. Thus (2.10) can be rewritten:

$$\bar{I}_n^k\left(\bar{r}\right) = \int_{\Delta k}\bar{\Lambda}_n\left(\bar{r}'\right)F\left(R\right)ds_k' = \int_0^{h'}\int_{u_l'(v')}^{u_u'(v')}\bar{\Lambda}_n\left(\bar{r}'\right)F\left(R\right)Rdu'dv'$$

$$\approx h'\sum_{i=1}^{N_v}\mathbf{w}_j^v\left(u_{uj}' - u_{lj}'\right)\sum_{i=1}^{N_u}\mathbf{w}_i^u\bar{\Lambda}_n^{i,j}\left(\bar{r}'\right)F\left(R_{i,j}\right)R_{i,j} \tag{2.17}$$

and

$$u_l'\left(v'\right) = \frac{1}{2}\ln\left(\frac{R+w_l'\left(v'\right)}{R-w_l'\left(v'\right)}\right), \; u_u'\left(v'\right) = \frac{1}{2}\ln\left(\frac{R+w_u'\left(v'\right)}{R-w_u'\left(v'\right)}\right) \tag{2.18}$$

where the position vector $\bar{r}'$ and R in the global coordinate system are expressed respectively as:

$$\bar{r}' = v'\hat{h} + \sqrt{\left(v'\right)^2 + z^2}\sinh\left(u'\right)\hat{w} + \bar{r}_m \tag{2.19}$$

$$R_{ij} = \sqrt{\left(w'\right)^2 + \left(v'\right)^2 + z^2} = \sqrt{\left(\sqrt{\left(v'\right)^2 + z^2}\sinh\left(u'\right)\right)^2 + \left(v'\right)^2 + z^2} = \sqrt{\left(v'\right)^2 + z^2}\cosh\left(u'\right). \tag{2.20}$$

The unit vector of the radial axis and orthogonal axis $\hat{h}$ and $\hat{w}$ are defined in (2.12).

In summary, the Khayat-Wilton Transformation is based on a transformation of physical coordinates of a triangle such that the kernel's 1/R singularity is exactly cancelled out using the transformation in (2.15). With the 1/R singularity being cancelled or removed, the remaining integrand is regular, and a Gauss-Legendre Quadrature rule is sufficient to yield accurate results.

Basis Function

The Khayat-Wilton Transform requires a transformation from the physical coordinates system to a local coordinates system. This requires a non-trivial transformation. For example consider the zero^h-order GWP divergence conforming basis function defined on a quadrilateral patch [21]:

$$\bar{\Lambda}_1 = \frac{u^1 - 1}{\sqrt{g}}, \quad \bar{\Lambda}_2 = \frac{u^2 - 1}{\sqrt{g}}, \quad \bar{\Lambda}_3 = \frac{u^1}{\sqrt{g}}, \quad \bar{\Lambda}_4 = \frac{u^2}{\sqrt{g}} \tag{2.21}$$

where $\sqrt{g}$ is the Jacobian of the quadrilateral surface, and is defined:

$$\sqrt{g} = \left| \bar{a}_1 \times \bar{a}_2 \right| \tag{2.22}$$

and $\bar{a}_1$ and $\bar{a}_2$ are the unitary vectors for a bi-linear quadrilateral patch:

$$\begin{aligned}
\bar{a}_1\left(u^1, u^2\right) &= \left(\bar{r}_2 - \bar{r}_1\right)\left(1 - u^2\right) + \left(\bar{r}_3 - \bar{r}_4\right)u^2 \\
\bar{a}_2\left(u^1, u^2\right) &= \left(\bar{r}_4 - \bar{r}_1\right)\left(1 - u^1\right) + \left(\bar{r}_3 - \bar{r}_2\right)u^1
\end{aligned} \tag{2.23}$$

After substituting (2.23) into (2.22), we observe that the basis function is a function of the *local coordinates* u^1 and u^2. However, the Khayat-Wilton transformation is based on the *physical coordinates* system. Thus, we need to project the physical coordinates system to local coordinates system given the observation point $\bar{r}$ by solving the mapping equation:

$$\bar{r}\left(u^1, u^2\right) = \bar{r}_1 + \left(\bar{r}_2 - \bar{r}_1\right)u^1 + \left(\bar{r}_4 - \bar{r}_1\right)u^2 + \left(\bar{r}_1 - \bar{r}_2 + \bar{r}_3 - \bar{r}_4\right)u^1 u^2 \tag{2.24}$$

$$\begin{aligned}
a_1 u^1_{i,j} + b_1 u^2_{i,j} + c_1 u^1_{i,j} u^2_{i,j} + d_1 &= 0 \\
a_2 u^1_{i,j} + b_2 u^2_{i,j} + c_2 u^1_{i,j} u^2_{i,j} + d_2 &= 0
\end{aligned} \tag{2.25}$$

where

$$\begin{aligned}
a_1 &= \vec{a} \cdot \vec{r}_{13}, & a_2 &= \vec{a} \cdot \vec{r}_{24}, \\
b_1 &= \vec{b} \cdot \vec{r}_{13}, & b_2 &= \vec{b} \cdot \vec{r}_{24}, \\
c_1 &= \vec{c} \cdot \vec{r}_{13}, & c_2 &= \vec{c} \cdot \vec{r}_{24}, \\
d_1 &= \vec{d} \cdot \vec{r}_{13}, & d_2 &= \vec{d} \cdot \vec{r}_{24},
\end{aligned} \tag{2.26}$$

The outline in Fortran code for the solutions of the quadratic equation is:

12

$$\mathbf{d} = small\ \#$$

$$if\ \left(b_1\ \&\ c_1 \neq 0 \right)\ then$$

$$if\ \left(\left| q_2 \right| < \mathbf{d} \right)\ then$$

$$u_{i,j}^1 = -\frac{q_0}{q_1}, \ u_{i,j}^2 = -\frac{a_1 u_{i,j}^1 + d_1}{b_1 + c_1 u_{i,j}^1}$$

$$else$$

$$u_{i,j}^1 = \frac{-q_1 \pm \sqrt{q_1^2 - 4 q_0 q_2}}{2 q_2}, \ u_{i,j}^2 = -\frac{a_1 u_{i,j}^1 + d_1}{b_1 + c_1 u_{i,j}^1}$$

$$endif$$

$$else$$

$$if\ \left(\left| q_2 \right| < \mathbf{d} \right)\ then$$

$$u_{i,j}^2 = -\frac{p_0}{p_1}, \ u_{i,j}^1 = -\frac{b_2 u_{i,j}^2 + d_2}{a_2 + c_2 u_{i,j}^2}$$

$$else$$

$$u_{i,j}^2 = -\frac{-p_1 \pm \sqrt{p_1^2 - 4 p_0 p_2}}{2 p_2}, \ u_{i,j}^1 = -\frac{b_2 u_{i,j}^2 + d_2}{a_2 + c_2 u_{i,j}^2} \tag{2.27}$$

$$endif$$

$$endif$$

where

$$
\begin{aligned}
q_2 &= a_2 c_1 - a_1 c_2, & p_2 &= b_1 c_2 - b_2 c_1, \\
q_1 &= b_1 a_2 - b_2 a_1 + c_1 d_2 - c_2 d_1, & p_1 &= b_1 a_2 - b_2 a_1 + c_2 d_1 - c_1 d_2, \\
q_0 &= b_1 d_2 - d_1 b_2, & p_0 &= a_2 d_1 - d_2 a_1,
\end{aligned} \tag{2.28}
$$

Since the system is quadratic, there are two solutions. To obtain a unique solution, constraints must be imposed, namely both u^1 and u^2 must be real numbers and lie between (0,1), to obtain a unique solution.

Near-singular Integral

Next, we must address the situation when the observation point falls outside the original quadrilateral, which poses a near-singularity. Unfortunately, following the algorithm can lead to a non-uniform solution as both u^1 and u^2 can be complex. To eliminate this problem, we replace the first-order bi-linear quadrilateral with two second-order triangles. This provides an exact mapping. In addition, the Jacobian

13

transformation of the triangle simply equals $2A_\Delta$, where A_Δ is the area of the triangle. For a flat quadrilateral patch, two linear triangles are sufficient.

Khayat-Wilton Transform in the Three-dimensional Space

In a three-dimensional space integral, the observation point may not lie in the plane of the quadrilateral patch. In this situation, the projected distance of the observation point to the patch is not zero. Thus, equation (2.18) actually has a logarithmic singularity. To resolve this, a specialized Linlog Quadrature rule [28] can be used along the v-directed integration. The Linlog rule integrates the log singularity exactly and converges rapidly. A 1D integration rule based on a Gauss-Legendre Quadrature can still apply along the orthogonal direction u'.

The affect of this logarithmic singularity can be demonstrated through a sample of examples. Fig 2.4 plots the difference of $u'_u - u'_l$ versus v' along the radial direction when both the source and observation points are in the same plane. Note that the contour is a straight line. Next, $u'_u - u'_l$ is plotted versus v when the observation point is moved a distance of 10^{-5} meter above the plane of integration. This is illustrated in Fig 2.5 and the logarithms singularity is observed.

The Linlog rule is used to approximate the integration of a logarithmic function using the summation

$$\int_0^1 f(x)\,dx \approx \sum_{i=1}^n w_i f(x_i) \tag{2.29}$$

where w_i and x_i is the weights and abscissas for the Linlog rule that can be computed based on the moments:

$$1, ln(x), x, xln(x), x^2, x^2ln(x),... \tag{2.30}$$

To effectively apply the Linlog integration rule, we need to determine the range over where the rule needs to be applied along the radial direction. We implement the following algorithm to determine the transitional point (*trspt*) to use either the Linlog or Guass-Legendre rules of integration. The algorithm is described as follows:

$$tt = |z| tan^{-1} (slope)$$
$$if \left(tt > h' \right) \ then$$
$$\quad trspt = 0$$
$$elseif \left(tan^{-1} (slope) > 1.5358897 \right) \& \left(tt < h' \right) then$$
$$\quad trspt = tt$$
$$else$$
$$\quad trspt = tt \cdot tan^{-1} (slope)$$
$$endif$$

$$(2.31)$$

where

$$slope = \frac{\left| u_u' (x_2) - u_l' (x_2) - u_u' (x_1) + u_l' (x_1) \right|}{x_2 - x_1}$$

$$x_2 = 1.1 |z|, \qquad x_1 = \frac{|z|}{1.1}$$

$$(2.32)$$

We observe that the transitional point for the logarithmic function in (2.18) occurs at z. Two adjacent points x_1 and x_2 are chosen to compute the slope at z in (2.32). We observe that when the angle at z is greater than 88 degrees, or 1.5358897 radians, the solution of the integral based on the Quadrature rule converges slowly because of the logarithmic singularity. Thus, in this case the Linlog rule is applied. If the angle at z is less than or equal to 88 degrees, the function in (2.18) is smooth, and applying a Gauss-Legendre integration rule is sufficient to integrate the function accurately.
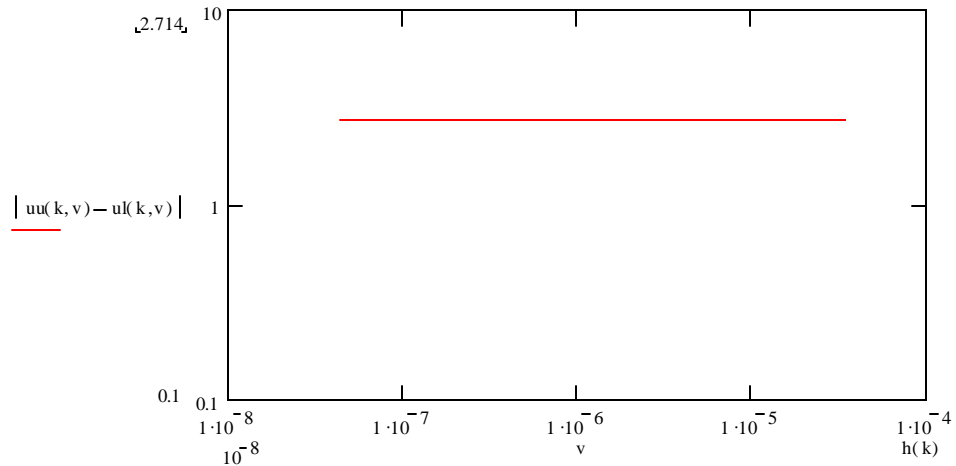
Fig. 2.3 The loglog plot of $u_u' (v) - u_l' (v)$ in (2.18). The projected distance is $z = 0$.
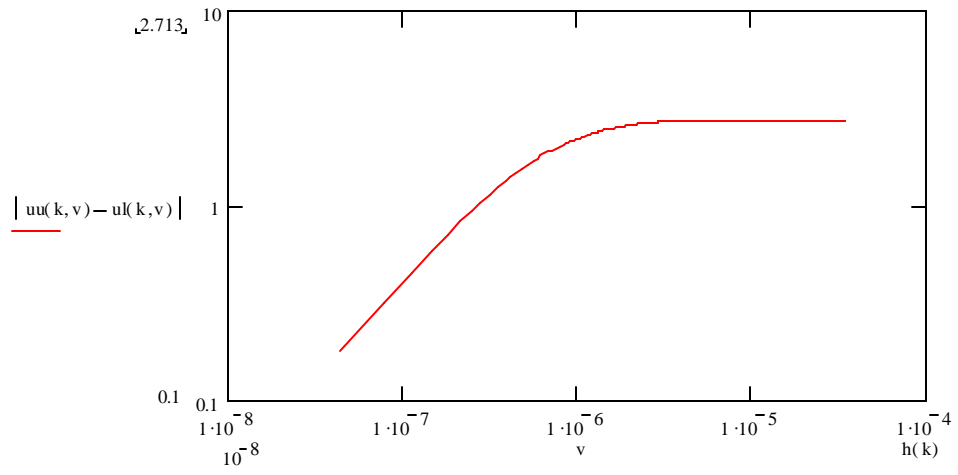
Fig. 2.4 The loglog plot of $u_u^{'}\left(v^{'}\right)-u_l^{'}\left(v^{'}\right)$ in (2.18). The projected distance is $z = 1\times10^{-5}$.

Chapter Three: Multilayered-media Green's function

The rapid development of RF and monolithic microwave integrated circuits (MMIC) has generated a demand for efficient and robust engineering CAD tools that perform full-wave EM analysis. Such tools that employ Method of Moment solutions must be able to efficiently evaluate the multilayered media Green's functions that are traditionally represented by Sommerfeld-type integrals (refer to Section 2.4). Specifically, an efficient general-purpose software is sought that is capable of modeling arbitrarily shaped objects in multilayered media. Development of such a general-purpose code requires solutions for both horizontal and vertical currents. Consider a current source in a multilayered medium, with each layer characterized by a relative permittivity e_r, relative permeability m_r, and thickness d_i as illustrated in Fig. 3.1.
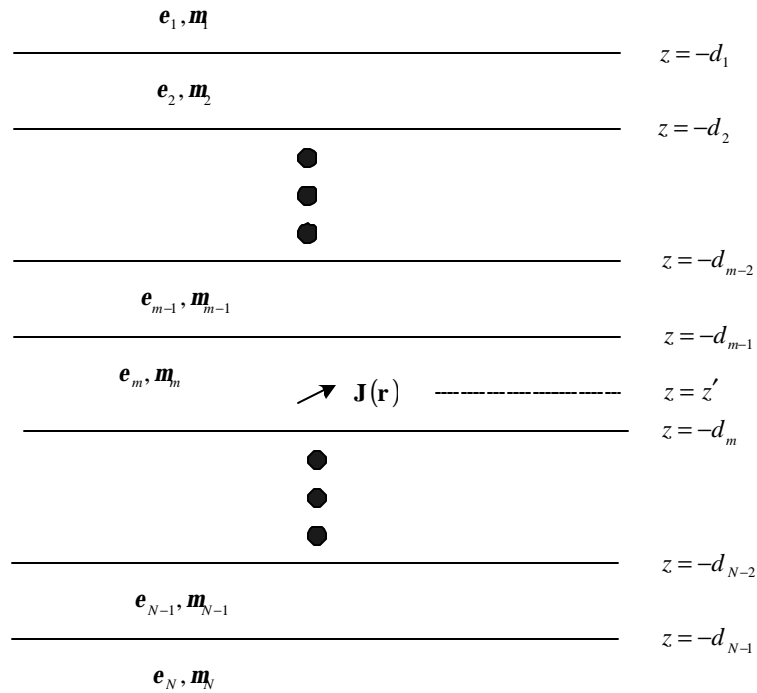
Fig. 3.1 Arbitrary point source embedded in the m-th layer of an N-layer medium.

In this chapter, we discuss the derivation of the layered media Green's function in Sommerfeld-type integrals, followed by presenting techniques to evaluate the

Sommerfeld integrals using the Michalski's extrapolation [29] and the Aksun's Two-level DCIM [12] schemes.

3.1 Formulations of Dyadic Green Function

An alternative formulation of the layered medium Green's function is introduced by Chew [30]. This formulation has the symmetrized vector-differential operator in the transverse fields E and H components such that the reciprocity of the solution is satisfied. The advantage of the symmetrized Green's function is that the singularity of the Green's function can be mitigated to the basis functions, avoiding the need to have special treatment for these singularities. Unlike Chew's approach, we superimpose the primary and reflected waves in the spectral domain in this dissertation. The reason is that when a source is embedded in a thin dielectric region backed by a ground plane, a significant rounding error occurs in the reflected wave, nearly canceling the primary wave. This difference can be as many as eight orders of magnitude smaller than the primary field. As a consequence, the reflected waves must be calculated to an extraordinary number of digits, requiring an inordinate amount of CPU time. Thus, splitting the field into primary and reflected waves loses its advantage. Under such conditions, we superimpose the primary and reflected waves in the spectral domain. In addition, we further decompose the reflected wave into *symmetric* and *asymmetric* forms so that the Dyadic Green function in the MPIE is more convenient to implement in the MoM code. For a detailed derivation of the Green's function, the reader can refer to Appendix A. Note that the derived Green's function is based on the current of the basis function and are either purely vertical or horizontal. When the Dyadic Green function is obtained, we can formulate the MPIE given in (2.6). The final formulations of the Green's function of the DGF in (2.7) due to the vector and scalar potentials, $G_{xx_m}^{EJ}$ and $G_{V_m}^{EJ}$ respectively, for the horizontal current given in (A.94)—(A.95) are expressed as:

$$G_{xx_m}^{EJ} = g_{h_m}^{TE} = \frac{-\omega\mu_m I}{4\pi} \int_0^\infty J_0\left(k_r r\right) \frac{k_r}{k_{m,z}} \left[e^{-jk_{m,z}|z-z'|} + \tilde{B}_m^{TE} e^{jk_{m,z}z} + \tilde{D}_m^{TE} e^{-jk_{m,z}z} \right] dk_r \tag{3.1}$$

$$G_{V_m}^{EJ} = \frac{-\omega\mu_m I}{4\pi} \int_0^\infty \frac{J_0\left(k_r r\right)}{k_r k_{m,z}} \left[\begin{matrix} k_r^2 e^{-jk_{m,z}|z-z'|} + \left(k_m^2 \tilde{B}_m^{TE} - k_{m,z}^2 \tilde{E}_m^{TM}\right) e^{jk_{m,z}z} \\ + \left(k_m^2 \tilde{D}_m^{TE} - k_{m,z}^2 \tilde{F}_m^{TM}\right) e^{-jk_{m,z}z} \end{matrix} \right] dk_r . \tag{3.2}$$

The Green's function due to the vector and scalar potentials, $G_{zz_m}^{EJ}$, $G_{zt_m}^{EJ}$ and $G_{vz_m}^{EJ}$, for the vertical current in (2.8), from (A.92)—(A.99) can be expressed as:

$$G_{zz_m}^{EJ} = g_{v_m}^{TM} = \frac{-w m_m I}{4p} \int_0^\infty J_0\left(k_r r\right) \frac{k_r}{k_{m,z}} \left[e^{-j k_{m,z}|z-z'|} + \tilde{B}_m^{TM} e^{j k_{m,z} z} + \tilde{D}_m^{TM} e^{-j k_{m,z} z} \right] dk_r \tag{3.3}$$

$$G_{zt_m}^{EJ} = \frac{i w m_m I}{4p} \int_0^\infty J_1\left(k_r r\right) \left[-\left(\tilde{E}_m^{TM} - \tilde{B}_m^{TE} \right) e^{j k_{m,z} z} + \left(\tilde{F}_m^{TM} - \tilde{D}_m^{TE} \right) e^{-j k_{m,z} z} \right] dk_r \tag{3.4}$$

$$G_{vz_m}^{EJ} = g_{h_m}^{TM} = \frac{-w m_m I}{4p} \int_0^\infty J_0\left(k_r r\right) \frac{k_r}{k_{m,z}} \left[e^{-j k_{m,z}|z-z'|} + \tilde{E}_m^{TM} e^{j k_{m,z} z} + \tilde{F}_m^{TM} e^{-j k_{m,z} z} \right] dk_r \tag{3.5}$$

for source and observation points embedded in the same layer. Note that the vector potential of the Green's function, $G_{zz_m}^{EJ}$, is contributed to when both the source and field basis situate on a vertical patch, while $G_{zt_m}^{EJ}$ is contribute d to when the source basis situates on a transverse patch while the field basis situates on a vertical patch. On the other hand, for a source embedded in the mth layer and observation embedded in the ith layer, the final formulas of the Green's function are given in (A.156)—(A.157) as:

$$G_{xx_{i,m}}^{EJ} = \begin{cases} \dfrac{-w m_m}{4p} \displaystyle\int_{k_r=0}^\infty J_0\left(k_r r\right) \frac{\tilde{A}_i^{TE<}}{k_{m,z}} e^{-j k_{i,z} d_i} \left[e^{-j k_{i,z} z} + \tilde{R}_{i,i-1}^{TE} e^{2 j k_{i,z} d_{i-1}} e^{j k_{i,z} z} \right] k_r dk_r, & (i<m) \\[4mm] \dfrac{-w m_m}{4p} \displaystyle\int_{k_r=0}^\infty J_0\left(k_r r\right) \frac{\tilde{A}_i^{TE>}}{k_{m,z}} e^{j k_{i,z} d_{i-1}} \left[e^{j k_{i,z} z} + \tilde{R}_{i,i+1}^{TE} e^{-2 j k_{i,z} d_i} e^{-j k_{i,z} z} \right] k_r dk_r, & (i>m) \end{cases} \tag{3.6}$$

for horizontal currents. For vector and scalar potentials due to the vertical current, the final formulas of the Green's function are given in (A.158)—(A.160), as:

$$G_{zz_{i,m}}^{EJ} = \begin{cases} \dfrac{-w m_m}{4p} \displaystyle\int_{k_r=0}^\infty J_0\left(k_r r\right) \frac{\tilde{A}_i^{TM<}}{k_{m,z}} e^{-j k_{i,z} d_i} \left[e^{-j k_{i,z} z} + \tilde{R}_{i,i-1}^{TM} e^{2 j k_{i,z} d_{i-1}} e^{-i k_{i,z} z} \right] k_r dk_r, & (i<m) \\[4mm] \dfrac{-w m_m}{4p} \displaystyle\int_{k_r=0}^\infty J_0\left(k_r r\right) \frac{\tilde{A}_i^{TM>}}{k_{m,z}} e^{j k_{i,z} d_{i-1}} \left[e^{j k_{i,z} z} + \tilde{R}_{i,i+1}^{TM} e^{-2 j k_{i,z} d_i} e^{i k_{i,z} z} \right] k_r dk_r, & (i>m) \end{cases} \tag{3.7}$$

$$G_{z_{i,m}}^{EJ} = \begin{cases} \dfrac{iw m_i}{4p} \int\limits_{k_r=0}^{\infty} J_1(k_r \boldsymbol{r}) \begin{bmatrix} \tilde{C}_i^{TM<} e^{-jk_{i,z}d_i}\left[e^{-jk_{i,z}z} + \tilde{R}_{i,i-1}^{TM} e^{2jk_{i,z}d_{i-1}} e^{jk_{i,z}z}\right] - \\ \tilde{A}_i^{TE<} \dfrac{k_{i,z}m_m}{k_{m,z}m_i} e^{-jk_{i,z}d_i}\left[e^{-jk_{i,z}z} - \tilde{R}_{i,i-1}^{TE} e^{2jk_{i,z}d_{i-1}} e^{jk_{i,z}z}\right] \end{bmatrix} dk_r, & (i<m) \\[2em] \dfrac{iw m_i}{4p} \int\limits_{k_r=0}^{\infty} J_1(k_r \boldsymbol{r}) \begin{bmatrix} \tilde{C}_i^{TM>} e^{jk_{i,z}d_{i-1}}\left[-e^{jk_{i,z}z} - \tilde{R}_{i,i+1}^{TM} e^{-2jk_{i,z}d_i} e^{-jk_{i,z}z}\right] - \\ \tilde{A}_i^{TE>} \dfrac{k_{i,z}m_m}{k_{m,z}m_i} e^{jk_{i,z}d_{i-1}}\left[-e^{jk_{i,z}z} + \tilde{R}_{i,i+1}^{TE} e^{-2jk_{i,z}d_i} e^{-jk_{i,z}z}\right] \end{bmatrix} dk_r, & (i>m) \end{cases} \tag{3.8}$$

$$G_{v_{z_{i,m}}}^{EJ} = \begin{cases} \dfrac{-w m_m}{4p} \int\limits_{k_r=0}^{\infty} J_0(k_r \boldsymbol{r}) \dfrac{k_{i,z}\tilde{C}_i^{TM<}}{k_{m,z}^2} e^{-jk_{i,z}d_i}\left[e^{-jk_{i,z}z} - \tilde{R}_{i,i-1}^{TM} e^{2jk_{i,z}d_{i-1}} e^{jk_{i,z}z}\right] k_r dk_r, & (i<m) \\[2em] \dfrac{-w m_m}{4p} \int\limits_{k_r=0}^{\infty} J_0(k_r \boldsymbol{r}) \dfrac{k_{i,z}\tilde{C}_i^{TM>}}{k_{m,z}^2} e^{jk_{i,z}d_{i-1}}\left[e^{jk_{i,z}z} - \tilde{R}_{i,i+1}^{TM} e^{-2jk_{i,z}d_i} e^{-jk_{i,z}z}\right] k_r dk_r, & (i>m) \end{cases} \tag{3.9}$$

where all the reflection coefficients are defined in Appendix A.

3.2 Sommerfeld Integral

Consider the Sommerfeld-type integral of the form [4]:

$$I = \int_0^{\infty} f(k_r) dk_r = \int_0^{\infty} \tilde{G}(z, z'; k_r) J_v(k_r \boldsymbol{r}) dk_r \qquad v = 0,1,2 \tag{3.10}$$

where $\tilde{G}$ is a spectral domain Green's function of the layered medium, J_v is the Bessel function of order v, and $\boldsymbol{r}$ is the radial distance between the field and source points:

$$\boldsymbol{r} = \sqrt{(x-x')^2 + (y-y')^2} \tag{3.11}$$

where z and z' are the vertical coordinates of the field and source points, respectively. The Sommerfeld integration must be performed numerically. This poses a number of challenges. Initially, J_v is oscillatory and slowly convergent. In fact, for a large $\boldsymbol{r}$ the integrand becomes very oscillatory. On the other hand, as $\boldsymbol{r} \to 0$, the integral over the semi-infinite domain is slowly convergent. The result can be singular when $\boldsymbol{r}=0$. Finally, the integration must be performed carefully to avoid branch point singularities and simple poles that lie on or near the contour integration. There are several techniques to estimate the Sommerfeld's tail efficiently and accurately. One of the techniques is the Extrapolation Method introduced by

Michalski [29]. The equation (3.10) is split into two integral paths — $(0, a)$ and (a, ∞) — as illustrated in Fig. 3.2. Therefore (3.10) becomes:

$$I = \int_{C^e} \tilde{G}(z, z'; k_r) J_v(k_r r) dk_r + \int_a^\infty \tilde{G}(z, z'; k_r) J_v(k_r r) dk_r \quad v = 0,1,2. \tag{3.12}$$

The first integral path is deformed into an elliptic path (C^e) in the first quadrant of the complex plane to avoid guided-wave poles and branch points of the integrand. The value of a is selected to ensure that the integrand is free of singularities on the remaining tail segment. In the layered media case, we find that the optimum value of a is:

$$a = 1.2 k_0 \sqrt{e_{r_{max}}} \tag{3.13}$$

where k_0 is the wave-number in free space, and $e_{r_{max}}$ is the largest relative permittivity for the dielectric in the layered media.
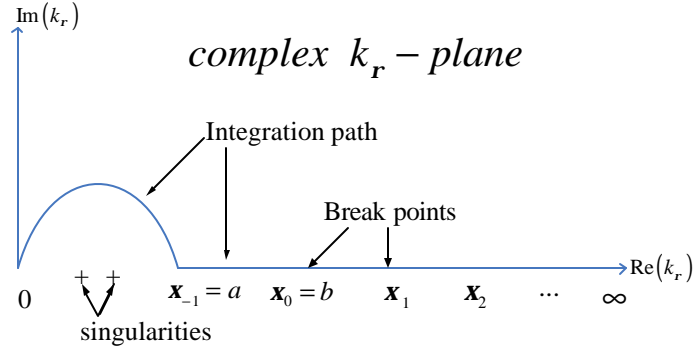
Fig. 3.2 Integration path in the complex k_r-plane. Between zero and a, the path is deformed from the real axis to avoid the integrand singularities. The partition-extrapolation method is applied over the real-axis tail segment (a, ∞).

The equation of the upper-half ellipse in Fig. 3.2 has a center at $\left(\dfrac{a}{2}, 0\right)$ and can be expressed as:

$$\frac{\left(x - \dfrac{a}{2}\right)^2}{\left(\dfrac{a}{2}\right)^2} + \frac{y^2}{b^2} = 1 \tag{3.14}$$

21

where a and b are the major and minor axes of ellipse where we assign a equals (3.13), and b equals $a/4$ in our code for an arbitrary value. Next, we introduce a variable t to transform the Cartesian coordinates (x, y) into the complex $k_r - plane$ using the change of variable:

$$y = b \sin t \tag{3.15}$$

in which x and Jacobian can be expressed respectively as

$$
\begin{aligned}
x &= \frac{b}{2}(1 - \cos t) \\
J &= \left(\frac{\partial x}{\partial t}, \frac{\partial y}{\partial t} \right) = \left(\frac{b}{2} \sin t, b \cos t \right)
\end{aligned}
\tag{3.16}
$$

Substituting (3.16) into (3.12), we obtain the final expression of the elliptic integration:

$$\int_{C^e} f(k_r) k_r = \int_0^p f\left(\frac{b}{2}(1 - \cos t) + jb \sin t \right)\left(\frac{b}{2} \cos t + jb \cos t \right) dt \tag{3.17}$$

This can then be applied to the integration over the contour C^e. Next, the Sommerfeld's tail is evaluated. A number of extrapolation techniques have been used to approximate the remainder of Sommerfeld's tails, such as the Euler Transformation [31], Iterated Aitken Transformation [32], E-Transformation [33-35], Shanks Transformation [36] and Generalized Levin Transformation [37]. We apply the method of weighted-average in this dissertation.

Weighted-Average Method

The interval (a, ∞) of Sommerfeld integral in (3.12) is subdivided into sections defined by break points, such as $(a, k r_0), (k r_0, k r_1)$ et cetera. A suitable break point is selected based on the asymptotic behavior of the integrand in order to accelerate the convergence rate. The simplest choice of break points is the equidistant points [38]:

$$k_{r_n} = b + nq \qquad n \geq 0 \tag{3.18}$$

where b denotes the first break point greater than a, we choose $b = a+q$, where $q = p/r$ is the asymptotic half-period of the Bessel function, which has the large argument approximation [39]:

$$J_v\left(k_r r\right) \sim \sqrt{\frac{2}{p k_r r}} \cos\left(k_r r - v\frac{r}{2} - \frac{p}{4}\right) \tag{3.19}$$

Thus, we can use a summation series $\{S_n\}$ to approximate the tail of the Sommerfeld integral. The second part of (3.12) is:

$$\int_a^\infty \tilde{G}\left(z, z'; k_r\right) J_v\left(rk_r\right) dk_r = \sum_{k=0}^n u_k = S_n, \quad n \to \infty \tag{3.20}$$

However, the summation series $\{S_n\}$ is slowly converging into a solution. Thus, a fast recursive approach is required to accelerate the convergence rate of the summation sequence $\{S_n\}$. Before applying the weighted-average method, we need to compute the initial summation series as:

$$S_0^{(k)} = \int_a^{N_{seg}} \tilde{G}\left(z, z'; k_r\right) J_v\left(rk_r\right) dk_r \tag{3.21}$$

where N_{seg} is the number of segments for the equidistant break point. In our code, we choose $N_{seg} = 4p/(ra)$. Subsequently, we can apply the recursive formulation with k iterative steps as:

$$S_n^{(k+1)} = \frac{S_n^{(k)} + h_n^{(k)} S_{n+1}^{(k)}}{1 + h_n^{(k)}}, \qquad h, k \geq 0 \tag{3.22}$$

where

$$h_n^{(k)} = 1 + \frac{0.5 + 2k}{b+n}, b = 1 + \frac{abr}{p} \tag{3.23}$$

The weighted-average method is recursively subdivided into equidistant break points defined in (3.18) until the relative error computed between the current and next step is within the given error tolerance:

$$\left| \frac{S_n^{(k+1)}}{S_n^k} \right| < tol \tag{3.24}$$

Finally, Michalski claimed that the recursive formula of (3.22) has a convergence rate for $z \neq z'$

$$O\left(\boldsymbol{x}^{-2}\right), \quad \boldsymbol{x} = \boldsymbol{p}\left|z - z'\right| / \boldsymbol{r} \tag{3.25}$$

where z and z' are the observation and source point in the layered media, respectively. For $z = z'$, the recursive formula exhibits linear monotone convergence.

3.3 Discrete Complex Image Method

When $\boldsymbol{r}$ is large the evaluation of the Sommerfeld integral is very time consuming and expensive due to the oscillatory behavior of the Bessel function. The Discrete Complex Image Method (DCIM) was developed to provide an accurate analytical approximation of the Sommerfeld integral. It was first developed by Fang *et al.* [10] to approximate the layered-media Green's function with a sum of complex coefficients and exponentials derived via Prony's method [40]. In this dissertation, the DCIM based on the original One-level approach is revised. The more robust Two-level approach developed by Aksun [41, 42] is also discussed in detail. In addition, the surface-wave terms of the Green's function extracted from DCIM are included to improve the accuracy of the Green's function in the far-field regions [10, 43, 44].

3.3.1 One-level DCIM

The spatial domain layered media Green's function can be obtained from the Sommerfeld integral as:

$$G(\boldsymbol{r}) = \int_{-\infty}^{\infty} dk_r k_r H_0^{(2)}\left(k_r \boldsymbol{r}\right) \tilde{G}\left(k_r\right) \tag{3.26}$$

It is recognized by Chow *et al.* [42] that if the spectral domain Green's function $\tilde{G}\left(k_r\right)$ can be approximated by exponentials, the Sommerfeld integral can be evaluated analytically using the well-known Sommerfeld identity [45]:

$$\frac{e^{-jk_m r}}{r} = \frac{1}{2j} \int_{-\infty}^{\infty} dk_r k_r H_0^{(2)}\left(k_r r\right) \frac{e^{-jk_{m,z}|z|}}{k_{m,z}}$$

$$= \frac{1}{j} \int_{0}^{\infty} dk_r k_r J_0\left(k_r r\right) \frac{e^{-jk_{m,z}|z|}}{k_{m,z}}$$

(3.27)

Fortunately, the approximation of a function on a series of complex exponentials can be performed via the Generalized Pencil of Function (GPOF), also known as Matrix Pencil (MP) that was first introduced by T. Sarkar [46, 47]. In order to approximate the spectral Green's function with the GPOF, the exponentials should be a function of k_r and sampled in the complex $k_r - plane$. A contour (C_{ap}) is defined as:

$$C_{ap} : k_{m,z} = k_m\left[-jt + \left(1 - \frac{t}{T_{02}}\right)\right], \quad 0 \leq t \leq T_0$$

(3.28)

This is illustrated in Fig 3.2.
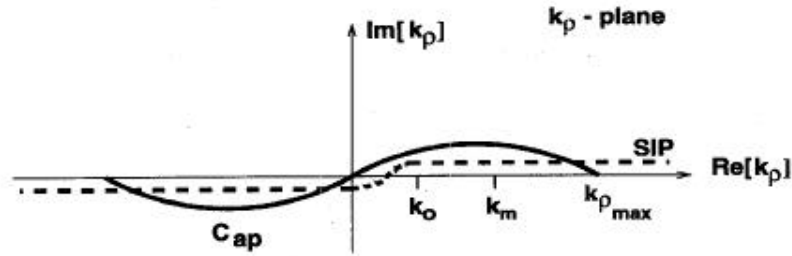
Fig. 3.3. Definition of the Sommerfeld integration path and the contours C_{ap1} used in the One-level approach [41, 42].

Observe that the contour path is defined similar to the Sommerfeld path in Fig 3.2. The combination of the GPOF and Sommerfeld identity allows the DCIM to yield accurate solutions for the layered media Green's function. Unfortunately, as mentioned by Aksun, not all the Green's functions have fast decaying spectral domain behavior. Thus, the spectral domain behavior of the Green's function must be investigated *a priori*. Consequently, a few iterations to find the optimized parameters must be performed. This drawback deterred the One-level approach from being fully robust, and hence it is not suitable for the development of CAD software. To circumvent this difficulty, a robust Two-level approximation scheme was developed by Aksun. This is discussed in the following section.

3.3.2 Aksun's Two-level method

To alleviate the necessity of investigating the spectral domain Green's function in advance and the difficulties caused by the trade-off between the sampling range T_0 and the sampling period, the approximation is preformed in two levels [11]. Define two contours on the complex $k_r-plane$, denoted by C_{ap1} and C_{ap2}, as illustrated in Fig. 3.4. The mapping of the contour is performed with a real variable t and is defined as:

$$
\begin{aligned}
&for \quad C_{ap1}: k_{m,z} = -jk_m\left(T_{02}+t\right), \quad 0 \le t \le T_{01} \\
&for \quad C_{ap2}: k_{m,z} = k_m\left[-jt+\left(1-\frac{t}{T_{02}}\right)\right], \quad 0 \le t \le T_{02}
\end{aligned} \tag{3.29}
$$
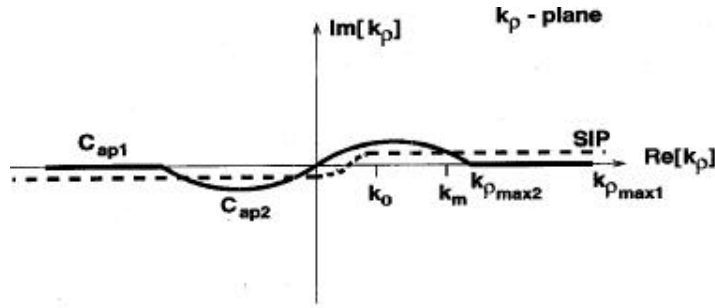
Fig. 3.4 Definition of the Sommerfeld integration path and the contours C_{ap1} used in the Two-level approach [41, 42].

Note that contour C_{ap2} is identical to that contour defined for the One-level approximation. The difference is that the value of T_{02} can be set in advance to a value such that $k_{r_{max2}} \ge k_{r_{max}}$, where $k_{r_{max}}$ is determined via the maximum value of the dielectric wave number in the layered media. The Green's function is uniformly sampled along each contour, $[0, T_{01}]$ and $[0, T_{02}]$. The details of how to define T_{01}, T_{02}, and other parameters can be referred to [42]. In summary, unlike the One-level approximation, the Two-level approximation does not require *a priori* knowledge of the Green's function behavior. The only input parameters are the sampling periods T_{01} and T_{02} which are typically set to a value between 100 to 300. The value of the sampling periods is set to 101 throughout all the numerical examples done in this dissertation.

The GPOF is applied in the spectral domain Green's function to approximate the function on the contours C_{ap1} and C_{ap2}. The approximation can be expressed as:

$$\tilde{G}_{c_{ap1}}\left(k_{m,z}\right) \approx \sum_{n=1}^{N_1} a_{1n} e^{-b_{1n}k_{m,z}} \qquad\qquad \text{for } C_{ap1}$$

$$\tilde{G}_{c_{ap2}}\left(k_{m,z}\right) = \tilde{G}\left(k_{m,z}\right) - \tilde{G}_{c_{ap1}}\left(k_{m,z}\right) \approx \sum_{n=1}^{N_2} a_{2n} e^{-b_{2n}k_{m,z}} \qquad \text{for } C_{ap2}$$

(3.30)

where b_n are the poles and a_n are the residues of the GPOF expansion. Subsequently,

$$\tilde{G}\left(k_r\right) \cong \frac{1}{j2k_{m,z}}\left[\tilde{G}_{c_{ap1}}\left(k_{m,z}\right) + \tilde{G}_{c_{ap1}}\left(k_{m,z}\right)\right]$$

$$\cong \frac{1}{j2k_{m,z}}\left[\sum_{n=1}^{N_1} a_{1n} e^{-b_{1n}k_{m,z}} + \sum_{n=1}^{N_2} a_{2n} e^{-b_{2n}k_{m,z}}\right]$$

(3.31)

where

$$k_r = \sqrt{k_m^2 - k_{m,z}^2} \qquad .$$

(3.32)

Equation (3.31) is then inserted into (3.26). This can then be computed in a closed form via the Sommerfeld identity. Consequently, the spatial domain Green's function can be approximated as:

$$G(\mathbf{r}) = \int_{-\infty}^{\infty} dk_r k_r H_0^{(2)}\left(k_r \mathbf{r}\right) \tilde{G}\left(k_r\right)$$

$$\cong \frac{1}{2j}\left[\sum_{n=1}^{N_1} a_{1n} \int_{-\infty}^{\infty} dk_r k_r H_0^{(2)}\left(k_r \mathbf{r}\right)\frac{e^{-\mathbf{a}_{1n}k_{m,z}}}{k_z} + \sum_{n=1}^{N_2} a_{2n} \int_{-\infty}^{\infty} dk_r k_r H_0^{(2)}\left(k_r \mathbf{r}\right)\frac{e^{-\mathbf{a}_{2n}k_{m,z}}}{k_z}\right]$$

$$\cong \frac{1}{2j}\left[\sum_{n=1}^{N_1} a_{1n} \int_{-\infty}^{\infty} dk_r k_r H_0^{(2)}\left(k_r \mathbf{r}\right)\frac{e^{-j(-j\mathbf{a}_{1n})k_{m,z}}}{k_z} + \sum_{n=1}^{N_2} a_{2n} \int_{-\infty}^{\infty} dk_r k_r H_0^{(2)}\left(k_r \mathbf{r}\right)\frac{e^{-j(-j\mathbf{a}_{2n})k_{m,z}}}{k_z}\right]$$

$$\cong G_{c_{ap1}}\left(\mathbf{r}\right) + G_{c_{ap2}}\left(\mathbf{r}\right)$$

(3.33)

where

$$G_{c_{ap1}}\left(\mathbf{r}\right) \cong \sum_{n=1}^{N_1} a_{1n} \frac{e^{-jk_m r_{i1}}}{r_{i1}} \qquad r_{i1} = \sqrt{\mathbf{r}^2 + \left(-jb_{1n}\right)^2} = \sqrt{\mathbf{r}^2 - b_{1n}^2}$$

$$G_{c_{ap2}}\left(\mathbf{r}\right) \cong \sum_{n=1}^{N_2} a_{2n} \frac{e^{-jk_m r_{i2}}}{r_{i2}} \qquad r_{i2} = \sqrt{\mathbf{r}^2 + \left(-jb_{2n}\right)^2} = \sqrt{\mathbf{r}^2 - b_{2n}^2}$$

(3.34)

The parameters a_{1n}, b_{1n} and a_{2n}, b_{2n} are the coefficients and exponents obtained from the application of the GPOF method in the first and second contour of the Two-level approach.

The Two-level DCIM can also be applied to the Sommerfeld integral of the form:

$$G(\mathbf{r}) = \int_{-\infty}^{\infty} dk_r \, \mathbf{r} H_1^{(2)}(k_r \mathbf{r}) \tilde{G}(k_r). \tag{3.35}$$

This is necessary for the DGF coefficient G_{zt} (A.98). To accommodate the first order Hankel function of second kind, we can use the identity [48]:

$$\int_0^{\infty} dk_r J_1(k_r \mathbf{r}) e^{-bk_{m,z}} = \frac{1}{\mathbf{r}}\left(e^{-bk_m} + \frac{jb}{\sqrt{\mathbf{r}^2 - b^2}} e^{-jk_m\sqrt{\mathbf{r}^2 - b^2}} \right). \tag{3.36}$$

By approximating $\tilde{G}$ with the Two-level approximation, we can derive the closed form expression as:

$$
\begin{aligned}
G(\mathbf{r}) &= \int_{-\infty}^{\infty} dk_r H_1^{(2)}(k_r \mathbf{r}) \tilde{g}_{zt}(k_r) \\
&\cong \sum_{n=1}^{N_1} a_{1n} \int_{-\infty}^{\infty} dk_r H_1^{(2)}(k_r \mathbf{r}) e^{-\mathbf{a}_{1n}k_{m,z}} + \sum_{n=1}^{N_2} a_{2n} \int_{-\infty}^{\infty} dk_r H_1^{(2)}(k_r \mathbf{r}) e^{-\mathbf{a}_{2n}k_{m,z}} \\
&\cong \frac{1}{\mathbf{r}}\left(G_{c_{ap1}}(\mathbf{r}) + G_{c_{ap2}}(\mathbf{r}) \right)
\end{aligned} \tag{3.37}
$$

where

$$
\begin{aligned}
G_{c_{ap1}}(\mathbf{r}) &= \sum_{n=1}^{N_1} a_{1n}\left(e^{-b_{1n}k_m} + \frac{jb_{1n}}{\sqrt{\mathbf{r}^2 - b_{1n}^2}} e^{-jk_m\sqrt{\mathbf{r}^2 - b_{1n}^2}} \right) \\
G_{c_{ap2}}(\mathbf{r}) &= \sum_{n=1}^{N_2} a_{2n}\left(e^{-b_{2n}k_m} + \frac{jb_{2n}}{\sqrt{\mathbf{r}^2 - b_{2n}^2}} e^{-jk_m\sqrt{\mathbf{r}^2 - b_{2n}^2}} \right)
\end{aligned} \tag{3.38}
$$

An alternative identity from (3.36) can be obtained by taking the derivative of the Sommerfeld identity in (3.27) with respect to $\mathbf{r}$ [49] is:

$$\int_0^{\infty} J_1(\mathbf{r}k_r) \frac{e^{-bk_{m,z}}}{k_{m,z}} k_r^2 dk_r = \frac{e^{jk_m\sqrt{\mathbf{r}^2 + b_n^2}}}{\left(\mathbf{r}^2 + b_n^2\right)^{3/2}}\left(1 - jk_m\sqrt{\mathbf{r}^2 + b_n^2}\right)\mathbf{r}. \tag{3.39}$$

Our investigation concludes that the DCIM scheme using the identity in (3.39) has large errors in the near-field region ($k_0 \mathbf{r} < 10^{-4}$). On the contrary, the DCIM scheme using the identity in (3.36) has controllable accuracy in the near-field region.

Many authors [8-10, 50-54] claimed that the DCIM could suffer significant inaccuracies mainly due to two problems: (1) not extracting the quasi-static terms from the Green's function; (2) introducing an incorrect branch point in the process to approximate the complex exponential. Regarding the first problem, the conventional DCIM that is similar to Aksun's One -level approach needed to extract the quasi-static terms to obtain accurate results in the near-field regions. However, that is not necessary for the Two-level approach. The approach yields highly accurate solutions without extracting the quasi-static terms. With regard to the second problem, it was reported by Kipp and Chow [9, 44] that the DCIM needed to be modified to take into account the additional branch cut that is present for multilayered media with an unbounded top or bottom region. The modified DCIM ($\tilde{G}_{\text{mod}}$) that they reported is rewritten as:

$$\tilde{G}_{\text{mod}} = \tilde{A} \frac{\tilde{G}'}{2jk_{z,0}}, \tilde{G}' = \tilde{G} \frac{k_{z,0}}{k_{z,m}} \qquad (3.40)$$

where $\tilde{A}$ are the reflection coefficients (A.19) — (A.21) and $\tilde{G}$ is the spectral Green's function. Notice that a factor $k_{z,0}/k_{z,m}$ is introduced to account for the branch cut. The GPOF approximation is now performed in terms of $k_{z,0}$ instead of $k_{z,m}$. This misunderstanding is clarified by Aksun [55] that the introduction of the artificial branch cut can be avoided by using the GPOF and enough sampling points for the Two-level approach (the period sampling of T_{01} and T_{02} set to 101 points or more is sufficient). The only error approximation of the solutions in the far-field regions for the Two-level approach is not extracting the surface-wave modes of the Green's function. Our investigation concludes Aksun's clarification. High accuracy of solution is obtained via the Two-level DCIM in the near-field region without extracting the quasi-static terms from the Green's function.

3.3.3 DCIM with Surface-wave-pole extraction

Green function approximated using the Two-level approach can be applied to controllable accuracy in the near-field region. However, the error becomes significant when r becomes large. This is due to the fact that DCIM does not accurately

approximate the $1/\sqrt{r}$ asymptotic behavior inherent in the surface-wave modes that are dominant in the far-field. This can be corrected by extracting the surface-wave modes from the DCIM approximation and adding them back in the spatial domain later.

In previous work on the DCIM, the evaluation of the surface-wave poles is carried out analytically using the Cauchy Residue theorem. The Cauchy Residue theorem is defined:

Cauchy Residue Theorem: If Γ is a simple closed positively oriented contour and f is analytic inside and on Γ except at the points $z_1, z_2, ..., z_n$ inside Γ, then

$$\oint_\Gamma f(z)\,dz = 2\boldsymbol{p}\, j \sum_{i=1}^{n} \mathrm{Res}(f; z_i)$$

$$\mathrm{Res}(f; z_i) = \lim_{z \to z_i} \frac{1}{(m-1)!} \frac{d^{m-1}}{dz^{m-1}}\left[(z - z_i)^m f(z)\right]$$

.(3.41)

The analytical approach is difficult to extend to multilayered cases since the residue might not have an analytical solution. A more robust approach to extract the surface-wave pole numerically is to use a simple recursive algorithm introduced in [56], which is based on the Cauchy Residue theorem. It begins with a rectangular contour enclosing the region of interest. The Green's function is integrated over the contour. If the integral process is nonzero, the contour is subdivided into four contours. This process is repeated until the location k_{rr_n} and residue Res_n of all the poles are found to be at the desired accuracy.

	ε_r	h
5	1.0	∞
4	2.1	0.7
3	12.5	0.3
2	9.8	0.5
1	8.6	0.3

(a)
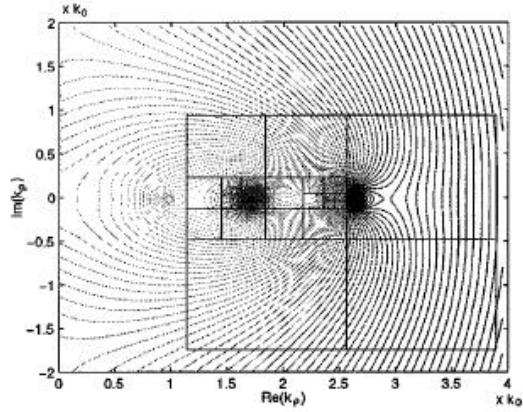
(b)

Fig. 3.5 Magnitude of G_v in the first and fourth quadrants of the complex k_ρ-plane for a four-layered medium. (a) The cross-sectional view of a five layered media backed with PEC ground plane (b) The rectangular contour is bisected until the surface-wave poles are located at $k_r = 1.736 k_0$ and $2.435 k_0$, source [57].[51]

Consider the five layers medium backed by a Perfectly Electric Conducting (PEC) ground plane as illustrated in Fig. 3. 5(a) as an example. The magnitude of the scalar Green's function G_v is plotted in Fig 3.5(b) in the first and fourth quadrants, the contour integral is repeated until we found the surface-wave poles at $k_r = 1.736 k_0$ and $2.435 k_0$, respectively.

Once the surface-wave poles are computed, the spectral Green's function due to the surface-wave mode is expressed as:

$$\tilde{G}_{sw}(k_r) = -j 2 k_z \sum_{n=0}^{M} \frac{2 k_{rrn}}{k_r^2 - k_{rrn}^2} \operatorname{Res}_n$$

$$\operatorname{Res}_n = \lim_{k_r \to k_{rrn}} (k_r - k_{rrn}) \frac{1}{j 2 k_z} \tilde{G}(k_r)$$

(3.42)

Then, applying the identity [48],

31

$$\frac{1}{2p} \int_0^\infty \frac{2k_{ri}R_i}{k_r^2 - k_{ri}^2} J_0\left(k_r \boldsymbol{r}\right) k_r dk_r = \frac{-jk_{ri}R_i}{2} H_0^{(2)}\left(k_{ri}\boldsymbol{r}\right) \tag{3.43}$$

the Green's function can be expressed in a closed form in the spatial domain as:

$$G_{sw}\left(\boldsymbol{r}\right) = -j2p \sum_{n=0}^{M} \left(\text{Res}_n k_{\boldsymbol{rrn}}\right) H_0^{(2)}\left(\boldsymbol{r}k_{\boldsymbol{rrn}}\right). \tag{3.44}$$

The surface-wave term is then superimposed into the layer media Green's function using the simple identity:

$$\begin{aligned}
\tilde{G} &= \left(\tilde{G} - \tilde{G}_{sw}\right) + \tilde{G}_{sw} \\
&= \left(\tilde{G}_{c_{ap1}} + \tilde{G}_{c_{ap2}}\right) + \tilde{G}_{sw}
\end{aligned} \tag{3.45}$$

where the DCIM is applied to the extracted term $\tilde{G} - \tilde{G}_{sw}$. Finally, the total Green's function is expressed as:

$$G\left(\boldsymbol{r}\right) = G_{c_{ap1}}\left(\boldsymbol{r}\right) + G_{c_{ap2}}\left(\boldsymbol{r}\right) + G_{sw}\left(\boldsymbol{r}\right). \tag{3.46}$$

Adding the surface-wave term into the DCIM approximation improves the far-field computation. However, a problem is encountered for the near-field evaluation. As discussed in [57], when $z \neq z'$, the Green's function is not singular at $\boldsymbol{r} = 0$; however, the surface-wave term becomes singular due to the evaluation of the Hankel function. Another drawback of adding the surface-wave term is the difficulty to derive a closed form integration equation in the MoM integration for the near-field regions. To circumvent these problems, we split the DCIM into two regions of $\boldsymbol{r}$: (1) Aksun's Two-level approach to approximate the spatial Green's function in near-field regions $\left(small\ \boldsymbol{r}\right)$; (2) in addition to the Two-level approach, include the surface-wave term to approximate the far-field regions. The transition point between these two regions can be safely fixed at $k_0 \boldsymbol{r} = 1$. A robust way we have found is to define a transition region with controllable error tolerance by computing the relative error between the numerical Sommerfeld integral and DCIM at distance points near $k_0 \boldsymbol{r} = 1$.

3.4 Computer implementation issues

There are three issues to be considered when implementing the MoM code, especially for developing automated CAD tools for solving microwave circuits. The first issue

is the implementation of DCIM. The most important parameter used in the Two-level DCM is T_{02} shown in Fig 3.4 which is defined as:

$$T_{02} = 1.2k_0 \sqrt{e_{r_{\max}}} \qquad\qquad (3.47)$$

where $e_{r_{\max}}$ is the maximum relative permittivity for the layered media in microwave circuits. The number of exponentials in the Two-level DCIM is automatically determined by equating the significant digits yielded from the Singular Value Decomposition (SVD) in the GPOF to the error tolerance.

Secondly, in order to save computer memory, we store the sample points of all tabulated Green's function into a compressed format, and several integer pointers are created to wisely determine the segment-window of the tabulated data to use. The interpolation scheme is discussed in Section 3.4.1.

Finally, during the process of filling the impedance matrix, the field cells are sorted in an ascending order according to the separation of radial distance from the source cell. For this procedure, we define two variables — *radius-near-field* and *radius-far-field* — to check which integration scheme to use (adaptive or fixed point Gauss quadrature) for the source and observation cells' interactions. We define the *radius-near-field* as the average of cells' diameters and the *radius-far-field* as two times the *radius-near-field*. Meanwhile, the separation distance for every reaction between source and field cells is calculated, and the separation distance is checked to ascertain whether an adaptive or fixed-point integration is used. If the separation distance is smaller than the *radius-near-field*, an adaptive integration based on the Gauss Quadrature rule is employed. If the separation distance falls between the range of *radius-near-field* and *radius-far-field*, we perform a fixed-point-order Gauss Quadrature integration proportional to the number of digits required for accuracy. When the separation distance is larger than the *radius-far-field*, integration with a fixed-point rule to an order of $p+1$ is performed, where p is the order of the basis function. We utilize the Khayat-Wilton transform for the singular and near singular cells.

3.4.1 Tabulated data for layered-media Green's functions

Lale, Aksun *et al.* [58] developed the analytical formulation to solve for planar microstrip problems using the DCIM. The approach is limited for rectangular mesh's discretization. The main drawback of this approach is incapable to solve for microwave circuits that have arbitrary shapes. For an arbitrary patch, one may use numerical integration. However, it is too expensive to compute. It is more efficient to tabulate the Green's functions as a function of r. Subsequently, an interpolation scheme can be used to interpolate the Green's function efficiently.

3.4.2 Efficient adaptive-window 1D interpolation

To reduce the overall fill time and compute the impedance matrix in MoM, an efficient 1D adaptive-window interpolation scheme is employed to interpolate the value of the Green's function in the spatial domain. The Green's function is pre-computed and tabulated via the DCIM. Subsequently, an interpolation scheme is utilized to approximate the Green's function. We employ the Silvester Lagrange Interpolation (SLI) scheme with order p and local simplex coordinate u, which is defined as [59]:

$$SLI_{p+1} = R_i(p, u) R_{p-1}(p, 1-u) \tag{3.48}$$

where $R_i(p, u)$ is the Silvester Lagrange polynomial defines as:

$$R_i(p, u) = \begin{cases} \dfrac{1}{i!} \displaystyle\prod_{k=0}^{i-1}(pu - k) & 1 \le i \le p \\ 1 & i = 0 \end{cases}. \tag{3.49}$$

The sample points of the interpolation scheme are adaptively chosen to yield a controllable accuracy. First, consider a segment (r_1, r_2) where r_1 and r_2 are the initial and end points respectively of Green's function. A new sample at the mid-point, $r_3 = (r_1 + r_2)/2$, is chosen by bisecting the segment (r_1, r_2). Subsequently, the first window enclosing all these 3 sample points are used to approximate the result — $Y_3(\rho_3)$ at r_3 via the interpolation scheme. Following the same procedure, we yield

5 sample points at the second window. We approximate the result — $Y_5(\rho_3)$ at point $\boldsymbol{r}_3$. The relative error is computed as:

$$\frac{\left|Y_5\left(\boldsymbol{r}_3\right)-Y_3\left(\boldsymbol{r}_3\right)\right|}{\left|Y_5\left(\boldsymbol{r}_3\right)\right|} \tag{3.50}$$

The bisecting procedure is repeated until the relative error is smaller than a given error tolerance. Note that the new sample points are bisected in the equidistant manner. In the interpolation scheme we implemented, a maximum of nine sample points are allowed within a window.

3.4.3 DOF for vertical basis reactions

To ensure that the LCTN property of the vertical basis function is satisfied, we define the number of Degree of Freedom (DOF) for the source and field cells. DOF equals *(nc-1)* where *nc* is the number of cells an edge shares. For example, two cells sharing an edge have one DOF, and three cells sharing an edge have two DOF. In order to satisfy the Kirchoff Current Law (KCL) in circuit theory, the direction of the current flows through the cells must be consistent. The direction of current that flows out from the cell has a positive sign. Otherwise a negative sign will be assigned to the current. In the MoM, the sign is determined by choosing the smallest cell number of cells sharing the common edge. For example, there are three cells that share an edge in Fig 3.6, hence the current is flowing into cell one and flowing out to cells two and three.
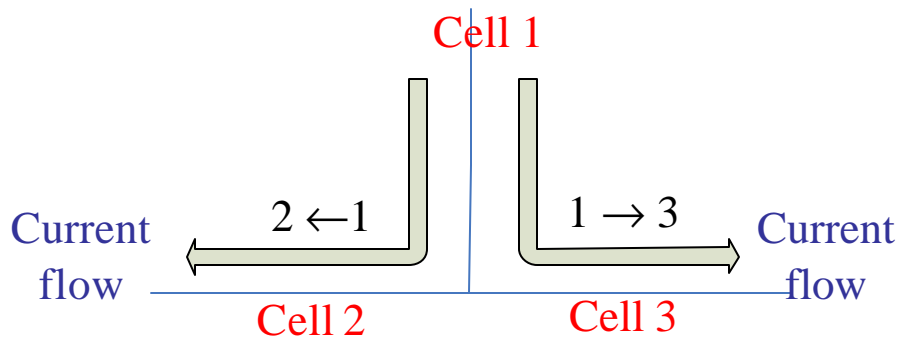
Fig. 3.6 The DOF of a vertical cell element. The sign of cell 1 has been assigned a positive value, while cell 2 and cell 3 are negative.

3.5 De-embedding scheme to extract scattering parameters

Usually the network parameters such as the radiation and scattering parameters of RF and MMIC are extracted using a full-wave simulation. The parameters being extracted are Y-parameters from discrete ports. Different wave guiding structures are associated with these discrete ports, including microstrip lines, co-planar waveguide lines (CPW) or co-planar line-pairs (CPLP).

Two popular de-embedding schemes in electromagnetic scattering problems are Chang and Rautio [60, 61]. In this dissertation, Rautio's approach is employed for solving two-port network scattering parameters. Next, the coefficients of current density are computed in MoM [25]. We excite each port with a delta-gap source and compute the port currents to find the Y-matrix as.

$$
\begin{pmatrix} I_1 \\ I_2 \\ \vdots \\ I_N \end{pmatrix} = \begin{pmatrix} Y_{11} & Y_{12} & \cdots & Y_{1N} \\ Y_{21} & Y_{22} & \cdots & Y_{2N} \\ \vdots & \vdots & \ddots & \\ Y_{N1} & Y_{N2} & & Y_{NN} \end{pmatrix} \begin{pmatrix} V_1 \\ V_2 \\ \vdots \\ V_3 \end{pmatrix}
\tag{3.51}
$$

where vector V is the delta-gap source that is placed across a gap between two cells in the limit so that the gap separation tended to zero. Thus, the Y-parameters can be extracted from a network by shorting all ports and exciting a single port with a voltage source. Subsequently, a virtual short and open circuit are symmetrically placed in the feed line network in the reference plane. The ABCD matrix can be computed by exciting the even and odd modes of the Device Under Test (DUT) under the feed line network. Finally, the S-parameters can be transformed once the ABCD matrix is known. A more detailed discussion about the DUT network can be found in the technical memorandum by Gedney [25].

3.6 Validation of Green's function with horizontal source/observation patches via DCIM

The advanced Two-level DCIM method presented in Section 3.3 is compared with the direct Sommerfeld integration, which is computed using the Weighted-average method. A number of examples are chosen to attempting fully validate the accuracy and efficiency of the DCIM method. Initially, consider the example of a microstrip

circuit printed on a single dielectric layer with the dielectric constant $e_r = 3.31$, that is backed by a ground plane with conductivity $s_m = 4.9 \times 10^7$ S/m. The cross-sectional view of the microstrip is illustrated in Fig 3.7 (a). With the presence of only a horizontal conductor, only two Green's function terms (G_{xx} and G_{vt}) in the DGF are required. The Green's functions are computed via the Two-level DCIM and the results are compared with the direct Sommerfeld integration. Fig 3.7 (b) shows the magnitude of the Green's functions versus $k_0 r$ where k_0 is the free-space wave number and r is the distance between the source and field points. Note that the surface-wave mode is included in the DCIM approximation at region $k_0 r > 1$.

$$z = 0.81\,\text{mm} \quad e_r = 1 \qquad z = z'$$

$$e_r = 3.31 \qquad \tan d = 0$$

$$z = 0 \qquad\qquad s = 4.9\text{x}10^7\text{S/m}$$
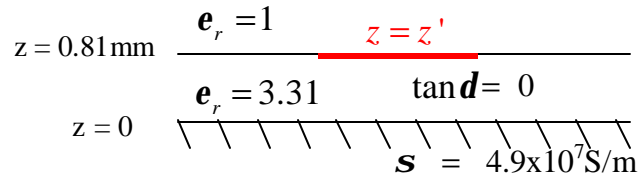
(a) The cross-sectional view of a microstrip, z is observation point, z' is source point.
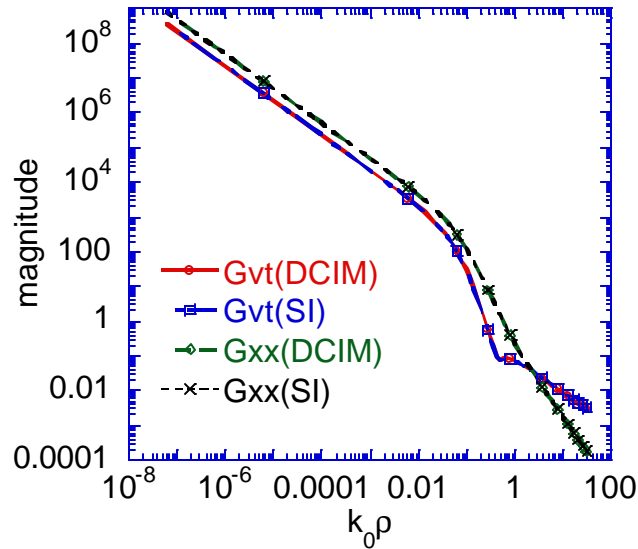
(b) The comparison between DCIM and Sommerfeld.

Fig. 3.7 Green's function for a single layer microstrip computed via DCIM and a direct Sommerfeld integration. The numerical Sommerfeld integration is based on the weighted average method in Michalski's paper. The operational frequency is at 2GHz. (a): The cross-sectional view of the microstrip; (b) The magnitude of Green's function versus $k_0 r$.

Next, Fig 3.8 (a) shows an example of a microstrip with four layers backed by a conductor plate, and each layer has a loss tangent of 0.001. Note that the source z' and observation z points are located at different layers. The layered media Green's functions G_{xx} and G_{vt} are computed via the DCIM, and compared with a direct Sommerfeld's results. Figure 3.8 (b) shows the magnitude of the Green's functions, and Fig 3.8 (d) shows the relative error of the DCIM. Note that in the region ($k_0 r > 3$) the surface-wave pole extraction defined in Section 3.3.3 is employed.
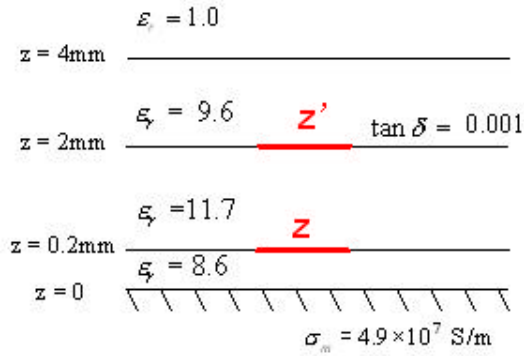
(a) The cross-sectional view of a microstrip, z is observation point, z' is source point. All dielectric layers have *tan d* of 0.001.
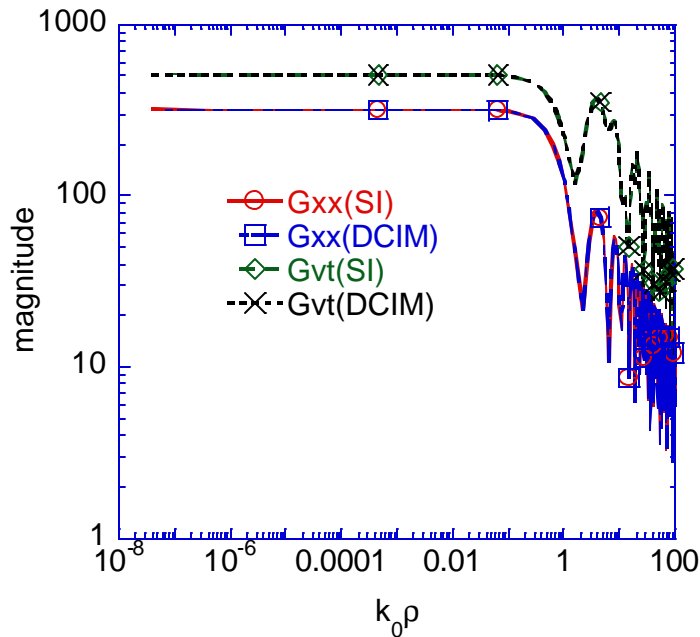
(b) Magnitude of Green's functions G_{xx}, G_{vt} for microstrip illustrated in (a).

38
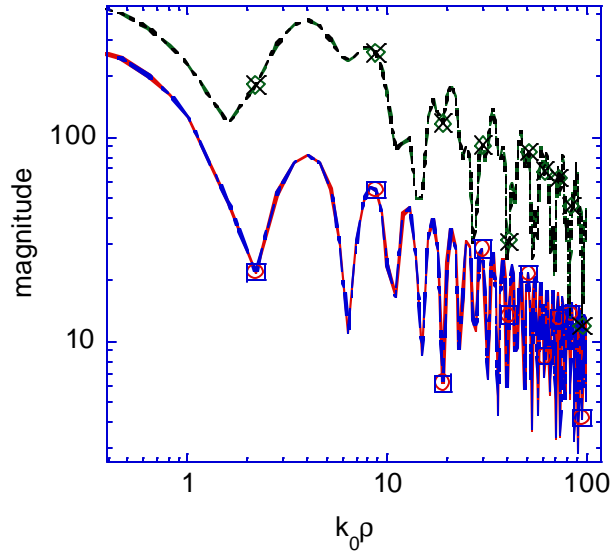
(c) Zoom-in view of far-field
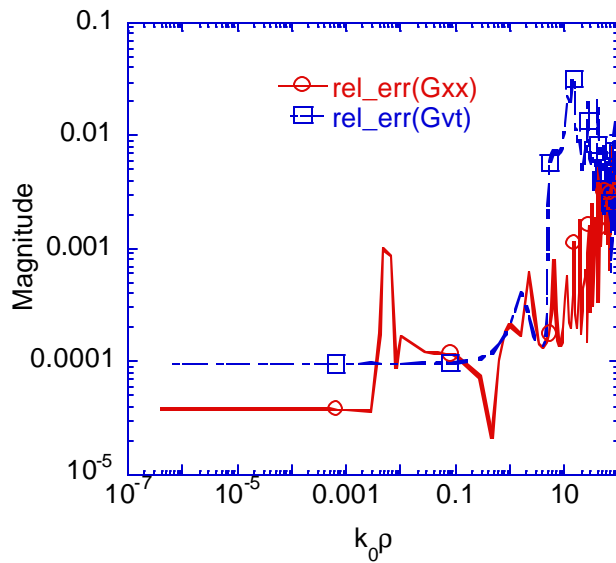
(d) Relative error of DCIM

Fig. 3.8 The comparison between the DCIM and Sommerfeld integration for the Green's functions G_{xx}, G_{vt} at 20GHz for the four-layer microstrip backed by a plate. Each layer has a loss tangent of 0.001. (a) Cross-sectional view. (b) The magnitude of Green's function z-integration versus $k_0 r$. (c) The zoom-in view of results in the far-field region. (d) The relative error of DCIM compared with a direct Sommerfeld results.

Chapter Four: Efficient pre-computation of the DGF for 2.5D circuits in multi-layered media

In Chapter 3 we considered the case of planar circuits printed on horizontal layered media. However, the objective is to be able to treat the more general case of arbitrary shaped circuits in layered media, namely with both vertical and horizontal conductors. In this chapter, we present an efficient methodology for using the DCIM to approximate the DGF for such circuits. The approach is limited to circuits with purely horizontal and purely vertical conductors — namely 2.5D problems. This is by no means limiting, since circuits fabricated with lithography, etching, or epitaxial growth-type processes grow metal layers along the vertical dimensions. Practical problems of interests are layered media for circuits with via, interconnects, air bridges, metal with thickness, et cetera. The work here can be extended to general 3D problems. An efficient approach to compute the DGF in layered media for microwave circuits with horizontal and vertical conductors is addressed next.

4.1 Circuits with horizontal conductors

It is expensive to directly utilize the DCIM to compute the DGF during the computation of the impedance matrix for the MoM. A more efficient approach is to pre-compute and tabulate the DGF via the DCIM in advance, and to utilize the adaptive 1D interpolation scheme presented in Section 3.4.1 to approximate the DGF with controllable accuracy. For metallization in different layers, we need to tabulate the DGF for each source-field layer pair. Reciprocity can be used to evaluate reciprocal DGF pairs, reducing the number of DGF pairs to $N(N+1)/2$, rather than N^2 operations, where N is the number of horizontal layers with metallizations.

4.2 Circuits with vertical and horizontal conductors

Circuits with vertical conductors require the pre-calculation of the DGF that is a function of the radial separation as well as the vertical separation of the source and field points. Furthermore, the DGF is also a function of the vertical coordinate of the source point. This is because the DGF is *not* translationally invariant with respect to z and z'. Thus, the DGF must be computed for every source position z' and every field

position z It must be noted that the DCIM only approximates the DGF as a function of the radial separation, r. Consequently, a DCIM approximation must be performed for every anticipated source coordinate z' as a function of r and the vertical field coordinate z This computation is very time consuming, especially in the near field where an adaptive Quadrature integration is needed for both r and z A solution to this problem is to pre-compute the DGF via the DCIM and tabulate it in a 2D table as functions of both r and z-z' pairs. Subsequently, multiple 2D interpolations must be employed to interpolate the DGF. For example, Ling [43] employed the DCIM to tabulate the DGF as a function of r, z, and z-z'. He utilized the Chebyshev interpolation scheme to interpolate the DGF for z-z' and the Lagrange interpolation scheme for r. Unfortunately, using a 2D interpolation scheme to interpolate the DGF can be very computationally intensive because the scheme requires fine sampling in z', z-z' and r in the near field to integrate through singularities. In addition, fine sampling is also required to yield accurate solutions in the far field due to oscillatory nature of the DGF.

4.2.1 Analytical evaluation of z-integration in the *spectral* domain.

To avoid a costly 2D interpolation scheme, an efficient approach is to perform the z integration of the DGF in the *spectral* domain analytically. Consider a source patch that has z-bounds $\left(z_1', z_2' \right)$ and field patch that has z-bounds $\left(z_1, z_2 \right)$. For each unique $\left(z_1', z_2' \right)$ — $\left(z_1, z_2 \right)$ pair, the DCIM is used to pre-compute and tabulate the Sommerfeld integral resulting from the analytical z-integration of the DGF, which is a function of r only. The tabulated data can then be computed using the adaptive 1D interpolation scheme presented in Section. 3.4.1. Therefore, a 2D interpolation scheme is avoided.

The vertical conductors are assumed to be rectangular patches. The basis functions on the vertical patches are the zero[th]-order GWP [21] basis functions. Both vertically and horizontally directional bases are supported on the vertical patch. A reaction integral assuming vertical source and field patches can be written as:

$$\int_{t_1}^{t_2} \int_{z_1}^{z_2} \int_{t_1'}^{t_2'} \int_{z_1'}^{z_2'} \left(\frac{z - z_2}{z_2 - z_1} \right) G\left(z, z'; k_r \right) \left(\frac{z' - z_1'}{z_2' - z_1'} \right) dz' dt' dz dt \qquad (4.1)$$

where primes indicate source coordinates. The Green's function can be rewritten in the spectral domain via the Sommerfeld integral:

$$\int_{t_1}^{t_2}\int_{z_1}^{z_2}\int_{t_1'}^{t_2'}\int_{z_1'}^{z_2'}\left(\frac{z-z_2}{z_2-z_1}\right)\left(\int_0^\infty \frac{J_0(k_r\boldsymbol{r})k_r}{k_{m,z}}\tilde{G}(z,z';k_r)dk_r\right)\left(\frac{z'-z_1'}{z_2'-z_1'}\right)dz'\,dt'\,dz\,dt. \tag{4.2}$$

The order of integral is interchanged that leads to:

$$\int_{t_1}^{t_2}\int_{t_1'}^{t_2'}\int_0^\infty \frac{J_0(k_r\boldsymbol{r})k_r}{k_{m,z}}\left[\int_{z_1}^{z_2}\int_{z_1'}^{z_2'}\left(\frac{z-z_2}{z_2-z_1}\right)\tilde{G}(z,z';k_r)\left(\frac{z'-z_1'}{z_2'-z_1'}\right)dz'\,dz\right]dk_r\,dt'\,dt \tag{4.3}$$

where $\tilde{G}$ is known in a closed form. Subsequently the z-integration can be performed analytically in the *spectral* domain. For example, consider G_{zz}, with the source and field patches in the same layer:

$$\int_{t_1}^{t_2}\int_{t_1'}^{t_2'}\int_0^\infty \frac{J_0(k_r\boldsymbol{r})k_r}{k_{m,z}}\left[\int_{z_1}^{z_2}\int_{z_1'}^{z_2'}\left(\frac{z-z_2}{z_2-z_1}\right)\tilde{G}_{zz}(z,z';k_r)\left(\frac{z'-z_1'}{z_2'-z_1'}\right)dz'\,dz\right]dk_r\,dt'\,dt \tag{4.4}$$

where the spectral domain $\tilde{G}_{zz}$ is defined as:

$$\tilde{G}_{zz}(z,z') = A_1 e^{jk_{m,z}(z+z'+2d_{m-1})} + A_2\left(e^{-jk_{m,z}(z'-z+2(d_m-d_{m-1}))} + e^{jk_{m,z}(z'-z-2(d_m-d_{m-1}))}\right) + A_3 e^{-jk_{m,z}(z'+z+2d_m)}$$

$$A_1 = \tilde{R}^{TM}_{m,m-1}\tilde{M}^{TM}_m \tag{4.5}$$

$$A_2 = \tilde{R}^{TM}_{m,m-1}\tilde{R}^{TM}_{m,m+1}\tilde{M}^{TM}_m$$

$$A_3 = \tilde{R}^{TM}_{m,m+1}\tilde{M}^{TM}_m$$

where the Fresnel reflection coefficients $\tilde{R}^{TM}_{i,j}$ and $\tilde{M}^{TM}_m$ are defined from (A.19) to (A.21). Subsequently, the bracketed terms in (4.4) can be derived analytically in a closed form as:

$$\int_{z_1}^{z_2}\int_{z_1'}^{z_2'}\left(\frac{z-z_2}{z_2-z_1}\right)\tilde{G}_{zz}(z,z';k_r)\left(\frac{z'-z_1'}{z_2'-z_1'}\right)dz'\,dz = \frac{1}{k_{m,z}^4}\sum_{i=1}^{13} c_i \tag{4.6}$$

where

$$c_1 = -jA_3\left[k_{m,z}\left(z_1' - z_2'\right) + j\right]e^{-jk_{m,z}\left(z_2 + z_2' + 2d_m\right)}$$

$$c_2 = -jA_2\left[k_{m,z}\left(z_1' - z_2'\right) + j\right]e^{jk_{m,z}\left(z_2 - z_2' - 2(d_m - d_{m-1})\right)}$$

$$c_3 = jA_2\left[k_{m,z}\left(z_1' - z_2'\right) - j\right]e^{-jk_{m,z}\left(z_2 - z_2' + 2(d_m - d_{m-1})\right)}$$

$$c_4 = jA_1\left[k_{m,z}\left(z_1' - z_2'\right) - j\right]e^{jk_{m,z}\left(z_2 + z_2' + 2d_{m-1}\right)}$$

$$c_5 = -A_2\left[k_{m,z}\left(z_2 - z_1\right) + j\right]\left[k_{m,z}\left(z_1' - z_2'\right) - j\right]e^{-jk_{m,z}\left(z_1 - z_2' + 2(d_m - d_{m-1})\right)}$$

$$c_6 = -A_2\left[k_{m,z}\left(z_2 - z_1\right) - j\right]\left[k_{m,z}\left(z_1' - z_2'\right) + j\right]e^{jk_{m,z}\left(z_1 - z_2' - 2(d_m - d_{m-1})\right)}$$

$$c_7 = A_1\left[k_{m,z}\left(z_2 - z_1\right) - j\right]\left[k_{m,z}\left(z_1' - z_2'\right) - j\right]e^{jk_{m,z}\left(z_1 + z_2' + 2d_{m-1}\right)}$$

$$c_8 = A_3\left[k_{m,z}\left(z_2 - z_1\right) + j\right]\left[k_{m,z}\left(z_1' - z_2'\right) + j\right]e^{-jk_{m,z}\left(z_1 + z_2' + 2d_m\right)}$$

$$c_9 = jA_1\left[k_{m,z}\left(z_2 - z_1\right) - j\right]e^{jk_{m,z}\left(z_1 + z_1' + 2d_{m-1}\right)}$$

$$c_{10} = -jA_3\left[k_{m,z}\left(z_2 - z_1\right) + j\right]e^{-jk_{m,z}\left(z_1 + z_1' + 2d_m\right)}$$

$$c_{11} = -2A_2\left\{(z_1 - z_2)k_{m,z}\sin\left[k_{m,z}\left(z_1' - z_1\right)\right] + \cos\left[k_{m,z}\left(z_2 - z_1'\right)\right] - \cos\left[k_{m,z}\left(z_1 - z_1'\right)\right]\right\}e^{-jk_{m,z}\,2(d_m - d_{m-1})}$$

$$c_{12} = -A_1 e^{jk_{m,z}\left(z_2 + z_1' + 2d_{m-1}\right)}$$

$$c_{13} = -A_3 e^{-jk_{m,z}\left(z_2 + z_1' + 2d_m\right)}$$

. (4.7)

All remaining reaction pairs of $G_{xx}, G_{zt}, G_{vt}, G_{vz}$ and G_{zz} for source and field patches in the same and different layers are discussed in detail in Appendix B. An important observation from (4.4) to (4.7) is that the singularity is reduced when performing the z-integration in the *spectral* domain. In addition, only the transverse-integration is to be performed in the spatial domain. However, care must be taken when evaluating the self-cell term. The kernel may still exhibit a logarithmic singularity at $r = 0$. While the kernel may not be numerically singular, its derivative is. To deal with the logarithmic singularity numerically, the transverse source integral t' can be split into two parts as:

$$\int_{t_1}^{t_2}\int_{t_1'}^{t_2'}\{\ \}dt'dt = \int_{t_1}^{t_2}\left[\int_{t_1'}^{t}\{\ \}dt' + \int_{t}^{t_2'}\{\ \}dt'\right]dt .$$
(4.8)

To ensure high accuracy and a fast convergence rate for the solution, numerical integration based on the Gauss Quadrature rule with fixed-point and high-order is performed for the transverse *field* integration, while the integration based on the Gauss Linlog rule is employed for the transverse *source* integration to capture the singularity.

43

4.2.2 Asymptotic extraction of analytical formulations with DCIM

As discussed in Section 4.2.1, the computation of the Sommerfeld integral in (4.4) is accelerated using the Two-level DCIM scheme. However, two issues are to be addressed before applying the DCIM. The first issue is that the DCIM cannot approximate a linear constant function accurately because a singularity occurs for computing the inverse vector via the Singular Value Decomposition (SVD) steps of the GPOF. Thus, exponentials with zero arguments in the closed form spectral domain equations must be extracted either numerically or analytically before applying the DCIM.

Secondly, the analytical forms of the integral in (4.4) approximated via the DCIM consist of higher-order complex poles associated with the branch cut as:

$$\int_0^\infty \frac{J_v\left(k_r \boldsymbol{r}\right) e^{-jk_{m,z}\sqrt{r^2-b_n^2}} k_r^n}{k_{m,z}^n \sqrt{\boldsymbol{r}^2-b_n^2}} dk_r \quad for \ v=0,1; n=1,2,3,4,... \tag{4.9}$$

Since DCIM only works well to approximate functions with a singularity of $1/\boldsymbol{r}$, (4.9) cannot be approximated via the DCIM accurately. In addition, it is difficult to apply analytical integral identities for the Sommerfeld integral in (4.9). Hence, the higher-order poles must be extracted analytically before applying the DCIM. The asymptotic extraction is presented in Appendix B. We observe that the higher-order poles are dominant in the near field, as $k_r \to \infty$.

4.3 Validation of Green's function with vertical source/observation patches via DCIM

In Section 4.2, a technique was presented where the vertical integrations for source and observation patches were performed analytically in the spectral domain. The advantage of this approach is that it avoids the expensive pre-computation and tabulation of the Green's functions over a 2D plane. Closed form expressions were also derived via the advanced Two-level DCIM algorithm. This methodology is validated in this section. First, consider a vertical conductor embedded in a multilayered dielectric substrate as illustrated in Fig 4.1. The conducting ground plane has a conductivity of $\boldsymbol{s}_m = 4.9 \times 10^7$ S/m. It is assumed at first that both the

vertical field and source patches have upper and lower z-bounds of 2.5 mm and 3 mm, respectively. As an example, we compute some of the closed form z-integrations that are derived in Appendix B, the reader can refer to (B.88), (B.98), (B.110), and (B.126). A comparison between the DCIM approximation and the direct Sommerfeld integration (the source and observation patch have the same z-bounds from 2mm to 3mm) is plotted in Fig 4.2. The relative error plot is illustrated in Fig 4.2 (c). For Fig 4.3 the source point is located at $z = 3$mm (source layer is at 2), while the observation layer has a z-bound from 2mm to 3mm (observation layer is at 3). The zoom-in view of the far-field and the relative error plots are illustrated in Fig 4.3 (b) and (c), respectively. Both results agreed very well. Note that in the region of $k_0 r > 3$, the surface-wave pole extraction defined in Section 3.3.3 is employed to approximate the $1/\sqrt{r}$ characteristic behavior in the far-region. The interpretations and derivations of other analytical closed forms are discussed in Appendix B and Table B.1.
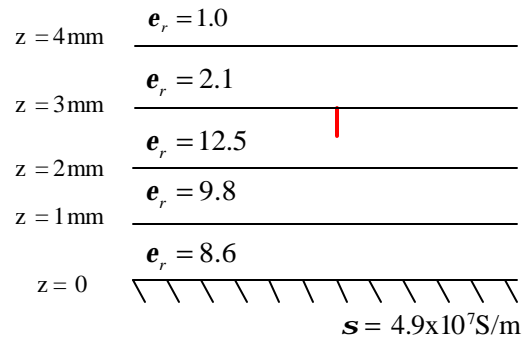
Fig. 4.1 Vertical strip embedded in a five layer media backed by a conducting ground plane with $s_m = 4.9 \times 10^7$ S/m. The vertical conductor is located between $z = 2.5$ mm and 3 mm and is assumed to be at $r = 0$. All layers have loss tangents ($\tan d$) of 0.001
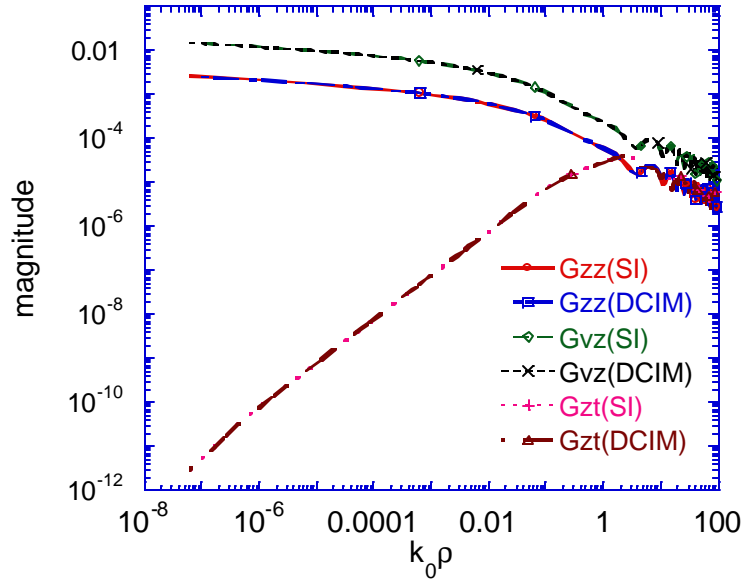
(a) magnitude of three pairs of closed-form Green's function in z-integration.
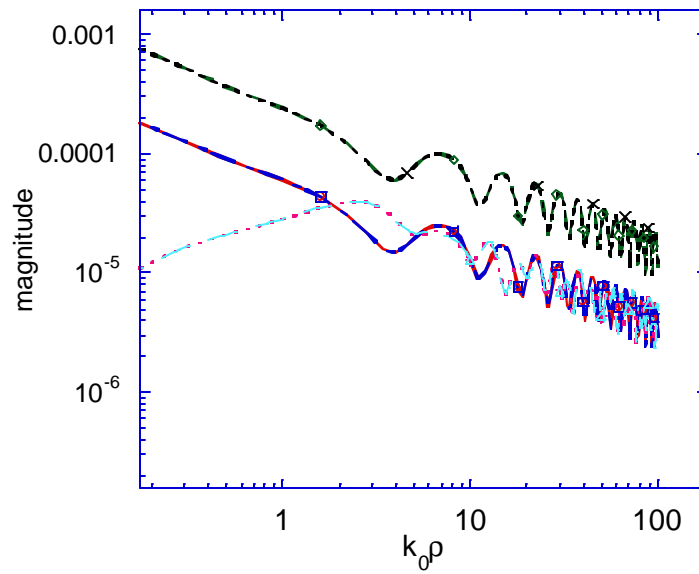
(b) zoom-in view of the far-field
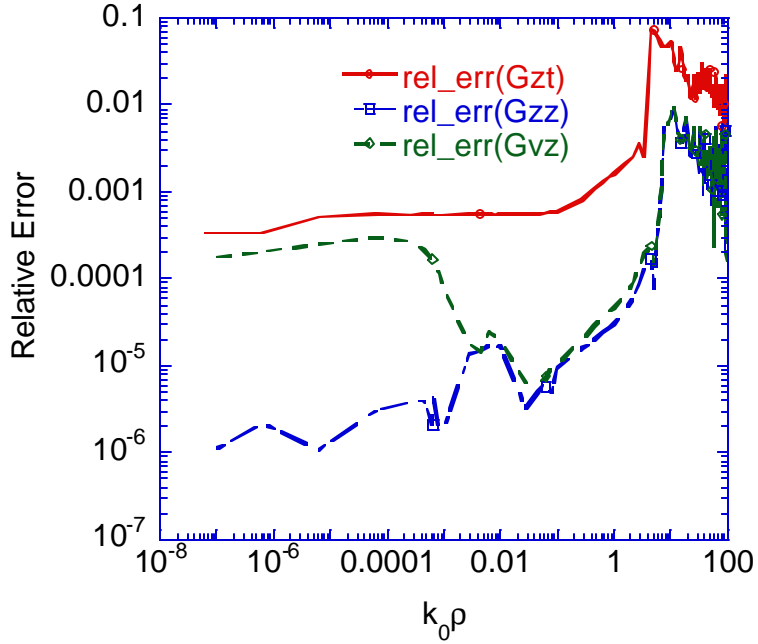
(c) The relative error for DCIM

Fig. 4.2 The comparison between the DCIM and Sommerfeld integration for the closed-form in (B.88), (B.98), and (B.110) at 30GHz for the microstrip case in Fig 4.1. (a) The magnitude of Green's function z-integration versus $k_0 r$. (b) The zoom-in view of results in the far-field region. (c) Relative error of DCIM compared with a direct Sommerfeld results.
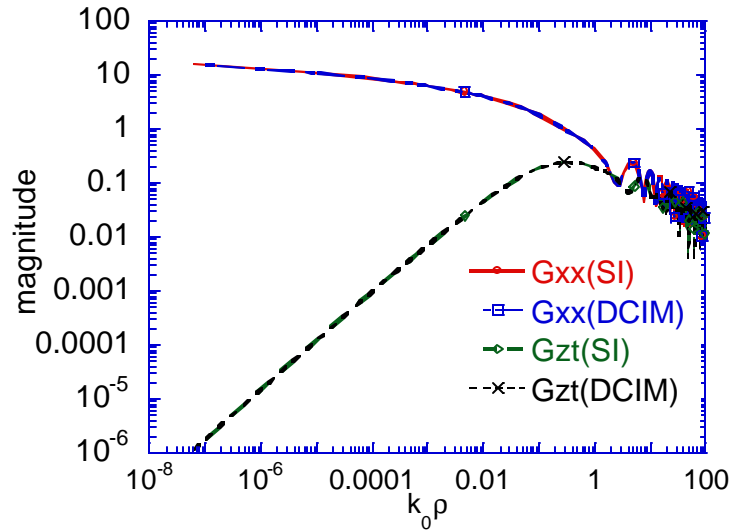
(a) magnitude of three pairs closed-form Green's function z-integration.
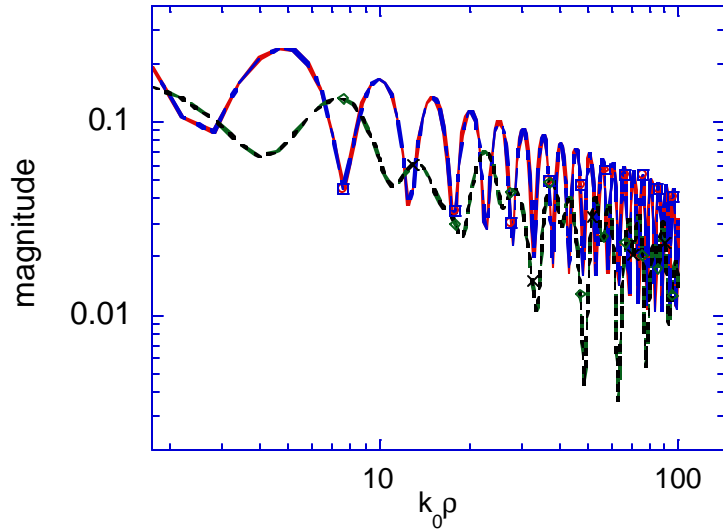
(b) zoom-in view of the far-field
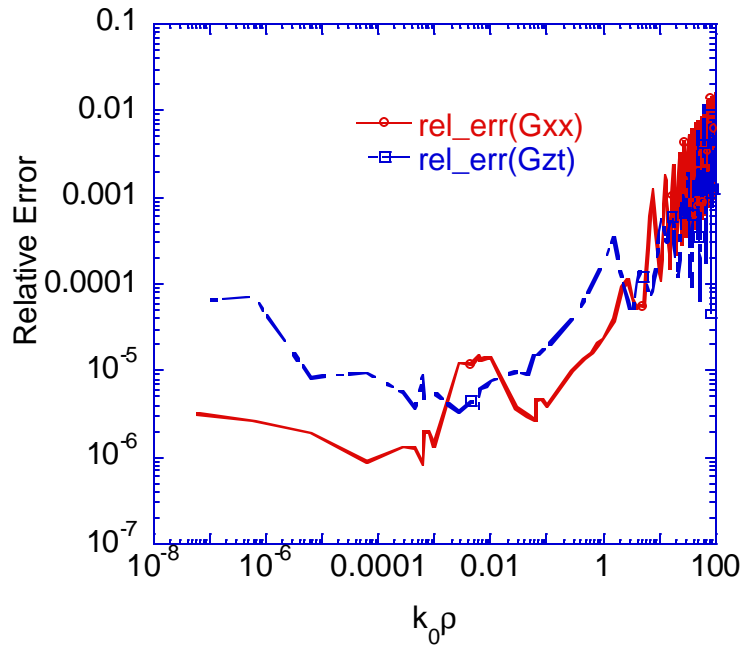
(c) The relative error of DCIM

Fig. 4.3 The comparison between the DCIM and Sommerfeld integration for the closed-form in (B.126) and (B.120). at frequency 30GHz for the microstrip case in Fig .4.1. Source point is located on the interface at 3mm, observation is located at z-bounds 2.5mm to 3mm. (a) The magnitude of Green's function z-integration versus $k_0 \boldsymbol{r}$. (b) The zoom-in view of the results in far-field region.

The next example is the case of a vertical stripline embedded in three dielectric layers, as illustrated in Fig 4.4. The vertical conductor is situated between $z = 0.508$ mm and 0.762 mm. Both source and field patches are assumed to be at transverse levels and the same bounds. The closed forms of (B.126) and (B.120) are computed via the DCIM and are compared with a direct Sommerfeld integration. The magnitudes of the closed form results are illustrated in Fig 4.5 (a) with a zoom-in view of the far-field region in Fig. 4.5 (b). Finally, the relative error of the DCIM versus a direct Sommerfeld integral is computed and illustrated in Fig 4.5 (c). From the figure, excellent results are observed via the DCIM with a relative error less than 10^{-4} at the near field, while the relative error is less than 0.005 at the far field.
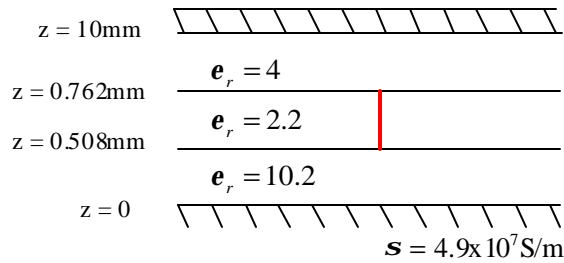
Fig 4.4 A strip structure embedded with three layers media between two conducting planes. The vertical conductor is located at z-level from 0.508 mm to 0.762 mm. All dielectric layers have loss tangents ($\tan d$) of 0.001.
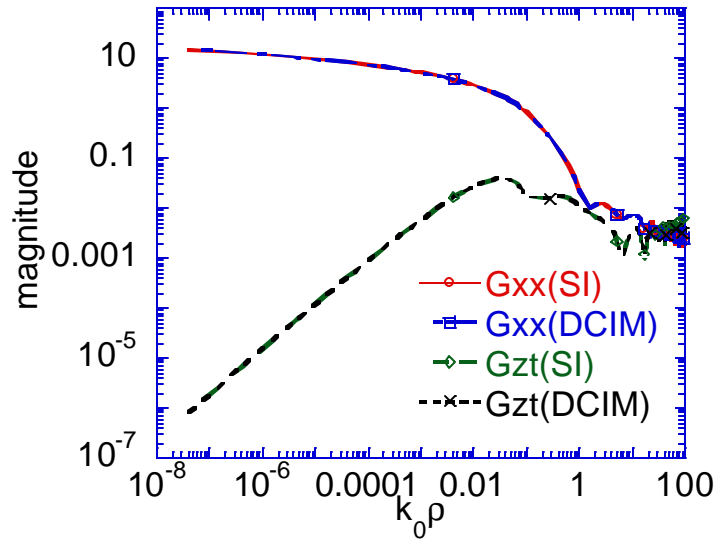
(a) magnitude of three pairs closed-form Green's function z-integration.
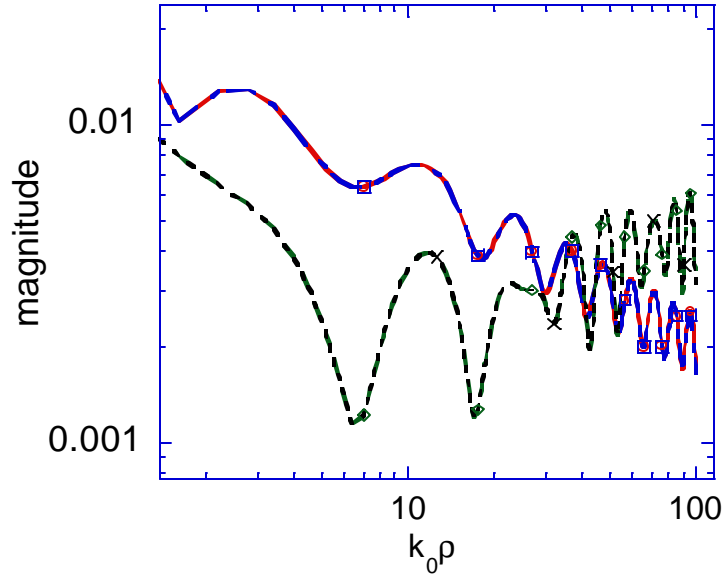
(b) zoom-in view of the far-field
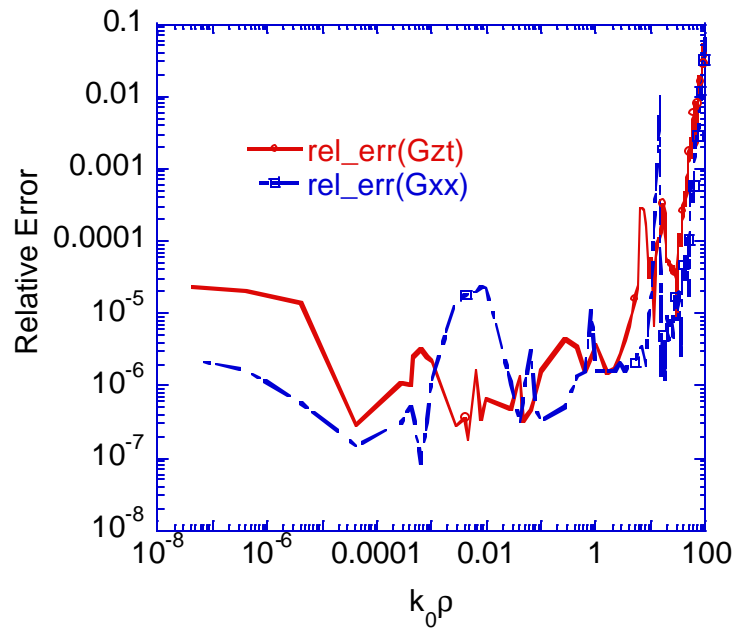
(c) Relative error of DCIM

Fig. 4.5 The comparison between the DCIM and Sommerfeld integration for the closed-form in (B.126) and (B.120) at frequency 20GHz for the stripline case in Fig 4.4. (a) The magnitude of Green's function z-integration versus $k_0 r$. (b) The zoom-in view of the results in far-field region (c) The relative error of DCIM compared to Direct Sommerfeld.

The surface-wave poles are again extracted in the far-field region when $k_0 r > 3$. The surface-wave poles for the microstrip line in Fig 4.1 and the stripline in Fig 4.4 are computed using the numerical contour-integral based on the Cauchy Residue Theorem. The computed surface-wave poles are listed in Table 4.1. Observe from Table 4.1 that the surface-wave poles for the TM and TE modes are complex numbers instead of real numbers, and they all lie in the fourth quadrant of the complex $k_r - plane$. This is due to the fact that all the dielectric substrates are embedded in a lossy material with a loss tangent of 0.001. A number of other examples were studied to fully validate the implementation of the robust Two-level DCIM method yet is too extensive to detail here.

Surface-wave modes	Microstrip line in Fig 4.1	Stripline in Fig 4.4
TM mode (k_0)	(2.9819, -0.0009948)	(1.3469, -0.0015890)
	(2.1406, -0.0015106)	(1.88049, -0.001114)
	(1.0151, -0.0001816)	(2.01825, -0.001034)
TE mode (k_0)	(1.7461, -0.0017487)	(1.32705, -0.001511)
	(2.9867, -0.0016297)	(1.8548, -0.0001114)

Table 4.1 TE and TM surface-wave modes for the microstrip line and stripline illustrated in Fig 4.1 and Fig 4.4, respectively, computed via the contour integration method.

Chapter Five: Validation

A number of methods have been introduced in the previous chapters, including the application of the Khayat-Wilton transform for singular and near singular integrals, a robust Two-level DCIM that includes surface-wave poles and quasi-image poles, and an efficient method for analyzing printed structures with both horizontal and vertical structures. The focus of this chapter is to validate the methods by studying both the accuracy and efficiency.

5.1 Singular and near singular integrals

Singular integral

In chapter two, the Duffy and Khayat-Wilton transforms were introduced as an efficient technique for integrating the 1/R singularity of the layered Green's function. Both techniques subdivided the surface of integration into continuous triangles that share a common vertex, which is the singular point. The transformation cancels the singularity. The unique nature of the Khayat-Wilton transform is that it exactly cancels the 1/R singularity kernel. Once the transformation is made, a numerical quadrature scheme is then introduced in the parametric space. A 1D fixed point Gauss Quadrature rule along the transverse direction u^1 and a 1D adaptive Quadrature rule in the radial u^2 direction are used respectively. In this way, the number of function evaluations can be significantly reduced, while maintaining an accuracy solution for the integration. To validate the convergence of the Khayat-Wilton transform, considers the example of the flat quadrilateral patch shown in Fig. 5.1:
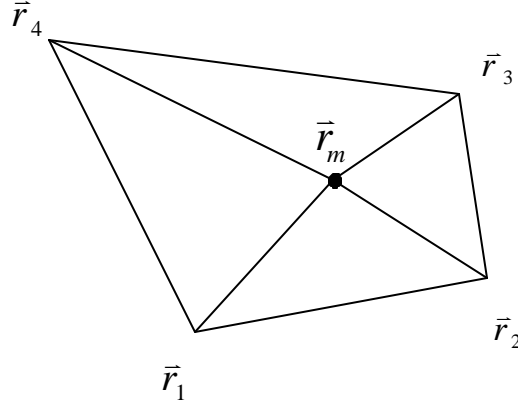
Fig. 5.1 A flat linear quadrilateral is divided into four sub-triangles with a common vertex at the singular point $\vec{r}_m$. The four vertexes are $\vec{r}_1 = (5.8 \times 10^{-4}, -5 \times 10^{-5}, 0)$, $\vec{r}_2 = (7.2 \times 10^{-4}, 0, 0)$, $\vec{r}_3 = (6.7 \times 10^{-4}, 1.3 \times 10^{-4}, 0)$, $\vec{r}_4 = (5.4 \times 10^{-4}, 1.8 \times 10^{-4}, 0)$.

Initially, the observation point $\vec{r}_m = (6.5 \times 10^{-4}, 8.72 \times 10^{-5}, 0)$. Consider the following integral:

$$\bar{I}_n(\bar{r}) = \int_s \bar{\Lambda}_n(\bar{r}')F(R)\,ds' \tag{5.1}$$

where $\bar{\Lambda}_n(\bar{r}')$ are zeroth-order-divergence-conforming GWP basis functions defined in chapter four defined as:

$$\bar{\Lambda}_1 = \frac{u^1 - 1}{\sqrt{g}}, \ \bar{\Lambda}_2 = \frac{u^2 - 1}{\sqrt{g}}, \ \bar{\Lambda}_3 = \frac{u^1}{\sqrt{g}}, \ \bar{\Lambda}_4 = \frac{u^2}{\sqrt{g}} \tag{5.2}$$

and $F(R)$ is the free-space Green function:

$$\frac{e^{-j2p\left|\bar{r}'-\bar{r}_m\right|}}{\left|\bar{r}'-\bar{r}_m\right|}. \tag{5.3}$$

A reference result I_{ref} for (5.1) — (5.3) was initially computed using an adaptive Duffy transform integral with an error tolerance of $k10^{-8}$. The mean error of the numerical integration that relates to the reference result is defined as:

$$mean\ error = \frac{1}{n}\sum_{i=1}^{n}\frac{\left|I_{i_{ref}} - I_i\right|}{\left|I_{i_{ref}}\right|} \quad for\ n = 4 \tag{5.4}$$

The plot of the mean error versus number of Gauss-Quadrature points based on integrations via the Khayat-Wilton and Duffy transforms are illustrated in Fig. 5.2. Note that the number of Gauss-Quadrature points in the orthogonal direction for the Khayat-Wilton transform is proportional to the number of digits of the given error tolerance. For example, two Gauss points were used along the orthogonal directions for an error tolerance of 0.01. The radial direction employs of an hp-adaptive scheme (h-refinement and p-refinement adaptive integration) based on a 3 and 5 points Quadrature rule. While the Duffy transform used a directional hp-adaptive scheme. Comparing the results in Fig 5.2, it is observed that the number of function evaluation using the Wilton method is at least three times less than the number used for the adaptive Duffy integration with the same accuracy.
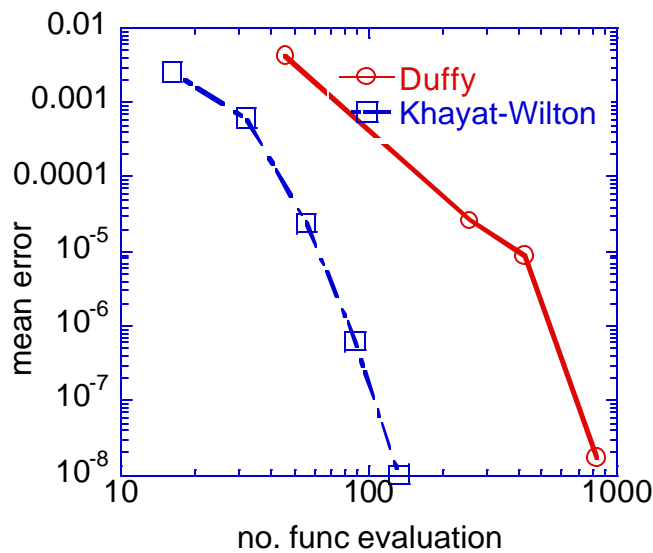
Fig. 5.2 Number of gauss points used for adaptive Duffy and Khayat-Wilton transforms to integrate (5.1). Each square and circle represents the digit of tolerance set in sequence from 1×10^{-1} to 1×10^{-7}. The singular point is placed at $(6.5 \times 10^{-4}, 8.72 \times 10^{-5}, 0)$.

Near-singular integral

Using the same quadrilateral patch in Fig 5.1, the observation point $\bar{r}_m$ is located at $(7 \times 10^{-4}, 8.72 \times 10^{-5}, 0)$. The location is near to the edge of the quadrilateral patch but outside the patch. A numerical integration based on an adaptive Gauss-Quadrature rule and the Khayat-Wilton transform is employed to compute the integration in (5.1).

The mean error defined in (5.4) versus the number of gauss points is plotted in Fig. 5.3. Observe that the solution computed via the Khayat-Wilton transform converges quickly, whereas the number of function evaluations required by the adaptive Gauss-Quadrature integration is significantly greater (4 to 10 times more) than the Khayat-Wilton transform. In the next example, we alleviate the observation point to a distance 1×10^{-5} meter above from the patch surface, i.e. $\vec{r}_m = (6.5 \times 10^{-4},\ 8.72 \times 10^{-5},$ $1 \times 10^{-5})$. As discussed in Chapter two, the Khayat-Wilton transform has a log-singularity in this case. Consequently, Linlog Quadrature rule is used to further accelerate the convergence rate of the solution. The number of function evaluations is significantly reduced when comparing to a conventional adaptive Quadrature integration. Furthermore, the Linlog rule maintains a rapid slope of convergence. This is illustrated in Fig 5.4. When the projected distance is gradually decreasing, the Linlog rule has a more rapid slope of convergence. This is further illustrated in Fig 5.5 and 5.6.
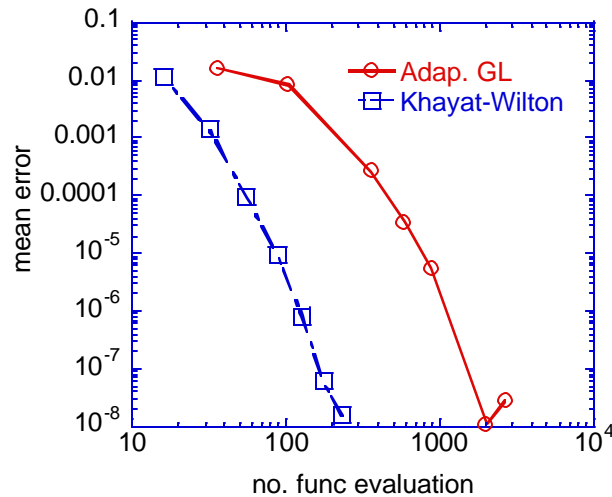
Fig. 5.3 Number of gauss points used for adaptive Duffy and Khayat-Wilton transform to integrate (5.1). Each square and circle represents the digit of tolerance set in sequence from 1×10^{-1} to 1×10^{-7}. The near singular point is placed at $(7 \times 10^{-4}, 8.72 \times 10^{-5}, 0)$.
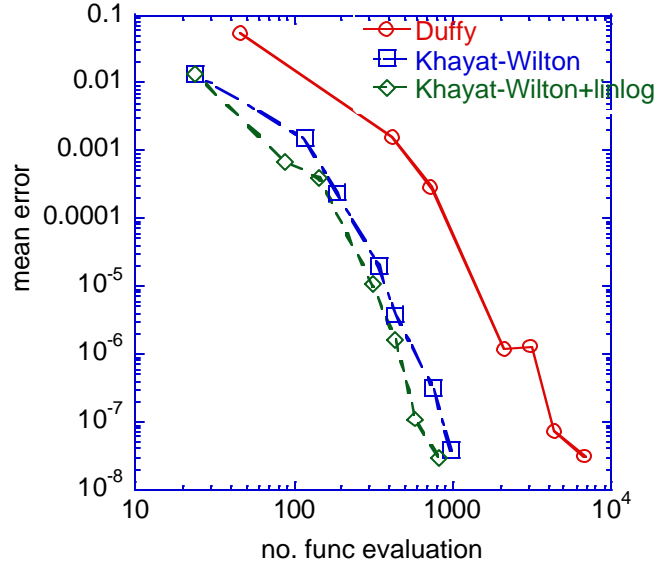
Fig. 5.4 Number of function evaluations for Duffy, Khayat-Wilton with and without using the Linlog integration rule to integrate (5.1). Quadrilateral patch is the same in Fig. 5.1, except the projected distance $projd = 1 \times 10^{-5}$. The singularity point is located at $(6.5 \times 10^{-4}, 8.72 \times 10^{-5}, 1 \times 10^{-5})$
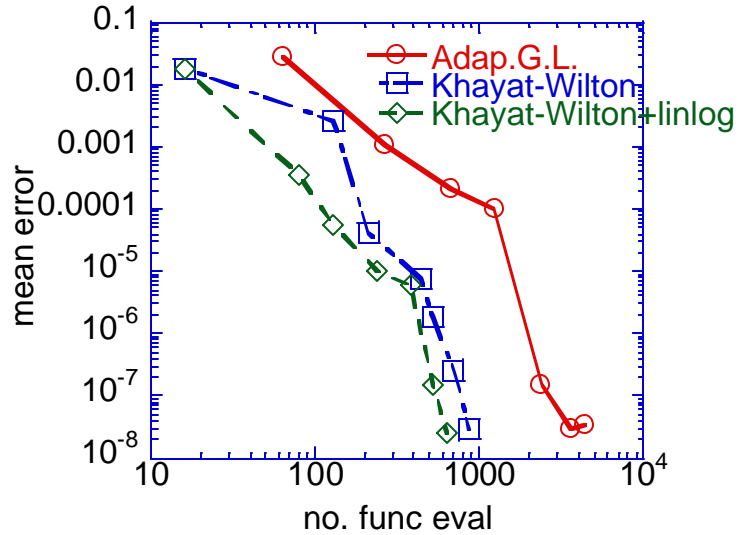
Fig. 5.5 Number of function evaluations for Duffy, Khayat-Wilton with and without using the Linlog integration rule to integrate (5.1). Quadrilateral patch is the same in Fig. 5.1, except the projected distance $projd = 1 \times 10^{-6}$. The singularity point is located at $(6.5 \times 10^{-4}, 8.72 \times 10^{-5}, 1 \times 10^{-5})$
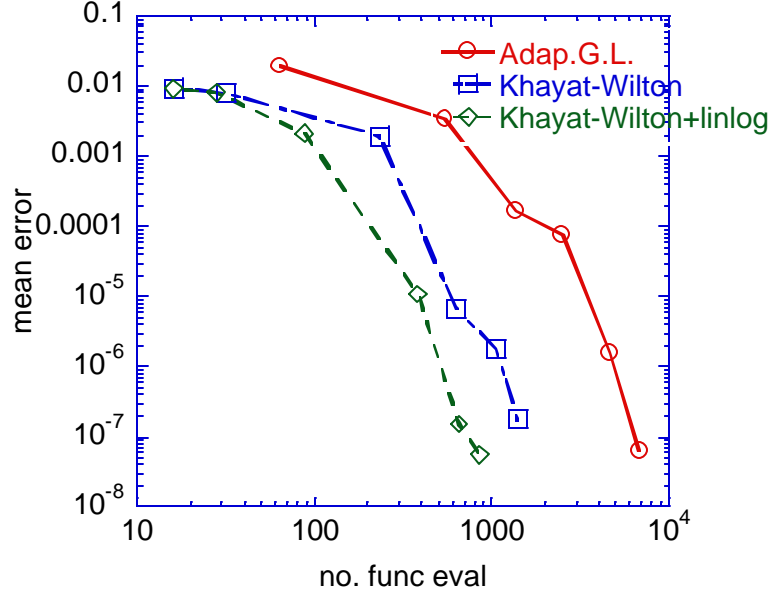
Fig. 5.6 Number of function evaluations for Duffy, Khayat-Wilton with and without using the Linlog integration rule to integrate (5.1). Quadrilateral patch is the same in Fig. 5.1, except the projected distance *projd* = 1×10^{-7}. The singularity point is located at $(6.5 \times 10^{-4}, 8.72 \times 10^{-5}, 1 \times 10^{-5})$

5.3 Planar microwave circuits

The DGF validated in the previous section were implemented within a computer program that performs a Method of Moment (MoM) solution for circuits and antennas printed in a multi-layered media. The MoM formulation is based on a Galerkin discretization of the MPIE as described in Section 2.1. The DGF were pre-computed via the Two-level DCIM method and were tabulated in a 1D table. The table is filled adaptively in order to maintain a desired level of accuracy. A fast interpolation scheme described in Section 4.3.1 is then used to approximate the DGF for the MoM reaction integrals. The Khayat-Wilton transformation is used to compute both singular and near singular integrations. The MoM code is validated first for circuits composed of only horizontal metallization. These results are presented in Section 5.3.1. Then more general circuits with multiple horizontal and vertical conductors in multilayered media are validated. These results are detailed in Section 5.3.2 —5.4.

5.3.1 Planar microwave circuits in single horizontal conducting layer

The first example we chose is a microstrip ring resonator printed on a Silicon substrate of dielectric constant 11.7 as illustrated in Fig 5.5 (a). The resonator is designed to yield resonant at 10GHz with radius equals to a quarter-wave length that is approximated as $3205\mu m$. The detail of designing the ring resonator is out of the scope of this dissertation. Reader can refer to papers [62-70]. The ring resonator is discretized with quadrilateral meshes as illustrated in Fig 5.5 (b). Subsequently, Fig 5.6 shows the magnitude and phase of the S-parameters of the resonator that computed via the DCIM. The results are compared with the computed results via the *IE3D* , and an excellent agreement between them is observed.

$z = 0.2mm$ $e_r = 1$

$e_r = 11.7$ $\tan d = 0$

$z = 0$

$s = 4.9 \times 10^7 S/m$
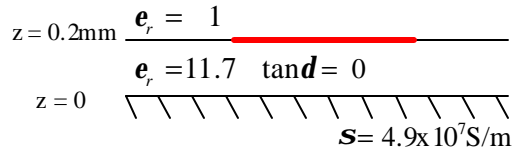
(a) The cross-sectional view of the microstrip ring resonator
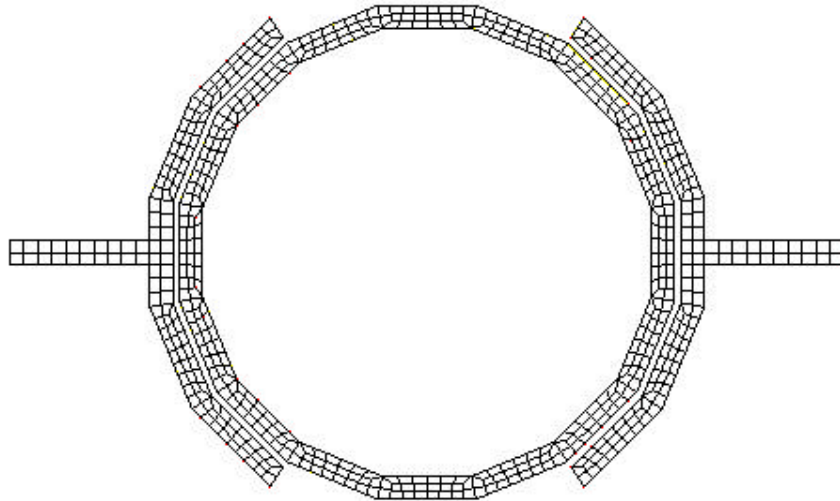
(b) The top-view of the microstrip ring resonator

Fig. 5.5 Geometry of the microstrip ring resonator. (a) The cross-sectional view of the microstrip ring resonator. (b) the top-view and the quadrilateral mesh of the resonator. The gap between the feedline and the resonator is 50μm, radius = 3205μm ≈ λ/4 at 10GHz.
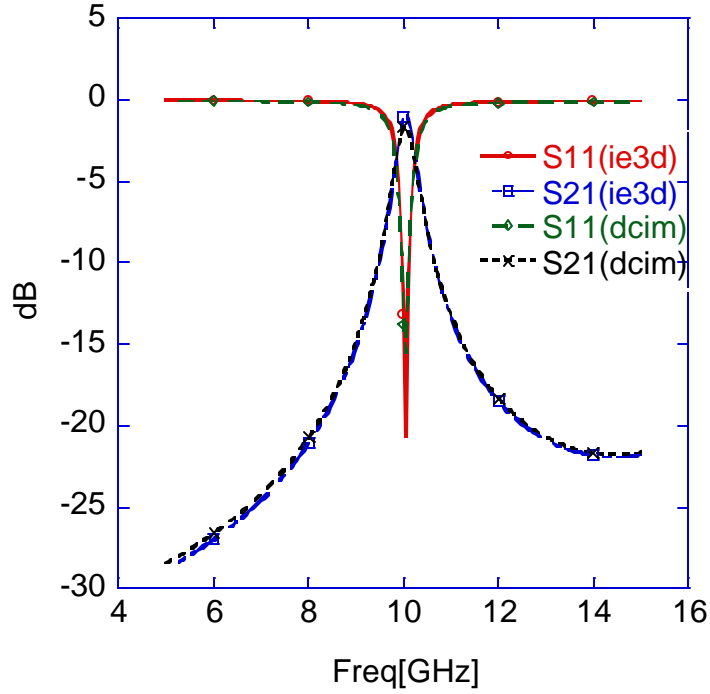
(a) Magnitude of S-parameters for a microstrip ring resonator
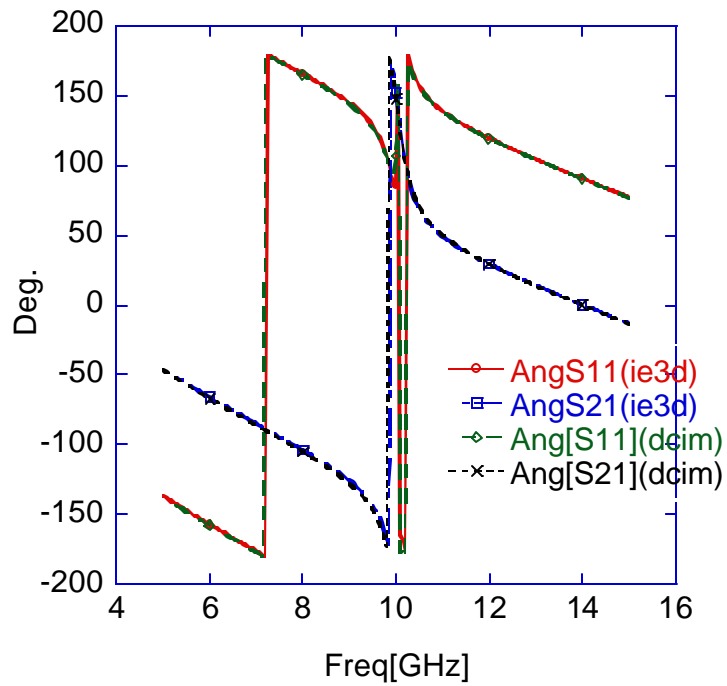
(b) Phase of the S-parameters for a microstrip ring resonator.

Fig. 5.6 The S-parameters of the microstrip ring resonator shown in Fig 5.5. (a) S-parameters versus frequency. (b) Angles for the S-parameters versus frequency. The computed results via DCIM are compared with Zeland's *IE3D*.

Next a 10GHz stripline ring resonator is modeled The layout of the stripline is illustrated in Fig 5.7 (a). The stripline is embedded in four layers and bounded by two planes. The dielectric constants and thickness of the layers are given in Fig 5.7 (a). The gap between the feed line and the resonator is 50 μm to exhibit a strong coupling effect Fig 5.7 (b) illustrates the quadrilateral mesh of the resonator. The S-parameters of the two-port network are computed with the DCIM. These results are compared with the results computed independently with *IE3D*. The magnitude and phase of the S-parameters are illustrated in Fig 5.8 (a) and (b), respectively. Both results agree very well.
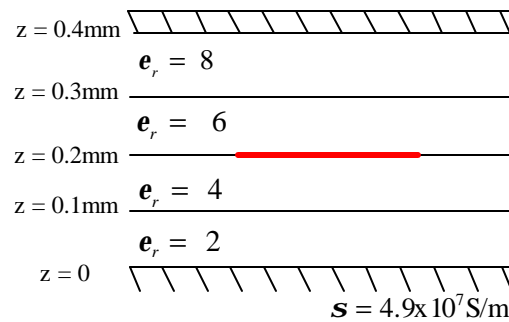
(a) Cross-sectional view of the stripline ring resonator.
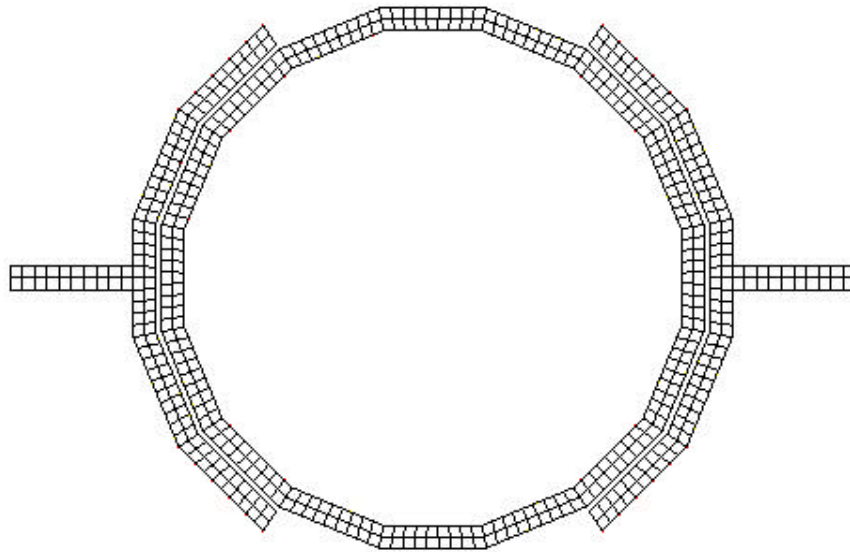
(b) Top-view of the stripline ring resonator.

Fig. 5.7 Geometry of the stripline ring resontor. (a) The cross-sectional view of the stripline ring resonator. (b) the top-view and the quadrilateral meshed of the resonator. The gap between the feed line and the resonator is 50μm, radius = 4035μm ≈ λ/4 at 10GHz. All dielectric layers have tan d of 0.
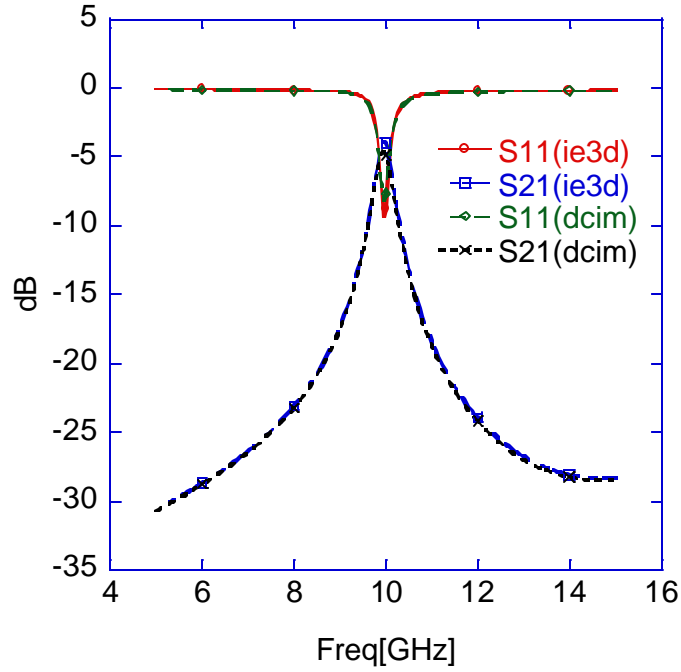
(a) S-parameters of t he stripline ring resonator.
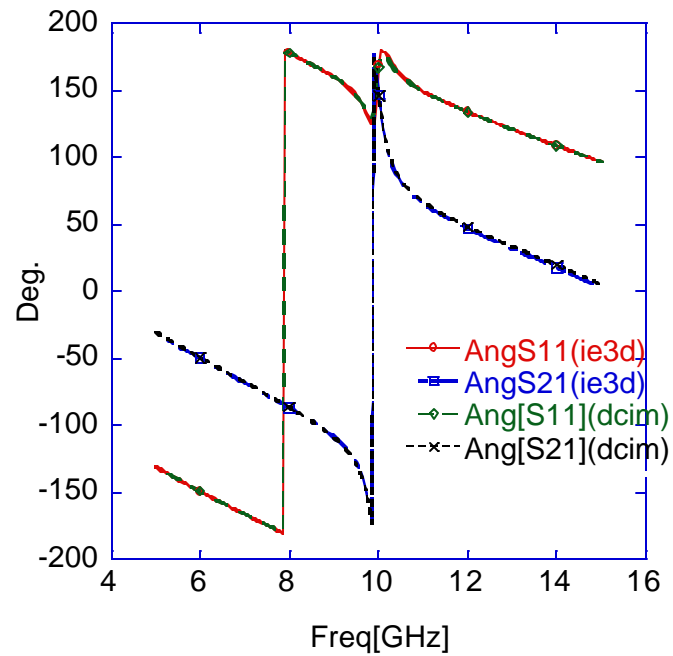
(b) Phase of the S-parameters of the stripline ring resonator.

Fig. 5.8 The S-parameters of the stripline ring resonator shown in Fig 5.7. (a) S-parameters versus frequency. (b) Phase for the S-parameters versus frequency. The computed results via DCIM are compared with Zeland's *IE3D*.

The surface current density on the stripline computed at the resonant frequency is illustrated as Fig 5.9. This is presented as a normalized current distribution in a dB scale. Interestingly, the smallest current is accumulated at the portion of the resonator that is parallel to the feed line, while the maximum current is present at the portion 90 degrees from the feed line.
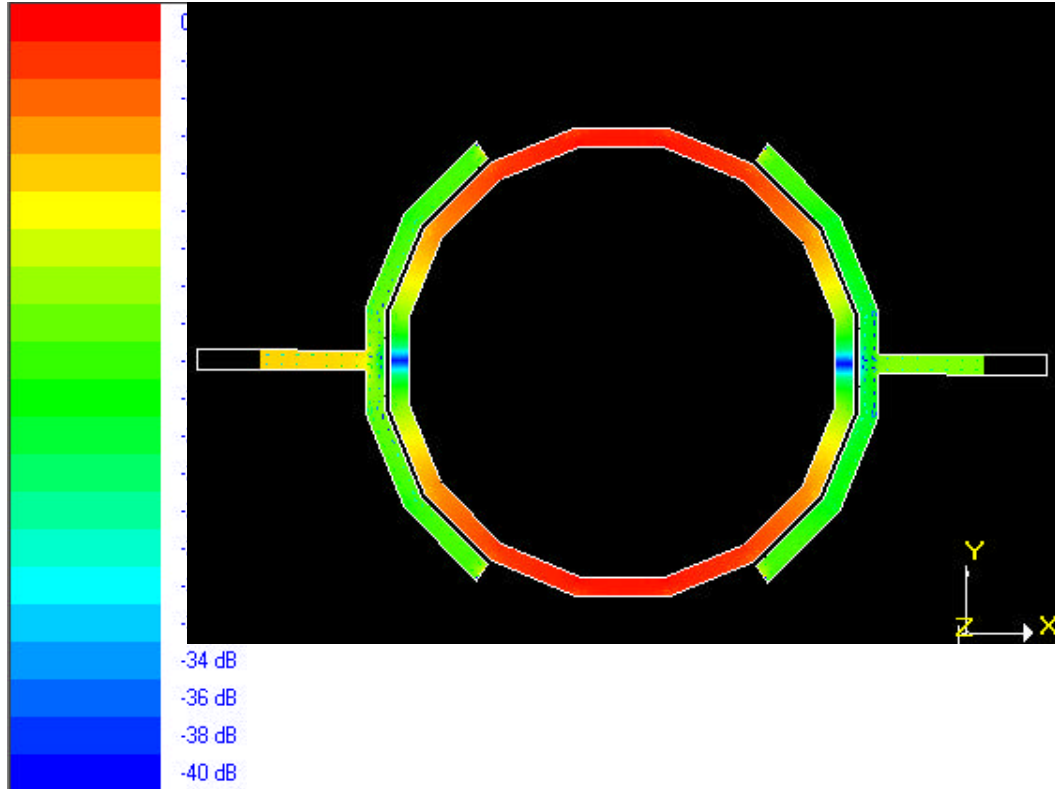
Fig. 5.9 The normalized current distribution of the stripline ring resonator showed in Fig 5.7. The magnitude of current is scaled in dB and the operational frequency is 10GHz.

Next, a six-pole hair-pin microstrip band pass filter printed on a RT/Duroid substrate with thickness of 0.81 mm and having a permittivity of $e_r = 3.31$ is analyzed. The cross-sectional view of the filter is illustrated in Fig 5.10 (a). The elliptic-type band pass filter has the feature that it has two steep gradients of attenuation poles outside the band of interests, which are due to the even and odd modes of the resonator. Figure 5.10 shows the top-view and layout of the six-pole band pass filter discretized with quadrilateral mesh. The magnitude and phase of the S-parameters computed with both the DCIM and *IE3D* are illustrated in Fig 5.11. The results agree extremely well. The filter has a reflection loss below -20dB within the

pass band, while the insertion loss within the pass band is about -1.2dB. The loss effect is mainly due to the conductor loss, dielectric loss, and surface-wave modes. The normalized current density distribution of the band pass filter computed at 2.18GHz is illustrated in Fig 5.12.
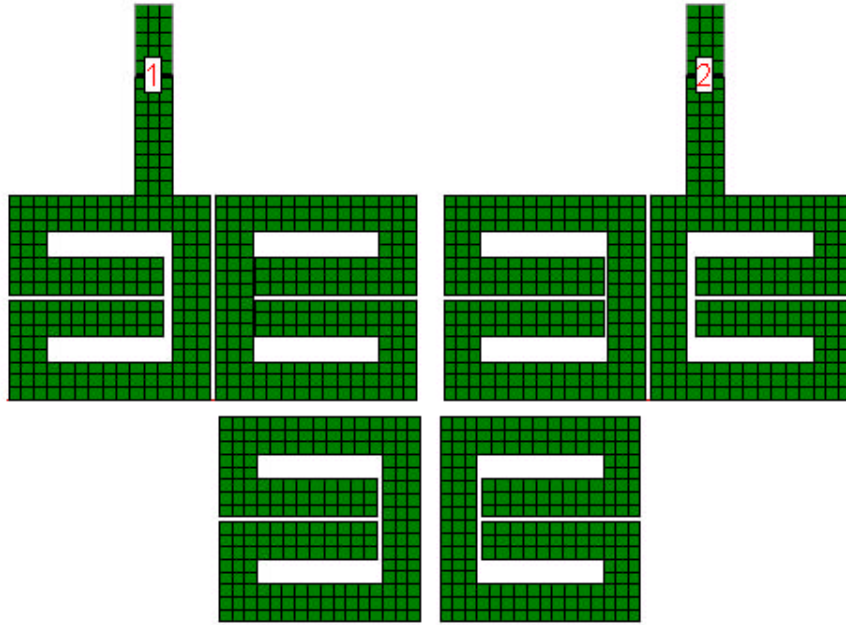
Fig. 5.10 The top-view of the six-pole band-pass filter. The filter is discretized with quadrilateral mesh.
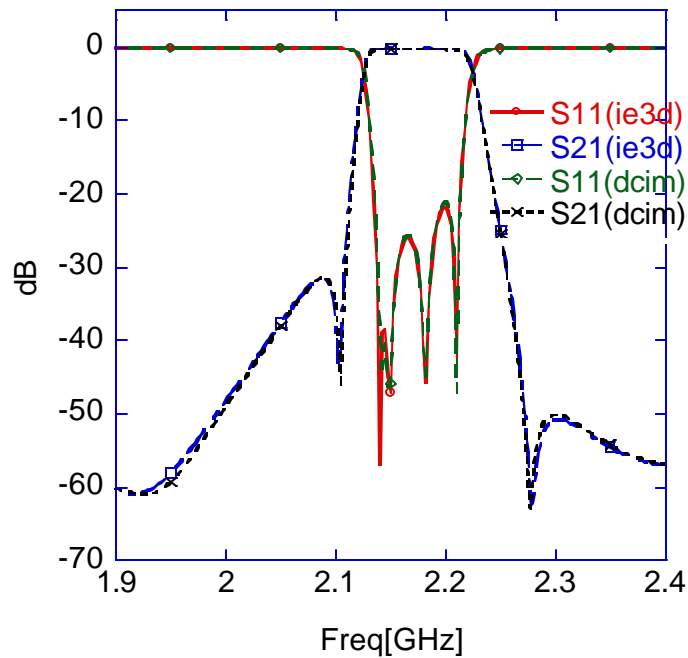
(a) Magnitude of S-parameters of stripline ring resonator
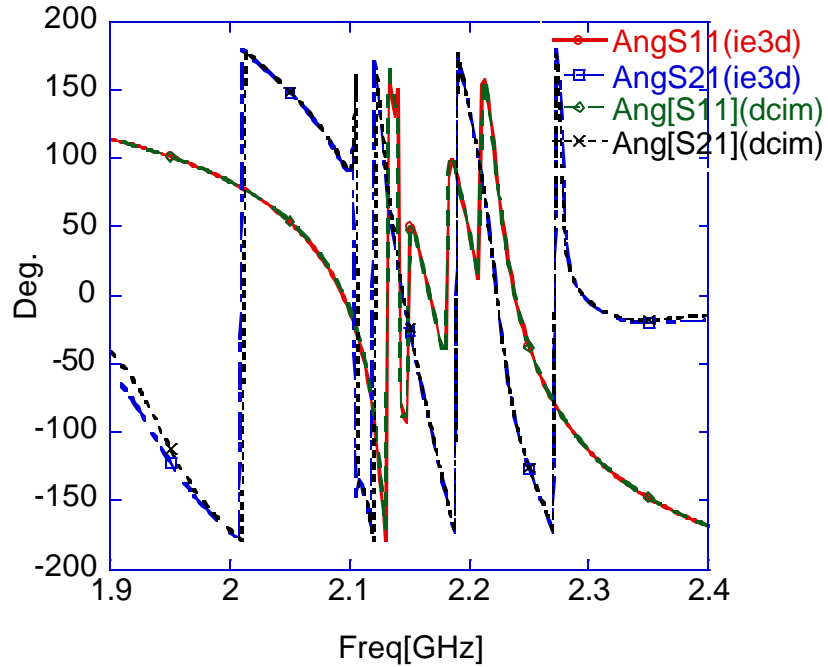
(b) Phase of S-parameters for stripline ring resonator

Fig. 5.11 The comparison of DCIM and Zeland's *IE3D* results of the six-pole band pass filter. (a).The S-parameters of the filter. (b) The Phase of the S-parameters.
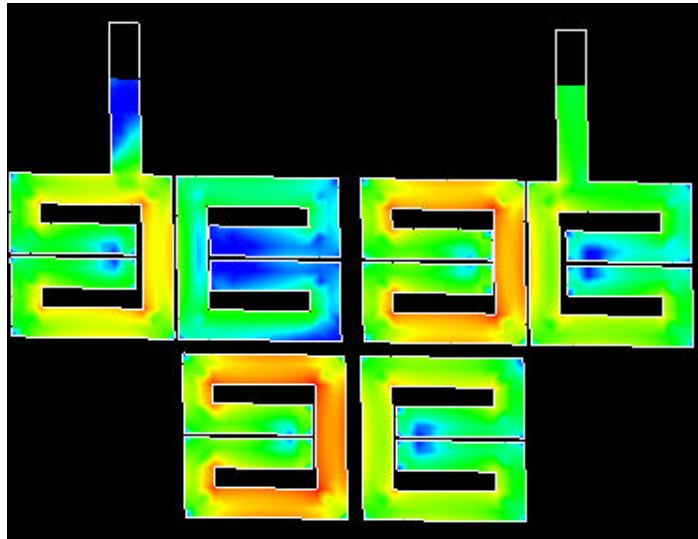
Fig. 5.12 The normalized current distribution of the six-pole band pass filter shown in Fig 5.10. The magnitude of current is scaled in dB and the operational frequency is 2.18GHz.

5.3.2 Planar microwave circuits in multiple horizontal conducting layers

For this section, a circuit with horizontal metallization at different layers is studied. The cross-sectional view of the layered media is illustrated in Fig 5.13 (a), except the relative permittivity for the lossless substrate ($\tan d = 0$) is $e_{r_1} = 2$, $e_{r_2} = 4$, $e_{r_3} = 6$ and $e_{r_4} = 8$. The cross-coupled resonators are located at multiple horizontal-layer interfaces at $z = 100$, 200, and 300 μm. The layout of the cross-coupled resonator in multiple horizontal layers media is showed in Fig 5.13 (b). The length and width of the resonators are 200 μm. The magnitude and phase of the S-parameters were computed and compared with *IE3D*. The results are illustrated in Fig 5.14, both results agree quite well. The normalized surface current density distribution of the cross-coupled filter at the resonant frequency (11.5 GHz) is illustrated in Fig 5.15. As a reference, the same MoM simulation is performed using a direct Sommerfeld evaluation of the Green's function. The results are identical to those computed via the DCIM.

(a) cross-sectional view

(b) 3D view
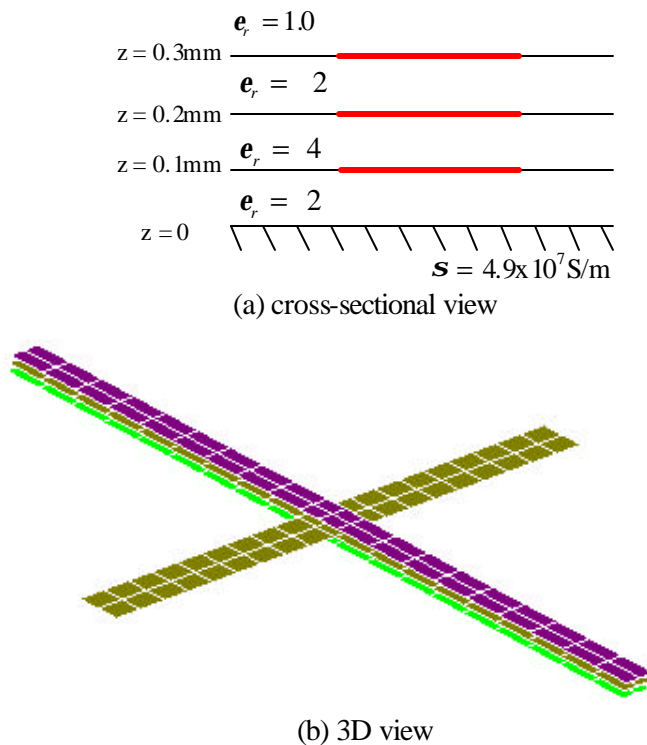
Fig. 5.13 The layout of the cross-coupled resonator in multiple horizontal layered media. The filter is discretized with quadrilateral mesh. Strip width = 540 μm, length = 9020 μm.
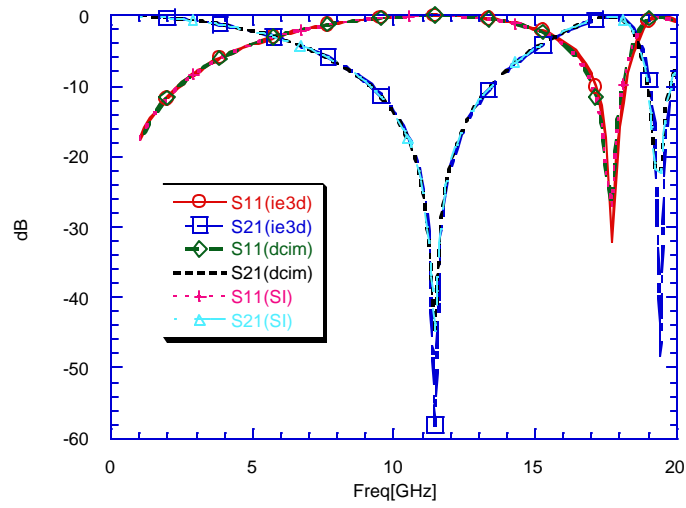
(a) Magnitude of S-parameters of the cross-couple resonator.
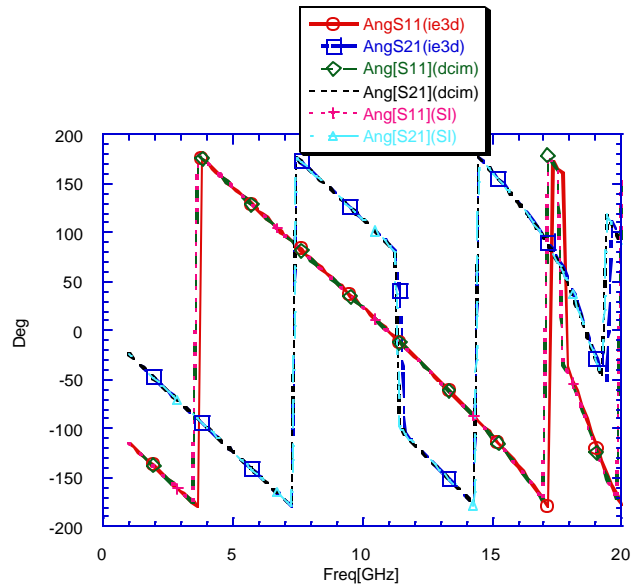
(b) Phase of the S-parameters of the cross-couple filter.

Fig. 5.14 The comparison of the DCIM, Sommerfeld integration and Zeland's *IE3D* results for the cross-coupled resonator. (a) The Magnitude of S-parameters for the resonator. (b) The Phase of the resonator.
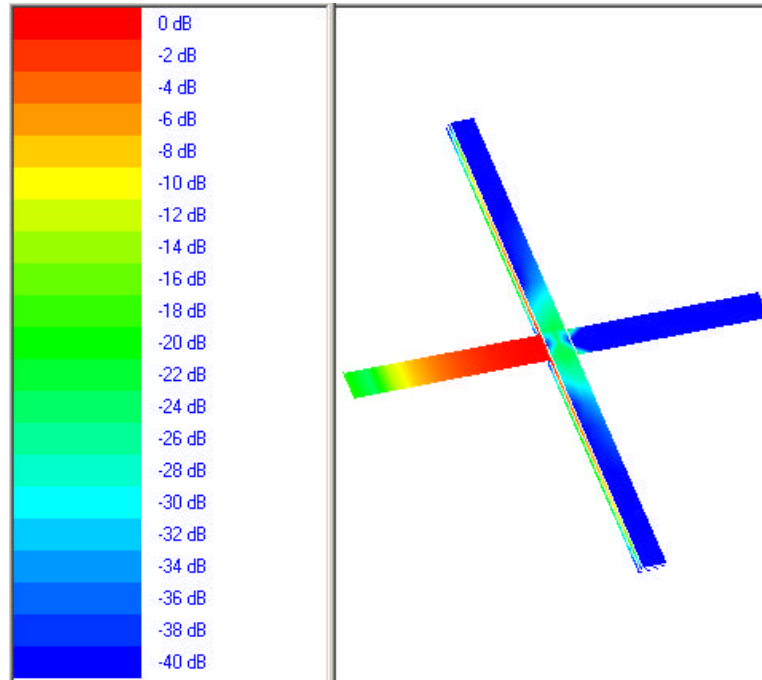
Fig. 5.15 The normalized current distribution of the cross-coupled resonator showed in Fig 5.13. The magnitude of current is scaled in dB and the operational frequency is 11.5GHz.

5.4 2.5D or 3D planar microwave circuits

In this section, examples of circuits with both vertical and horizontal conductors in multi-layered media are studied. A practical example of a 3D planar microwave circuit is the microstrip spiral inductor illustrated in Fig 5.16. The structure of the spiral inductor is a rectangular that consists of two air bridges across one of the feed lines. The height and span of the air bridges are 1.0 mm and 6.0 mm, respectively. The material substrate used for the inductor is RT/Duroid with permittivity of 9.6 and thickness of 2 mm. The S-parameters were computed using the DCIM and closed form Green's function for vertical basis reactions. These results are illustrated in Fig 5.17. The computed results agree quite well with *IE3D* even at resonant frequency. Moreover, the computed results are also agree very well with data published by Ling in [43]. The normalized current distribution of the spiral inductor at the resonant frequency (3.55 GHz) is illustrated in Fig 5.18.

$e_r = 1$

z = 0.2mm

$e_r = 9.6$ tan$d$=0.01

z = 0

$s = 4.9 \times 10^7$ S/m
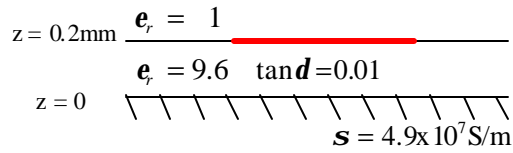
(a) cross-sectional view
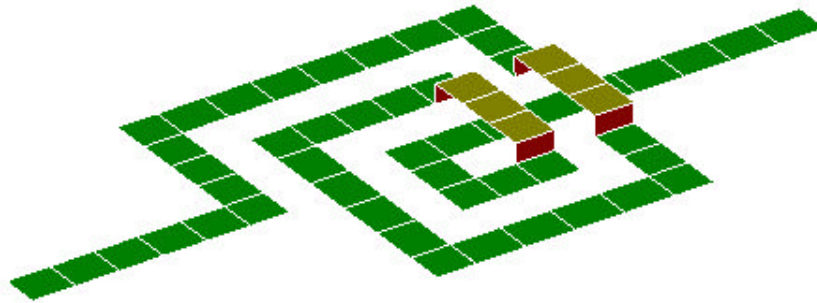
(b) 3D view

Fig. 5.16 The layout of microstrip spiral inductor. The inductor is discretized with a quadrilateral mesh. The substrate of the microstrip used is RT/Duroid with loss tangent of 0.01 ($e_r = 9.6$-j0.096), the thickness of the substrate is 2mm. The conductor width and the spacing between the conductors is 2mm, the height and span of the air bridges is 1mm and 6mm, respectively.
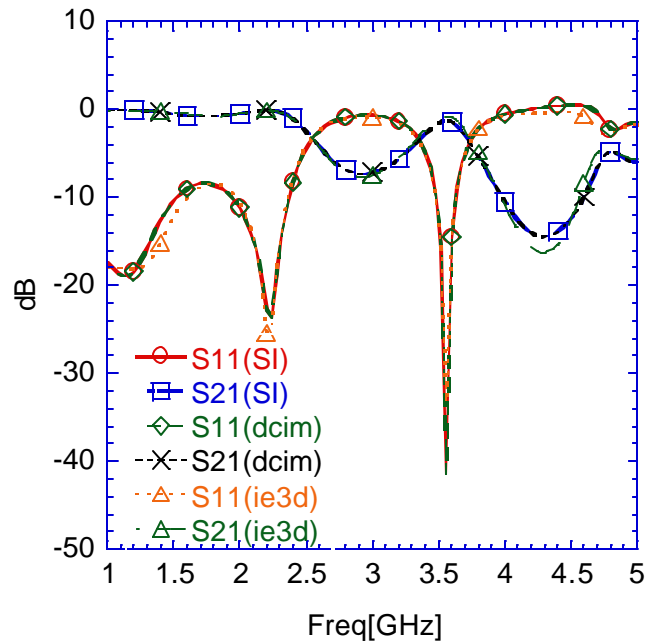
(a) Magnitude of S-parameters of the microstrip spiral inductor.
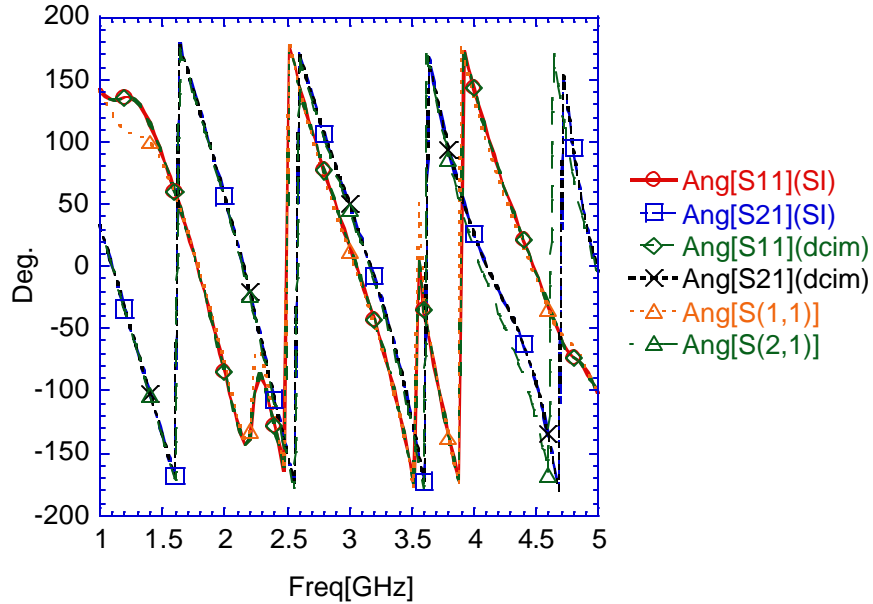
(b) Phase of the microstrip spiral inductor.

Fig. 5.17 The comparison of the DCIM, Sommerfeld integration and Zeland's *IE3D* results for the microstrip spiral inductor shown in Fig 5. 16. (a) The S-parameters of the inductor. (b) Phase of the inductor.
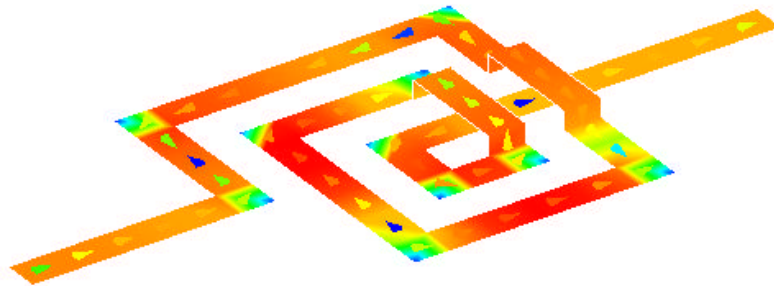
Fig. 5.18 The normalized current distribution of the microstrip spiral inductor shown in Fig 5.16. The magnitude of current is scaled in dB and the operational frequency is 3.55GHz.

Next, we conduct two examples of 3D planar microwave circuits that require junction bases. The first example is a microstrip rectangular spiral that has the RT/Duroid substrate with loss tangent of 0.01 (e_r = 9.6-j0.096) as illustrated in Fig. 5.19. Observe from the figure that the air bridge connects the end of spiral and the feed line, hence there are two junctions located at the pad bases of the microstrip. The S-parameters were computed using the DCIM and a direct Sommerfeld using the closed form Green's function with vertical basis reactions. These results are illustrated in

Fig 5.20. The computed results agree quite well with *IE3D* even at the resonant frequency. The normalized current density distribution of the microstrip spiral at the resonant frequency (11.5 GHz) is illustrated in Fig 5.21.

$z = 0.2$mm $e_r = 1$

$e_r = 9.6$ $\tan d = 0.01$

$z = 0$

$s = 4.9 \times 10^7$ S/m

(a) cross-sectional view
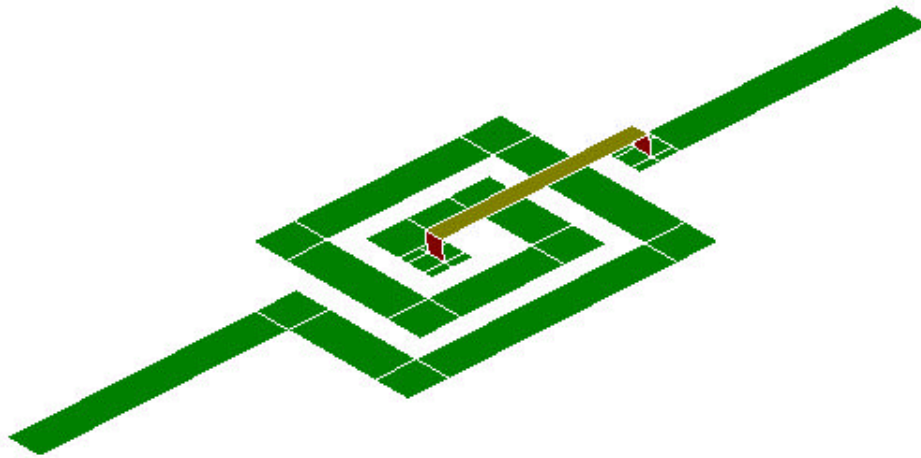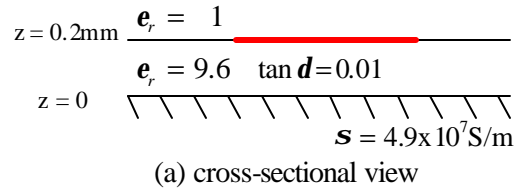
(b) 3D view

Fig. 5.19 The layout of microstrip spiral inductor with two junctions. The inductor is discretized with quadrilateral mesh. The substrate of the microstrip used is RT/Duroid with loss tangent of 0.01 ($e_r = 9.6$-j0.096), the thickness of the substrate is 0.2mm. The conductor width and the spacing between the conductors is 0.2mm, the height and span of the air bridges is 0.1mm and 1.1mm, respectively. (a) cross-sectional view (b) 3D view of the layout.
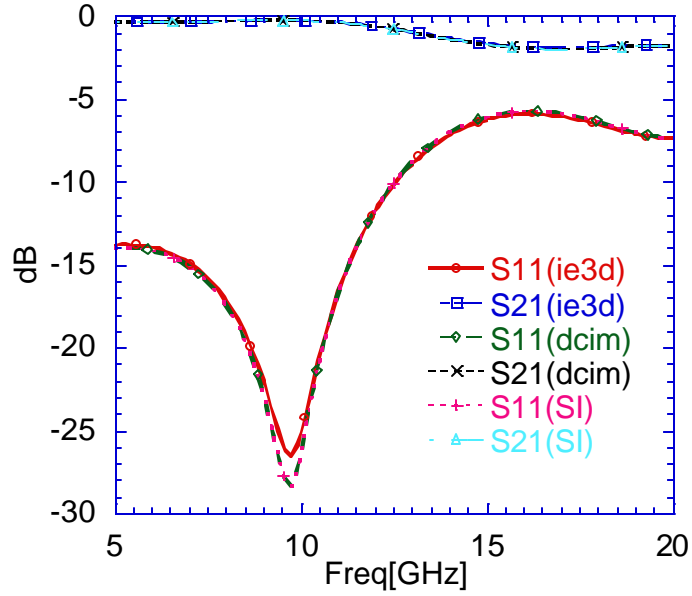
(a) Magnitude of S-parameters of the microstrip spiral inductor.
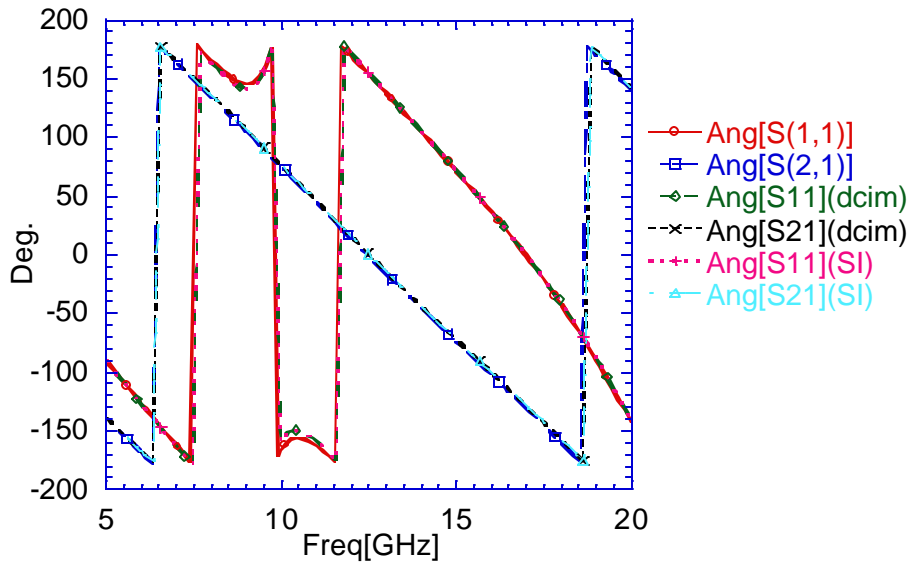
(b) Phase of the microstrip spiral inductor.

Fig. 5.20 The comparison of the DCIM, Sommerfeld integration and Zeland's *IE3D* results for the microstrip spiral inductor shown in Fig 5.19. (a) The S-parameters of the inductor. (b) Phase of the inductor.
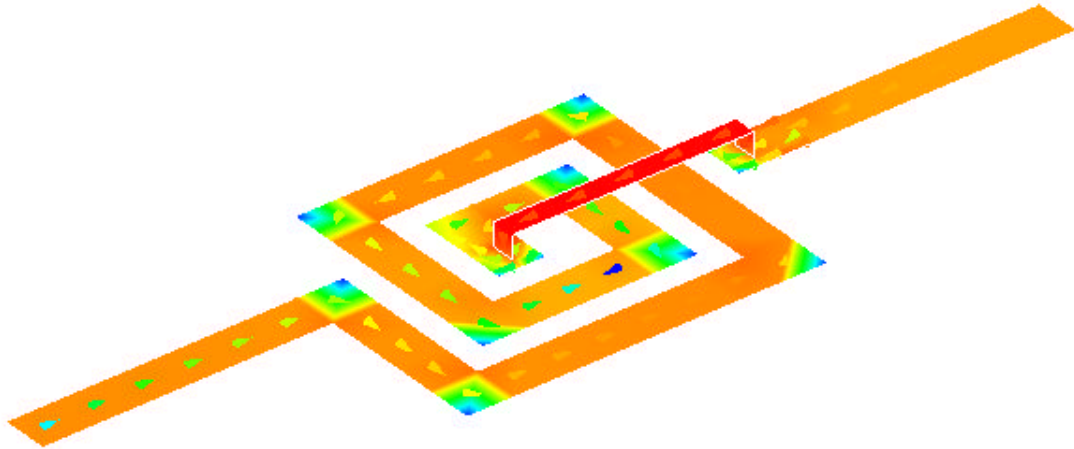
Fig. 5.21 The normalized current distribution of the microstrip spiral inductor shown in Fig 5.19. The magnitude of current is scaled in dB and the operational frequency is 3.55GHz.

We compare the CPU time of the fill and the matrix solved times for the impedance matrix via the DCIM and *IE3D* with the examples shown above. The data is summarized in Table 5.1. Integration techniques based on the Duffy and the Khayat-Wilton transform are compared, while the layered media Green's function is approximated using DCIM. All the simulations were performed using the HP superdome (SDX) cluster at the University of Kentucky. This cluster has 248 3.4GHz Intel Xeon em64t processors @ 2GB per processor. Only simulations performed on a single processor are reported here.

	# cells/unks	DGF. (s)	fill/solve per freq. (s)	total/freq(s)
Ie3d	692/1066	na	na	11
Duffy& Adap Q.L.+SI	644/1066	1.71	20.42/0.78	22.91
Duffy& Adap Q.L.+DCIM	644/1066	0.04	19.77/0.79	20.60
Khayat-Wilton +DCIM	644/1066	0.04	13.66/0.78	14.48

(a) microstrip ring resonator in Fig 5.5

	# cells/unks	DGF. (s)	fill/solve per freq. (s)	total/freq(s)
Ie3d	588/852	na	na	8
Duffy& Adap Q.L.+SI	548/822	2.2	21.22/0.30	23.72
Duffy& Adap Q.L.+DCIM	548/822	0.04	21.28/0.30	21.62
Khayat-Wilton +DCIM	548/822	0.04	11.44/0.31	11.79

(b) stripline ring resonator in Fig 5.7

	# cells/unks	DGF. (s)	fill/solve per freq. (s)	total/freq(s)
Ie3d	1320/2188	na	na	96
Duffy& Adap Q.L.+SI	1320/2188	2.65	56.18/5.96	64.79
Duffy& Adap Q.L.+DCIM	1320/2188	0.05	49.14/5.96	55.15
Khayat-Wilton +DCIM	1320/2188	0.05	34.59/6.28	40.92

(c) Six-pole bandpass filter in Fig 5.10

Table 5.1 The comparison of the CPU time for DCIM, Sommerfeld integration and Zeland's *IE3D* results for the microstrip ring resonator, stripline ring resonator, and six-pole band pass filter.

	# cells/unks	DGF. (s)	fill/solve per freq. (s)	total/freq (s)
SI	284/424	9.53	20.49/0.04	30.06
DCIM	284/424	0.77	20.92/0.05	21.74

Multiple-horizontal cross-coupled in Fig 5.13

	# cells/unks	DGF. (s)	fill/solve per freq. (s)	total/freq (s)
SI	71/72	6.9	4.13/0.0	11.03
DCIM	71/72	1.06	4.13/0.0	5.19

Microstrip air-bridge spiral inductor in Fig 5.16

	# cells/unks	DGF. (s)	fill/solve per freq. (s)	total/freq (s)
SI	82/95	8.5	4.52/0.01	13.03
DCIM	82/95	1.07	4.49/0.01	5.57

Microstrip air-bridge spiral inductor with junction in Fig 5.19

Table 5.2 The comparison of the CPU time for DCIM and Sommerfeld integration with analytically closed-form of z-integration in *spectral* domain on the vertical patch for the multiple horizontal cross-coupled, microstrip air-bridge spiral inductor with and without junction.

Observe from Table 5.1 and Table 5.2 that the pre-computation and tabulation time of Green's functions using the DCIM was an order of magnitude faster than a direct Sommerfeld integration. Meanwhile, the time to fill the impedance matrix using the integration scheme based on the Khayat-Wilton transform was about twice as fast as the integration based on the Duffy and adaptive Gauss Legendre.

Finally, we model the inductor with a solid air bridge that has a thickness of t = 0.1 mm. The layout of the circuit is illustrated in Fig 5.20 (a). The magnitude and phase of the S-parameters computed via the DCIM are illustrated in Fig 5.20 (b) and (c), respectively. From these figures, a good agreement is observed comparing with *IE3D*.
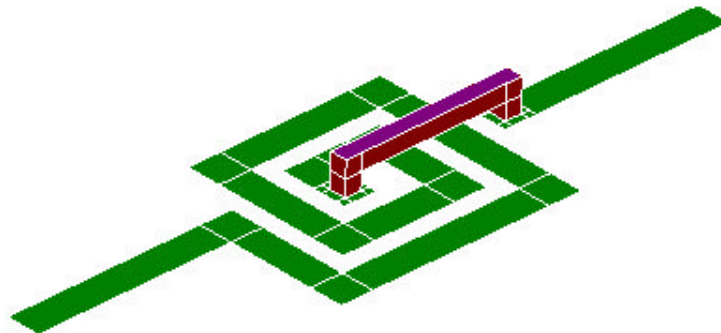
(a) 3D view
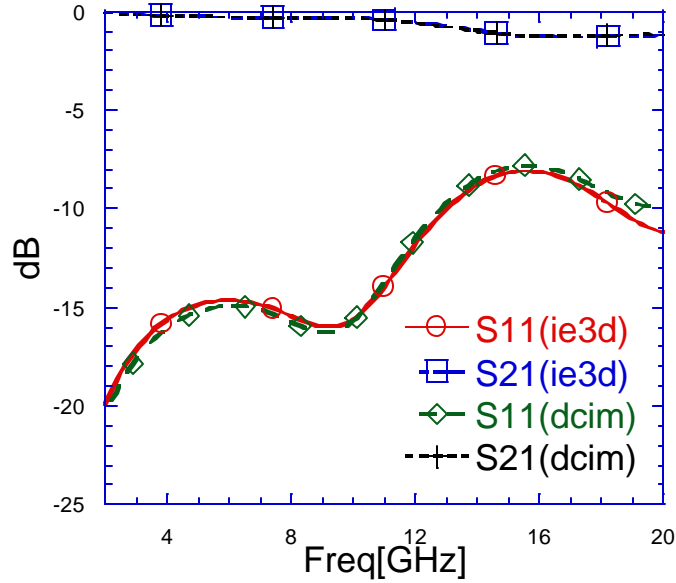
(b) Magnitude of S-parameters.
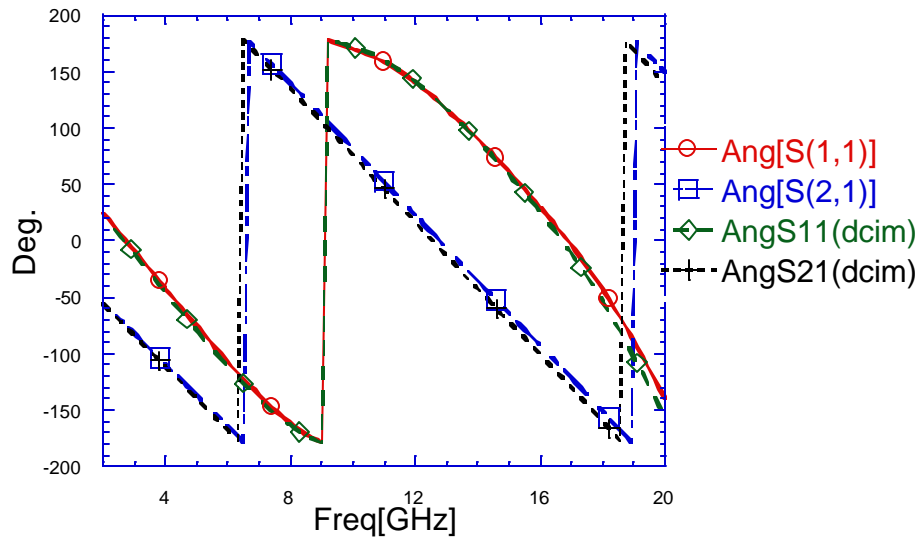
(c) Phase of S-parameters.

Fig. 5.20 The layout of microstrip spiral inductor with thickness $t = 0.1$mm. The inductor is discretized with quadrilateral mesh. The substrate of the microstrip used is RT/Duroid with loss tangent of 0.01 ($e_r = 9.6$-j0.096), the thickness of the substrate is 0.2mm. The conductor width and the spacing between the conductors is 0.2mm, the height and span of the air bridges is 0.1mm and 1.1mm, respectively. (a) The 3D layout view (b) Magnitude of S-parameters (c) Phase of S-parameters.

Chapter Six: Fast Solution Technique

6.1 Introduction

In this chapter, a fast method of moment solution for the network parameter extraction of passive circuit structures printed in a layered medium is presented. The method of moments procedure is founded on a Galerkin based solution of MPIE in Section 2.1 that employs a GWP zero[th]-order divergence conforming basis functions. To accelerate the computation, a fast solution procedure based on the Quadrature Sampled Pre-Corrected FFT (QSPCFFT) method is presented [71]. The QSPCFFT is in the same class of techniques as the adaptive integral method (AIM) [72], the pre-corrected FFT [50, 73, 74], the sparse matrix/canonical grid algorithm [75] and the Fast Multipole Method (FMM) [76-79]. Near interactions are computed using the traditional integral equation formulation and stored in a compressed format. Far interactions are not directly computed or stored. Rather, when performing a matrix-vector multiplication, the contribution from far interactions is accelerated via the FFT. What distinguishes the QSPCFFT method from previous techniques, is that it does not explicitly require the computation of moments or an expansion of the Green's function. Rather, the FFT of the surface current density is computed directly using the discontinuous FFT of Fan and Liu [80]. It is shown herein that the QSPCFFT method is highly accurate and efficient. The solution scales with a computational complexity of $O(N \log N)$ and memory as $O(N)$. It is worth it to mention that the DCIM is also suitable to be applied to the FMM. However, a separation of multipole expansion must be done for each complex exponential, DGF term or coefficient, and each $z - z'$ pair.

6.2 Quadrature -Sampled FFT (QSFFT)

The discretization of the MPIE in (2.6) leads to a linear system of equations,

$$Z\mathbf{j} = \mathbf{v} \tag{6.1}$$

where $\mathbf{j}$ is the unknown current density vector.

The linear system in (6.1) will be solved using an iterative solution technique. This requires a series of matrix vector products with the impedance matrix Z. To accelerate these products, the impedance matrix is broken up into its *near* and *far*-field contributions as:

$$Z^{near}\mathbf{j} + Z^{far}\mathbf{j} = \mathbf{v} \ . \tag{6.2}$$

Z^{near} is a sparse matrix representing the *near* interactions and is stored in a compressed format. The entries of Z^{near} are computed to a specified accuracy using adaptive numerical Quadrature. Z^{far} represents *far* interactions. More explicitly, these are entries of Z that can be computed to a specified accuracy using a fixed N_q-point quadrature rule for both the inner and outer integrals of (6.1). Z^{far} is not actually stored. Rather a fast matrix-vector product that computes $Z^{far}\mathbf{a}$ is applied using FFT techniques.

Taking advantage of the translational invariance of the Green function along a horizontal plane, the matrix-vector product $Z^{far}\mathbf{j}$ is accelerated via the FFT. This far interaction represents the convolution of a source current and the Green's function assuming that the observation point is sufficiently far removed from the source. When computing multiple source interactions with multiple fields points, the convolution can be accelerated via the operation $F^{-1}\left\{F\left\{\bar{\bar{G}}\right\} \cdot F\left\{\mathbf{J}\right\}\right\}$, where F denotes the fast Fourier transform (FFT). The standard FFT requires that the data be sampled at the vertices of a uniformly spaced grid. However, the current density is supported by GWP basis functions on an arbitrary mesh discretization. It is shown here that the Fast Fourier transform of the current can be performed using the discontinuous FFT of Fan and Liu [80]. At this point, assume that the current density to be Fourier transformed is situated in a horizontal x,y-plane (that is parallel to the layered media interface). The surfaces describing the printed circuit in this plane are discretized into N_c curvilinear triangle or quadrilateral cells. An N_q-point quadrature rule is then enforced over each cell so that the Fourier transform of the current is approximated as:

$$\tilde{\mathbf{J}}(\tilde{\mathbf{k}}) = \iiint\limits_{S} \mathbf{J}\left(\mathbf{r}\right) e^{j2p\tilde{\mathbf{k}}_t \cdot \mathbf{r}} ds \approx \sum_{l=1}^{N_c} \sum_{q_l=1}^{N_q} \sqrt{g_{q_l}} w_{q_l} \mathbf{J}_{q_l} e^{j2p\tilde{\mathbf{k}}_t \cdot \mathbf{r}_{q_l}} \ , \tag{6.3}$$

where $\tilde{\mathbf{k}}_t = \left(\tilde{k}_x, \tilde{k}_y \right)$ is the transverse wave-vector, $\mathbf{J}_{q_l} \left(= \mathbf{J}(\mathbf{r}_{q_l}) \right)$ represents the current density sampled at the quadrature abscissa point $\mathbf{r}_{q_l}$ on the l-th patch, $\mathbf{w}_{q_l}$ is the quadrature weight, and $\sqrt{g_{q_l}}$ is the Jacobian evaluated at $\mathbf{r}_{q_l}$.

The exponential function in (6.3) is a smooth function over all space. Thus, it can be interpolated from the uniform grid indices to the quadrature points as [80]:

$$e^{j2\boldsymbol{p}\tilde{\mathbf{k}}_t \cdot \mathbf{r}_{q_l}} = \sum_{n_x=0}^{N_x} \sum_{n_y=0}^{N_y} \Phi_{n_x,n_y} \left(\mathbf{r}_{q_l} \right) e^{j2\boldsymbol{p}\tilde{\mathbf{k}} \cdot \mathbf{r}_{n_x n_y}} \;, \tag{6.4}$$

where $\Phi_{n_x,n_y}(\mathbf{r}_{q_l})$ are smooth interpolation polynomials with finite support. For simplicity in notation, the summation in (6.4) is taken over the entire uniform grid. However, the interpolation polynomials $\Phi_{n_x,n_y}(\mathbf{r}_{q_l})$ are non-zero only in a region local to $\mathbf{r}_{q_l}$. Combining (6.4) with (6.3), leads to

$$\tilde{\mathbf{J}}(\tilde{\mathbf{k}}_t) \approx \sum_{l=1}^{N_c} \sum_{q_l=1}^{N_{q_l}} \sqrt{g_{q_l}} \, \boldsymbol{w}_{q_l} \mathbf{J}_{q_l} \sum_{n_x=0}^{N_x} \sum_{n_y=0}^{N_y} \Phi_{n_x,n_y} \left(\mathbf{r}_{q_l} \right) e^{j2\boldsymbol{p}\tilde{\mathbf{k}} \cdot \mathbf{r}_{n_x n_y}} \;. \tag{6.5}$$

The order of summation is then rearranged [80], leading to:

$$\tilde{\mathbf{J}}(\tilde{\mathbf{k}}) \approx \sum_{n_x=0}^{N_x} \sum_{n_y=0}^{N_y} e^{j2\boldsymbol{p}\tilde{\mathbf{k}} \cdot \mathbf{r}_{n_x,n_y}} \left(\sum_{l=1}^{N_c} \sum_{q_l=1}^{N_q} \Phi_{n_x,n_y} \left(\mathbf{r}_{q_l} \right) \mathbf{J}_q \sqrt{g_{q_l}} \, \boldsymbol{w}_{q_l} \right). \tag{6.6}$$

This can be expressed as:

$$\tilde{\mathbf{J}}(\tilde{\mathbf{k}}) \approx \sum_{n_x=0}^{N_x} \sum_{n_y=0}^{N_y} e^{j2\boldsymbol{p}\tilde{\mathbf{k}} \cdot \mathbf{r}_{n_x n_y}} \tilde{j}_{n_x,n_y} \;, \tag{6.7}$$

where $\tilde{j}_{n_x,n_y}$ represents the interior double summation of the expression in (6.6). Letting $\tilde{j}_{n_x,n_y}$ be a single entry of the column vector $\tilde{\mathbf{j}}$, then $\tilde{\mathbf{j}}$ can be expressed in operator form as:

$$\tilde{\mathbf{j}} = WL \, \mathbf{j} \;. \tag{6.8}$$

where $\mathbf{j}$ is the vector of unknown coefficients, $L \, \mathbf{j}$ represents the total current sampled at the quadrature points and weighted by $\sqrt{g_{q_l}} \, \boldsymbol{w}_{q_l}$, and W is a sparse matrix,

78

where the $l \times q_l$-th entry of the $n_x \times n_y$-th row is $\Phi_{n_x, n_y}(\mathbf{r}_{q_l})$. It is noted that W is sparse since only local interpolation functions are used.

Next, from (6.7) it is seen that $\tilde{\mathbf{J}}(\tilde{\mathbf{k}})$ is efficiently evaluated for discrete values of $\tilde{\mathbf{k}}$ via the FFT as:

$$\tilde{\mathbf{J}}(\tilde{\mathbf{k}}) = F\{WL\,\mathbf{j}\}. \tag{6.9}$$

The convolution of the Green's function with the current is then approximated as:

$$F^{-1}\left\{F\left\{\bar{\bar{G}}\right\} \cdot F\{WL\,\mathbf{j}\}\right\} = H\{WL\,\mathbf{j}\}, \tag{6.10}$$

where $\bar{\bar{G}}$ is the dyadic Green function in (2.7) evaluated at the uniform FFT grid points, but set to zero at the origin avoiding the near-field singularity. Thus, it is referred to as the *windowed* dyadic Green's function.

The convolutional expression in (6.10) computes the field at the *uniform grid points*. However, what remains is the compute the inner product of the test vector $\mathbf{T}$ with the electric field. To perform this operation, fields are interpolated from the uniform grid to the quadrature points. Then, the inner product of the test vector is performed by weighting the interpolated fields by the quadrature weights and the Jacobian and then summing up this quantity over the quadrature points. The final expression can then be expressed in operator form as:

$$Z^{far}\mathbf{j} = L^T W^T H\{WL\,\mathbf{j}\} \tag{6.11}$$

where the operator W^T interpolates the fields to the quadrature points, and the product with L^T then performs the inner product with the test vector – effectively using an N_{q_l}-point quadrature rule for the l-th patch.

Since the FFT is a global operation, the operation on the right-hand-side of (6.11) has overlapping support in the near field region. Consequently, the product $Z^{near}\mathbf{j}$ must be corrected. This is done *a priori* and is thus referred to as a *pre-correction* of the sparse near field matrix Z^{near}. This is expressed as [73]:

$$\tilde{Z}^{near} = Z^{near} - U\left[L^T W^T H\{WL\,\mathbf{j}\}\right], \tag{6.12}$$

where U restricts the results to the support of the non-zero entries of Z^{near}. The pre-corrections can be performed very efficiently by effectively using a discrete impulse response. Let

$$\mathbf{j}_k = \begin{cases} 1, & k = j \\ 0, & k \neq j \end{cases} \tag{6.13}$$

Then, the pre-correction can be computed as:

$$\tilde{Z}_{i,j}^{near} = Z_{i,j}^{near} - U_i \left[L^T W^T \cdot \bar{\bar{G}}_{w_{i,j}} \otimes WL \, \mathbf{j}_j \right], \tag{6.14}$$

where $\bar{\bar{G}}_{w_{i,j}}$ is sampled at the uniform grid points, and $\otimes$ implies a discrete convolution. It is noted that the products with WL and $L^T W^T$ can be done locally and do not require the global sparse matrices. Furthermore, the support of $\bar{\bar{G}}_{w_{i,j}}$ used for the discrete convolution is determined by the support of the test function and the basis function relative to the uniform grid.

If the circuit lies entirely within a single plane of the layered medium, then only a single FFT will need to be done. However, if there is vertical metallization and multiple horizontal metal layers, then multiple FFT's will need to be performed. The reason for this is that the dyadic Green's function is translationally invariant along the horizontal direction, but not the vertical direction. However, it can be set up so that only one FFT per layer (of the layered medium) needs be performed.

6.3 Validation

To validate the QSPCFFT algorithm, consider a microstrip patch array antenna, as illustrated in Fig. 6.1. The antennas are printed on a 31 mil substrate with $e_r = 4.4$. The scattering parameters of the 2 element array are also illustrated in Fig. 6.1 and are compared to those computed via Zeland *IE3D*™. The array of the antenna was increased from 2 to 16. The solution was obtained via the QSPCFFT algorithm with a BiCGSTAB(l) iterative solver [81] with l = 4. The CPU times required to compute the near field matrix and its pre-corrections are graphed in Fig. 6.2 as a function of N. Also, the CPU time per iteration is also presented. The memory required by the QSPCFFT algorithm is presented in Fig. 6.2 as well and is compared to that required

by a full-direct solve (assuming complex double precision for both approaches). Observing these results, it is seen that the fill time scales close to $O(N)$, the cost per iteration scales close to $O(N\log N)$, and the memory as $O(N)$, as expected by the algorithm.

A final example is a spiral inductor array loaded microstrip line, illustrated in Fig. 6.3 (a). The line is printed on a 10 µm InP substrate. Each inductor has a radius of 200 µm. The spacing between inductor load pairs is also 200 µm. The scattering parameters were extracted via the QSPCFFT accelerated method of moment solution over the frequency range of 0.1 – 100 GHz. These results are illustrated in Fig. 6.3 (c). These results are also compared to those computed via Zeland *IE3D*. Excellent agreement is observed. Results obtained via the QSPCFFT solution are compared to those obtained via a direct solver in Fig. 6.3 (d). These results compare to better than 2 digits.
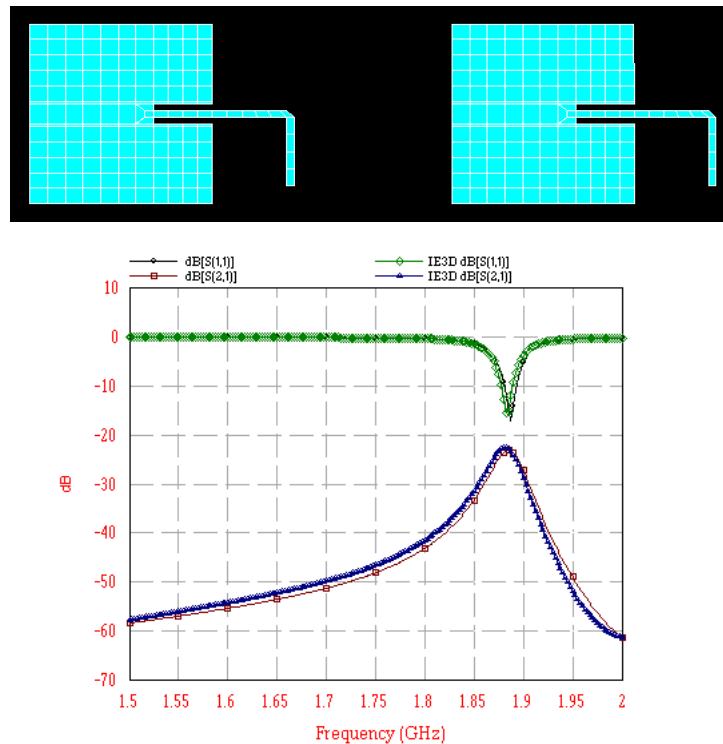
Fig. 6.1 2-element microstrip patch antenna array filter printed on a 31 mil substrate ($e_r = 4.4$) and the scattering parameters computed by QSPCFFT and Zeland *IE3D*.
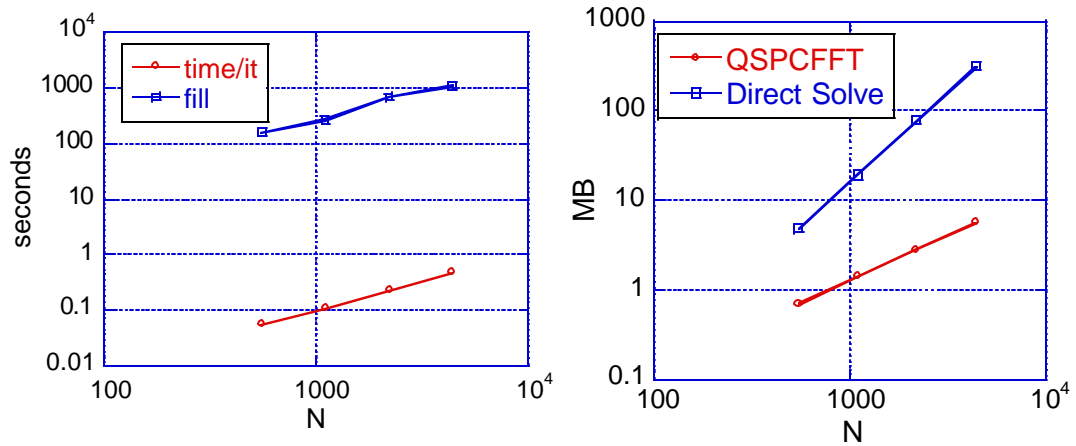
Fig. 6.2 Scaling of CPU time and memory as the patch array in Fig 6.1 is increased from 2 to 16 patch antennas. The memory compares the QSPCFFT solution with a direct solution method with full-matrix storage.
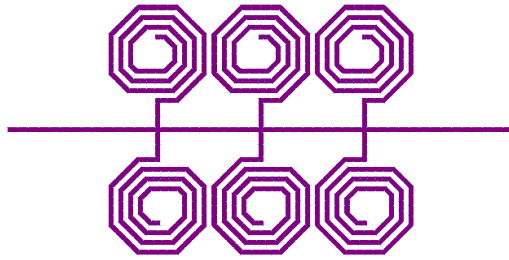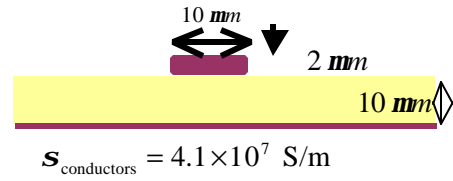
(a) Top view   (b) Cross section view
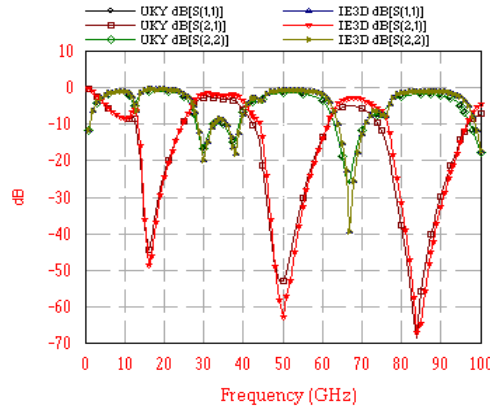
(c) S-parameters of UKY and *IE3D*   (d) QSPCFFT and direct LU
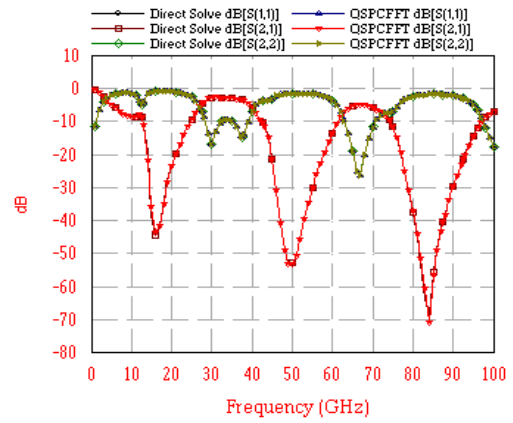
Fig. 6.3 Spiral inductor loaded microstrip line. (a) Top view, (b) Cross section of the microstrip line and substrate, (c) Comparison of the QSPCFFT solution (denotes as UKY) and Zeland's *IE3D*, and (d) Comparison of QSPCFFT and direct LU factorization solutions.

Chapter Seven: Conclusion and Future work

7.1 Conclusion

In this dissertation, an efficient integral equation technique based on the MPIE has been implemented for the analysis of microwave circuits. The GWP zero[th]-order divergence conforming basis function is employed in the MoM analysis. An adaptive numerical integration based on the Khayat-Wilton transform is employed to deal with the 1/R singularity and near-singularity of the kernels. The time consuming direct Sommerfeld integration of the layered media Green's function is circumvented by applying the Two-level DCIM scheme. Furthermore, for circuits with both horizontal and vertical conductors, a costly 2D interpolation of the Dyadic Green's Function (DGF) is avoided by using a closed-form evaluation of the z-integrations in the *spectral* domain in layered media. The calculation of the closed-form is further accelerated by using the Two-level DCIM. Moreover, the singularity of the z-integration is removed. Finally, the use of the QSPCFFT in the MoM analysis accelerates the iterative costs of complexity to a scale of $O(NlogN)$, rather than a scale of $O(N^2)$ with a direct solver.

7.2 Future work

The current algorithm is only valid to solve microwave circuits with either purely horizontal or vertical conductors in layered media. In order to solve for more general and complicated structures such as antennas with conical shapes, coaxial lines, and antennas with wire-bonds, several tasks are outlined in the next section.

7.2.1 Modify the layered-media Green's function

For solving arbitrary 3D microwave structures, the DGF with both horizontal and vertical currents is required. A suitable DGF is based on the formulation C proposed by Michalski and Zhang [3]. The new dyadic kernel for the MPIE formulation in MoM is defined as:

$$\begin{bmatrix} \tilde{G}_{xx} & 0 & \tilde{G}_{xz} \\ 0 & \tilde{G}_{yy} & \tilde{G}_{yz} \\ \tilde{G}_{zx} & \tilde{G}_{zy} & \tilde{G}_{zz} \end{bmatrix} \tag{7.1}$$

where the Green's functions in (7.1) are presented in their paper from (43) to (53). Meanwhile, the *correlation factor* Φ^e in (2.4) is required for the scalar potential kernel.

7.2.2 Incorporate Pre-corrected Fast Fourier Transform for 3D structures

The fast technique based on the QSPCFFT is presented in Chapter six for 2D problems with horizontal conductors. For problems with vertical conductors, the closed form z-integrations in the *spectral* domain are required to compute via FFT for each layer and maintain $O(N \log N)$ complexity for the matrix-vector multiplication.

7.2.3 Extension to higher-order basis functions

For complicated microwave circuit structures, a very fine detail in mesh discretization is necessary for low-order basis functions in order to yield accurate results in the MoM analysis. As a result, a large matrix is to be solved, which is very time consuming. A better approach is to utilize higher-order interpolatory basis functions that result in a better convergence rate and yield an accurate solution even with a coarse discretization. Thus, the derivation of the closed-form z-integration in the *spectral* domain with higher-order basis functions is necessary.

7.2.4 Optimization algorithm

For microwave circuit design, an optimization process is essential to meet specifications and to minimize attenuation loss. Many efficient optimization algorithms have been reported in literature, such as the optimization scheme based on the Genetic Algorithm [89, 90]. In the optimization process, one can refill the entire z-matrix every time when a parameter is changed. However this approach is inefficient and expensive. A more efficient optimization approach is to refill the z matrix entries corresponding to the points where the parameters are modified [91, 92].

The remaining entries of the z-matrix are unaltered. Hence, a large amount of time is saved in filling the impedance matrix.

Appendix A

A.1 Introduction

Assume an arbitrary point source representing an electric current density $\mathbf{J}(\mathbf{r}) = \hat{a}' I d(\mathbf{r} - \mathbf{r}')$, where $\hat{a}'$ is an arbitrary unit vector. The vertical electric field can then be expressed as [93]:

$$E_z(\mathbf{r}) = \frac{-j w \boldsymbol{m}_m I}{4\boldsymbol{p}} \left[\hat{z} \cdot \hat{a}' + \frac{1}{k_m^2} \frac{\partial}{\partial z} \nabla \cdot \hat{a}' \right] \frac{e^{-jk_m|\mathbf{r}-\mathbf{r}'|}}{|\mathbf{r}-\mathbf{r}'|} . \tag{A.1}$$

Similarly, the vertical magnetic field is:

$$H_z(\mathbf{r}) = \frac{I}{4\boldsymbol{p}} \left[\hat{z} \cdot \nabla_t \times \hat{a}' \right] \frac{e^{-jk_m|\mathbf{r}-\mathbf{r}'|}}{|\mathbf{r}-\mathbf{r}'|} \tag{A.2}$$

where ∇_t indicates the transverse projection of the Nabla operator.
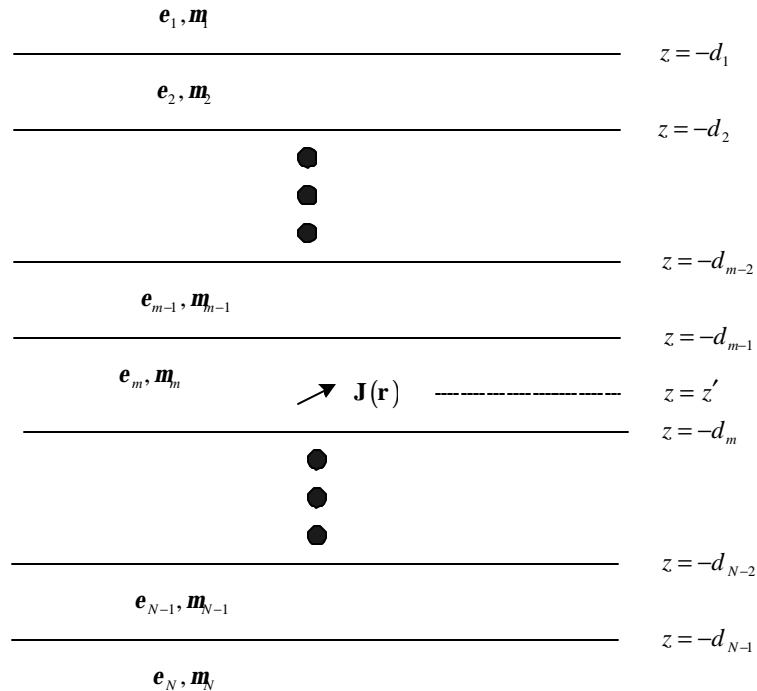
Fig. A.1   arbitrary point source embedded in the *m*-th layer of an N-layer medium.

Next, assume the source to be located in the mth-layer of an N-layer medium as illustrated in Fig. A.1. Initially, assume that the source is radiating in a homogeneous

space with physical material parameters $(\boldsymbol{e}_{r_m}, \boldsymbol{m}_{r_m}, \boldsymbol{s}_m, \tan \boldsymbol{d}_m)$, where $\boldsymbol{e}_{r_m}$ is the relative permittivity (F/m) (a real number), $\boldsymbol{m}_{r_m}$ (H/m) is the relative permeability, $\boldsymbol{s}_m$ is the conductivity (S/m), and $\tan \boldsymbol{d}_m$ is the loss tangent. Meanwhile, the complex relative permittivity is defined as:

$$\hat{\boldsymbol{e}}_{r_m} = \boldsymbol{e}_{r_m}(1 - j \tan \boldsymbol{d}_m) + \frac{\boldsymbol{s}_m}{j\boldsymbol{w}\boldsymbol{e}_o} \tag{A.3}$$

To determine the fields within the layered medium, we will first apply the Weyl identity and express the current as a continuous spectral of planar current sheets [30, 94]. Each sheet emanates a plane wave, for which a closed form solution of the integral exists. The spatial domain Green's function will then be found through Sommerfeld integrals. This is derived in the following. It is noted that the notation used herein is adopted directly from [95, 96].

The point source is initially projected into the k-space through the Weyl identity [94]:

$$\frac{e^{-jk_m|\mathbf{r}-\mathbf{r}'|}}{|\mathbf{r}-\mathbf{r}'|} = \frac{-j}{2\boldsymbol{p}} \int_{-\infty}^{\infty} \int_{-\infty}^{\infty} d\mathbf{k}_t \, \frac{e^{-j\mathbf{k}_t \cdot (\mathbf{r}_t - \mathbf{r}_t') - jk_{m,z}|z-z'|}}{k_{m,z}} \tag{A.4}$$

where, $\mathbf{k}_t = \hat{x}k_x + \hat{y}k_y$ is the transverse wave vector, $k_m = \boldsymbol{w}\sqrt{\boldsymbol{m}_m \boldsymbol{e}_m}$, and

$$k_{m,z} = \begin{cases} \sqrt{k_m^2 - \mathbf{k}_t \cdot \mathbf{k}_t} & k_m^2 > \mathbf{k}_t \cdot \mathbf{k}_t \\ -j\sqrt{\mathbf{k}_t \cdot \mathbf{k}_t - k_m^2} & k_m^2 < \mathbf{k}_t \cdot \mathbf{k}_t \end{cases}. \tag{A.5}$$

Consequently, in the k-space, we can define from (A.1):

$$\tilde{E}_z(\mathbf{r}) = \frac{-\boldsymbol{w}\boldsymbol{m}_m I}{8\boldsymbol{p}^2}\left[\hat{z}\cdot\hat{\boldsymbol{a}}' + \frac{1}{k_m^2}\frac{\partial}{\partial z}\nabla\cdot\hat{\boldsymbol{a}}'\right]\frac{e^{-j\mathbf{k}_t \cdot (\mathbf{r}_t - \mathbf{r}_t') - jk_{m,z}|z-z'|}}{k_{m,z}} \tag{A.6}$$

and from (A.2)

$$H_z(\mathbf{r}) = \frac{I}{8\boldsymbol{p}^2}\left[\hat{z}\cdot\nabla_t\times\hat{\boldsymbol{a}}'\right]\frac{e^{-j\mathbf{k}_t \cdot (\mathbf{r}_t - \mathbf{r}_t') - jk_{m,z}|z-z'|}}{k_{m,z}}. \tag{A.7}$$

The transverse fields can be derived directly from the vertical fields. These are easily derived from Maxwell's equations [96]:

$$\tilde{\mathbf{E}}_t = \frac{1}{k_t^2}\left[\nabla_t \frac{\partial}{\partial z}\tilde{E}_z + jw\mathbf{m}_m \hat{z}\times\nabla_t \tilde{H}_z\right] \tag{A.8}$$

$$\tilde{\mathbf{H}}_t = \frac{1}{k_t^2}\left[\nabla_t \frac{\partial}{\partial z}\tilde{H}_z - jw\mathbf{e}_m \hat{z}\times\nabla_t \tilde{E}_z\right] \tag{A.9}$$

Now, we can assume that the source lies in the mth layer of an N-layer medium. Given this, we will proceed to compute the fields radiated by the source in the mth layer as well as an arbitrary layer i either above or below the source level (i.e., $i < m$, or $i > m$, respectively). This is addressed in each of the following subsections.

A.2 Observation field in the m$^{\text{th}}$ layer

Initially, consider the field radiated in the mth layer due to the arbitrary point source in the mth layer. We can derive that:

$$\tilde{E}_z^m = \hat{z}\cdot\hat{\boldsymbol{a}}'\left(1+\frac{1}{k_m^2}\frac{\partial^2}{\partial z^2}\right)\tilde{g}_{v_m}^{TM} + \frac{1}{k_m^2}\frac{\partial}{\partial z}\nabla\cdot\hat{\boldsymbol{a}}'\tilde{g}_{h_m}^{TM} \tag{A.10}$$

and

$$\tilde{H}_z^m = \hat{z}\cdot\nabla_t\times\hat{\boldsymbol{a}}'\frac{\tilde{g}_{h_m}^{TE}}{-jw\mathbf{m}_m} \tag{A.11}$$

where the k-space Green's function are defined as:

$$\tilde{g}_{v_m}^{TM} = \frac{-w\mathbf{m}_m I}{8\mathbf{p}^2}\frac{e^{-j\mathbf{k}_t\cdot(\mathbf{r}_t-\mathbf{r}_t')}}{k_{m,z}}\left[e^{-jk_{m,z}|z-z'|} + \tilde{B}_m^{TM}e^{jk_{m,z}z} + \tilde{D}_m^{TM}e^{-jk_{m,z}z}\right] \tag{A.12}$$

$$\tilde{g}_{h_m}^{TM} = \frac{-w\mathbf{m}_m I}{8\mathbf{p}^2}\frac{e^{-j\mathbf{k}_t\cdot(\mathbf{r}_t-\mathbf{r}_t')}}{k_{m,z}}\left[e^{-jk_{m,z}|z-z'|} + \tilde{E}_m^{TM}e^{jk_{m,z}z} + \tilde{F}_m^{TM}e^{-jk_{m,z}z}\right] \tag{A.13}$$

$$\tilde{g}_{h_m}^{TE} = \frac{-w\mathbf{m}_m I}{8\mathbf{p}^2}\frac{e^{-j\mathbf{k}_t\cdot(\mathbf{r}_t-\mathbf{r}_t')}}{k_{m,z}}\left[e^{-jk_{m,z}|z-z'|} + \tilde{B}_m^{TE}e^{jk_{m,z}z} + \tilde{D}_m^{TE}e^{-jk_{m,z}z}\right] \tag{A.14}$$

where

$$\tilde{B}_m^{TM/TE} = \tilde{R}_{m,m-1}^{TM/TE}\tilde{M}_m^{TM/TE}e^{jk_{m,z}d_{m-1}}\left[e^{jk_{m,z}(d_{m-1}+z')} + \tilde{R}_{m,m+1}^{TM/TE}e^{-jk_{m,z}(d_m-d_{m-1})}e^{-jk_{m,z}(d_m+z')}\right], \tag{A.15}$$

$$\tilde{D}_m^{TM/TE} = \tilde{R}_{m,m+1}^{TM/TE}\tilde{M}_m^{TM/TE}e^{-jk_{m,z}d_m}\left[e^{-jk_{m,z}(d_m+z')} + \tilde{R}_{m,m-1}^{TM/TE}e^{-jk_{m,z}(d_m-d_{m-1})}e^{jk_{m,z}(d_{m-1}+z')}\right], \tag{A.16}$$

$$\tilde{E}_m^{TM} = \tilde{R}_{m,m-1}^{TM}\tilde{M}_m^{TM}e^{jk_{m,}d_{m-1}}\left[-e^{jk_{m,z}(d_{m-1}+z')} + \tilde{R}_{m,m+1}^{TM}e^{-jk_{m,z}(d_m-d_{m-1})}e^{-jk_{m,z}(d_m+z')}\right], \qquad (A.17)$$

$$\tilde{F}_m^{TM} = \tilde{R}_{m,m+1}^{TM}\tilde{M}_m^{TM}e^{-jk_{m,z}d_m}\left[-e^{-jk_{m,z}(d_m+z')} + \tilde{R}_{m,m-1}^{TM}e^{-jk_{m,z}(d_m-d_{m-1})}e^{jk_{m,z}(d_{n-1}+z')}\right], \qquad (A.18)$$

$$\tilde{M}_m^{TM/TE} = \left[1 - \tilde{R}_{m,m-1}^{TM/TE}\tilde{R}_{m,m+1}^{TM/TE}e^{-2jk_{m,z}(d_m-d_{m-1})}\right]^{-1} \qquad (A.19)$$

$$\tilde{R}_{m,m+1}^{TM/TE} = \frac{R_{m,m+1}^{TM/TE} + \tilde{R}_{m+1,m+2}^{TM/TE}e^{-2jk_{m+1,z}(d_{m+1}-d_m)}}{1 + R_{m,m+1}^{TM/TE}\tilde{R}_{m+1,m+2}^{TM/TE}e^{-2jk_{m+1,z}(d_{m+1}-d_m)}} \qquad (A.20)$$

$$\tilde{R}_{m,m-1}^{TM/TE} = \frac{R_{m,m-1}^{TM/TE} + \tilde{R}_{m-1,m-2}^{TM/TE}e^{-2jk_{m-1,z}(d_{m-1}-d_{m-2})}}{1 + R_{m,m-1}^{TM/TE}\tilde{R}_{m-1,m-2}^{TM/TE}e^{-2jk_{m-1,z}(d_{m-1}-d_{m-2})}} \qquad (A.21)$$

where *TM/TE* refers to either *TM* or *TE*, and $R_{m,m+1}^{TM/TE}$ are the Fresnel reflection coefficients resulting from the reflection of a *TM* or *TE*-polarized plane wave (respectively) by a material half space. These are defined as:

$$R_{m,m+1}^{TM} = \frac{\boldsymbol{e}_{m+1}k_{m,z} - \boldsymbol{e}_m k_{m+1,z}}{\boldsymbol{e}_{m+1}k_{m,z} + \boldsymbol{e}_m k_{m+1,z}} \qquad (A.22)$$

$$R_{m,m+1}^{TE} = \frac{\boldsymbol{m}_{m+1}k_{m,z} - \boldsymbol{m}_m k_{m+1,z}}{\boldsymbol{m}_{m+1}k_{m,z} + \boldsymbol{m}_m k_{m+1,z}} . \qquad (A.23)$$

The Fresnel coefficients satisfy the identity: $R_{m+1,m}^{TMTE} = -R_{m,m+1}^{TMTE}$. We can also define the Fresnel transmission coefficients:

$$T_{m,m+1}^{TM} = 1 + R_{m,m+1}^{TM} = \frac{2\boldsymbol{e}_{m+1}k_{m,z}}{\boldsymbol{e}_{m+1}k_{m,z} + \boldsymbol{e}_m k_{m+1,z}} \qquad (A.24)$$

$$T_{m,m+1}^{TE} = 1 + R_{m,m+1}^{TE} = \frac{2\boldsymbol{m}_{m+1}k_{m,z}}{\boldsymbol{m}_{m+1}k_{m,z} + \boldsymbol{m}_m k_{m+1,z}} . \qquad (A.25)$$

The coefficients $\tilde{R}$ in (A.20) and (A.21) are referred to as the generalized reflection coefficients, and include multiple reflections due to the layers beyond the interface. The generalized reflection coefficients can be found recursively. That is, if region 1 and region *N* are half spaces, then we can define $\tilde{R}_{N,N+1}^{TM/TE} = 0$. Consequently, starting with $\tilde{R}_{N-1,N}^{TM/TE}$, we can find all $\tilde{R}_{m,m+1}^{TM/TE}$ recursively through $\tilde{R}_{1,2}^{TM/TE}$ using (A.20). Similarly, defining $\tilde{R}_{1,0}^{TM/TE} = 0$, then starting with $\tilde{R}_{2,1}^{TM/TE}$, we can find all $\tilde{R}_{m,m-1}^{TM/TE}$

recursively through $\tilde{R}_{N,N-1}^{TM/TE}$ using (A.21). Finally, in the event that region N is PEC, then $\tilde{R}_{N-1,N}^{TM} = +1$ and $\tilde{R}_{N-1,N}^{TE} = -1$, and again $\tilde{R}_{m,m+1}^{TM/TE}$ can be found recursively using (A.21). A similar statement can be made if region 1 is PEC.

In (A.12) - (A.14), the k-space Green's function can be expressed as a superposition of the *primary field* and the *reflected* field. The primary field is simply the field due to the direct radiation of the Green's function. The reflected field is due to multiple reflections off the boundary interfaces. To this end, we express:

$$\tilde{g}_{v_m}^{TM} = \tilde{g}_{v_m}^{TM^P} + \tilde{g}_{v_m}^{TM^R}, \quad \tilde{g}_{h_m}^{TM} = \tilde{g}_{h_m}^{TM^P} + \tilde{g}_{h_m}^{TM^R}, \quad \tilde{g}_{h_m}^{TE} = \tilde{g}_{h_m}^{TE^P} + \tilde{g}_{h_m}^{TE^R} \qquad (A.26)$$

where

$$\tilde{g}_m^P = \tilde{g}_{v_m}^{TM^P} = \tilde{g}_{h_m}^{TM^P} = \tilde{g}_{h_m}^{TE^P} = \frac{-w\boldsymbol{m}_m I}{8\boldsymbol{p}^2} \frac{e^{-j\mathbf{k}_t\cdot(\mathbf{r}_t-\mathbf{r}_t')}}{k_{m,z}} e^{-jk_{m,z}|z-z|} \qquad (A.27)$$

$$\tilde{g}_{v_m}^{TM^R} = \frac{-w\boldsymbol{m}_m I}{8\boldsymbol{p}^2} \frac{e^{-j\mathbf{k}_t\cdot(\mathbf{r}_t-\mathbf{r}_t')}}{k_{m,z}} \left[\tilde{B}_m^{TM} e^{jk_{m,z}z} + \tilde{D}_m^{TM} e^{-jk_{m,z}z} \right] \qquad (A.28)$$

$$\tilde{g}_{h_m}^{TM^R} = \frac{-w\boldsymbol{m}_m I}{8\boldsymbol{p}^2} \frac{e^{-j\mathbf{k}_t\cdot(\mathbf{r}_t-\mathbf{r}_t')}}{k_{m,z}} \left[\tilde{E}_m^{TM} e^{jk_{m,z}z} + \tilde{F}_m^{TM} e^{-jk_{m,z}z} \right] \qquad (A.29)$$

$$\tilde{g}_{h_m}^{TE^R} = \frac{-w\boldsymbol{m}_m I}{8\boldsymbol{p}^2} \frac{e^{-j\mathbf{k}_t\cdot(\mathbf{r}_t-\mathbf{r}_t')}}{k_{m,z}} \left[\tilde{B}_m^{TE} e^{jk_{m,z}z} + \tilde{D}_m^{TE} e^{-jk_{m,z}z} \right]. \qquad (A.30)$$

Due to the linearity of the operators in (A.10) and (A.11), we can also express:

$$\tilde{E}_z^m = \tilde{E}_z^{m^P} + \tilde{E}_z^{m^R}, \quad \tilde{H}_z^m = \tilde{H}_z^{m^P} + \tilde{H}_z^{m^R}. \qquad (A.31)$$

Following (15) – (24) of [95], the total primary electric field is expressed in the spectral domain as:

$$\hat{\boldsymbol{a}} \cdot \tilde{\mathbf{E}}_m^P = \left[\hat{\boldsymbol{a}} \cdot \hat{\boldsymbol{a}}' + \frac{1}{k_m^2} \hat{\boldsymbol{a}} \cdot \nabla\nabla \cdot \hat{\boldsymbol{a}}' \right] \tilde{g}_m^P \qquad (A.32)$$

Given the Weyl identity in (A.4), this can be readily expressed back in the spatial domain as:

91

$$\hat{a} \cdot \mathbf{E}_m^P(\mathbf{r}) = -jw\boldsymbol{m}_m \left[\hat{a} \cdot \hat{a}' + \frac{1}{k_m^2} \hat{a} \cdot \nabla \nabla \cdot \hat{a}' \right] g_m^p(\mathbf{r}, \mathbf{r}') \tag{A.33}$$

where

$$g_m^p(\mathbf{r}, \mathbf{r}') = \frac{I}{4\boldsymbol{p}} \frac{e^{-jk_m|\mathbf{r}-\mathbf{r}'|}}{|\mathbf{r}-\mathbf{r}'|}. \tag{A.34}$$

Next, we consider the multiple reflected wave. Before deriving a symmetric operator similar to that expressed in (A.33), it is recognized that vertical electric field radiated by the vertical and horizontal have symmetric and anti-symmetric components. This is predominately due to the flipping of the sign of the field radiated above or below the current sheet for the horizontal dipole case due to a reflecting boundary either above or below the source. This is immediately observed from comparing (A.15) and (A.16) with (A.17) and (A.18). Namely, the first term in the parenthesis of (A.15) and the second term in the parenthesis of (A.16) is equal to the first term of (A.17) and the second term of (A.18), respectively, for the TM-polarization. These correspond to the symmetric term. Similarly, the second term in (A.15) and the first term in (A.16) is equal to the negative of the second term of (A.17) and the first term of (A.18), respectively, for the TM-polarization. These translate to the asymmetric terms. Based on this observation, it appears to be advantageous to further decompose $\tilde{g}_m^{TE^R}$ and $\tilde{g}_m^{TM^R}$ as:

$$\begin{aligned} \tilde{g}_{v_m}^{TM^R} &= \tilde{g}_m^{TM^{RS}} + \tilde{g}_m^{TM^{RA}} \\ \tilde{g}_{h_m}^{TM^R} &= \tilde{g}_m^{TM^{RS}} - \tilde{g}_m^{TM^{RA}} \\ \tilde{g}_{h_m}^{TE^R} &= \tilde{g}_m^{TE^{RS}} + \tilde{g}_m^{TE^{RA}} \end{aligned} \tag{A.35}$$

where, from (A.12) — (A.18), the *asymmetric* terms are:

$$\tilde{g}_m^{TM/TE^{RA}} =$$

$$\frac{-w\boldsymbol{m}_m I}{8\boldsymbol{p}^2} \frac{e^{-j\mathbf{k}_t(\mathbf{r}_t - \mathbf{r}_t')}}{k_{m,z}} \left[\tilde{R}_{m,m-1}^{TM/TE} e^{jk_{m,z}(z+z')} e^{2jk_{m,z}d_{m-1}} + \tilde{R}_{m,m+1}^{TM/TE} e^{-jk_{m,z}(z+z')} e^{-2jk_{m,z}d_m} \right] \tilde{M}_m^{TM/TE} \tag{A.36}$$

and the *symmetric* terms are:

$$\tilde{g}_m^{TM/TE^{RS}} =$$

$$\frac{-\boldsymbol{wm}_m I}{8\boldsymbol{p}^2} \frac{e^{-j\mathbf{k}_t\cdot(\mathbf{r}_t-\mathbf{r}_t')}}{k_{m,z}} \tilde{R}_{m,m+1}^{TM/TE} \tilde{R}_{m,m-1}^{TM/TE} e^{-2jk_{m,z}(d_m-d_{m-1})} \left[e^{jk_{m,z}(z-z')} + e^{-jk_{m,z}(z-z')} \right] \tilde{M}_m^{TM/TE} \qquad (A.37)$$

The contribution to $\tilde{g}_m^{TM/TE^{RA}}$ can be thought of as the principal reflections off the upper and lower boundaries (weighted by the multiple reflection term $\tilde{M}_m^{TM/TE}$) and the contribution to $\tilde{g}_m^{TM/TE^{RS}}$ can be thought of as due to the secondary reflections. It is noted that the *asymmetric* term $\tilde{g}_m^{TM/TE^{RA}}$ arises from the sign difference in the leading terms of $\tilde{E}_m^{TM}$ and $\tilde{F}_m^{TM}$ as compared to $\tilde{B}_m^{TM}$ and $\tilde{D}_m^{TM}$.

Next, the electric due to the reflecting boundaries will be decomposed into $\tilde{\mathbf{E}}^{RS}$ and $\tilde{\mathbf{E}}^{RA}$. Initially, we will explicitly construct the contribution due to the upper boundary, where in general:

$$\hat{\boldsymbol{a}} \cdot \tilde{\mathbf{E}}^{m^{RS}} = \hat{\boldsymbol{a}} \cdot \hat{z} E_z^{m^{RS}} + \hat{\boldsymbol{a}} \cdot \mathbf{E}_t^{m^{RS}} \qquad (A.38)$$

where

$$\tilde{E}_z^{m^{RS}} = \left(\hat{z}\cdot\hat{\boldsymbol{a}}' \right) \left(1 + \frac{1}{k_m^2}\frac{\partial^2}{\partial z^2} \right) \tilde{g}_m^{TM^{RS}} + \frac{1}{k_m^2}\frac{\partial}{\partial z}\nabla_t\cdot\hat{\boldsymbol{a}}'\,\tilde{g}_m^{TM^{RS}}$$
$$= \left[\hat{z}\cdot\hat{\boldsymbol{a}}' + \frac{1}{k_m^2}\frac{\partial}{\partial z}\nabla\cdot\hat{\boldsymbol{a}}' \right] \tilde{g}_m^{TM^{RS}} \qquad (A.39)$$

and

$$\tilde{H}_z^{m^{RS}} = \hat{z}\cdot\nabla_t\times\hat{\boldsymbol{a}}'\frac{\tilde{g}_m^{TE^{RS}}}{-j\boldsymbol{wm}_m}, \qquad (A.40)$$

$$\hat{\boldsymbol{a}} \cdot \tilde{\mathbf{E}}_t^{m^{RS}} = \frac{1}{k_t^2}\left[\hat{\boldsymbol{a}}\cdot\nabla_t\frac{\partial}{\partial z}\tilde{E}_z^{m^{RS}} + j\boldsymbol{wm}_m\hat{\boldsymbol{a}}\cdot\hat{z}\times\nabla_t\tilde{H}_z^{m^{RS}} \right]. \qquad (A.41)$$

The first term in (A.41) can be expanded as:

$$\frac{1}{k_t^2}\hat{\boldsymbol{a}}\cdot\nabla_t\frac{\partial}{\partial z}\tilde{E}_z^{m^{RS}} = \frac{1}{k_t^2}\hat{\boldsymbol{a}}\cdot\nabla_t\frac{\partial}{\partial z}\left[\hat{z}\cdot\hat{\boldsymbol{a}}' + \frac{1}{k_m^2}\frac{\partial}{\partial z}\nabla\cdot\hat{\boldsymbol{a}}' \right]\tilde{g}_m^{TM^{RS}}$$
$$= -\frac{1}{k_t^2}\hat{\boldsymbol{a}}\cdot\nabla_t\nabla_t\cdot\hat{\boldsymbol{a}}'\tilde{g}_m^{TM^{RS}} + \frac{1}{k_m^2}\hat{\boldsymbol{a}}\cdot\nabla_t\nabla\cdot\hat{\boldsymbol{a}}'\tilde{g}_m^{TM^{RS}} \qquad (A.42)$$

93

Then, combining (A.42), (A.41), (A.39) and (A.40) with leads to:

$$\hat{\boldsymbol{a}} \cdot \tilde{\mathbf{E}}_m^{RS} = \left[\hat{z} \cdot \hat{\boldsymbol{a}} \hat{z} \cdot \hat{\boldsymbol{a}}' + \hat{z} \cdot \hat{\boldsymbol{a}}' \frac{1}{k_m^2} \frac{\partial}{\partial z} \nabla \cdot \hat{\boldsymbol{a}}' \right] \tilde{g}_m^{TM^{RS}} - \frac{1}{k_t^2} \hat{\boldsymbol{a}} \cdot \nabla_t \nabla_t \cdot \hat{\boldsymbol{a}}' \tilde{g}_m^{TM^{RS}}$$
$$+ \frac{1}{k_m^2} \hat{\boldsymbol{a}} \cdot \nabla_t \nabla \cdot \hat{\boldsymbol{a}}' \tilde{g}_m^{TM^{RS}} - \frac{1}{k_t^2} (\hat{\boldsymbol{a}} \cdot \hat{z} \times \nabla_t)(\hat{\boldsymbol{a}}' \cdot \hat{z} \times \nabla_t) \tilde{g}_m^{TE^{RS}}$$
(A.43)

Recognizing that

$$\left[\hat{\boldsymbol{a}} \cdot \hat{z}\hat{z} \cdot \hat{\boldsymbol{a}}' - \frac{1}{k_t^2} \hat{\boldsymbol{a}} \cdot \nabla_t \nabla_t \cdot \hat{\boldsymbol{a}}' \right] \tilde{g}_m^{TM^{RS}} = \left[\hat{\boldsymbol{a}} \cdot \hat{\boldsymbol{a}}' + \frac{1}{k_t^2} (\hat{\boldsymbol{a}} \cdot \hat{z} \times \nabla_t)(\hat{\boldsymbol{a}}' \cdot \hat{z} \times \nabla_t) \right] \tilde{g}_m^{TM^{RS}} \quad (A.44)$$

then (A.43) can be rewritten as:

$$\hat{\boldsymbol{a}} \cdot \tilde{\mathbf{E}}_m^{RS} = \left[\hat{\boldsymbol{a}} \cdot \hat{\boldsymbol{a}}' + \frac{1}{k_m^2} \hat{\boldsymbol{a}} \cdot \nabla \nabla \cdot \hat{\boldsymbol{a}}' \right] \tilde{g}_m^{TM^{RS}} + \frac{1}{k_t^2} (\hat{\boldsymbol{a}} \cdot \hat{z} \times \nabla_t)(\hat{\boldsymbol{a}}' \cdot \hat{z} \times \nabla_t) \left(\tilde{g}_m^{TM^{RS}} - \tilde{g}_m^{TE^{RS}} \right)$$
(A.45)

The above procedure can be repeated for the reflective term due to the lower boundary. Following this procedure we derive:

$$\hat{\boldsymbol{a}} \cdot \tilde{\mathbf{E}}_m^{RA} = \left[\hat{\boldsymbol{a}} \cdot \hat{\boldsymbol{a}}_I' + \frac{1}{k_m^2} \hat{\boldsymbol{a}} \cdot \nabla \nabla \cdot \hat{\boldsymbol{a}}_I' \right] \tilde{g}_m^{TM^{RA}} + \frac{1}{k_t^2} (\hat{\boldsymbol{a}} \cdot \hat{z} \times \nabla_t)(\hat{\boldsymbol{a}}_I' \cdot \hat{z} \times \nabla_t) \left(\tilde{g}_m^{TM^{RA}} + \tilde{g}_m^{TE^{RA}} \right) \quad (A.46)$$

where $\hat{\boldsymbol{a}}_I'$ is the imaged source vector defined as:

$$\hat{\boldsymbol{a}}_I' = -\hat{x}\boldsymbol{a}_x' - \hat{y}\boldsymbol{a}_y' + \hat{z}\boldsymbol{a}_z' \quad (A.47)$$

Applying an inverse transform, (A.45) and (A.46) can be expressed in the spatial domain as:

$$\hat{\boldsymbol{a}} \cdot \mathbf{E}_m^{RS} = \left[\hat{\boldsymbol{a}} \cdot \hat{\boldsymbol{a}}' + \frac{1}{k_m^2} \hat{\boldsymbol{a}} \cdot \nabla \nabla \cdot \hat{\boldsymbol{a}}' \right] g_m^{TM^{RS}} + \frac{(\hat{\boldsymbol{a}} \cdot \hat{z} \times \nabla_t)(\hat{\boldsymbol{a}}' \cdot \hat{z} \times \nabla_t) g_m^{ME^{RS}}}{k_t^2} \quad (A.48)$$

$$\hat{\boldsymbol{a}} \cdot \mathbf{E}_m^{RA} = \left[\hat{\boldsymbol{a}} \cdot \hat{\boldsymbol{a}}_I' + \frac{1}{k_m^2} \hat{\boldsymbol{a}} \cdot \nabla \nabla \cdot \hat{\boldsymbol{a}}_I' \right] g_m^{TM^{RA}} + \frac{(\hat{\boldsymbol{a}} \cdot \hat{z} \times \nabla_t)(\hat{\boldsymbol{a}}_I' \cdot \hat{z} \times \nabla_t) g_m^{ME^{RA}}}{k_t^2} \quad (A.49)$$

where, $g_m^{TM^{RA/S}}$, $g_m^{ME^{RA/S}}$ are spatial domain equivalents that are computed from the Sommerfeld integrals. These are evaluated directly from (A.36) – (A.37). In each of these, the Sommerfeld integrals are of the form:

$$\int\limits_{-\infty}^{\infty}\int\limits_{-\infty}^{\infty} e^{-j\mathbf{k}_t \cdot \mathbf{r}_t} F\left(k_{m,z}\right) dk_x dk_y \qquad (A.50)$$

where the source point is assumed to be at the origin. Next, let

$$\mathbf{k}_t = \hat{\mathbf{x}} k_r \cos \boldsymbol{a} + \hat{\mathbf{y}} k_r \sin \boldsymbol{a}$$
$$\mathbf{r}_t - \mathbf{r}_t' = \hat{\mathbf{x}} r \cos \boldsymbol{f} + \hat{\mathbf{y}} r \sin \boldsymbol{f} \qquad (A.51)$$

Then, (A.50) can be rewritten as:

$$\int\limits_{0}^{\infty} \left(\int\limits_{0}^{2p} e^{-jk_r r \cos(\boldsymbol{a}-\boldsymbol{f})} F\left(k_{m,z}\right) d\boldsymbol{a} \right) k_r dk_r \qquad (A.52)$$

where $k_{m,z} = \sqrt{k_m^2 - k_r^2}$. Applying the identity:

$$J_o\left(k_r r\right) = \frac{1}{2\boldsymbol{p}} \int_0^{2p} e^{-jk_r r \cos(\boldsymbol{a}-\boldsymbol{f})} d\boldsymbol{a} \qquad (A.53)$$

then, (A.52) can be rewritten as:

$$2\boldsymbol{p} \int\limits_{0}^{\infty} k_r J_o\left(k_r r\right) F\left(k_{m,z}\right) dk_r \quad . \qquad (A.54)$$

$${g_m^{TM}}^{RA} =$$

$$\frac{-\boldsymbol{wm}_m I}{4\boldsymbol{p}} \int\limits_0^\infty \frac{k_r}{k_{m,z}} J_o\left(k_r r\right) \tilde{M}_m^{TM} \left[\tilde{R}_{m,m-1}^{TM} e^{jk_{m,z}(z+z')} e^{2jk_{m,z}d_{m-1}} + \tilde{R}_{m,m+1}^{TM} e^{-jk_{m,z}(z+z')} e^{-2jk_{m,z}d_m} \right] dk_r \qquad (A.55)$$

$${g_m^{TM}}^{RS} =$$

$$\frac{-\boldsymbol{wm}_m I}{4\boldsymbol{p}} \int\limits_0^\infty \frac{k_r}{k_{m,z}} J_o\left(k_r r\right) \tilde{M}_m^{TM/TE} \left[\tilde{R}_{m,m+1}^{TM/TE} \tilde{R}_{m,m-1}^{TM/TE} e^{-2jk_{m,z}(d_m-d_{m-1})} \left[e^{jk_{m,z}(z-z')} + e^{-jk_{m,z}(z-z')} \right] \right] dk_r$$
$$(A.56)$$

$${g_m^{ME}}^{RA} =$$

$$\frac{-\boldsymbol{wm}_m I}{4\boldsymbol{p}} \int\limits_0^\infty \frac{1}{k_r \cdot k_{m,z}} J_o\left(k_r r\right) \left\{ e^{jk_{m,z}(z+z')} e^{2jk_{m,z}d_{m-1}} \left[\tilde{M}_m^{TM} \tilde{R}_{m,m-1}^{TM} + \tilde{M}_m^{TE} \tilde{R}_{m,m-1}^{TE} \right] \right. \qquad (A.57)$$
$$\left. + e^{-jk_{m,z}(z+z')} e^{-2jk_{m,z}d_m} \left[\tilde{M}_m^{TM} \tilde{R}_{m,m+1}^{TM} + \tilde{M}_m^{TE} \tilde{R}_{m,m+1}^{TE} \right] dk_r \right\}$$

and

$$g_m^{ME^{RS}} =$$

$$\frac{-\boldsymbol{w}\boldsymbol{m}_m I}{4\boldsymbol{p}} \int_0^\infty \frac{1}{k_r \cdot k_{m,z}} J_o\left(k_r \boldsymbol{r}\right) \left\{ e^{-2\,jk_{m,z}(d_m-d_{m-1})} \left(e^{jk_{m,z}(z-z')} + e^{-jk_{m,z}(z-z')} \right) \begin{bmatrix} \tilde{M}_m^{TM} \tilde{R}_{m,m+1}^{TM} \tilde{R}_{m,m-1}^{TM} & - \\ \tilde{M}_m^{TE} \tilde{R}_{m,m+1}^{TE} \tilde{R}_{m,m-1}^{TE} \end{bmatrix} dk_r \right\}$$

$$(A.58)$$

The expressions in (A.48) and (A.49) represent the EFIE operator for the reflected Green's function. This expression can be used for a method of moment solution. To this end, assume a test function $\vec{T}_m(\vec{r})$ and basis function $\vec{J}_n(\vec{r})$, where the vector functions are assumed to be tangential to a surface element. The EFIE operator is then expressed as:

$$\int_{S_m} \vec{T}_m(\vec{r}) \cdot \mathbf{E}_m^{RS} ds = \int_{S_m} \int_{S_n'} \left[\vec{T}_m(\vec{r}) \cdot \vec{J}_n(\vec{r}') + \frac{1}{k_m^2} \vec{T}_m(\vec{r}) \cdot \nabla \nabla \cdot \vec{J}_n(\vec{r}') \right] g_m^{TM^{RS}} ds'ds$$
$$+ \int_{S_m} \int_{S_n'} \left(\vec{T}_m(\vec{r}) \cdot \hat{z} \times \nabla_t \right) \left(\vec{J}_n(\vec{r}') \cdot \hat{z} \times \nabla_t \right) g_m^{ME^{RS}} ds'ds$$

$$(A.59)$$

for RS, where S_m is the surface of the patch supporting the test function, and S_n' is the surface of the patch supporting the basis function. A similar expression is derived for RA.

Next, the dyad is introduced:

$$\frac{1}{k_t^2} \left(\hat{\boldsymbol{a}} \cdot \hat{z} \times \nabla_t \right) \left(\hat{\boldsymbol{a}}' \cdot \hat{z} \times \nabla_t \right) \tilde{g}_m^{ME^{RS}} = \hat{\boldsymbol{a}} \cdot \tilde{\bar{G}}_m^{ME^{RS}} \cdot \hat{\boldsymbol{a}}' \tag{A.60}$$

where,

$$\tilde{\bar{G}}_m^{ME^{RS}} = \begin{pmatrix} \dfrac{\partial^2}{\partial y^2} & -\dfrac{\partial^2}{\partial x \partial y} & 0 \\[2mm] -\dfrac{\partial^2}{\partial x \partial y} & \dfrac{\partial^2}{\partial x^2} & 0 \\[2mm] 0 & 0 & 0 \end{pmatrix} \dfrac{\left(\tilde{g}_m^{TM^{RS}} - \tilde{g}_m^{TE^{RS}} \right)}{k_t^2} \tag{A.61}$$

It is noted that only the transverse components of $\hat{\boldsymbol{a}}'$ are impacted by the dyadic. Thus, we similarly have that:

$$\frac{1}{k_t^2} \left(\hat{\boldsymbol{a}} \cdot \hat{z} \times \nabla_t \right) \left(\hat{\boldsymbol{a}}'_t \cdot \hat{z} \times \nabla_t \right) \tilde{g}_m^{ME^{RA}} = -\hat{\boldsymbol{a}} \cdot \tilde{\bar{G}}_m^{ME^{RA}} \cdot \hat{\boldsymbol{a}}' \tag{A.62}$$

where, we have defined,

$$
\tilde{\tilde{G}}_m^{ME^{RA}} = \begin{pmatrix} \dfrac{\partial^2}{\partial y^2} & -\dfrac{\partial^2}{\partial x \partial y} & 0 \\[2ex] -\dfrac{\partial^2}{\partial x \partial y} & \dfrac{\partial^2}{\partial x^2} & 0 \\[2ex] 0 & 0 & 0 \end{pmatrix} \dfrac{\left(\tilde{g}_m^{TM^{RA}} + \tilde{g}_m^{TE^{RA}} \right)}{k_t^2}
\tag{A.63}
$$

For the generalized case, the symmetry property loses its advantage since the derivatives must be applied to the Green's function. Consequently, the *RS* and *RA* terms are combined, leading to:

$$
\tilde{\tilde{G}}_m^{ME^{R}} = \tilde{\tilde{G}}_m^{ME^{RS}} - \tilde{\tilde{G}}_m^{ME^{RA}} = \begin{pmatrix} \dfrac{\partial^2}{\partial y^2} & -\dfrac{\partial^2}{\partial x \partial y} & 0 \\[2ex] -\dfrac{\partial^2}{\partial x \partial y} & \dfrac{\partial^2}{\partial x^2} & 0 \\[2ex] 0 & 0 & 0 \end{pmatrix} \left(\dfrac{\left(\tilde{g}_m^{TM^{RS}} - \tilde{g}_m^{TM^{RA}} \right)}{k_t^2} - \dfrac{\left(\tilde{g}_m^{TE^{RS}} + \tilde{g}_m^{TE^{RA}} \right)}{k_t^2} \right)
\tag{A.64}
$$

From (A.35), this is rewritten as:

$$
\tilde{\tilde{G}}_m^{ME^{R}} = \begin{pmatrix} \dfrac{\partial^2}{\partial y^2} & -\dfrac{\partial^2}{\partial x \partial y} & 0 \\[2ex] -\dfrac{\partial^2}{\partial x \partial y} & \dfrac{\partial^2}{\partial x^2} & 0 \\[2ex] 0 & 0 & 0 \end{pmatrix} \dfrac{\left(\tilde{g}_{h_m}^{TM^{R}} - \tilde{g}_{h_m}^{TE^{R}} \right)}{k_t^2}
\tag{A.65}
$$

where $\tilde{g}_{h_m}^{TM^{R}}$ and $\tilde{g}_{h_m}^{TE^{R}}$ are defined in (A.29) and (A.30), respectively. The spatial derivatives are then expressed in the spectral domain, where,

$$
\frac{\partial^2}{\partial x^2} \rightarrow -k_r^2 \cos^2 \boldsymbol{q}, \quad \frac{\partial^2}{\partial y^2} \rightarrow -k_r^2 \sin^2 \boldsymbol{q}, \quad \frac{\partial^2}{\partial x \partial y} \rightarrow -k_r^2 \cos \boldsymbol{q} \sin \boldsymbol{q}
\tag{A.66}
$$

The dyadic is $\tilde{\tilde{G}}_m^{ME^{R}}$ is then mapped back into the spatial domain. To this end, the Weyl identity is used. The integral is reduced to a Sommerfeld integral by expressing the integral in cylindrical coordinates $(k_r, \boldsymbol{q})$. The $\boldsymbol{q}$ integrals can be performed analytically from the following identities:

$$\int_{q=0}^{2p} e^{-jk_r r\cos(q-f)}dq = 2p J_0\left(k_r r\right) \tag{A.67}$$

$$\int_{q=0}^{2p} \cos q\, e^{-jk_r r\cos(q-f)}dq = -2pj\cos f J_1\left(k_r r\right) \tag{A.68}$$

$$\int_{q=0}^{2p} \sin q\, e^{-jk_r r\cos(q-f)}dq = -2p\, j\sin f J_1\left(k_r r\right) \tag{A.69}$$

$$\int_{q=0}^{2p} \cos^2 q\, e^{-jk_r r\cos(q-f)}dq = \begin{cases} p\left[J_0\left(k_r r\right)-\cos\left(2f\right)J_2\left(k_r r\right)\right] \\ 2p\left[\cos^2 f\left(J_0\left(k_r r\right)-2\dfrac{J_1\left(k_r r\right)}{k_r r}\right)+\dfrac{J_1\left(k_r r\right)}{k_r r}\right] \end{cases} \tag{A.70}$$

$$\int_{q=0}^{2p} \sin^2 q\, e^{-jk_r r\cos(q-f)}dq = \begin{cases} p\left[J_0\left(k_r r\right)+\cos\left(2f\right)J_2\left(k_r r\right)\right] \\ 2p\left[\sin^2 f\left(J_0\left(k_r r\right)-2\dfrac{J_1\left(k_r r\right)}{k_r r}\right)+\dfrac{J_1\left(k_r r\right)}{k_r r}\right] \end{cases} \tag{A.71}$$

$$\int_{q=0}^{2p} \cos q\,\sin q\, e^{-jk_r r\cos(q-f)}dq = \begin{cases} -p\sin\left(2f\right)J_2\left(k_r r\right) \\ 2p\sin f\cos f\left(J_0\left(k_r r\right)-2\dfrac{J_1\left(k_r r\right)}{k_r r}\right) \end{cases} \tag{A.72}$$

where f is the observation angle defined such that and $\cos f = (x-x')/r, \sin f = (y-y')/r$. Two analytical forms for the integrals in (A.67) – (A.72) are provided. It is unclear if one offers any advantage over the other. In either case, the observation angle f is extracted from the Sommerfeld integral.

Finally,

$$\overline{\overline{G}}_m^{ME^R} = \begin{pmatrix} \sin^2 f S_1^{ME}\left(r\right)+S_2^{ME}\left(r\right) & -\sin f\cos f S_1^{ME}\left(r\right) & 0 \\ -\sin f\cos f S_1^{ME}\left(r\right) & \cos^2 f S_1^{ME}\left(r\right)+S_2^{ME}\left(r\right) & 0 \\ 0 & 0 & 0 \end{pmatrix} \tag{A.73}$$

A.2.1 A Total Field Representation for the Electric Field Dyadic Green Function

When a source is embedded in a thin dielectric region backed by a ground plane, there is the potential for significant rounding error to occur within the decoupled form of

the DGF presented in the previous section. The reason for this is that the reflected wave is nearly canceling the primary wave. This difference can be as many as 8 orders of magnitude smaller than the primary field. As a consequence, the reflected waves must be calculated to an extraordinary number of digits, requiring an inordinate amount of CPU time. Thus, splitting the field into primary and reflected waves loses its advantage. Rather different from Chew's paper [30], under such conditions, we superimpose the primary and reflected waves in the spectral domain. Thus, the Sommerfeld integrals can be performed to reasonable precision with reasonable CPU times. In this section, we will combine (A.32), (A.48) and (A.49) to transform the Dyadic Green function into a more convenient form to work with. We begin with (A.33), (A.48) and (A.49), which provide the differential operators for the *primary*, and *symmetric* and *asymmetric reflected* fields:

$$\hat{a} \cdot \mathbf{E}_m^P(\mathbf{r}) = iwm_m \left[\hat{a} \cdot \hat{a}' + \frac{1}{k_m^2} \hat{a} \cdot \nabla\nabla \cdot \hat{a}' \right] g_m^p(\mathbf{r},\mathbf{r}') \qquad (A.74)$$

$$\hat{a} \cdot \mathbf{E}_m^{RS} = \left[\hat{a} \cdot \hat{a}' + \frac{1}{k_m^2} \hat{a} \cdot \nabla\nabla \cdot \hat{a}' \right] g_m^{TM^{RS}} + (\hat{a} \cdot \hat{z} \times \nabla_t)(\hat{a}' \cdot \hat{z} \times \nabla_t) \left(\frac{\tilde{g}_m^{TM^{RS}} - \tilde{g}_m^{TE^{RS}}}{k_r^2} \right) \qquad (A.75)$$

$$\hat{a} \cdot \mathbf{E}_m^{RA} = \left[\hat{a} \cdot \hat{a}_I' + \frac{1}{k_m^2} \hat{a} \cdot \nabla\nabla \cdot \hat{a}_I' \right] g_m^{TM^{RA}} + (\hat{a} \cdot \hat{z} \times \nabla_t)(\hat{a}_I' \cdot \hat{z} \times \nabla_t) \left(\frac{\tilde{g}_m^{TM^{RA}} + \tilde{g}_m^{TE^{RA}}}{k_r^2} \right) \qquad (A.76)$$

Initially, the goal will be to express the $(\hat{a} \cdot \hat{z} \times \nabla_t)(\hat{a}' \cdot \hat{z} \times \nabla_t)$ operator in a more convenient form. We start out by expressing this term as a dyadic operator:

$$(\hat{a} \cdot \hat{z} \times \nabla_t)(\hat{a}' \cdot \hat{z} \times \nabla_t) = \hat{a} \cdot \begin{bmatrix} \dfrac{\partial^2}{\partial y^2}\hat{x}\hat{x} & -\dfrac{\partial^2}{\partial x \partial y}\hat{x}\hat{y} & 0 \\[3mm] -\dfrac{\partial^2}{\partial x \partial y}\hat{y}\hat{x} & \dfrac{\partial^2}{\partial x^2}\hat{y}\hat{y} & 0 \\[3mm] 0 & 0 & 0 \end{bmatrix} \cdot \hat{a}'. \qquad (A.77)$$

This is then expressed in the spectral domain as:

$$\hat{a} \cdot \begin{bmatrix} -k_y^2\hat{x}\hat{x} & k_x k_y \hat{x}\hat{y} & 0 \\ k_x k_y \hat{y}\hat{x} & -k_x^2\hat{y}\hat{y} & 0 \\ 0 & 0 & 0 \end{bmatrix} \cdot \hat{a}' \qquad (A.78)$$

99

The dispersion relationship dictates that $k_x^2 = k_\mathbf{r}^2 - k_y^2$ and $k_y^2 = k_\mathbf{r}^2 - k_x^2$. Therefore, (A.78) can be expressed as:

$$\hat{\boldsymbol{a}} \cdot \begin{bmatrix} -k_\mathbf{r}^2 \hat{x}\hat{x} & 0 & 0 \\ 0 & -k_\mathbf{r}^2 \hat{y}\hat{y} & 0 \\ 0 & 0 & 0 \end{bmatrix} \cdot \hat{\boldsymbol{a}}' + \hat{\boldsymbol{a}} \cdot \begin{bmatrix} k_x^2 \hat{x}\hat{x} & k_x k_y \hat{x}\hat{y} & 0 \\ k_x k_y \hat{y}\hat{x} & k_x^2 \hat{y}\hat{y} & 0 \\ 0 & 0 & 0 \end{bmatrix} \cdot \hat{\boldsymbol{a}}'. \tag{A.79}$$

This is then mapped back into the spatial domain as:

$$-k_\mathbf{r}^2 \hat{\boldsymbol{a}}_t \cdot \hat{\boldsymbol{a}}_t' - \hat{\boldsymbol{a}} \cdot \nabla_t \nabla_t \cdot \hat{\boldsymbol{a}}', \tag{A.80}$$

where ∇_t represents the gradient operator along the transverse direction only. Therefore, we conclude that:

$$\left(\hat{\boldsymbol{a}} \cdot \hat{z} \times \nabla_t\right)\left(\hat{\boldsymbol{a}}' \cdot \hat{z} \times \nabla_t\right) = -k_\mathbf{r}^2 \hat{\boldsymbol{a}}_t \cdot \hat{\boldsymbol{a}}_t' - \hat{\boldsymbol{a}} \cdot \nabla_t \nabla_t \cdot \hat{\boldsymbol{a}}' \tag{A.81}$$

Similarly, we can show that:

$$\left(\hat{\boldsymbol{a}} \cdot \hat{z} \times \nabla_t\right)\left(\hat{\boldsymbol{a}}_I' \cdot \hat{z} \times \nabla_t\right) = k_\mathbf{r}^2 \hat{\boldsymbol{a}}_t \cdot \hat{\boldsymbol{a}}_t' + \hat{\boldsymbol{a}} \cdot \nabla_t \nabla_t \cdot \hat{\boldsymbol{a}}'. \tag{A.82}$$

Combining the leading terms of (A.81) and (A.75), it is found that:

$$\hat{\boldsymbol{a}} \cdot \hat{\boldsymbol{a}}' g_m^{TM^{RS}} - k_\mathbf{r}^2 \hat{\boldsymbol{a}}_t \cdot \hat{\boldsymbol{a}}_t' \left(\frac{\tilde{g}_m^{TM^{RS}} - \tilde{g}_m^{TE^{RS}}}{k_\mathbf{r}^2} \right) = \hat{\boldsymbol{a}} \cdot \begin{bmatrix} \tilde{g}_m^{TE^{RS}} \hat{x}\hat{x} & 0 & 0 \\ 0 & \tilde{g}_m^{TE^{RS}} \hat{y}\hat{y} & 0 \\ 0 & 0 & g_m^{TM^{RS}} \hat{z}\hat{z} \end{bmatrix} \cdot \hat{\boldsymbol{a}}' \tag{A.83}$$

and from (A.82) and (A.76):

$$\hat{\boldsymbol{a}} \cdot \hat{\boldsymbol{a}}_I' g_m^{TM^{RA}} + k_\mathbf{r}^2 \hat{\boldsymbol{a}}_t \cdot \hat{\boldsymbol{a}}_t' \left(\frac{\tilde{g}_m^{TM^{RA}} + \tilde{g}_m^{TE^{RA}}}{k_\mathbf{r}^2} \right) = \hat{\boldsymbol{a}} \cdot \begin{bmatrix} \tilde{g}_m^{TE^{RA}} \hat{x}\hat{x} & 0 & 0 \\ 0 & \tilde{g}_m^{TE^{RA}} \hat{y}\hat{y} & 0 \\ 0 & 0 & g_m^{TM^{RA}} \hat{z}\hat{z} \end{bmatrix} \cdot \hat{\boldsymbol{a}}'. \tag{A.84}$$

Then, combining the leading terms in (A.74) - (A.76) and using (A.83) and (A.84), leads to:

100

$$
\hat{\boldsymbol{a}} \cdot \begin{bmatrix} \tilde{g}_m^P + \tilde{g}_m^{TE^{RS}} + \tilde{g}_m^{TE^{RA}} \hat{x}\hat{x} & 0 & 0 \\ 0 & \tilde{g}_m^P + \tilde{g}_m^{TE^{RS}} + \tilde{g}_m^{TE^{RA}} \hat{y}\hat{y} & 0 \\ 0 & 0 & \tilde{g}_m^P + \tilde{g}_m^{TM^{RS}} + \tilde{g}_m^{TM^{RA}} \hat{z}\hat{z} \end{bmatrix} \cdot \hat{\boldsymbol{a}}'
$$

$$
= \hat{\boldsymbol{a}} \cdot \begin{bmatrix} g_{h_m}^{TE} \hat{x}\hat{x} & 0 & 0 \\ 0 & g_{h_m}^{TE} \hat{y}\hat{y} & 0 \\ 0 & 0 & g_{v_m}^{TM} \hat{z}\hat{z} \end{bmatrix} \cdot \hat{\boldsymbol{a}}'
$$

(A.85)

Next, the $\hat{\boldsymbol{a}} \cdot \nabla \nabla \cdot \hat{\boldsymbol{a}}'$ terms in (A.74) - (A.76) and the $\hat{\boldsymbol{a}} \cdot \nabla_t \nabla_t \cdot \hat{\boldsymbol{a}}'$ terms in (A.81) and (A.82) are combined. Before doing so, the following identities are realized:

$$
\hat{\boldsymbol{a}} \cdot \nabla \nabla \cdot \hat{\boldsymbol{a}}' = \hat{\boldsymbol{a}} \cdot \nabla \nabla_t \cdot \hat{\boldsymbol{a}}' + \hat{\boldsymbol{a}} \cdot \nabla \nabla_z \cdot \hat{\boldsymbol{a}}'
$$

(A.86)

$$
\left(\hat{\boldsymbol{a}} \cdot \nabla \nabla \cdot \hat{\boldsymbol{a}}'_I \right)^{RA} = -\hat{\boldsymbol{a}} \cdot \nabla \nabla_t \cdot \hat{\boldsymbol{a}}' - \hat{\boldsymbol{a}} \cdot \nabla \nabla_z \cdot \hat{\boldsymbol{a}}'
$$

(A.87)

$$
\hat{\boldsymbol{a}} \cdot \nabla_t \nabla_t \cdot \hat{\boldsymbol{a}}' = \hat{\boldsymbol{a}} \cdot \nabla \nabla_t \cdot \hat{\boldsymbol{a}}' - \hat{\boldsymbol{a}} \cdot \nabla_z \nabla_t \cdot \hat{\boldsymbol{a}}'
$$

(A.88)

where $\nabla_z = \hat{z} \dfrac{\partial}{\partial z}$. Note that the term $\left(\hat{\boldsymbol{a}} \cdot \nabla \nabla_z \cdot \hat{\boldsymbol{a}}' \right)^{RA}$ of (A.87) is the *asymmetric* term that contributes to the scalar potential term in the MPIE. Note that the second term in (A.87) from the image is negative. This term represents the image of the electric charge density, which distribute the charge uniformly for transverse and vertical currents. Subsequently, we combine the terms from (A.74) - (A.76) and (A.81) - (A.82), which leads to:

101

$$\frac{1}{k_m^2}\hat{\pmb{a}}\cdot\nabla\nabla_t\cdot\hat{\pmb{a}}'\tilde{g}_m^p+\frac{1}{k_m^2}\hat{\pmb{a}}\cdot\nabla\nabla_t\cdot\hat{\pmb{a}}'\tilde{g}_m^{TM^{RS}}-\frac{1}{k_m^2}\hat{\pmb{a}}\cdot\nabla\nabla_t\cdot\hat{\pmb{a}}'\tilde{g}_m^{TM^{RA}}$$

$$+\frac{1}{k_m^2}\hat{\pmb{a}}\cdot\nabla\nabla_z\cdot\hat{\pmb{a}}'\tilde{g}_m^p+\frac{1}{k_m^2}\hat{\pmb{a}}\cdot\nabla\nabla_z\cdot\hat{\pmb{a}}'\tilde{g}_m^{TM^{RS}}-\frac{1}{k_m^2}\hat{\pmb{a}}\cdot\nabla\nabla_z\cdot\hat{\pmb{a}}'\tilde{g}_m^{TM^{RA}}$$

$$+\hat{\pmb{a}}\cdot\nabla\nabla_t\cdot\hat{\pmb{a}}'\left(-\frac{\tilde{g}_m^{TM^{RS}}-\tilde{g}_m^{TE^{RS}}}{k_{\mathbf{r}}^2}+\frac{\tilde{g}_m^{TM^{RA}}+\tilde{g}_m^{TE^{RA}}}{k_{\mathbf{r}}^2}\right)+\hat{\pmb{a}}\cdot\nabla_z\nabla_t\cdot\hat{\pmb{a}}'\left(\frac{\tilde{g}_m^{TM^{RS}}-\tilde{g}_m^{TE^{RS}}}{k_{\mathbf{r}}^2}-\frac{\tilde{g}_m^{TM^{RA}}+\tilde{g}_m^{TE^{RA}}}{k_{\mathbf{r}}^2}\right)$$

$$=\frac{1}{k_m^2}\hat{\pmb{a}}\cdot\nabla\nabla_t\cdot\hat{\pmb{a}}'\left(\tilde{g}_m^p+\frac{k_m^2\tilde{g}_{h_m}^{TE^R}-k_{m,z}^2\tilde{g}_{h_m}^{TM^R}}{k_{\mathbf{r}}^2}\right)+\frac{1}{k_m^2}\hat{\pmb{a}}\cdot\nabla\nabla_z\cdot\hat{\pmb{a}}'\left(\tilde{g}_m^p+\tilde{g}_{h_m}^{TM^R}\right)$$

$$+\hat{\pmb{a}}\cdot\begin{pmatrix}0 & 0 & 0\\ 0 & 0 & 0\\ \cos\pmb{a}\,\hat{z}\hat{x} & \sin\pmb{a}\,\hat{z}\hat{y} & 0\end{pmatrix}\cdot\hat{\pmb{a}}'ik_{\mathbf{r}}\frac{\partial}{\partial z}\left(\frac{g_{h_m}^{TM^R}-g_{h_m}^{TE^R}}{k_{\mathbf{r}}^2}\right)$$

$$(A.89)$$

where the relationship $1/k_{\mathbf{r}}^2-1/k_m^2=k_{m,z}^2/k_{\mathbf{r}}^2k_m^2$ is used. Finally, combining (A.85) and (A.89) leads to the relationship:

$$\hat{\pmb{a}}\cdot\mathbf{E}_M(\mathbf{r})=$$

$$\hat{\pmb{a}}\cdot\begin{bmatrix}\tilde{G}_{xx_m}^{EJ}\,\hat{x}\hat{x} & 0 & 0\\ 0 & \tilde{G}_{xx_m}^{EJ}\,\hat{y}\hat{y} & 0\\ \tilde{G}_{zx_m}^{EJ}\,\hat{z}\hat{x} & \tilde{G}_{zy_m}^{EJ}\,\hat{z}\hat{y} & \tilde{G}_{zz_m}^{EJ}\,\hat{z}\hat{z}\end{bmatrix}\cdot\hat{\pmb{a}}'+\frac{1}{k_m^2}\hat{\pmb{a}}\cdot\nabla\nabla_t\cdot\hat{\pmb{a}}'\tilde{G}_{V_{t_m}}^{EJ}+\frac{1}{k_m^2}\hat{\pmb{a}}\cdot\nabla\nabla_z\cdot\hat{\pmb{a}}'\tilde{G}_{V_{z_m}}^{EJ}\quad(A.90)$$

where

$$\tilde{G}_{xx_m}^{EJ}=\tilde{g}_{h_m}^{TE},\ \tilde{G}_{zz_m}^{EJ}=\tilde{g}_{v_m}^{TM},\tag{A.91}$$

$$\tilde{G}_{V_{t_m}}^{EJ}=\tilde{g}_m^p+\frac{k_m^2\tilde{g}_{h_m}^{TE^R}-k_{m,z}^2\tilde{g}_{h_m}^{TM^R}}{k_{\mathbf{r}}^2},\ \tilde{G}_{V_{z_m}}^{EJ}=\tilde{g}_{h_m}^{TM}\tag{A.92}$$

$$\tilde{G}_{zx_m}^{EJ}=\cos\pmb{a}\,\tilde{g}_{zt_m}^{EJ},\ \tilde{G}_{zy_m}^{EJ}=\sin\pmb{a}\,\tilde{g}_{zt_m}^{EJ},\ \tilde{g}_{zt_m}^{EJ}=-jk_{\mathbf{r}}\frac{\partial}{\partial z}\left(\frac{\tilde{g}_{h_m}^{TM^R}-\tilde{g}_{h_m}^{TE^R}}{k_{\mathbf{r}}^2}\right)\tag{A.93}$$

From (A.90), it is evident that this formulation will only be directly applicable to current densities that are either purely transverse or purely vertical. A more general form that handles an arbitrary current density will require further derivation. Nevertheless, the present form is still applicable under many circumstances and has much merit.

The next step is to derive the Sommerfeld integrals used to strictly express (A.90) in the physical spatial domain. Observing (A.91) – (A.93), five Sommerfeld integrals are required:

$$G_{xx_m}^{EJ} = g_{h_m}^{TE} = \frac{-w m_m I}{4p} \int_0^\infty J_0(k_r r) \frac{k_r}{k_{m,z}} \left[e^{-jk_{m,z}|z-z'|} + \tilde{B}_m^{TE} e^{jk_{m,z}z} + \tilde{D}_m^{TE} e^{-jk_{m,z}z} \right] dk_r . \qquad (A.94)$$

Next, from (A.92), (A.29) and (A.30):

$$G_{V_{t_m}}^{EJ} = \frac{-w m_m I}{4p} \int_0^\infty \frac{J_0(k_r r)}{k_r k_{m,z}} \left[\begin{array}{c} k_r^2 e^{-jk_{m,z}|z-z'|} + \left(k_m^2 \tilde{B}_m^{TE} - k_{m,z}^2 \tilde{E}_m^{TM} \right) e^{jk_{m,z}z} \\ + \left(k_m^2 \tilde{D}_m^{TE} - k_{m,z}^2 \tilde{F}_m^{TM} \right) e^{-jk_{m,z}z} \end{array} \right] dk_r \qquad (A.95)$$

From (A.12), (A.91), and

$$G_{zz_m}^{EJ} = g_{v_m}^{TM} = \frac{-w m_m I}{4p} \int_0^\infty J_0(k_r r) \frac{k_r}{k_{m,z}} \left[e^{-jk_{m,z}|z-z'|} + \tilde{B}_m^{TM} e^{jk_{m,z}z} + \tilde{D}_m^{TM} e^{-jk_{m,z}z} \right] dk_r . \qquad (A.96)$$

$$G_{vz_m}^{EJ} = g_{h_m}^{TM} = \frac{-w m_m I}{4p} \int_0^\infty J_0(k_r r) \frac{k_r}{k_{m,z}} \left[e^{-jk_{m,z}|z-z'|} + \tilde{E}_m^{TM} e^{jk_{m,z}z} + \tilde{F}_m^{TM} e^{-jk_{m,z}z} \right] dk_r \qquad (A.97)$$

Finally, from (A.93) (A.29), (A.30), (A.68), and (A.69):

$$G_{zt_m}^{EJ} = \frac{-jw m_m I}{4p} \int_0^\infty J_1(k_r r) \left[-\left(\tilde{E}_m^{TM} - \tilde{B}_m^{TE} \right) e^{jk_{mz}z} + \left(\tilde{F}_m^{TM} - \tilde{D}_m^{TE} \right) e^{-jk_{m,z}z} \right] dk_r \qquad (A.98)$$

and

$$G_{zx_m}^{EJ} = \cos f G_{zt_m}^{EJ}, \quad G_{zy_m}^{EJ} = \sin f G_{zt_m}^{EJ} . \qquad (A.99)$$

At this point, we can express an integral operator based on (A.90) assuming a Galerkin formulation. To this end, we expand the current with basis functions and perform the inner product of the electric field with a test function. Thus, from (A.90), this leads to:

$$\int_{S_m} \vec{T}_m(\vec{r}) \cdot \mathbf{E}_m^{RS} ds = \int_{S_m} \int_{S'_n} \left[\vec{T}_m(\vec{r}) \cdot \overline{\overline{G}}_m^{EJ} \cdot \vec{J}_n(\vec{r}') + \frac{1}{k_m^2} \vec{T}_m(\vec{r}) \cdot \nabla \nabla \cdot \vec{J}_n(\vec{r}') \overline{G}_V^{EJ} \right] ds' ds \qquad (A.100)$$

where

103

$$\overline{\overline{G}}_m^{EJ} = \begin{bmatrix} G_{xx_m}^{EJ}\hat{x}\hat{x} & 0 & 0 \\ 0 & G_{xx_m}^{EJ}\hat{y}\hat{y} & 0 \\ \cos \boldsymbol{f} g_{zt_m}^{EJ}\hat{z}\hat{x} & \sin \boldsymbol{f} g_{zt_m}^{EJ}\hat{z}\hat{y} & G_{zz_m}^{EJ}\hat{z}\hat{z} \end{bmatrix} \tag{A.101}$$

and

$$\overline{G}_V^{EJ} = \begin{cases} G_{V_{t_m}}^{EJ} & \text{for } \vec{J}_t \\ G_{V_{z_m}}^{EJ} & \text{for } \vec{J}_z \end{cases} . \tag{A.102}$$

Finally, the derivatives can then be moved onto the test or basis function, leading to:

$$\int_{S_m} \vec{T}_m(\vec{r}) \cdot \mathbf{E}_m^{RS} ds = \int_{S_m} \int_{S_n'} \left[\vec{T}_m(\vec{r}) \cdot \overline{\overline{G}}_m^{EJ} \cdot \vec{J}_n(\vec{r}') - \frac{1}{k_m^2} \nabla \cdot \vec{T}_m(\vec{r}) \nabla' \cdot \vec{J}_n(\vec{r}') \overline{G}_V^{EJ} \right] ds' ds \tag{A.103}$$

where for this to be valid $\vec{J}_n$ must be either purely horizontal or vertical.

Given the final forms of the layered Green's function, the choice of sign for the scalar potential term $\hat{a} \cdot \nabla \nabla_z \cdot \hat{a}'$ in (A.87) can be validated by applying the Lorentz Gauge. The definition of the Lorentz Gauge that is defined as:

$$\nabla \cdot \vec{A}(\vec{r}) = -j \boldsymbol{wme} \Phi(\vec{r}) \tag{A.104}$$

where $\vec{A}(\vec{r})$ and $\Phi(\vec{r})$ are the vector and scalar potentials, respectively, defined as:

$$\vec{A}(\vec{r}) = \int_V d\vec{r}' \overline{G}^A(\vec{r},\vec{r}') \cdot \vec{J}(\vec{r}')$$
$$\Phi(\vec{r}) = \int_V d\vec{r}' G^q(\vec{r},\vec{r}') \boldsymbol{r}(\vec{r}') \tag{A.105}$$

where $\boldsymbol{r}$ is the total charge density and $\vec{J}$ is the surface electric current density on the conducting surface. Applying the continuity equation:

$$\nabla' \cdot \vec{J}(\vec{r}') = -j \boldsymbol{wr}(\vec{r}') \tag{A.106}$$

and some manipulation using some vector identities [97], we can show that:

$$\nabla \cdot \overline{G}^A(\vec{r},\vec{r}') = -\boldsymbol{me} \nabla' G^q(\vec{r},\vec{r}') \tag{A.107}$$

For a z-directed field, (A.107) can be rewritten as:

$$\frac{\partial}{\partial z}\tilde{G}_{vz} = -\frac{w^2}{k_{i,z}^2}\frac{\partial}{\partial z}\tilde{G}_{zz} \tag{A.108}$$

Equation (A.108) relates the vector and scalar potential for a vertical electric dipole. Finally we can show that the vector potential and scalar potential derived in (A.91) and (A.92) satisfy (A.108).

A.3 Observation field in the ith layer

In this section, we consider the case when the source and observation coordinates are in different layers. For distinction, let the observation point lie in layer i, and the source point lie in layer m. Further, we will distinguish between observation layers that are above the source layer (i.e., $i < m$ and $z > z'$) and observation layers that are below the source layer (i.e., $i > m$ and $z < z'$).

A.3.1 A Total Field Representation for the Electric Field Dyadic Green Function

Initially, consider the situation when the observation layer is above the source layer $(i < m)$. In this region, the vertical electric and magnetic fields in the k-space are expressed as:

$$\tilde{E}_z^{i<} = \hat{z}\cdot\hat{\boldsymbol{a}}'\left(1+\frac{1}{k_i^2}\frac{\partial^2}{\partial z^2}\right)\tilde{g}_{v_i}^{TM<} + \frac{1}{k_i^2}\frac{\partial}{\partial z}\nabla\cdot\hat{\boldsymbol{a}}'\tilde{g}_{h_i}^{TM<} \tag{A.109}$$

$$\tilde{H}_z^{i<} = \hat{z}\cdot\nabla_t\times\hat{\boldsymbol{a}}'\frac{\tilde{g}_{h_i}^{TE<}}{-jw\boldsymbol{m}_i} \tag{A.110}$$

where the k-space Green's function are defined as:

$$\tilde{g}_{v_i}^{TM<} = \frac{-w\boldsymbol{m}_i I}{8\boldsymbol{p}^2}\frac{e^{-j\mathbf{k}_t\cdot(\mathbf{r}_t-\mathbf{r}_t')}}{k_{m,z}}\tilde{A}_i^{TM<}e^{-jk_{i,z}d_i}\left[e^{-jk_{i,z}z}+\tilde{R}_{i,i-1}^{TM}e^{2jk_{i,z}d_{i-1}}e^{jk_{i,z}z}\right] \tag{A.111}$$

$$\tilde{g}_{h_i}^{TM<} = \frac{-w\boldsymbol{m}_i I}{8\boldsymbol{p}^2}\frac{e^{-j\mathbf{k}_t\cdot(\mathbf{r}_t-\mathbf{r}_t')}}{k_{m,z}}\frac{k_{m,z}}{k_{i,z}}\tilde{C}_i^{TM<}e^{-jk_{i,z}d_i}\left[e^{-jk_{i,z}z}-\tilde{R}_{i,i-1}^{TM}e^{2jk_{i,z}d_{i-1}}e^{jk_{i,z}z}\right] \tag{A.112}$$

$$\tilde{g}_{h_i}^{TE<} = \frac{-w\boldsymbol{m}_i I}{8\boldsymbol{p}^2}\frac{e^{-j\mathbf{k}_t\cdot(\mathbf{r}_t-\mathbf{r}_t')}}{k_{m,z}}\frac{\boldsymbol{m}_m}{\boldsymbol{m}_i}\tilde{A}_i^{TE<}e^{-jk_{i,z}d_i}\left[e^{-jk_{i,z}z}+\tilde{R}_{i,i-1}^{TE}e^{2jk_{i,z}d_{i-1}}e^{jk_{i,z}z}\right] \tag{A.113}$$

where

$$\tilde{A}_i^{TM/TE^<} = \tilde{T}_{m,i}^{TM/TE^<} e^{jk_{m,z}d_{m-1}} \left[e^{jk_{m,z}z'} + \tilde{D}_m^{TM/TE} \right],$$ (A.114)

$$\tilde{C}_i^{TM^<} = \tilde{T}_{m,i}^{TM^<} e^{jk_{m,z}d_{m-1}} \left[e^{jk_{m,z}z'} + \tilde{F}_m^{TM} \right],$$ (A.115)

$$\tilde{T}_{m,i}^{TM/TE^<} = \prod_{\substack{j=m \\ (i<m)}}^{i+1} S_{j,j-1}^{TM/TE^<} \Theta_j$$ (A.116)

$$S_{j,j-1}^{TM/TE^<} = \frac{T_{j,j-1}^{TM/TE}}{1 + R_{j,j-1}^{TM/TE} \tilde{R}_{j-1,j-2}^{TM/TE} e^{-2jk_{j-1,z}\left(d_{j-1}-d_{j-2}\right)}}$$ (A.117)

$$\Theta_l = \begin{cases} 1 & , l = m \\ e^{jk_{l,z}\left(d_{l-1}-d_l\right)} & , l \neq m \end{cases}$$ (A.118)

where, the indices of the product symbol in (A.116) are stepped with -1. It is noted that $\tilde{A}_i^{TM/TE^<}$ and $\tilde{C}_i^{TM^<}$ can be further simplified by plugging in the values from (A.16) and (A.18) for $\tilde{D}_m^{TM/TE}$ and $\tilde{F}_m^{TM}$, respectively. Then, after applying the identity:

$$e^{jk_{m,z}z'} + \tilde{M}_m^{TM/TE} \tilde{R}_{m,m+1}^{TM/TE} \tilde{R}_{m,m-1}^{TM/TE} e^{-2jk_{m,z}\left(d_m-d_{m-1}\right)} e^{jk_{m,z}z'} = \tilde{M}_m^{TM/TE} e^{jk_{m,z}z'}$$ (A.119)

$\tilde{A}_i^{TM/TE^<}$ and $\tilde{C}_i^{TM^<}$ can be rewritten as

$$\tilde{A}_i^{TM/TE^<} = \tilde{T}_{m,i}^{TM/TE^<} e^{jk_{m,z}d_{m-1}} \left[e^{jk_{m,z}z'} + \tilde{R}_{m,m+1}^{TM/TE} e^{-2jk_{m,z}d_m} e^{-jk_{m,z}z'} \right] \tilde{M}_m^{TM/TE}$$ (A.120)

$$\tilde{C}_i^{TM^<} = \tilde{T}_{m,i}^{TM^<} e^{jk_{m,z}d_{m-1}} \left[e^{jk_{m,z}z'} - \tilde{R}_{m,m+1}^{TM} e^{-2jk_{m,z}d_m} e^{-jk_{m,z}z'} \right] \tilde{M}_m^{TM}$$ (A.121)

In the region $i > m$ ($z < z'$), the fields in the k-space are expressed as:

$$\tilde{E}_z^{i^>} = \hat{z} \cdot \hat{\boldsymbol{a}}' \left(1 + \frac{1}{k_i^2} \frac{\partial^2}{\partial z^2} \right) \tilde{g}_{v_i}^{TM^>} + \frac{1}{k_i^2} \frac{\partial}{\partial z} \nabla \cdot \hat{\boldsymbol{a}}' \tilde{g}_{h_i}^{TM^>}$$ (A.122)

$$\tilde{H}_z^{i^>} = \hat{z} \cdot \nabla_t \times \hat{\boldsymbol{a}}' \frac{\tilde{g}_{h_i}^{TE^>}}{-jw m_i}$$ (A.123)

where the k-space Green's function are defined as:

$$\tilde{g}_{v_i}^{TM^>} = \frac{-\boldsymbol{wm}_i I}{8\boldsymbol{p}^2} \frac{e^{-j\mathbf{k}_i\cdot(\mathbf{r}_t-\mathbf{r}_t')}}{k_{m,z}} \tilde{A}_i^{TM^>} e^{jk_{i,z}d_{i-1}} \left[e^{jk_{i,z}z} + \tilde{R}_{i,i+1}^{TM} e^{-2jk_{i,z}d_i} e^{-jk_{i,z}z} \right] \tag{A.124}$$

$$\tilde{g}_{h_i}^{TM^>} = \frac{-\boldsymbol{wm}_i I}{8\boldsymbol{p}^2} \frac{e^{-j\mathbf{k}_i\cdot(\mathbf{r}_t-\mathbf{r}_t')}}{k_{m,z}} \frac{k_{m,z}}{k_{i,z}} \tilde{C}_i^{TM^>} e^{jk_{i,z}d_{i-1}} \left[e^{jk_{i,z}z} - \tilde{R}_{i,i+1}^{TM} e^{-2jk_{i,z}d_i} e^{-jk_{i,z}z} \right] \tag{A.125}$$

$$\tilde{g}_{h_i}^{TE^>} = \frac{-\boldsymbol{wm}_i I}{8\boldsymbol{p}^2} \frac{e^{-j\mathbf{k}_i\cdot(\mathbf{r}_t-\mathbf{r}_t')}}{k_{m,z}} \frac{\boldsymbol{m}_m}{\boldsymbol{m}_i} \tilde{A}_i^{TE^>} e^{jk_{i,z}d_{i-1}} \left[e^{jk_{i,z}z} + \tilde{R}_{i,i+1}^{TE} e^{-2jk_{i,z}d_i} e^{-jk_{i,z}z} \right] \tag{A.126}$$

where,

$$\tilde{A}_i^{TM/TE^>} = \tilde{T}_{m,i}^{TM/TE^>} e^{-jk_{m,z}d_m} \left[e^{-jk_{m,z}z'} + \tilde{B}_m^{TM} \right], \tag{A.127}$$

$$\tilde{C}_i^{TM^>} = \tilde{T}_{m,i}^{TM^>} e^{-jk_{m,z}d_m} \left[e^{-jk_{m,z}z'} + \tilde{E}_m^{TM} \right] \tag{A.128}$$

$$\tilde{T}_{m,i}^{TM/TE^>} = \prod_{j=m}^{i-1} S_{j,j+1}^{TM/TE^>} \Theta_j \tag{A.129}$$

$$S_{l,l+1}^{TM/TE^>} = \frac{T_{l,l+1}^{TM/TE}}{1 + R_{l,l+1}^{TM/TE} \tilde{R}_{l+1,l+2}^{TM/TE} e^{-2jk_{l+1,z}(d_{l+1}-d_l)}} \tag{A.130}$$

and Θ_j is detailed in (A.118). Again, substituting in for $\tilde{B}_m^{TM}$ and $\tilde{E}_m^{TM}$ from (A.15) and (A.17), respectively, (A.127) and (A.128) can be expressed as:

$$\tilde{A}_i^{TM/TE^>} = \tilde{T}_{m,i}^{TM/TE^>} e^{-jk_{m,z}d_m} \left[e^{-jk_{m,z}z'} + \tilde{R}_{m,m-1}^{TM/TE} e^{j2k_{m,z}d_{m-1}} e^{jk_{m,z}z'} \right] \tilde{M}_m^{TM/TE} \tag{A.131}$$

$$\tilde{C}_i^{TM^>} = \tilde{T}_{m,i}^{TM^>} e^{-jk_{m,z}d_m} \left[e^{-jk_{m,z}z'} - \tilde{R}_{m,m-1}^{TM} e^{j2k_{m,z}d_{m-1}} e^{jk_{m,z}z'} \right] \tilde{M}_m^{TM} \tag{A.132}$$

Once again, it is desirable to derive a symmetric operator for the transmitted waves in the ith region. To this end, the spectral domain Green's function will again be segregated into symmetric and anti-symmetric components:

$$\begin{aligned}
\tilde{g}_{v_i}^{TM^{<\!/\!>}} &= \tilde{g}_{i^{<\!/\!>}}^{TM^{TS}} + \tilde{g}_{i^{<\!/\!>}}^{TM^{TA}} \\
\tilde{g}_{h_i}^{TM^{<\!/\!>}} &= \frac{k_{m,z}}{k_{i,z}} \left(\tilde{g}_{i^{<\!/\!>}}^{TM^{TS}} - \tilde{g}_{i^{<\!/\!>}}^{TM^{TA}} \right) \\
\tilde{g}_{h_i}^{TE^{<\!/\!>}} &= \frac{\boldsymbol{m}_m}{\boldsymbol{m}_i} \left(\tilde{g}_{i^{<\!/\!>}}^{TE^{TS}} + \tilde{g}_{i^{<\!/\!>}}^{TE^{TA}} \right)
\end{aligned} \tag{A.133}$$

where, from (A.111) - (A.121):

$$\tilde{g}_{i^<}^{TM/TE^{TS}} = \frac{-w m_i I}{8p^2} \frac{e^{-j\mathbf{k}_i \cdot (\mathbf{r}_t - \mathbf{r}_t')}}{k_{m,z}} \cdot$$

$$\tilde{T}_{m,i}^{TM/TE^<} \left[e^{-jk_{i,z}(z+d_i)} e^{jk_{m,z}(z'+d_{m-1})} + \tilde{R}_{i,i-1}^{TM/TE} e^{jk_{i,z}(2d_{i-1}-d_i+z)} \tilde{R}_{m,m+1}^{TM \, TE} e^{-jk_{m,z}(2d_m-d_{m-1}+z')} \right] \tilde{M}_m^{TM TE} \tag{A.134}$$

$$\tilde{g}_{i^<}^{TM TE^{TA}} = \frac{-w m_i I}{8p^2} \frac{e^{-j\mathbf{k}_i \cdot (\mathbf{r}_t - \mathbf{r}_t')}}{k_{m,z}} \cdot$$

$$\tilde{T}_{m,i}^{TM/TE^<} \left[e^{-jk_{i,z}(z+d_i)} \tilde{R}_{m,m+1}^{TM/TE} e^{-jk_{m,z}(2d_m-d_{m-1}+z')} + e^{jk_{m,z}(z'+d_{m-1})} \tilde{R}_{i,i-1}^{TM/TE} e^{jk_{i,z}(2d_{i-1}-d_i+z)} \right] \tilde{M}_m^{TM/TE} \tag{A.135}$$

Similarly, from (A.124) - (A.132):

$$\tilde{g}_{i^>}^{TM TE^{TS}} = \frac{-w m_i I}{8p^2} \frac{e^{-j\mathbf{k}_i \cdot (\mathbf{r}_t - \mathbf{r}_t')}}{k_{m,z}} \cdot$$

$$\tilde{T}_{m,i}^{TM/TE^>} \left[e^{jk_{i,z}(z+d_{i-1})} e^{-jk_{m,z}(z'+d_m)} + \tilde{R}_{i,i+1}^{TM \, TE} e^{-jk_{i,z}(2d_i-d_{i-1}+z)} \tilde{R}_{m,m-1}^{TM/TE} e^{jk_{m,z}(2d_{m-1}-d_m+z')} \right] \tilde{M}_m^{TM TE} \tag{A.136}$$

$$\tilde{g}_{i^>}^{TM TE^{TA}} = \frac{-w m_i I}{8p^2} \frac{e^{-j\mathbf{k}_i \cdot (\mathbf{r}_t - \mathbf{r}_t')}}{k_{m,z}} \cdot$$

$$\tilde{T}_{m,i}^{TM TE^>} \left[e^{jk_{i,z}(z+d_{i-1})} \tilde{R}_{m,m-1}^{TM/TE} e^{jk_{m,z}(2d_{m-1}-d_m+z')} + e^{-jk_{m,z}(z'+d_m)} \tilde{R}_{i,i+1}^{TM/TE} e^{-jk_{i,z}(2d_i-d_{i-1}+z)} \right] \tilde{M}_m^{TM TE} \tag{A.137}$$

The vertical electric and magnetic fields radiated in the *i*-th region due to the symmetric and anti-symmetric parts of the Green's function are defined as:

$$\tilde{E}_z^{i^{TS^{<>}}} = \hat{z} \cdot \hat{\mathbf{a}}' \left(1 + \frac{1}{k_i^2} \frac{\partial^2}{\partial z^2} \right) \tilde{g}_{i^{<>}}^{TM^{TS}} + \frac{1}{k_i^2} \frac{\partial}{\partial z} \nabla_t \cdot \hat{\mathbf{a}}_2' \tilde{g}_{i^{<>}}^{TM^{TS}} \tag{A.138}$$

$$\tilde{H}_z^{i^{TS^{<>}}} = \hat{z} \cdot \nabla_t \times \hat{\mathbf{a}}_2' \left(\frac{k_{i,z}}{k_{m,z}} \frac{m_m}{m_i} \right) \left(\frac{\tilde{g}_{h_i}^{TE^{TS}}}{-jwm_i} \right) \tag{A.139}$$

$$\tilde{E}_z^{i^{TA^{<>}}} = \hat{z} \cdot \hat{\mathbf{a}}' \left(1 + \frac{1}{k_i^2} \frac{\partial^2}{\partial z^2} \right) \tilde{g}_{i^{<>}}^{TM^{TA}} + \frac{1}{k_i^2} \frac{\partial}{\partial z} \nabla \cdot \hat{\mathbf{a}}_{2I}' \tilde{g}_{i^{<>}}^{TM^{TA}} \tag{A.140}$$

$$\tilde{H}_z^{i^{TS^{<>}}} = -\hat{z} \cdot \nabla_t \times \hat{\mathbf{a}}_{2I}' \left(\frac{k_{i,z}}{k_{m,z}} \frac{m_m}{m_i} \right) \left(\frac{\tilde{g}_{h_i}^{TE^{TS}}}{-jwm_i} \right) \tag{A.141}$$

where,

$$\hat{\mathbf{a}}_2' = \frac{k_{m,z}}{k_{i,z}} \left(\mathbf{a}_x \hat{x}' + \mathbf{a}_y \hat{y}' \right) + P_e^{VED} \mathbf{a}_z \hat{z}, \quad \hat{\mathbf{a}}_{2I}' = -\frac{k_{m,z}}{k_{i,z}} \left(\mathbf{a}_x \hat{x}' + \mathbf{a}_y \hat{y}' \right) - P_e^{VED} \mathbf{a}_z \hat{z} \tag{A.142}$$

in which the constant P_e^{VED} is associated with the scalar potential and can be determined from applying the Lorentz Gauge in (A.108) from $\tilde{G}_{zz}$. The constant coefficient P_e^{VED} is derived at the end of this section. Following the derivations of (A.38) - (A.46)

$$\hat{\boldsymbol{a}} \cdot \tilde{\mathbf{E}}_{i^{<,>}}^{TS} = \left[\hat{\boldsymbol{a}} \cdot \hat{\boldsymbol{a}}_2' + \frac{1}{k_i^2} \hat{\boldsymbol{a}} \cdot \nabla\nabla \cdot \hat{\boldsymbol{a}}_2' \right] \tilde{g}_{i^{<>}}^{TM^{TS}} + $$
$$\frac{1}{k_t^2} \left(\hat{\boldsymbol{a}} \cdot \hat{z} \times \nabla_t \right) \left(\hat{\boldsymbol{a}}_2' \cdot \hat{z} \times \nabla_t \right) \tilde{g}_{i^{<>}}^{ME^{TS}} \qquad (A.143)$$

$$\hat{\boldsymbol{a}} \cdot \tilde{\mathbf{E}}_{i^{<,>}}^{TA} = \left[\hat{\boldsymbol{a}} \cdot \hat{\boldsymbol{a}}_{2I}' + \frac{1}{k_i^2} \hat{\boldsymbol{a}} \cdot \nabla\nabla \cdot \hat{\boldsymbol{a}}_{2I}' \right] \tilde{g}_{i^{<>}}^{TM^{TA}} + $$
$$\frac{1}{k_t^2} \left(\hat{\boldsymbol{a}} \cdot \hat{z} \times \nabla_t \right) \left(\hat{\boldsymbol{a}}_{2I}' \cdot \hat{z} \times \nabla_t \right) \tilde{g}_{i^{<>}}^{ME^{TA}} \qquad (A.144)$$

where

$$\tilde{g}_{i^{<,>}}^{ME^{TS}} = \left(\tilde{g}_{i^{<,>}}^{TM^{TS}} - \left(\frac{k_{i,z}}{k_{m,z}} \frac{\boldsymbol{m}_m}{\boldsymbol{m}_I} \right) \tilde{g}_{i^{<>}}^{TE^{TS}} \right) \qquad (A.145)$$

$$\tilde{g}_{i^{<,>}}^{ME^{TA}} = \left(\tilde{g}_{i^{<,>}}^{TM^{TA}} + \left(\frac{k_{i,z}}{k_{m,z}} \frac{\boldsymbol{m}_m}{\boldsymbol{m}_I} \right) \tilde{g}_{i^{<,>}}^{TE^{TA}} \right) \qquad (A.146)$$

The spectral form for the electric field in (A.143) and (A.144) can be transformed back into the spatial domain. However, difficulty arises since $\hat{\boldsymbol{a}}_2'$ and $\hat{\boldsymbol{a}}_{2I}'$ are functions of k_r. To appropriately compensate for this, the method of moment formulation can be first introduced in the spectral domain using (A.143) and (A.144) are then appropriately inversing transformed back to obtain the spatial domain equivalent. We begin by expressing the electric field dyadic Green function due to an electric current source in a similar form as that presented in section II.A.2. This can be easily done using basically the same procedure as that outlined in (A.74) – (A.90), while using the transmitted fields as outlined in (A.109) – (A.142). In the development of this derivation it is realized that only the transmitted waves in region i are the total field – that is there is no primary wave. Thus, one can derive for the i-th region:

$$\hat{\mathbf{a}} \cdot \tilde{\mathbf{E}}_{i,m}(\mathbf{r}) =$$

$$\hat{\mathbf{a}} \cdot \begin{bmatrix} \tilde{G}^{EJ}_{xx_{i,m}} \hat{x}\hat{x} & 0 & 0 \\ 0 & \tilde{G}^{EJ}_{xx_{i,m}} \hat{y}\hat{y} & 0 \\ \tilde{G}^{EJ}_{zx_{i,m}} \hat{z}\hat{x} & \tilde{G}^{EJ}_{zy_{i,m}} \hat{z}\hat{y} & \tilde{G}^{EJ}_{zz_{i,m}} \hat{z}\hat{z} \end{bmatrix} \cdot \hat{\mathbf{a}}' + \frac{1}{k_i^2} \hat{\mathbf{a}} \cdot \nabla\nabla_t \cdot \hat{\mathbf{a}}' \tilde{G}^{EJ}_{V_{i,m}} + \frac{1}{k_i^2} \hat{\mathbf{a}} \cdot \nabla\nabla_z \cdot \hat{\mathbf{a}}' \tilde{G}^{EJ}_{V_{z_{i,m}}} \tag{A.147}$$

where the subscript i,m indicates the field in the i-th layer due to a source in the m-th layer, and:

$$\tilde{G}^{EJ}_{xx_{i,m}} = \tilde{g}^{TE}_{h_{i,m}}, \tag{A.148}$$

$$\tilde{G}^{EJ}_{zz_{i,m}} = \tilde{g}^{TM}_{v_{i,m}}, \tag{A.149}$$

$$\tilde{G}^{EJ}_{zx_{i,m}} = \cos\mathbf{a} \cdot \tilde{g}^{TM}_{z_{i,m}}, \quad \tilde{G}^{EJ}_{zy_{i,m}} = \sin\mathbf{a} \cdot \tilde{g}^{TM}_{z_{i,m}}, \tag{A.150}$$

$$\tilde{G}^{EJ}_{z_{i,m}} = -j\frac{\partial}{\partial z}\left(\frac{\tilde{g}^{TM}_{h_{i,m}} - \tilde{g}^{TE}_{h_{i,m}}}{k_r}\right) \tag{A.151}$$

$$\tilde{G}^{EJ}_{V_{i,m}} = \frac{k_i^2 \tilde{g}^{TE}_{h_{i,m}} - k_{z,i}^2 \tilde{g}^{TM}_{h_i}}{k_r^2}. \tag{A.152}$$

In order to determine $\tilde{G}^{EJ}_{vz}$, we needed to derive the constant coefficient of P_e^{VED} in (A.142) using the Lorentz Gauge relationship between the scalar and vector potential in (A.108). From (A.108) we interchange the derivative of $\tilde{G}_{zz}$ from with respect to z to with respect to z', and perform proper sign change that lead to:

$$\frac{\partial}{\partial z}\tilde{G}_{zz} = -jk_{i,z}A_k\left(e^{-jk_{i,z}z} - B_k e^{jk_{i,z}z}\right)\left(e^{jk_{m,z}z'} + D_1 e^{-jk_{m,z}z'} + E_2 e^{jk_{m,z}z'}\right)$$

where

$$A_k = \frac{-\mathbf{w}\mathbf{m}_i J_0}{8\mathbf{p}^2} \frac{e^{-j\bar{k}_t \cdot \left(\bar{r}_t - \bar{r}_t'\right)} e^{-jk_{i,z}d_i + jk_{m,z}d_{m-1}}}{k_{m,z}} \tilde{T}^{TM<}_{m,i} \tag{A.153}$$

$$B_k = \tilde{R}^{TM}_{i,i-1} e^{2jk_{i,z}d_{i-1}}$$

$$D_1 = \tilde{R}^{TM}_{m,m+1} \tilde{M}^{TM}_m e^{-jk_{m,z}2d_m} \qquad E_2 = \tilde{R}^{TM}_{m,m-1} \tilde{M}^{TM}_m \tilde{R}^{TM}_{m,m+1} e^{-jk_{m,z}2(d_m - d_{m-1})}$$

Subsequently $\tilde{G}_{vz}$ is expressed as:

$$\tilde{g}_{vz} = -\int_{z'} \frac{\partial}{\partial z} \tilde{g}_{zz} dz' = -ik_{i,z} A_k \left(e^{ik_{i,z}z} - B_k e^{-ik_{i,z}z} \right) \left(\frac{e^{-ik_{m,z}z'}}{-ik_{m,z}} + \frac{D_1 e^{ik_{m,z}z'}}{ik_{m,z}} - \frac{E_2 e^{-ik_{m,z}z'}}{ik_{m,z}} \right)$$

$$= \left(\frac{k_{i,z}}{k_{m,z}} \right) A_k \left(e^{ik_{i,z}z} - B_k e^{-ik_{i,z}z} \right) \tilde{F}_m^{TM} = \left(\frac{k_{i,z}}{k_{m,z}} \right)^2 \tilde{g}_{h_i}^{TM<}$$

(A.154)

for $i < m$ case. From (A.154) we conclude that the constant coefficient of P_e^{VED} is $k_{i,z}/k_{m,z}$. Following similar procedure above, we can derive $\tilde{G}_{vz}$ for case $i > m$. We showed that the constant coefficient of P_e^{VED} is the same with case $i < m$. Finally, the spatial domain form of (A.147) is expressed as:

$$\hat{a} \cdot \mathbf{E}_{i,m}(\mathbf{r}) =$$
$$\hat{a} \cdot \begin{bmatrix} G_{xx_{i,m}}^{EJ} \hat{x}\hat{x} & 0 & 0 \\ 0 & G_{xx_{i,m}}^{EJ} \hat{y}\hat{y} & 0 \\ \cos f g_{zt_{i,m}}^{EJ} \hat{z}\hat{x} & \sin f g_{zt_{i,m}}^{EJ} \hat{z}\hat{y} & G_{zz_{i,m}}^{EJ} \hat{z}\hat{z} \end{bmatrix} \cdot \hat{a}' + \frac{1}{k_i^2} \hat{a} \cdot \nabla\nabla_t \cdot \hat{a}' G_{V_{t_{i,m}}}^{EJ} + \frac{1}{k_i^2} \hat{a} \cdot \nabla\nabla_z \cdot \hat{a}' G_{V_{z_{i,m}}}^{EJ}$$

(A.155)

where, from (A.113) and (A.126),

$$G_{xx_{i,m}}^{EJ} = \begin{cases} \dfrac{-wm_m}{4p} \displaystyle\int_{k_r=0}^{\infty} J_0(k_r r) \dfrac{\tilde{A}_i^{TE<}}{k_{m,z}} e^{-jk_{i,z}d_i} \left[e^{-jk_{i,z}z} + \tilde{R}_{i,i-1}^{TE} e^{2jk_{i,z}d_{i-1}} e^{jk_{i,z}z} \right] k_r dk_r, & (i < m) \\[2em] \dfrac{-wm_m}{4p} \displaystyle\int_{k_r=0}^{\infty} J_0(k_r r) \dfrac{\tilde{A}_i^{TE>}}{k_{m,z}} e^{jk_{i,z}d_{i-1}} \left[e^{jk_{i,z}z} + \tilde{R}_{i,i+1}^{TE} e^{-2jk_{i,z}d_i} e^{-jk_{i,z}z} \right] k_r dk_r, & (i > m) \end{cases}$$

(A.156)

$$G_{V_{t_{i,m}}}^{EJ} = \begin{cases} \dfrac{-wm_m}{4p} \displaystyle\int_{k_r=0}^{\infty} \dfrac{J_0(k_r r)}{k_r k_{m,z}} \begin{bmatrix} k_o^2 e_r m_{r_m} \tilde{A}_i^{TE<} e^{-jk_{i,z}d_i} \left[e^{-jk_{i,z}z} + \tilde{R}_{i,i-1}^{TE} e^{2jk_{i,z}d_{i-1}} e^{jk_{i,z}z} \right] - \\ k_{i,z} k_{m,z} \tilde{C}_i^{TM<} e^{-jk_{i,z}d_i} \left[e^{-jk_{i,z}z} - \tilde{R}_{i,i-1}^{TM} e^{2jk_{i,z}d_{i-1}} e^{jk_{i,z}z} \right] \end{bmatrix} dk_r, & (i < m) \\[2em] \dfrac{-wm_m}{4p} \displaystyle\int_{k_r=0}^{\infty} \dfrac{J_0(k_r r)}{k_r k_{m,z}} \begin{bmatrix} k_o^2 e_r m_{r_m} \tilde{A}_i^{TE>} e^{jk_{i,z}d_{i-1}} \left[e^{jk_{i,z}z} + \tilde{R}_{i,i+1}^{TE} e^{-2jk_{i,z}d_i} e^{-jk_{i,z}z} \right] - \\ k_{i,z} k_{m,z} \tilde{C}_i^{TM>} e^{jk_{i,z}d_{i-1}} \left[e^{jk_{i,z}z} - \tilde{R}_{i,i+1}^{TM} e^{-2jk_{i,z}d_i} e^{-jk_{i,z}z} \right] \end{bmatrix} dk_r, & (i > m) \end{cases}$$

(A.157)

$$G_{zz_{i,m}}^{EJ} = \begin{cases} \dfrac{-wm_m}{4p} \displaystyle\int_{k_r=0}^{\infty} J_0(k_r r) \dfrac{\tilde{A}_i^{TM<}}{k_{m,z}} e^{-jk_{i,z}d_i} \left[e^{-jk_{i,z}z} + \tilde{R}_{i,i-1}^{TM} e^{2jk_{i,z}d_{i-1}} e^{jk_{i,z}z} \right] k_r dk_r, & (i < m) \\[2em] \dfrac{-wm_m}{4p} \displaystyle\int_{k_r=0}^{\infty} J_0(k_r r) \dfrac{\tilde{A}_i^{TM>}}{k_{m,z}} e^{jk_{i,z}d_{i-1}} \left[e^{jk_{i,z}z} + \tilde{R}_{i,i+1}^{TM} e^{-2jk_{i,z}d_i} e^{-jk_{i,z}z} \right] k_r dk_r, & (i > m) \end{cases}$$

, (A.158)

$$G_{zt_{i,m}}^{EJ} = \begin{cases} \dfrac{i\boldsymbol{w}\boldsymbol{m}_i}{4\boldsymbol{p}} \displaystyle\int_{k_r=0}^{\infty} J_1\left(k_r \boldsymbol{r}\right) \begin{bmatrix} \tilde{C}_i^{TM^<} e^{-jk_{i,z}d_i} \left[e^{-jk_{i,z}z} + \tilde{R}_{i,i-1}^{TM} e^{2jk_{i,z}d_{i-1}} e^{jk_{i,z}z} \right] - \\ \tilde{A}_i^{TE^<} \dfrac{k_{i,z}\boldsymbol{m}_m}{k_{m,z}\boldsymbol{m}_i} e^{-jk_{i,z}d_i} \left[e^{-jk_{i,z}z} - \tilde{R}_{i,i-1}^{TE} e^{2jk_{i,z}d_{i-1}} e^{jk_{i,z}z} \right] \end{bmatrix} dk_r, \quad (i<m) \\[4em] \dfrac{i\boldsymbol{w}\boldsymbol{m}_i}{4\boldsymbol{p}} \displaystyle\int_{k_r=0}^{\infty} J_1\left(k_r \boldsymbol{r}\right) \begin{bmatrix} \tilde{C}_i^{TM^>} e^{jk_{i,z}d_{i-1}} \left[-e^{jk_{i,z}z} - \tilde{R}_{i,i+1}^{TM} e^{-2jk_{i,z}d_i} e^{-jk_{i,z}z} \right] - \\ \tilde{A}_i^{TE^>} \dfrac{k_{i,z}\boldsymbol{m}_m}{k_{m,z}\boldsymbol{m}_i} e^{jk_{i,z}d_{i-1}} \left[-e^{jk_{i,z}z} + \tilde{R}_{i,i+1}^{TE} e^{-2jk_{i,z}d_i} e^{-jk_{i,z}z} \right] \end{bmatrix} dk_r, \quad (i>m) \end{cases} \qquad (A.159)$$

and

$$G_{v_{z_{i,m}}}^{EJ} = \begin{cases} \dfrac{-\boldsymbol{w}\boldsymbol{m}_m}{4\boldsymbol{p}} \displaystyle\int_{k_r=0}^{\infty} J_0\left(k_r \boldsymbol{r}\right) \dfrac{k_{i,z}\tilde{C}_i^{TM^<}}{k_{m,z}^2} e^{-jk_{i,z}d_i} \left[e^{-jk_{i,z}z} - \tilde{R}_{i,i-1}^{TM} e^{2jk_{i,z}d_{i-1}} e^{jk_{i,z}z} \right] k_r dk_r, \quad (i<m) \\[3em] \dfrac{-\boldsymbol{w}\boldsymbol{m}_m}{4\boldsymbol{p}} \displaystyle\int_{k_r=0}^{\infty} J_0\left(k_r \boldsymbol{r}\right) \dfrac{k_{i,z}\tilde{C}_i^{TM^>}}{k_{m,z}^2} e^{jk_{i,z}d_{i-1}} \left[e^{jk_{i,z}z} - \tilde{R}_{i,i+1}^{TM} e^{-2jk_{i,z}d_i} e^{-jk_{i,z}z} \right] k_r dk_r, \quad (i>m) \end{cases} \qquad (A.160)$$

where, $\tilde{A}_i^{TM/TE^<}$ and $\tilde{A}_i^{TM/TE^>}$ are given by (A.120) and (A.131), respectively, and $\tilde{C}_i^{TM^<}$ and $\tilde{C}_i^{TM^>}$ are given by (A.121) and (A.132), respectively. More specifically,

$$\tilde{A}_i^{TM/TE^<} = \tilde{T}_{m,i}^{TM/TE^<} e^{jk_{m,z}d_{m-1}} \left[e^{jk_{m,z}z'} + \tilde{R}_{m,m+1}^{TM/TE} e^{-2jk_{m,z}d_m} e^{-jk_{m,z}z'} \right] \tilde{M}_m^{TM/TE}, \qquad (A.161)$$

$$\tilde{A}_i^{TM/TE^>} = \tilde{T}_{m,i}^{TM/TE^>} e^{-jk_{m,z}d_m} \left[e^{-jk_{m,z}z'} + \tilde{R}_{m,m-1}^{TM/TE} e^{j2k_{m,z}d_{m-1}} e^{jk_{m,z}z'} \right] \tilde{M}_m^{TM/TE}, \qquad (A.162)$$

$$\tilde{C}_i^{TM^<} = \tilde{T}_{m,i}^{TM^<} e^{jk_{m,z}d_{m-1}} \left[e^{jk_{m,z}z'} - \tilde{R}_{m,m+1}^{TM} e^{-2jk_{m,z}d_m} e^{-jk_{m,z}z'} \right] \tilde{M}_m^{TM}, \qquad (A.163)$$

and

$$\tilde{C}_i^{TM^>} = \tilde{T}_{m,i}^{TM^>} e^{-jk_{m,z}d_m} \left[e^{-jk_{m,z}z'} - \tilde{R}_{m,m-1}^{TM} e^{2jk_{m,z}d_{m-1}} e^{jk_{m,z}z'} \right] \tilde{M}_m^{TM} \qquad (A.164)$$

where,

$$\tilde{T}_{m,i}^{TM/TE^<} = \prod_{\substack{j=m \\ (i<m)}}^{i+1} S_{j,j-1}^{TM/TE^<} \Theta_j, \qquad (A.165)$$

$$S_{l,l-1}^{TM/TE^<} = \frac{T_{l,l-1}^{TM/TE}}{1 + R_{l,l-1}^{TM/TE} \tilde{R}_{l-1,l-2}^{TM/TE} e^{-2jk_{l-1,z}(d_{l+1}-d_{l-2})}}, \qquad (A.166)$$

$$\tilde{T}_{m,i}^{TM/TE^>} = \prod_{j=m}^{i-1} S_{j,j+1}^{TM/TE^>} \Theta_j, \qquad (A.167)$$

$$S_{l,l+1}^{TM/TE^{>}} = \frac{T_{l,l+1}^{TM/TE}}{1 + R_{l,l+1}^{TM/TE} \tilde{R}_{l+1,l+2}^{TM/TE} e^{-2jk_{l+1,z}(d_{l+1}-d_l)}} \, , \tag{A.168}$$

and

$$\Theta_l = \begin{cases} 1 & , l = m \\ e^{jk_{l,z}(d_{l-1}-d_l)} & , l \neq m \end{cases} . \tag{A.169}$$

(A.156) — (A.169) is the final expression of the layered media Green's function in the Dyadic Green Function for source and observation points place at different layers.

Appendix B

B.1 Introduction

In this appendix B, the closed-form expressions for the z-integrations in the spectral domain basis functions and Green's for arbitrary layered media are derived. The asymptotic extraction of the closed-form expression via an analytical formulation is also included. As stated in the Section 4.4, the basis function used is the GWP zero[th] order basis function or the RWG rooftop basis function for a quadrilateral patch.

There are three different types reactions between basis: 1) vertical-to-vertical (vertical source basis and vertical field basis functions); 2) horizontal-to-vertical (horizontal source basis and vertical field basis functions); 3) vertical-to-horizontal (vertical source basis and horizontal field basis functions). It is also noted that the horizontal functions are not necessarily planar, but can also have a vertical distribution (e.g., a horizontally directed current on a vertical strip). All these reactions are presented below.

Consider the MPIE formulation with a Galerkin discretization:

$$\iiiint\limits_{t\ z\ t'\ z'} \left(\vec{\Lambda} \cdot \overline{\overline{G}} \cdot \vec{\Lambda'} - \frac{1}{k_m} G_v \left(\nabla \cdot \vec{\Lambda} \right) \left(\nabla' \cdot \vec{\Lambda'} \right) \right) dz' dt' dz dt \tag{B.1}$$

in which $\vec{\Lambda}$ and $\vec{\Lambda}'$ are the testing and source basis functions, respectively, where the surface integrals are performed in the transverse and z-direction. Subsequently, we can distinguish the three different types of basis reactions with the MPIE formulation.

B.2 Vertical-to-vertical basis reactions

Assume that both the current and field basis functions are located on vertical patches. The integration in (B.1) resulting from the dyadic kernel $\overline{\overline{G}}$ can be expressed as:

$$\begin{aligned}
&\iiiint\limits_{t\ z\ t'\ z'} \vec{\Lambda} \cdot \overline{\overline{G}} \cdot \vec{\Lambda'} dz'\, dt'\, dz\, dt \\
&= \iiiint\limits_{t\ z\ t'\ z'} \hat{z} g(z) l_z \cdot \overline{\overline{G}} \cdot l_z' \hat{z}'\, g(z')\, dz' dv' dz dv
\end{aligned} \tag{B.2}$$

The DGF in (B.2) is expanded in terms of a Sommerfeld integral:

$$l_z l_z' \iiint\limits_{t\ t'\ 0}^{\infty} \frac{J_0\left(k_r \boldsymbol{r}\right) k_r}{k_{m,z}} \left[\iint\limits_{z\ z'} g\left(z\right) \tilde{G}\left(z, z', k_r\right) g\left(z'\right) dz' dz \right] dk_r\, dt'\, dt \tag{B.3}$$

where l_z and $l_{z'}$ are the tangential edge length of the field basis and current basis, respectively. Similarly for the scalar potential G_v, the order of integration is changed so that the z-integration falls on the spectral DGF:

$$\iiiint\limits_{t\ z\ t'\ z'} \left(\nabla \cdot \overrightarrow{\Lambda}\right) G_v\left(\boldsymbol{r}\right) \left(\nabla' \cdot \overrightarrow{\Lambda'}\right) dz'\,dt'\,dz\,dt$$
$$= \iiiint\limits_{t\ z\ t'\ z'} l_z G_v\left(\boldsymbol{r}\right) l_{z'} dz'\,dt'\,dz\,dt \tag{B.4}$$

The DGF in (B.4) is expanded in terms of a Sommerfeld integral:

$$l_z l_{z'} \iiint\limits_{t\ t'\ 0}^{\infty} \frac{J_0\left(k_r \boldsymbol{r}\right) k_r}{k_{m,z}} \left[\iint\limits_{z\ z'} \tilde{G}_v\left(z, z', k_r\right) dz'\,dz \right] dk_r\, dt'\, dt . \tag{B.5}$$

Notice that the z-and $\dot{z}$-integrations are performed in the spectral domain before applying the Sommerfeld integral to transform to the spatial domain.

B.3 Horizontal-to-vertical basis reactions

Next assume that the current basis is located on a horizontal patch and field basis on a vertical patch. The surface integral is performed in a local simplex coordinate system that transforms the physical coordinate system into a local system $\left(u^1, u^2\right)$. The local system has a range of $(0,1)$. The integration in (B.1) resulting from the dyadic kernel $\overline{\overline{G}}$ can be expressed as:

$$\iiint\limits_{t\ z\ s'} \overrightarrow{\Lambda} \cdot \overline{\overline{G}} \cdot \overrightarrow{\Lambda'} ds'\,dz\,dt$$
$$= \iiint\limits_{s'\ t\ z} g\left(z\right) l_z\, \hat{z} \cdot \overline{\overline{G}} \cdot \hat{a}'\ g\left(z'\right) l_{z'} dz\,dt\,ds' \tag{B.6}$$

where *ds'* denotes the surface integral of the current patch. The DGF in (B.6) is expanded in terms of a Sommerfeld integral:

$$l_z \iint\limits_{s'\ t} g\left(z'\right) \hat{a}' \cdot \langle \cos \boldsymbol{f}', \sin \boldsymbol{f}' \rangle \int\limits_0^{\infty} J_1\left(k_r \boldsymbol{r}\right) \left[\int\limits_z g\left(z\right) \tilde{G}_{zt}\left(z, z', k_r\right) dz \right] dk_r\,dt\,ds' \tag{B.7}$$

where $\langle \ \rangle$ denotes the inner product, and $\tilde{G}_{zt}$ is the Green's function reaction associates with the vertical current and horizontal field. Similarly for the scalar potential G_v, the order of integration is changed so that the z-integration falls on the spectral DGF:

$$\iiint_{s't\,z} (\nabla \cdot \vec{\Lambda}) G_v(\boldsymbol{r})(\nabla \cdot \vec{\Lambda'}) dz dt ds'$$
$$= l_z l_{z'} \iiint_{s't\,z} G_v(\boldsymbol{r}) dz dt ds' \tag{B.8}$$

The DGF in (B.8) is expanded in terms of a Sommerfeld integral:

$$l_z l_{z'} \iiint_{s't\,0}^{\infty} \frac{J_0(k_r \boldsymbol{r}) k_r}{k_{m,z}} \left[\int_z \tilde{G}_v(z, z', k_r) dz \right] dk_r dt ds' \tag{B.9}$$

where the z-integration is derived analytically in the spectral domain before performing the Sommerfeld integration.

B.4 Vertical-to-horizontal basis reactions

Next assume that the current basis is located on a vertical patc h and field basis on a horizontal patch. The surface integral is performed in a local simplex coordinate system that transforms the physical coordinate system into a local system (u^1, u^2). The local system has a range of (0,1). The integration in (B.1) resulting from the dyadic kernel $\overline{\overline{G}}$ can be expressed as:

$$\iiint_{t'\,z'\,s} \vec{\Lambda} \cdot \overline{\overline{G}} \cdot \vec{\Lambda'} ds dz' dt'$$
$$= \iiint_{s\,t'\,z'} g(z') l_{z'} \hat{z}' \cdot \overline{\overline{G}} \hat{a} g(z) l_z dz' dt' ds \tag{B.10}$$

The DGF in (B.10) is expanded in terms of a Sommerfeld integral:

$$l_z \iint_{s\,t'} g(z) \hat{a} \cdot \langle \cos \boldsymbol{f}, \sin \boldsymbol{f} \rangle \int_0^{\infty} J_1(k_r \boldsymbol{r}) \left[\int_{z'} g(z') \tilde{G}_{tz'}(z, z', k_r) dz \right] dk_r dt' ds$$
$$= 0 \qquad \because (\tilde{G}_{tz'} = 0) \tag{B.11}$$

116

Similarly for the scalar potential G_v, the order of integration is changed so that the z'-integration falls on the spectral DGF:

$$
\begin{aligned}
&\iiint_{s\ t'\ z'}\left(\nabla\cdot\vec{\Lambda}\right)G_v\left(\boldsymbol{r}\right)\left(\nabla'\cdot\overline{\Lambda'}\right)dz'\,dt'\,ds \\
&=\iiint_{s\ t'\ z'}l_z G_v\left(\boldsymbol{r}\right)l_z dz'\,dt'\,ds
\end{aligned}
\tag{B.12}
$$

The DGF in (B.12) is expanded in terms of a Sommerfeld integral:

$$
l_z l_{z'}\iiint_{s\ t'\ 0}^{\infty}\frac{J_0\left(k_r\boldsymbol{r}\right)k_r}{k_{m,z}}\left[\int_{z'}\tilde{G}_v\left(z,z',k_r\right)dz'\right]dk_r dt'\,ds
\tag{B.13}
$$

where the z'-integration is derived analytically in the spectral domain before performing the Sommerfeld integration.

Once the reaction typed of basis functions are determined, we began to derive the closed-form formulations for all the reactions in free-space and layered media Green's function. The zero[th]-order divergence-conforming GWP basis function is employed assuming that the vertical current patch has z bounds $\left(z_1',z_2'\right)$ and vertical field patch has z-bounds $\left(z_1,z_2\right)$ expressed as:

$$
\begin{aligned}
g\left(z\right)=\frac{z-z_1}{z_2-z_1}\ ;\ g\left(z\right)=\frac{z_2-z}{z_2-z_1} \\
g\left(z'\right)=\frac{z'-z_1'}{z_2'-z_1'}\ ;\ g\left(z'\right)=\frac{z_2'-z'}{z_2'-z_1'}
\end{aligned}
\tag{B.14}
$$

For horizontal currents that are transverse directed, the basis is constant in z. The divergences of the z-directed source and field basis can be stated explicitly as l_z and $l_{z'}$. Combining this with the (B.2) — (B.14) is what then leads to the 16 different closed form expressions showed in Table B1. From the table, the closed-forms expressions from 1 to 9 are associated with the vertical-to-vertical basis reactions, expressions from 10 to 13 are associated with the horizontal-to-vertical basis reactions, and expressions from 14 to 16 are associated with the vertical-to-horizontal basis reactions.

no.	Sommerfeld-typed integral of closed-form formulations for z-integration in the spectral domain
1	$\displaystyle \int_0^\infty J_0\left(k_r\boldsymbol{r}\right)\frac{k_r}{k_{m,z}}\left[\iint_{z\,z'}\left(z'-z_1'\right)\tilde{G}_{zz}\left(z,z',k_r\right)\left(z-z_2\right)dz'dz\right]dk_r$
2	$\displaystyle \int_0^\infty J_0\left(k_r\boldsymbol{r}\right)\frac{k_r}{k_{m,z}}\left[\iint_{z\,z'}\left(z'-z_2'\right)\tilde{G}_{zz}\left(z,z',k_r\right)\left(z-z_1\right)dz'dz\right]dk_r$
3	$\displaystyle \int_0^\infty J_0\left(k_r\boldsymbol{r}\right)\frac{k_r}{k_{m,z}}\left[\iint_{z\,z'}\left(z'-z_1'\right)\tilde{G}_{zz}\left(z,z',k_r\right)\left(z-z_1\right)dz'dz\right]dk_r$
4	$\displaystyle \int_0^\infty J_0\left(k_r\boldsymbol{r}\right)\frac{k_r}{k_{m,z}}\left[\iint_{z\,z'}\left(z'-z_2'\right)\tilde{G}_{zz}\left(z,z',k_r\right)\left(z-z_2\right)dz'dz\right]dk_r$
5	$\displaystyle \int_0^\infty J_0\left(k_r\boldsymbol{r}\right)\frac{k_r}{k_{m,z}}\left[\iint_{z\,z'}\tilde{G}_{xx}\left(z,z',k_r\right)dz'dz\right]dk_r$
6	$\displaystyle \int_0^\infty J_0\left(k_r\boldsymbol{r}\right)\frac{k_r}{k_{m,z}}\left[\iint_{z\,z'}\tilde{G}_{vz}\left(z,z',k_r\right)dz'dz\right]dk_r$
7	$\displaystyle \int_0^\infty J_0\left(k_r\boldsymbol{r}\right)\frac{k_r}{k_{m,z}}\left[\iint_{z\,z'}\tilde{G}_{vt}\left(z,z',k_r\right)dz'dz\right]dk_r$
8	$\displaystyle \int_0^\infty J_1\left(k_r\boldsymbol{r}\right)\left[\iint_{z\,z'}\left(z-z_1\right)\tilde{g}_{zt}\left(z,z',k_r\right)dz'dz\right]dk_r$
9	$\displaystyle \int_0^\infty J_1\left(k_r\boldsymbol{r}\right)\left[\iint_{z\,z'}\left(z-z_2\right)\tilde{g}_{zt}\left(z,z',k_r\right)dz'dz\right]dk_r$
10	$\displaystyle \int_0^\infty J_1\left(k_r\boldsymbol{r}\right)\left[\int_z\left(z-z_1\right)\tilde{g}_{zt}\left(z,z',k_r\right)dz\right]dk_r$
11	$\displaystyle \int_0^\infty J_1\left(k_r\boldsymbol{r}\right)\left[\int_z\left(z-z_2\right)\tilde{g}_{zt}\left(z,z',k_r\right)dz\right]dk_r$
12	$\displaystyle \int_0^\infty J_0\left(k_r\boldsymbol{r}\right)\frac{k_r}{k_{m,z}}\left[\int_z\tilde{G}_{xx}\left(z,z',k_r\right)dz\right]dk_r$
13	$\displaystyle \int_0^\infty J_0\left(k_r\boldsymbol{r}\right)\frac{k_r}{k_{m,z}}\left[\int_z\tilde{G}_{vt}\left(z,z',k_r\right)dz\right]dk_r$
14	$\displaystyle \int_0^\infty J_0\left(k_r\boldsymbol{r}\right)\frac{k_r}{k_{m,z}}\left[\int_z\tilde{G}_{vt}\left(z,z',k_r\right)dz'\right]dk_r$
15	$\displaystyle \int_0^\infty J_0\left(k_r\boldsymbol{r}\right)\frac{k_r}{k_{m,z}}\left[\int_{z'}\tilde{G}_{vz}\left(z,z',k_r\right)dz'\right]dk_r$
16	$\displaystyle \int_0^\infty J_0\left(k_r\boldsymbol{r}\right)\frac{k_r}{k_{m,z}}\left[\int_{z'}\tilde{G}_{xx}\left(z,z',k_r\right)dz'\right]dk_r$

Table B.1: Closed-form z-integration in *spectral* domain for the reaction between layered media Green's function and zero[h]-order divergence-conforming GWP basis functions

B.5 Free-space case

For sake of illustration, we begin by performing the z-integrations in the spectral domain when the host media is free-space. The source and field patches are assumed to be rectangular, and to be either purely vertical or purely horizontal. The source patch has the vertical bounds $\left(z_1^{'}, z_2^{'}\right)$, and the field patch has the vertical bounds $\left(z_1, z_2\right)$. The closed-form formulations (in the order of Table B1) for the free-space case are expressed in the following.

Closed-form formulation (1):

$$\tilde{I}_z\left(\tilde{G}\right) = \int\limits_{z_1}^{z_2}\int\limits_{z_1^{'}}^{z_2^{'}}\left(z' - z_1^{'}\right)e^{-jk_{m,z}|z-z'|}\left(z - z_2\right)dz'dz \qquad \text{(B.15)}$$

case (I): when $z_1 = z_1^{'}$ and $z_2 = z_2^{'}$:

$$
\begin{aligned}
&\int\limits_{z_1}^{z_2}\int\limits_{z_1^{'}}^{z_2^{'}}\left(z - z_2\right)e^{-jk_{m,z}|z-z'|}\left(z' - z_1^{'}\right)dz'dz \\
&= \int\limits_{z_1}^{z_2}\int\limits_{z_1^{'}}^{z}\left(z - z_2\right)e^{-jk_{m,z}\left(z-z'\right)}\left(z' - z_1\right)dz'dz + \int\limits_{z_1}^{z_2}\int\limits_{z}^{z_2^{'}}\left(z - z_2\right)e^{+jk_{m,z}\left(z-z'\right)}\left(z' - z_1\right)dz'dz \\
&= \frac{3\left[\left(k_{m,z}\left(z_2 - z_1\right) - j\right)^2 - 1\right]e^{-jk_{m,z}\left(z_2 - z_1\right)} + 6 + j\left[\left(z_2 - z_1\right)k_{m,z}\right]^3}{3k_{m,z}^4}
\end{aligned}
\qquad \text{(B.16)}
$$

case (II) when $z > z'$ or $z_1 \geq z_2^{'}$:

$$
\begin{aligned}
&\int\limits_{z_1}^{z_2}\int\limits_{z_1^{'}}^{z_2^{'}}\left(z - z_2\right)e^{-jk_{m,z}\left(z-z'\right)}\left(z' - z_1^{'}\right)dz'dz \\
&= \frac{e_1 + e_2 + e_3 + e_4}{k_{m,z}^4}
\end{aligned}
\qquad \text{(B.17)}
$$

where

$$e_1 = j\left[k_{m,z}\left(z_1' - z_2'\right) - j\right]e^{-jk_{m,z}\left(z_2 - z_2'\right)}$$

$$e_2 = \left[k_{m,z}\left(z_2 - z_1\right) + j\right]\left[k_{m,z}\left(z_2' - z_1'\right) + j\right]e^{jk_{m,z}\left(z_2' - z_1\right)}$$

$$e_3 = j\left[k_{m,z}\left(z_1 - z_2\right) - j\right]e^{jk_{m,z}\left(z_1' - z_1\right)}$$

$$e_4 = -e^{-jk_{m,z}\left(z_2 - z_1'\right)}$$

(B.18)

case (III) when $z' > z$ or $z_1' \geq z_1$:

$$\int_{z_1}^{z_2}\int_{z_1'}^{z_2'}(z - z_2)e^{-jk_{m,z}\left(z' - z\right)}\left(z' - z_1'\right)dz'dz$$

$$= \frac{e_5 + e_6 + e_7 + e_8}{k_{m,z}^4}$$

(B.19)

where

$$e_5 = j\left[k_{m,z}\left(z_2 - z_1\right) - j\right]e^{jk_{m,z}\left(z_1 - z_1'\right)}$$

$$e_6 = \left[k_{m,z}\left(z_2 - z_1\right) - j\right]\left[k_{m,z}\left(z_2' - z_1'\right) - j\right]e^{-jk_{m,z}\left(z_2 - z_1\right)}$$

$$e_7 = j\left[k_{m,z}\left(z_2' - z_1'\right) - j\right]e^{jk_{m,z}\left(z_2 - z_2'\right)}$$

$$e_8 = -e^{jk_{m,z}\left(z_2 - z_1'\right)}$$

(B.20)

It is observed that (B.18) and (B.20) are the conjugate of each other as expected.

Closed-form formulation (2):

case (I) when $z_1 = z_1'$ and $z_2 = z_2'$:

$$\int_{z_1}^{z_2}\int_{z_1'}^{z_2'}(z - z_1)e^{-jk_{m,z}|z - z'|}\left(z' - z_2'\right)dz'dz$$

$$= \frac{3\left[k_{m,z}\left(z_2 - z_1\right) - 1 - j\right]\left[k_{m,z}\left(z_2 - z_1\right) + 1 - j\right]e^{-jk_{m,z}\left(z_2 - z_1\right)} + 6 + j\left[k_{m,z}\left(z_2 - z_1\right)\right]^3}{3k_{m,z}^4}$$

(B.21)

case (II) when $z > z'$ or $z_1 \geq z_2'$:

$$\int_{z_1}^{z_2}\int_{z_1'}^{z_2'}(z-z_1)e^{-jk_{m,z}(z-z')}(z'-z_2')dz'dz$$

$$= \frac{c_1+c_2+c_3+c_4}{k_{m,z}^4}$$

(B.22)

$$c_1 = \left[k_{m,z}(z_2-z_1)-j\right]\left[k_{m,z}(z_2'-z_1')-j\right]e^{-jk_{m,z}(z_2-z_1')}$$

$$c_2 = j\left[k_{m,z}(z_2-z_1)-j\right]e^{-jk_{m,z}(z_2-z_2')}$$

$$c_3 = j\left[k_{m,z}(z_2'-z_1')-j\right]e^{jk_{m,z}(z_1'-z_1)}$$

$$c_4 = -e^{jk_{m,z}(z_2-z_1')}$$

(B.23)

case (III) when $z' > z$ or $z_1' \geq z_1$:

$$\int_{z_1}^{z_2}\int_{z_1'}^{z_2'}(z-z_1)e^{-jk_{m,z}(z'-z)}(z'-z_2')dz'dz$$

$$= \frac{c_1+c_2+c_3+c_4}{k_{m,z}^4}$$

(B.24)

$$c_1 = \left[k_{m,z}(z_2-z_1)+j\right]\left[k_{m,z}(z_2'-z_1')+j\right]e^{jk_{m,z}(z_2-z_1')}$$

$$c_2 = j\left[k_{m,z}(z_1-z_2)-j\right]e^{jk_{m,z}(z_2-z_2')}$$

$$c_3 = j\left[k_{m,z}(z_1'-z_2')-j\right]e^{-jk_{m,z}(z_1'-z_1)}$$

$$c_4 = -e^{-jk_{m,z}(z_2-z_1')}$$

(B.25)

Closed-form formulation (3):

case (I) when $z_1 = z_1'$ and $z_2 = z_2'$:

$$\int_{z_1}^{z_2}\int_{z_1'}^{z_2'}(z-z_1)e^{-jk_{m,z}|z-z'|}(z'-z_1')dz'dz$$

$$= \frac{6j\left[k_{m,z}(z_1-z_2)+j\right]e^{-jk_{m,z}(z_2-z_1)}+6-2j\left[(z_2-z_1)k_{m,z}\right]^3+3\left[(z_2-z_1)k_{m,z}\right]^2}{3k_{m,z}^4}$$

$$= -\frac{2j(z_2-z_1)}{3k_{m,z}^2}+\frac{6j\left[k_{m,z}(z_1-z_2)+j\right]e^{-jk_{m,z}(z_2-z_1)}+6+3\left[(z_2-z_1)k_{m,z}\right]^2}{3k_{m,z}^4}$$

(B.26)

case (II) when $z > z'$ or $z_1 \geq z_2'$:

$$\int_{z_1}^{z_2}\int_{z_1'}^{z_2'}(z-z_1)e^{-jk_{m,z}\left(z-z'\right)}\left(z'-z_1'\right)dz'dz$$

$$=\frac{c_1+c_2+c_3+c_4}{k_{m,z}^4}$$
(B.27)

$$c_1=\left[k_{m,z}\left(z_2-z_1\right)-j\right]\left[k_{m,z}\left(z_2'-z_1'\right)+j\right]e^{-jk_{m,z}\left(z_2-z_2'\right)}$$

$$c_2=j\left[k_{m,z}\left(z_1-z_2\right)+j\right]e^{-jk_{m,z}\left(z_2-z_1'\right)}$$

$$c_3=j\left[k_{m,z}\left(z_2'-z_1'\right)+j\right]e^{-jk_{m,z}\left(z_1-z_2'\right)}$$

$$c_4=e^{-jk_{m,z}\left(z_1-z_1'\right)}$$
(B.28)

case (III) when $z'>z$ or $z_1'\geq z_1$:

$$\int_{z_1}^{z_2}\int_{z_1'}^{z_2'}(z-z_1)e^{-jk_{m,z}\left(z'-z\right)}\left(z'-z_1'\right)dz'dz$$

$$=\frac{c_1+c_2+c_3+c_4}{k_{m,z}^4}$$
(B.29)

$$c_1=\left[k_{m,z}\left(z_2-z_1\right)+j\right]\left[k_{m,z}\left(z_2'-z_1'\right)-j\right]e^{jk_{m,z}\left(z_2-z_2'\right)}$$

$$c_2=j\left[k_{m,z}\left(z_2-z_1\right)+j\right]e^{jk_{m,z}\left(z_2-z_1'\right)}$$

$$c_3=j\left[k_{m,z}\left(z_1'-z_2'\right)+j\right]e^{jk_{m,z}\left(z_1-z_2'\right)}$$

$$c_4=e^{jk_{m,z}\left(z_1-z_1'\right)}$$
(B.30)

Closed-form formulation (4):

case (I) when $z_1=z_1'$ and $z_2=z_2'$:

$$\int_{z_1}^{z_2}\int_{z_1'}^{z_2'}(z-z_2)e^{-jk_{m,z}\left|z-z'\right|}\left(z'-z_2'\right)dz'dz$$

$$=\frac{6j\left[k_{m,z}\left(z_1-z_2\right)+j\right]e^{-jk_{m,z}\left(z_2-z_1\right)}+6-2j\left[k_{m,z}\left(z_2-z_1\right)\right]^3+3\left[k_{m,z}\left(z_2-z_1\right)\right]^2}{3k_{m,z}^4}$$
(B.31)

case (II) when $z>z'$ or $z_1\geq z_2'$:

$$\int_{z_1}^{z_2}\int_{z_1'}^{z_2'}(z-z_2)e^{-jk_{m,z}(z-z')}\left(z'-z_1'\right)dz'dz$$

$$=\frac{c_1+c_2+c_3+c_4}{k_{m,z}^4}$$

(B.32)

$$c_1 = j\left[k_{m,z}\left(z_2-z_1\right)+j\right]e^{-jk_{m,z}\left(z_1-z_2'\right)}$$

$$c_2 = \left[k_{m,z}\left(z_2-z_1\right)+j\right]\left[k_{m,z}\left(z_2'-z_1'\right)-j\right]e^{-jk_{m,z}\left(z_1-z_1'\right)}$$

$$c_3 = j\left[k_{m,z}\left(z_1'-z_2'\right)+j\right]e^{-jk_{m,z}\left(z_2-z_1'\right)}$$

$$c_4 = e^{-jk_{m,z}\left(z_2-z_2'\right)}$$

(B.33)

case (III) when $z' > z$ or $z_1' \geq z_1$:

$$\int_{z_1}^{z_2}\int_{z_1'}^{z_2'}(z-z_2)e^{-jk_{m,z}(z'-z)}\left(z'-z_1'\right)dz'dz$$

$$=\frac{c_1+c_2+c_3+c_4}{k_{m,z}^4}$$

(B.34)

$$c_1 = e^{jk_{m,z}\left(z_2-z_2'\right)}$$

$$c_2 = j\left[k_{m,z}\left(z_1-z_2\right)+j\right]e^{jk_{m,z}\left(z_1-z_2'\right)}$$

$$c_3 = \left[k_{m,z}\left(z_2-z_1\right)-j\right]\left[k_{m,z}\left(z_2'-z_1'\right)+j\right]e^{jk_{m,z}\left(z_1-z_1'\right)}$$

$$c_4 = j\left[k_{m,z}\left(z_2'-z_1'\right)+j\right]e^{jk_{m,z}\left(z_2-z_1'\right)}$$

(B.35)

Closed-form formulation (5-7):

case (I) when $z_1 = z_1'$ and $z_2 = z_2'$:

$$\int_{z_1}^{z_2}\int_{z_1'}^{z_2'}e^{-jk_{m,z}|z-z'|}dz'\,dz$$

$$=\frac{2j\left(z_1-z_2\right)}{k_{m,z}}+\frac{2-e^{-jk_{m,z}\left(z_2-z_1'\right)}-e^{jk_{m,z}\left(z_1-z_2'\right)}}{k_{m,z}^2}$$

(B.36)

case (II) when $z > z'$ or $z_1 \geq z_2'$:

$$\int_{z_1}^{z_2}\int_{z_1'}^{z_2'} e^{-jk_{m,z}\left|z-z'\right|}\,dz'\,dz$$

$$= \frac{e^{jk_{m,z}\left(z_1'-z_1\right)} - e^{jk_{m,z}\left(z_2'-z_1\right)} - e^{jk_{m,z}\left(z_1'-z_2\right)} + e^{jk_{m,z}\left(z_2'-z_2\right)}}{k_{m,z}^2}$$

(B.37)

case (III) when $z' > z$ or $z_1' \geq z_1$:

$$\int_{z_1}^{z_2}\int_{z_1'}^{z_2'} e^{-jk_{m,z}\left|z-z'\right|}\,dz'\,dz$$

$$= \frac{e^{-jk_{m,z}\left(z_1'-z_1\right)} - e^{-jk_{m,z}\left(z_2'-z_1\right)} - e^{-jk_{m,z}\left(z_1'-z_2\right)} + e^{-jk_{m,z}\left(z_2'-z_2\right)}}{k_{m,z}^2}$$

(B.38)

Closed-form formulation (8-11):

There is no free-space Green's function (or the primary term of the Green's function) associated with the g_{zt} term in DGF as showed in Appendix A.

Closed-form formulation (12-13):

case (I) when $z_1 = z_1'$ and $z_2 = z_2'$:

$$\int_{z_1}^{z_2} e^{-jk_{m,z}\left|z-z'\right|}\,dz$$

$$= \begin{cases} \dfrac{je^{-jk_{m,z}\left(z'-z_2\right)}}{k_{m,z}} - \dfrac{j}{k_{m,z}} & if\left(z'=z1\right) \\[2mm] \dfrac{je^{-jk_{m,z}\left(z'-z_1\right)}}{k_{m,z}} - \dfrac{j}{k_{m,z}} & if\left(z'=z2\right) \\[2mm] \dfrac{j\left(e^{-jk_{m,z}\left(z'-z_1\right)} + e^{-jk_{m,z}\left(z'-z_2\right)}\right)}{k_{m,z}} - \dfrac{2j}{k_{m,z}} & elsewhere \end{cases}$$

(B.39)

case (II) when $z > z'$ or $z_1 \geq z_2'$:

$$\int_{z_1}^{z_2} e^{-jk_{m,z}\left|z-z'\right|}\,dz = \frac{j\left(e^{-jk_{m,z}\left(z_2-z'\right)} - e^{-jk_{m,z}\left(z_1-z'\right)}\right)}{k_{m,z}}$$

(B.40)

case (III) when $z' > z$ or $z_1' \geq z_1$:

$$\int_{z_1}^{z_2} e^{-jk_{m,z}|z-z'|} dz = \frac{j\left(e^{-jk_{m,z}(z'-z_1)} - e^{-jk_{m,z}(z'-z_2)}\right)}{k_{m,z}} \tag{B.41}$$

Closed-form formulation (14-16):

case (I) when $z_1 = z_1'$ and $z_2 = z_2'$:

$$\int_{z_1'}^{z_2'} e^{-jk_{m,z}|z-z'|} dz'$$

$$= \begin{cases} \dfrac{je^{-jk_{m,z}(z_2'-z)}}{k_{m,z}} - \dfrac{j}{k_{m,z}} & if\left(z = z_1'\right) \\[4mm] \dfrac{je^{-jk_{m,z}(z-z_1')}}{k_{m,z}} - \dfrac{j}{k_{m,z}} & if\left(z = z_2'\right) \\[4mm] \dfrac{j\left(e^{-jk_{m,z}(z_2'-z)} + e^{-jk_{m,z}(z-z_1')}\right)}{k_{m,z}} - \dfrac{2j}{k_{m,z}} & elsewhere \end{cases} \tag{B.42}$$

case (II) when $z > z'$ or $z_1 \geq z_2'$:

$$\int_{z_1'}^{z_2'} e^{-jk_{m,z}|z-z'|} dz' = \frac{j\left(e^{-jk_{m,z}(z-z_1')} - e^{-jk_{m,z}(z-z_2')}\right)}{k_{m,z}} \tag{B.43}$$

case (III) when $z' > z$ or $z_1' \geq z_1$:

$$\int_{z_1'}^{z_2'} e^{-jk_{m,z}|z-z'|} dz' = \frac{j\left(e^{-jk_{m,z}(z_2'-z)} - e^{-jk_{m,z}(z_1'-z)}\right)}{k_{m,z}} \tag{B.44}$$

B.6 Source and field points located at the same layer in the layered media

In this section, we present the closed-form formulation for a multi-layered Green's function as illustrated in Fig A.1. For the vertical-to-vertical basis reactions, we need to consider only vertical field and source patches. For vertical-to-horizontal and horizontal-to-vertical basis reactions, we need to consider both horizontal or vertical patches since both can support horizontally-directed basis functions.

Closed-form formulation (1):

$$\int_{z_1}^{z_2}\int_{z_1'}^{z_2'}(z-z_2)\tilde{G}_{zz}\left(k_r,z,z'\right)\left(z'-z_1'\right)dz'dz = \frac{\sum_{i=1}^{13}c_i}{k_{m,z}^4} \tag{B.45}$$

in which the layered media Green's function $\tilde{G}_{zz}$ is due to a z-directed source and field. The Fresnel reflection coefficients A_1, A_2, A_3 associated with $\tilde{G}_{zz}$ (A.91) are defined as:

$$\tilde{G}_{zz}\left(z,z'\right)=A_1 e^{jk_{m,z}\left(z+z'+2d_{m-1}\right)}+A_2\left(e^{-jk_{m,z}\left(z'-z+2(d_m-d_{m-1})\right)}+e^{jk_{m,z}\left(z'-z-2(d_m-d_{m-1})\right)}\right)+A_3 e^{-jk_{m,z}\left(z'+z+2d_m\right)}$$

$$A_1 = \tilde{R}_{m,m-1}^{TM}\tilde{M}_m^{TM}$$

$$A_2 = \tilde{R}_{m,m-1}^{TM}\tilde{R}_{m,m+1}^{TM}\tilde{M}_m^{TM}$$

$$A_3 = \tilde{R}_{m,m+1}^{TM}\tilde{M}_m^{TM}$$

$$\tag{B.46}$$

and

$$c_1 = -jA_3 \left[k_{m\,z} \left(z_1' - z_2' \right) + j \right] e^{-jk_{m\,z} \left(z_2 + z_2' + 2 d_m \right)}$$

$$c_2 = -jA_2 \left[k_{m\,z} \left(z_1' - z_2' \right) + j \right] e^{jk_{m,z} \left(z_2 - z_2' - 2(d_m - d_{m-1}) \right)}$$

$$c_3 = jA_2 \left[k_{m\,z} \left(z_1' - z_2' \right) - j \right] e^{-jk_{m,z} \left(z_2 - z_2' + 2(d_m - d_{m-1}) \right)}$$

$$c_4 = jA_1 \left[k_{m,z} \left(z_1' - z_2' \right) - j \right] e^{jk_{m,z} \left(z_2 + z_2' + 2 d_{m-1} \right)}$$

$$c_5 = -A_2 \left[k_{m\,z} \left(z_2 - z_1 \right) + j \right] \left[k_{m,z} \left(z_1' - z_2' \right) - j \right] e^{-jk_{m,z} \left(z_1 - z_2' + 2(d_m - d_{m-1}) \right)}$$

$$c_6 = -A_2 \left[k_{m\,z} \left(z_2 - z_1 \right) - j \right] \left[k_{m,z} \left(z_1' - z_2' \right) + j \right] e^{jk_{m,z} \left(z_1 - z_2' - 2(d_m - d_{m-1}) \right)}$$

$$c_7 = A_1 \left[k_{m\,z} \left(z_2 - z_1 \right) - j \right] \left[k_{m,z} \left(z_1' - z_2' \right) - j \right] e^{jk_{m,z} \left(z_1 + z_2' + 2 d_{m-1} \right)}$$

$$c_8 = A_3 \left[k_{m\,z} \left(z_2 - z_1 \right) + j \right] \left[k_{m,z} \left(z_1' - z_2' \right) + j \right] e^{-jk_{m,z} \left(z_1 + z_2' + 2 d_m \right)}$$

$$c_9 = jA_1 \left[k_{m\,z} \left(z_2 - z_1 \right) - j \right] e^{jk_{m,z} \left(z_1 + z_1' + 2 d_{m-1} \right)}$$

$$c_{10} = -jA_3 \left[k_{m\,z} \left(z_2 - z_1 \right) + j \right] e^{-jk_{m,z} \left(z_1 + z_1' + 2 d_m \right)}$$

$$c_{11} = -2A_2 \left\{ \left(z_1 - z_2 \right) k_{m,z} \sin \left[k_{m,z} \left(z_1' - z_1 \right) \right] + \cos \left[k_{m,z} \left(z_2 - z_1' \right) \right] - \cos \left[k_{m,z} \left(z_1 - z_1' \right) \right] \right\} e^{-jk_{m,z} \, 2(d_m - d_{m-1})}$$

$$c_{12} = -A_1 e^{jk_{m,z} \left(z_2 + z_1' + 2 d_{m-1} \right)}$$

$$c_{13} = -A_3 e^{-jk_{m,z} \left(z_2 + z_1' + 2 d_m \right)}$$

(B.47)

Closed-form formulation (2):

$$\int_{z_1}^{z_2} \int_{z_1'}^{z_2'} (z - z_1) \tilde{G}_{zz} \left(k_r, z, z' \right) \left(z' - z_2' \right) dz' dz = \frac{\sum\limits_{i=1}^{16} c_i}{k_{m,z}^4}$$

(B.48)

in which

$$c_1 = jA_2\left[k_{m,z}\left(z_1' - z_2'\right) - j\right]e^{-jk_{m,z}\left(z_1' - z_1 + 2\left(d_m - d_{m-1}\right)\right)}$$

$$c_2 = -jA_1\left[k_{m,z}\left(z_1' - z_2'\right) + j\right]e^{jk_{m,z}\left(z_1 + z_1' + 2d_{m-1}\right)}$$

$$c_3 = -jA_2\left[k_{m,z}\left(z_1' - z_2'\right) + j\right]e^{-jk_{m,z}\left(z_1 - z_1' + 2\left(d_m - d_{m-1}\right)\right)}$$

$$c_4 = jA_3\left[k_{m,z}\left(z_1' - z_2'\right) - j\right]e^{-jk_{m,z}\left(z_1 + z_1' + 2d_m\right)}$$

$$c_5 = jA_2\left[k_{m,z}\left(z_1 - z_2\right) - j\right]e^{-jk_{m,z}\left(z_2' - z_2 + 2\left(d_m - d_{m-1}\right)\right)}$$

$$c_6 = jA_1\left[k_{m,z}\left(z_1 - z_2\right) - j\right]e^{jk_{m,z}\left(z_2 + z_2' + 2d_{m-1}\right)}$$

$$c_7 = -jA_2\left[k_{m,z}\left(z_1 - z_2\right) + j\right]e^{-jk_{m,z}\left(z_2 - z_2' + 2\left(d_m - d_{m-1}\right)\right)}$$

$$c_8 = -jA_3\left[k_{m,z}\left(z_1 - z_2\right) + j\right]e^{-jk_{m,z}\left(z_2 + z_2' + 2d_m\right)}$$

$$c_9 = -A_1\left[k_{m,z}\left(z_1 - z_2\right) - j\right]\left[k_{m,z}\left(z_1' - z_2'\right) + j\right]e^{jk_{m,z}\left(z_2 + z_1' + 2d_{m-1}\right)}$$

$$c_{10} = A_2\left[k_{m,z}\left(z_1 - z_2\right) - j\right]\left[k_{m,z}\left(z_1' - z_2'\right) - j\right]e^{-jk_{m,z}\left(z_1' - z_2 + 2\left(d_m - d_{m-1}\right)\right)}$$

$$c_{11} = A_2\left[k_{m,z}\left(z_1 - z_2\right) + j\right]\left[k_{m,z}\left(z_1' - z_2'\right) + j\right]e^{-jk_{m,z}\left(z_2 - z_1' + 2\left(d_m - d_{m-1}\right)\right)}$$

$$c_{12} = -A_3\left[k_{m,z}\left(z_1 - z_2\right) + j\right]\left[k_{m,z}\left(z_1' - z_2'\right) - j\right]e^{-jk_{m,z}\left(z_2 + z_1' + 2d_m\right)}$$

$$c_{13} = -A_3 e^{-jk_{m,z}\left(z_1 + z_2' + 2d_m\right)} \tag{B.49}$$

$$c_{14} = -A_2 e^{-jk_{m,z}\left(z_2 - z_1 + 2\left(d_m - d_{m-1}\right)\right)}$$

$$c_{15} = -A_2 e^{-jk_{m,z}\left(z_1 - z_2' + 2\left(d_m - d_{m-1}\right)\right)}$$

$$c_{16} = -A_1 e^{jk_{m,z}\left(z_1 + z_2' + 2d_{m-1}\right)}$$

Closed-form formulation (3):

$$\int_{z_1}^{z_2}\int_{z_1'}^{z_2'}\left(z - z_1\right)\tilde{G}_{zz}\left(k_r, z, z'\right)\left(z' - z_1'\right)dz'dz = \frac{\sum_{i=1}^{16} c_i}{k_{m,z}^4} \tag{B.50}$$

in which

128

$$c_1 = -jA_3\left[k_{m\,z}\left(z_1^{'}-z_2^{'}\right)+j\right]e^{-jk_{m,z}\left(z_1^{'}+z_2^{'}+2d_m\right)}$$

$$c_2 = -jA_2\left[k_{m,z}\left(z_1^{'}-z_2^{'}\right)+j\right]e^{-jk_{m,z}\left(z_2^{'}-z_1^{'}+2\left(d_m-d_{m-1}\right)\right)}$$

$$c_3 = jA_2\left[k_{m\,z}\left(z_1^{'}-z_2^{'}\right)-j\right]e^{-jk_{m,z}\left(z_1^{'}-z_2^{'}+2\left(d_m-d_{m-1}\right)\right)}$$

$$c_4 = jA_1\left[k_{m\,z}\left(z_1^{'}-z_2^{'}\right)-j\right]e^{jk_{m,z}\left(z_1^{'}+z_2^{'}+2d_{m-1}\right)}$$

$$c_5 = -A_2\left[k_{m\,z}\left(z_1-z_2\right)-j\right]\left[k_{m,z}\left(z_1^{'}-z_2^{'}\right)+j\right]e^{-jk_{m,z}\left(z_2^{'}-z_2+2\left(d_m-d_{m-1}\right)\right)}$$

$$c_6 = A_1\left[k_{m,z}\left(z_1-z_2\right)-j\right]\left[k_{m,z}\left(z_1^{'}-z_2^{'}\right)-j\right]e^{jk_{m,z}\left(z_2+z_2^{'}+2d_{m-1}\right)}$$

$$c_7 = -A_2\left[k_{m\,z}\left(z_1-z_2\right)+j\right]\left[k_{m,z}\left(z_1^{'}-z_2^{'}\right)-j\right]e^{-jk_{m,z}\left(z_2-z_2^{'}+2\left(d_m-d_{m-1}\right)\right)}$$

$$c_8 = A_3\left[k_{m,z}\left(z_1-z_2\right)+j\right]\left[k_{m,z}\left(z_1^{'}-z_2^{'}\right)+j\right]e^{-jk_{m,z}\left(z_2+z_2^{'}+2d_m\right)}$$

$$c_9 = jA_1\left[k_{m\,z}\left(z_1-z_2\right)-j\right]e^{jk_{m,z}\left(z_2+z_1^{'}+2d_{m-1}\right)}$$

$$c_{10} = jA_2\left[k_{m\,z}\left(z_1-z_2\right)-j\right]e^{-jk_{m,z}\left(z_1^{'}-z_2+2\left(d_m-d_{m-1}\right)\right)}$$

$$c_{11} = -jA_2\left[k_{m\,z}\left(z_1-z_2\right)+j\right]e^{-jk_{m,z}\left(z_2-z_1^{'}+2\left(d_m-d_{m-1}\right)\right)}$$

$$c_{12} = -jA_3\left[k_{m,z}\left(z_1-z_2\right)+j\right]e^{-jk_{m,z}\left(z_2+z_1^{'}+2d_m\right)}$$

$$c_{13} = -A_2e^{-jk_{m,z}\left(z_1^{'}-z_1+2\left(d_m-d_{m-1}\right)\right)}$$

$$c_{14} = -A_1e^{jk_{m,z}\left(z_1+z_1^{'}+2d_{m-1}\right)}$$

$$c_{15} = -A_2e^{-jk_{m,z}\left(z_1-z_1^{'}+2\left(d_m-d_{m-1}\right)\right)}$$

$$c_{16} = -A_3e^{-jk_{m,z}\left(z_1^{'}+z_1+2d_m\right)}$$

(B.51)

Closed-form formulation (4):

$$\int_{z_1}^{z_2}\int_{z_1^{'}}^{z_2^{'}}(z-z_2)\tilde{G}_{zz}\left(k_r,z,z^{'}\right)\left(z^{'}-z_2^{'}\right)dz^{'}dz = \frac{\sum\limits_{i=1}^{16}c_i}{k_{m,z}^4}$$

(B.52)

in which

$$c_1 = jA_2\left[k_{m\,z}\left(z_2' - z_1'\right) + j\right]e^{-jk_{m,z}\left(z_1' - z_2' + 2\left(d_m - d_{m-1}\right)\right)}$$

$$c_2 = jA_3\left[k_{m\,z}\left(z_2' - z_1'\right) + j\right]e^{-jk_{m,z}\left(z_1' + z_2' + 2d_m\right)}$$

$$c_3 = jA_2\left[k_{m\,z}\left(z_1' - z_2'\right) + j\right]e^{-jk_{m,z}\left(z_2' - z_1' + 2\left(d_m - d_{m-1}\right)\right)}$$

$$c_4 = jA_1\left[k_{m\,z}\left(z_1' - z_2'\right) + j\right]e^{jk_{m,z}\left(z_1' + z_2' + 2d_{m-1}\right)}$$

$$c_5 = -A_3\left[k_{m\,z}\left(z_2 - z_1\right) + j\right]\left[k_{m,z}\left(z_2' - z_1'\right) + j\right]e^{-jk_{m,z}\left(z_1 + z_2' + 2\,d_m\right)}$$

$$c_6 = -A_1\left[k_{m\,z}\left(z_2 - z_1\right) - j\right]\left[k_{m,z}\left(z_2' - z_1'\right) - j\right]e^{jk_{m,z}\left(z_1 + z_1' + 2\,d_{m-1}\right)}$$

$$c_7 = jA_2\left[k_{m\,z}\left(z_1 - z_2\right) + j\right]e^{-jk_{m,z}\left(z_2' - z_1 + 2\left(d_m - d_{m-1}\right)\right)}$$

$$c_8 = jA_2\left[k_{m\,z}\left(z_2 - z_1\right) + j\right]e^{-jk_{m,z}\left(z_1 - z_2' + 2\left(d_m - d_{m-1}\right)\right)}$$

$$c_9 = A_2\left[k_{m,z}\left(z_2 - z_1\right) - j\right]\left[k_{m,z}\left(z'_2 - z_1'\right) + j\right]e^{-jk_{m,z}\left(z_1' - z_1 + 2\left(d_m - d_{m-1}\right)\right)}$$

$$c_{10} = jA_1\left[k_{m\,z}\left(z_1 - z_2\right) + j\right]e^{jk_{m,z}\left(z_1 + z_2' + 2d_{m-1}\right)}$$

$$c_{11} = jA_3\left[k_{m\,z}\left(z_2 - z_1\right) + j\right]e^{-jk_{m,z}\left(z_1 + z_2' + 2d_m\right)}$$

$$c_{12} = A_2\left[k_{m\,z}\left(z_2 - z_1\right) + j\right]\left[k_{m,z}\left(z'_2 - z_1'\right) - j\right]e^{-jk_{m,z}\left(z_1 - z_1' + 2\left(d_m - d_{m-1}\right)\right)}$$

$$c_{13} = A_1 e^{jk_{mz}\left(z_2 + z_2' + 2d_{m-1}\right)}$$

$$c_{14} = A_3 e^{-jk_{m,z}\left(z_2 + z_2' + 2\,d_m\right)}$$

$$c_{15} = A_2 e^{-jk_{m,z}\left(z_2' - z_2 + 2\left(d_m - d_{m-1}\right)\right)}$$

$$c_{16} = A_2 e^{-jk_{m,z}\left(z_2 - z_2' + 2\left(d_m - d_{m-1}\right)\right)} \tag{B.53}$$

Closed-form formulation (5):

$$\int_{z_1}^{z_2}\int_{z_1'}^{z_2'} \tilde{G}_{xx}\left(k_r, z, z'\right)dz'dz = \frac{c_1 + c_2 + c_3}{k_{m,z}^2} \tag{B.54}$$

in which the layered media Green's function $\tilde{G}_{xx}$ is due to an x-directed field and an x-directed source projection. The Fresnel reflection coefficients A_1, A_2, A_3 associated with $\tilde{G}_{xx}$ (A.91) are defined as:

$$\tilde{G}_{xx}\left(z,z'\right) = A_1 e^{jk_{m,z}\left(z+z'+2d_{m-1}\right)} + A_2\left(e^{-jk_{m,z}\left(z'-z+2(d_m-d_{m-1})\right)} + e^{jk_{m,z}\left(z'-z-2(d_m-d_{m-1})\right)}\right) + A_3 e^{-jk_{m,z}\left(z'+z+2d_m\right)}$$

$$A_1 = \tilde{R}_{m,m-1}^{TE}\tilde{M}_m^{TE}$$

$$A_2 = \tilde{R}_{m,m-1}^{TE}\tilde{R}_{m,m+1}^{TE}\tilde{M}_m^{TE}$$

$$A_3 = \tilde{R}_{m,m+1}^{TE}\tilde{M}_m^{TE}$$

$$(\text{B.55})$$

and

$$c_1 = -A_1\left\{e^{jk_{m,z}\left(z_1'+z_1+2d_{m-1}\right)} - e^{jk_{m,z}\left(z_1+z_2'+2d_{m-1}\right)} - e^{jk_{m,z}\left(z_2+z_1'+2d_{m-1}\right)} + e^{jk_{m,z}\left(z_2+z_2'+2d_{m-1}\right)}\right\}$$

$$c_2 = -A_2\left\{\begin{matrix} -e^{-jk_{m,z}\left(z_1-z_1'+2(d_m-d_{m-1})\right)} + e^{-jk_{m,z}\left(z_1-z_2'+2(d_m-d_{m-1})\right)} + e^{-jk_{m,z}\left(z_2'-z_1+2(d_m-d_{m-1})\right)} + e^{-jk_{m,z}\left(z_2-z_1'+2(d_m-d_{m-1})\right)} \\ +e^{-jk_{m,z}\left(z_1'-z_2+2(d_m-d_{m-1})\right)} - e^{-jk_{m,z}\left(z_2-z_2'+2(d_m-d_{m-1})\right)} - e^{-jk_{m,z}\left(z_2'-z_2+2(d_m-d_{m-1})\right)} - e^{-jk_{m,z}\left(z_1-z_1'+2(d_m-d_{m-1})\right)} \end{matrix}\right\}$$

$$c_3 = -A_3\left\{e^{-jk_{m,z}\left(z_1'+z_1+2d_m\right)} - e^{-jk_{m,z}\left(z_1+z_2'+2d_m\right)} - e^{-jk_{m,z}\left(z_2+z_1'+2d_m\right)} + e^{-jk_{m,z}\left(z_2+z_2'+2d_m\right)}\right\}$$

$$(\text{B.56})$$

Closed-form formulation (6):

$$\int_{z_1}^{z_2}\int_{z_1'}^{z_2'}\tilde{G}_{vz}\left(k_r,z,z'\right)dz'dz = \frac{c_1+c_2+c_3}{k_{m,z}^2}$$

$$(\text{B.57})$$

The layered media Green's function of $\tilde{G}_{vz}$ (A.92) is the scalar potential of the MPIE due to a vertical current. For this case it is assumed that both the source and field basis are situated in vertical patches. The analytical formulation of (B.57) is derived as the following:

$$c_1 = A_1\left\{e^{jk_{m,z}\left(z_1'+z_1+2d_{m-1}\right)} - e^{jk_{m,z}\left(z_1+z_2'+2d_{m-1}\right)} - e^{jk_{m,z}\left(z_2+z_1'+2d_{m-1}\right)} + e^{jk_{m,z}\left(z_2+z_2'+2d_{m-1}\right)}\right\}$$

$$c_2 = A_2\left\{\begin{matrix} e^{jk_{m,z}\left(z_1'-z_1-2(d_m-d_{m-1})\right)} - e^{jk_{m,z}\left(z_2'-z_1-2(d_m-d_{m-1})\right)} - e^{-jk_{m,z}\left(z_2'-z_1+2(d_m-d_{m-1})\right)} - e^{jk_{m,z}\left(z_1'-z_2-2(d_m-d_{m-1})\right)} \\ -e^{-jk_{m,z}\left(z_1'-z_2+2(d_m-d_{m-1})\right)} + e^{jk_{m,z}\left(z_2'-z_2-2(d_m-d_{m-1})\right)} + e^{-jk_{m,z}\left(z_2'-z_2+2(d_m-d_{m-1})\right)} + e^{-jk_{m,z}\left(z_1'-z_1+2(d_m-d_{m-1})\right)} \end{matrix}\right\}$$

$$c_3 = A_3\left\{-e^{-jk_{m,z}\left(z_2'+z_1+2d_m\right)} - e^{-jk_{m,z}\left(z_2+z_1'+2d_m\right)} + e^{-jk_{m,z}\left(z_2+z_2'+2d_m\right)} + e^{-jk_{m,z}\left(z_1+z_1'+2d_m\right)}\right\}$$

$$(\text{B.58})$$

where the Fresnel reflection coefficients A_1, A_2, and A_3 are defined in (B.46) for the TM$_z$-polarization.

Closed-form formulation (7):

$$\int\limits_{z_1}^{z_2}\int\limits_{z_1'}^{z_2'}\tilde{G}_{vt}\left(k_r,z,z'\right)dz'dz=\frac{\sum\limits_{i=1}^{16}c_i}{k_{m,z}^2 k_r^2}$$

(B.59)

in which the layered media Green's function $\tilde{G}_{vt}$ is the scalar potential term of the MPIE. For this case, it is assumed that the horizontal current is supported by a vertical patch, and the field basis is supported by a vertical patch. The Fresnel reflection coefficients A_1 to A_6 associated with $\tilde{G}_{vt}$ (A.92) are defined as:

$$\tilde{G}_{vt}=\frac{\left(A_1 k_m^2 + A_3 k_{m,z}^2\right)e^{jk_{m,z}\left(2d_{m-1}+z+z'\right)}+\left(A_2 k_m^2 - A_4 k_{m,z}^2\right)\left(e^{-jk_{m,z}\left(z'-z+2(d_m-d_{m-1})\right)}+e^{-jk_{m,z}\left(z-z'+2(d_m-d_{m-1})\right)}\right)}{k_r^2}$$
$$\frac{+\left(A_5 k_{m,z}^2 + A_6 k_m^2\right)e^{-jk_{m,z}\left(z+z'+2d_m\right)}}{}$$

$$A_1 = \tilde{R}_{m,m-1}^{TE}\tilde{M}_m^{TE} \qquad A_4 = \tilde{R}_{m,m-1}^{TM}\tilde{M}_m^{TM}\tilde{R}_{m,m+1}^{TM}$$
$$A_2 = \tilde{R}_{m,m-1}^{TE}\tilde{R}_{m,m+1}^{TE}\tilde{M}_m^{TE} \qquad A_5 = \tilde{R}_{m,m+1}^{TM}\tilde{M}_m^{TM}$$
$$A_3 = \tilde{R}_{m,m-1}^{TM}\tilde{M}_m^{TM} \qquad A_6 = \tilde{R}_{m,m+1}^{TE}\tilde{M}_m^{TE}$$

(B.60)

and

$$c_1 = \left(A_2 k_m^2 - A_4 k_{m,z}^2\right) e^{-jk_{m,z}\left(z_2 - z_2' + 2(d_m - d_{m-1})\right)}$$

$$c_2 = \left(A_5 k_{m,z}^2 + A_6 k_m^2\right) e^{-jk_{m,z}\left(z_1 + z_2' + 2d_m\right)}$$

$$c_3 = \left(A_1 k_m^2 + A_3 k_{m,z}^2\right) e^{jk_{m,z}\left(z_1 + z_2' + 2d_{m-1}\right)}$$

$$c_4 = \left(A_4 k_{m,z}^2 - A_2 k_m^2\right) e^{-jk_{m,z}\left(z_1 - z_2' + 2(d_m - d_{m-1})\right)}$$

$$c_5 = -\left(A_3 k_{m,z}^2 + A_1 k_m^2\right) e^{jk_{m,z}\left(z_1 + z_1' + 2d_{m-1}\right)}$$

$$c_6 = \left(A_2 k_m^2 - A_4 k_{m,z}^2\right) e^{-jk_{m,z}\left(z_1 - z_1' + 2(d_m - d_{m-1})\right)}$$

$$c_7 = -\left(A_5 k_{m,z}^2 + A_6 k_m^2\right) e^{-jk_{m,z}\left(z_1 + z_1' + 2d_m\right)}$$

$$c_8 = -\left(A_5 k_{m,z}^2 + A_6 k_m^2\right) e^{-jk_{m,z}\left(z_2 + z_2' + 2d_m\right)}$$

$$c_9 = -\left(A_3 k_{m,z}^2 + A_1 k_m^2\right) e^{jk_{m,z}\left(z_2 + z_2' + 2d_{m-1}\right)}$$

$$c_{10} = \left(A_1 k_m^2 + A_3 k_{m,z}^2\right) e^{jk_{m,z}\left(z_2 + z_1' + 2d_{m-1}\right)}$$

$$c_{11} = \left(A_4 k_{m,z}^2 - A_2 k_m^2\right) e^{-jk_{m,z}\left(z_2 - z_1' + 2(d_m - d_{m-1})\right)}$$

$$c_{12} = \left(A_5 k_{m,z}^2 + A_6 k_m^2\right) e^{-jk_{m,z}\left(z_2 + z_1' + 2d_m\right)}$$

$$c_{13} = \left(A_4 k_{m,z}^2 - A_2 k_m^2\right) e^{-jk_{m,z}\left(z_2' - z_1 + 2(d_m - d_{m-1})\right)}$$

$$c_{14} = \left(A_2 k_m^2 - A_4 k_{m,z}^2\right) e^{-jk_{m,z}\left(z_1' - z_1 + 2(d_m - d_{m-1})\right)}$$

$$c_{15} = \left(A_2 k_m^2 - A_4 k_{m,z}^2\right) e^{-jk_{m,z}\left(z_2' - z_2 + 2(d_m - d_{m-1})\right)}$$

$$c_{16} = \left(A_4 k_{m,z}^2 - A_2 k_m^2\right) e^{-jk_{m,z}\left(z_1' - z_2 + 2(d_m - d_{m-1})\right)}$$

(B.61)

Closed-form formulation (8):

$$\int_{z_1}^{z_2}\int_{z_1'}^{z_2'} \tilde{g}_{zt}\left(k_r, z, z'\right)\left(z - z_1\right) dz' dz = \frac{\displaystyle\sum_{i=1}^{16} c_i}{k_{m,z}^3}$$

(B.62)

for the reaction of a horizontal source basis with a vertical field basis. For this case, it is assumed that the horizontal source basis is supported by a vertical patch. The closed-form expression of (B.62) is:

$$\tilde{g}_{zt} = \left(A_1 + A_3\right) e^{jk_{m,z}\left(2d_{m-1} + z + z'\right)} + \left(A_2 - A_4\right)\left(e^{-jk_{m,z}\left(z' - z + 2(d_m - d_{m-1})\right)} - e^{-jk_{m,z}\left(z - z' + 2(d_m - d_{m-1})\right)}\right)$$
$$- \left(A_5 + A_6\right) e^{-jk_{m,z}\left(z + z' + 2(d_m - d_{m-1})\right)}$$

(B.63)

in which the Fresnel reflection coefficients A_1 to A_6 are defined in (B.60), and

$$c_1 = -(A_5 + A_6)\left[k_{m,z}(z_1 - z_2) + j\right]e^{-jk_{m,z}\left(z_2 + z_2' + 2d_m\right)}$$

$$c_2 = (A_5 + A_6)\left[k_{m,z}(z_1 - z_2) + j\right]e^{-jk_{m,z}\left(z_2 + z_1' + 2d_m\right)}$$

$$c_3 = (A_2 - A_4)\left[k_{m,z}(z_1 - z_2) + j\right]e^{-jk_{m,z}\left(z_2 - z_2' + 2(d_m - d_{m-1})\right)}$$

$$c_4 = (A_2 - A_4)\left[k_{m,z}(z_1 - z_2) - j\right]e^{-jk_{m,z}\left(z_1' - z_2 + 2(d_m - d_{m-1})\right)}$$

$$c_5 = (A_4 - A_2)\left[k_{m,z}(z_1 - z_2) + j\right]e^{-jk_{m,z}\left(z_2 - z_1' + 2(d_m - d_{m-1})\right)}$$

$$c_6 = -(A_1 + A_3)\left[k_{m,z}(z_1 - z_2) - j\right]e^{jk_{m,z}\left(z_2 + z_1' + 2d_{m-1}\right)}$$

$$c_7 = (A_4 - A_2)\left[k_{m,z}(z_1 - z_2) - j\right]e^{-jk_{m,z}\left(z_2' - z_2 + 2(d_m - d_{m-1})\right)}$$

$$c_8 = (A_1 + A_3)\left[k_{m,z}(z_1 - z_2) - j\right]e^{jk_{m,z}\left(z_2 + z_2' + 2d_{m-1}\right)}$$

$$c_9 = j(A_2 - A_4)e^{-jk_{m,z}\left(z_1 - z_1' + 2(d_m - d_{m-1})\right)}$$

$$c_{10} = j(A_4 - A_2)e^{-jk_{m,z}\left(z_1 - z_2' + 2(d_m - d_{m-1})\right)}$$

$$c_{11} = j(A_5 + A_6)e^{-jk_{m,z}\left(z_1 + z_2' + 2d_m\right)}$$

$$c_{12} = j(A_1 + A_3)e^{jk_{m,z}\left(z_1 + z_2' + 2d_{m-1}\right)} \qquad \text{(B.64)}$$

$$c_{13} = -j(A_5 + A_6)e^{-jk_{m,z}\left(z_1 + z_1' + 2d_m\right)}$$

$$c_{14} = j(A_2 - A_4)e^{-jk_{m,z}\left(z_1' - z_1 + 2(d_m - d_{m-1})\right)}$$

$$c_{15} = -j(A_1 + A_3)e^{jk_{m,z}\left(z_1 + z_1' + 2d_{m-1}\right)}$$

$$c_{16} = j(A_4 - A_2)e^{-jk_{m,z}\left(z_2' - z_1 + 2(d_m - d_{m-1})\right)}$$

Closed-form formulation (9):

$$\int_{z_1}^{z_2}\int_{z_1'}^{z_2'} \tilde{g}_{zt}\left(k_{\boldsymbol{r}}, z, z'\right)(z - z_2)\, dz'dz = \frac{\sum\limits_{i=1}^{16} c_i}{k_{m,z}^3} \qquad \text{(B.65)}$$

in which

$$c_1 = -j\left(A_4 - A_2\right)e^{-jk_{m,z}\left(z_2 - z_2' + 2\left(d_m - d_{m-1}\right)\right)}$$

$$c_2 = j\left(A_4 - A_2\right)e^{-jk_{m,z}\left(z_1' - z_2 + 2\left(d_m - d_{m-1}\right)\right)}$$

$$c_3 = j\left(A_4 - A_2\right)e^{-jk_{m,z}\left(z_2 - z_1' + 2\left(d_m - d_{m-1}\right)\right)}$$

$$c_4 = -j\left(A_4 - A_2\right)e^{-jk_{m,z}\left(z_2' - z_2 + 2\left(d_m - d_{m-1}\right)\right)}$$

$$c_5 = j\left(A_1 + A_3\right)e^{jk_{m,z}\left(z_2 + z_1' + 2d_{m-1}\right)}$$

$$c_6 = j\left(A_5 + A_6\right)e^{-jk_{m,z}\left(z_1' + z_2 + 2d_m\right)}$$

$$c_7 = -j\left(A_1 + A_3\right)e^{jk_{m,z}\left(z_2 + z_2' + 2d_{m-1}\right)}$$

$$c_8 = -j\left(A_5 + A_6\right)e^{-jk_{m,z}\left(z_2 + z_2' + 2d_m\right)}$$

$$c_9 = \left(A_4 - A_2\right)\left[k_{m,z}\left(z_2 - z_1\right) + j\right]e^{-jk_{m,z}\left(z_1 - z_2' + 2\left(d_m - d_{m-1}\right)\right)}$$

$$c_{10} = \left(A_2 - A_4\right)\left[k_{m,z}\left(z_2 - z_1\right) + j\right]e^{-jk_{m,z}\left(z_1 - z_1' + 2\left(d_m - d_{m-1}\right)\right)}$$

$$c_{11} = \left(A_2 - A_4\right)\left[k_{m,z}\left(z_2 - z_1\right) - j\right]e^{-jk_{m,z}\left(z_2' - z_1 + 2\left(d_m - d_{m-1}\right)\right)}$$

$$c_{12} = \left(A_4 - A_2\right)\left[k_{m,z}\left(z_2 - z_1\right) - j\right]e^{-jk_{m,z}\left(z_1' - z_1 + 2\left(d_m - d_{m-1}\right)\right)}$$

$$c_{13} = \left(A_1 + A_3\right)\left[k_{m,z}\left(z_2 - z_1\right) - j\right]e^{jk_{m,z}\left(z_1 + z_1' + 2d_{m-1}\right)}$$

$$c_{14} = -\left(A_1 + A_3\right)\left[k_{m,z}\left(z_2 - z_1\right) - j\right]e^{jk_{m,z}\left(z_1 + z_2' + 2d_{m-1}\right)}$$

$$c_{15} = -\left(A_5 + A_6\right)\left[k_{m,z}\left(z_2 - z_1\right) + j\right]e^{-jk_{m,z}\left(z_1' + z_1 + 2d_m\right)}$$

$$c_{16} = \left(A_5 + A_6\right)\left[k_{m,z}\left(z_2 - z_1\right) + j\right]e^{-jk_{m,z}\left(z_2' + z_1 + 2d_m\right)}$$

(B.66)

Closed-form formulation (10):

$$\int_{z_1}^{z_2} \tilde{g}_{zt}\left(k_r, z, z'\right)\left(z - z_1\right)dz = \frac{\displaystyle\sum_{i=1}^{8} c_i}{k_{m,z}^2}$$

(B.67)

for the reaction of a horizontal source with a vertical field. In this case, the horizontal source is assumed to be supported by a horizontal patch. The closed-form expression of (B.67) is:

135

$$c_1 = -\left(A_1 + A_3\right)e^{jk_{m,z}\left(z_1 + z' + 2\,d_{m-1}\right)}$$

$$c_2 = \left(A_2 - A_4\right)e^{jk_{m,z}\left(z' - z_1 - 2\left(d_m - d_{m-1}\right)\right)}$$

$$c_3 = \left(A_5 + A_6\right)e^{-jk_{m,z}\left(z_1 + z' + 2\,d_m\right)}$$

$$c_4 = \left(A_4 - A_2\right)e^{-jk_{m,z}\left(z' - z_1 + 2\left(d_m - d_{m-1}\right)\right)}$$

$$c_5 = j\left(A_4 - A_2\right)\left[k_{m,z}\left(z_2 - z_1\right) + j\right]e^{-jk_{m,z}\left(z' - z_2 + 2\left(d_m - d_{m-1}\right)\right)}$$

$$c_6 = j\left(A_4 - A_2\right)\left[k_{m,z}\left(z_2 - z_1\right) - j\right]e^{jk_{m,z}\left(z' - z_2 - 2\left(d_m - d_{m-1}\right)\right)}$$

$$c_7 = -j\left(A_1 + A_3\right)\left[k_{m,z}\left(z_2 - z_1\right) + j\right]e^{jk_{m,z}\left(z_2 + z' + 2\,d_{m-1}\right)}$$

$$c_8 = -j\left(A_5 + A_6\right)\left[k_{m,z}\left(z_2 - z_1\right) - j\right]e^{-jk_{m,z}\left(z_2 + z' + 2\,d_m\right)}$$

(B.68)

in which the Fresnel reflection coefficients A_1 to A_6 are defined in (B.60).

Closed-form formulation (11):

$$\int_{z_1}^{z_2} \tilde{g}_{zt}\left(k_r, z, z'\right)\left(z - z_2\right)dz = \frac{\displaystyle\sum_{i=1}^{8} c_i}{k_{m,z}^2}$$

(B.69)

in which

$$c_1 = j\left(A_4 - A_2\right)\left[k_{m,z}\left(z_2 - z_1\right) + j\right]e^{jk_{m,z}\left(z' - z_1 - 2\left(d_m - d_{m-1}\right)\right)}$$

$$c_2 = -j\left(A_5 + A_6\right)\left[k_{m,z}\left(z_2 - z_1\right) + j\right]e^{-jk_{m,z}\left(z_1 + z' + 2\,d_m\right)}$$

$$c_3 = -j\left(A_1 + A_3\right)\left[k_{m,z}\left(z_2 - z_1\right) - j\right]e^{jk_{m,z}\left(z_1 + z' + 2\,d_{m-1}\right)}$$

$$c_4 = j\left(A_4 - A_2\right)\left[k_{m,z}\left(z_2 - z_1\right) - j\right]e^{-jk_{m,z}\left(z' - z_1 + 2\left(d_m - d_{m-1}\right)\right)}$$

$$c_5 = \left(A_4 - A_2\right)e^{jk_{m,z}\left(z' - z_2 - 2\left(d_m - d_{m-1}\right)\right)}$$

$$c_6 = -\left(A_5 + A_6\right)e^{-jk_{m,z}\left(z' + z_2 + 2\,d_m\right)}$$

$$c_7 = \left(A_1 + A_3\right)e^{jk_{m,z}\left(z_2 + z' + 2\,d_{m-1}\right)}$$

$$c_8 = \left(A_2 - A_4\right)e^{-jk_{m,z}\left(z' - z_2 + 2\left(d_m - d_{m-1}\right)\right)}$$

(B.70)

Closed-form formulation (12):

$$\int_{z_1}^{z_2} \tilde{G}_{xx}\left(k_r, z, z'\right)dz = \frac{c_1 + c_2 + c_3}{k_{m,z}}$$

(B.71)

for the reaction of a horizontal source with a horizontal field. In this case, the horizontal field is assumed to be supported by a vertical patch. The closed-form expression of (B.71) is:

$$c_1 = jA_1 \left\{ e^{jk_{m,z}\left(z_1 + \dot{z} + 2d_{m-1}\right)} - e^{jk_{m,z}\left(z_2 + \dot{z} + 2d_{m-1}\right)} \right\}$$

$$c_2 = jA_2 \left\{ e^{-jk_{m,z}\left(\dot{z} - z_1 + 2\left(d_m - d_{m-1}\right)\right)} - e^{jk_{m,z}\left(\dot{z} - z_1 - 2\left(d_m - d_{m-1}\right)\right)} - e^{-jk_{m,z}\left(\dot{z} - z_2 + 2\left(d_m - d_{m-1}\right)\right)} + e^{jk_{m,z}\left(\dot{z} - z_2 - 2\left(d_m - d_{m-1}\right)\right)} \right\}$$

$$c_3 = jA_3 \left\{ e^{-jk_{m,z}\left(z_2 + \dot{z} + 2d_m\right)} - e^{-jk_{m,z}\left(z_1 + \dot{z} + 2d_m\right)} \right\}$$

$$(B.72)$$

where the Fresnel reflection coefficients A_1 to A_3 are defined in (B.55).

Closed-form formulation (13):

$$\int_{z_1}^{z_2} \tilde{G}_{vt}\left(k_r, z, \dot{z}\right) dz = \frac{\sum_{i=1}^{8} c_i}{k_{m,z} k_r^2} \tag{B.73}$$

for the reaction through the scalar potential with a vertical source. In this case, the reaction with a source basis on a horizontal patch is considered. The closed-form expression of (B.73) is:

$$c_1 = j\left(A_1 k_m^2 + A_3 k_{m,z}^2\right) e^{jk_{m,z}\left(z_1 + \dot{z} + 2d_{m-1}\right)}$$

$$c_2 = j\left(A_2 k_m^2 - A_4 k_{m,z}^2\right) e^{-jk_{m,z}\left(\dot{z} - z_1 + 2\left(d_m - d_{m-1}\right)\right)}$$

$$c_3 = -j\left(A_5 k_{m,z}^2 + A_6 k_m^2\right) e^{-jk_{m,z}\left(z_1 + \dot{z} + 2d_m\right)}$$

$$c_4 = j\left(A_4 k_{m,z}^2 - A_2 k_m^2\right) e^{jk_{m,z}\left(\dot{z} - z_1 - 2\left(d_m - d_{m-1}\right)\right)}$$

$$c_5 = j\left(A_2 k_m^2 - A_4 k_{m,z}^2\right) e^{jk_{m,z}\left(\dot{z} - z_2 - 2\left(d_m - d_{m-1}\right)\right)} \tag{B.74}$$

$$c_6 = -j\left(A_1 k_m^2 + A_3 k_{m,z}^2\right) e^{jk_{m,z}\left(z_2 + \dot{z} + 2d_{m-1}\right)}$$

$$c_7 = j\left(A_4 k_{m,z}^2 - A_2 k_m^2\right) e^{-jk_{m,z}\left(\dot{z} - z_2 + 2\left(d_m - d_{m-1}\right)\right)}$$

$$c_8 = j\left(A_5 k_{m,z}^2 + A_6 k_m^2\right) e^{-jk_{m,z}\left(\dot{z} + z_2 + 2d_m\right)}$$

Closed-form formulation (14):

$$\int_{z_1}^{z_2'} \tilde{G}_{vt}\left(k_r, z, z'\right) dz = \frac{\displaystyle\sum_{i=1}^{8} c_i}{k_{m,z} k_r^2} \tag{B.75}$$

for the reaction through the scalar potential with a vertical source. In this case, the reaction with a field basis on a horizontal patch is considered. The closed-form expression is:

$$
\begin{aligned}
c_1 &= j\left(A_1 k_m^2 + A_3 k_{m,z}^2\right) e^{jk_{m,z}\left(2d_{m-1}+z+z_1'\right)} \\
c_2 &= j\left(A_2 k_m^2 - A_4 k_{m,z}^2\right) e^{-jk_{m,z}\left(2\left(d_m - d_{m-1}\right)+z-z_1'\right)} \\
c_3 &= -j\left(A_5 k_{m,z}^2 + A_6 k_m^2\right) e^{-jk_{m,z}\left(2d_m + z + z_1'\right)} \\
c_4 &= -j\left(A_1 k_m^2 + A_3 k_{m,z}^2\right) e^{jk_{m,z}\left(2d_{m-1}+z+z_2'\right)} \\
c_5 &= j\left(A_4 k_{m,z}^2 - A_2 k_m^2\right) e^{-jk_{m,z}\left(2\left(d_m - d_{m-1}\right)+z-z_2'\right)} \\
c_6 &= j\left(A_5 k_{m,z}^2 + A_6 k_m^2\right) e^{-jk_{m,z}\left(2d_m + z + z_2'\right)} \\
c_7 &= j\left(A_4 k_{m,z}^2 - A_2 k_m^2\right) e^{jk_{m,z}\left(-2\left(d_m - d_{m-1}\right)-z_1'+z\right)} \\
c_8 &= j\left(A_2 k_m^2 - A_4 k_{m,z}^2\right) e^{jk_{m,z}\left(-2\left(d_m - d_{m-1}\right)-z_2'+z\right)}
\end{aligned}
\tag{B.76}
$$

Closed-form formulation (15):

$$\int_{z_1'}^{z_2'} \tilde{G}_{vz}\left(k_r, z, z'\right) dz' = \frac{c_1 + c_2 + c_3}{k_{m,z}} \tag{B.77}$$

for the reaction through the scalar potential with a vertical source. In this case, the reaction with a source basis on a vertical patch is considered. The closed-form expression of (B.77) is:

$$
\begin{aligned}
c_1 &= jA_1 \left\{ -e^{jk_{m,z}\left(z+z_1'+2d_{m-1}\right)} + e^{jk_{m,z}\left(z_2'+z+2d_{m-1}\right)} \right\} \\
c_3 &= jA_3 \left\{ e^{-jk_{m,z}\left(z_1'+z+2d_m\right)} - e^{-jk_{m,z}\left(z+z_2'+2d_m\right)} \right\} \\
c_2 &= jA_2 \left\{ e^{-jk_{m,z}\left(z-z_1'+2\left(d_m-d_{m-1}\right)\right)} - e^{jk_{m,z}\left(z-z_1'-2\left(d_m-d_{m-1}\right)\right)} - e^{-jk_{m,z}\left(z-z_2'+2\left(d_m-d_{m-1}\right)\right)} + e^{jk_{m,z}\left(z-z_2'-2\left(d_m-d_{m-1}\right)\right)} \right\}
\end{aligned}
$$

$$\tag{B.78}$$

Closed-form formulation (16):

$$\int_{z_1'}^{z_2'} \tilde{G}_{xx}\left(k_r, z, z'\right) dz' = \frac{c_1 + c_2 + c_3}{k_{m,z}} \tag{B.79}$$

for the reaction of a horizontal source and field. In this case, the horizontal source is assumed to be supported by a vertical patch and the horizontal field is assumed to be supported by a horizontal patch. The coefficie nts for closed-form expression of (B.79) are:

$$c_1 = jA_1\left\{e^{jk_{m,z}\left(z+z_1'+2d_{m-1}\right)} - e^{jk_{m,z}\left(z+z_2'+2d_{m-1}\right)}\right\}$$

$$c_2 = jA_2\left\{e^{-jk_{m,z}\left(z-z_1'+2\left(d_m-d_{m-1}\right)\right)} - e^{jk_{m,z}\left(z-z_1'-2\left(d_m-d_{m-1}\right)\right)} - e^{-jk_{m,z}\left(z-z_2'+2\left(d_m-d_{m-1}\right)\right)} + e^{jk_{m,z}\left(z-z_2'-2\left(d_m-d_{m-1}\right)\right)}\right\}$$

$$c_3 = jA_3\left\{e^{-jk_{m,z}\left(z+z_2'+2d_m\right)} - e^{-jk_{m,z}\left(z+z_1'+2d_m\right)}\right\}$$

$$\tag{B.80}$$

B.7 Source at m^{th}-layer and field at the ith-layer in the layered media

In this section, we present the closed-form formulation of the basis reaction for a multi-layered Green's function that the source and field points are in different layers as illustrated in Fig A.1. Similarly, we need to consider the basis reaction for all three cases: (1) vertical-to-vertical, (2) vertical-to-horizontal, (3) horizontal-to-vertical.

Closed-form formulation (1):

$$\int_{z_1}^{z_2}\int_{z_1'}^{z_2'}\left(z-z_2\right)\tilde{G}_{zz}\left(k_r, z, z'\right)\left(z'-z_1'\right) dz' dz = \frac{\displaystyle\sum_{i=1}^{16} C_i}{k_{m,z}^2 k_{i,z}^2} \tag{B.81}$$

in which the layered media Green's function $\tilde{G}_{zz}$ (A.149) due to a z-directed source and field that are in different layered media is expressed as:

$$\tilde{G}_{zz} = \begin{cases} \left[A_1 e^{jk_{m,z}(d_{m-1}+z')} + A_2 e^{-jk_{m,z}(2d_m-d_{m-1}+z')} \right]\left[e^{-jk_{i,z}(d_i+z)} + A_3 e^{jk_{i,z}(2d_{i-1}-d_i+z)} \right] & for\,(i<m) \\[2mm] \left[B_1 e^{-jk_{m,z}(d_m+z')} + B_2 e^{jk_{m,z}(2d_{m-1}-d_m+z')} \right]\left[e^{jk_{i,z}(d_{i-1}+z)} + B_3 e^{-jk_{i,z}(2d_i-d_{i-1}+z)} \right] & for\,(i>m) \end{cases}$$

$$A_1 = \tilde{T}_{m,i}^{TM^<} \tilde{M}_m^{TM} \qquad\qquad B_1 = \tilde{T}_{m,i}^{TM^>} \tilde{M}_m^{TM}$$

$$A_2 = \tilde{T}_{m,i}^{TM^<} \tilde{M}_m^{TM} \tilde{R}_{m,m+1}^{TM} \qquad B_2 = \tilde{T}_{m,i}^{TM^>} \tilde{M}_m^{TM} \tilde{R}_{m,m-1}^{TM}$$

$$A_3 = \tilde{R}_{i,i-1}^{TM} \qquad\qquad\qquad B_3 = \tilde{R}_{i,i+1}^{TM}$$

(B.82)

where the Fresnel reflection $\tilde{R}$ and transmission coefficients $\tilde{T}$ are defined in the Appendix A. The analytical form of (B.81) for the cases of $(i<m)$ and $(i>m)$, respectively are derived as:

$$c_1 = -A_2 e^{-j\left[k_{m,z}\left(z_1'+2d_m-d_{m-1}\right)+k_{i,z}\left(z_2+d_i\right)\right]}$$

$$c_2 = -A_1\left[jk_{m,z}\left(z_2'-z_1'\right)-1\right]e^{j\left[k_{m,z}\left(z_2'+d_{m-1}\right)-k_{i,z}\left(z_2+d_i\right)\right]}$$

$$c_3 = -A_1 A_3\left[jk_{m,z}\left(z_2'-z_1'\right)-1\right]e^{j\left[k_{m,z}\left(z_2'+d_{m-1}\right)+k_{i,z}\left(z_2+2d_{i-1}-d_i\right)\right]}$$

$$c_4 = -A_2 A_3\left[jk_{m,z}\left(z_1'-z_2'\right)-1\right]e^{-j\left[k_{m,z}\left(z_2'+2d_m-d_{m-1}\right)-k_{i,z}\left(z_2+2d_{i-1}-d_i\right)\right]}$$

$$c_5 = -A_1 A_3 e^{j\left[k_{m,z}\left(z_1'+d_{m-1}\right)+k_{i,z}\left(z_2+2d_{i-1}-d_i\right)\right]}$$

$$c_6 = -A_2\left[jk_{m,z}\left(z_1'-z_2'\right)-1\right]e^{-j\left[k_{m,z}\left(z_2'+2d_m-d_{m-1}\right)+k_{i,z}\left(z_2+d_i\right)\right]}$$

$$c_7 = -A_2 A_3 e^{-j\left[k_{m,z}\left(z_1'+2d_m-d_{m-1}\right)-k_{i,z}\left(z_2+2d_{i-1}-d_i\right)\right]}$$

$$c_8 = -A_1 e^{j\left[k_{m,z}\left(z_1'+d_{m-1}\right)-k_{i,z}\left(z_2+d_i\right)\right]}$$

$$c_9 = A_2\left[k_{m,z}\left(z_1'-z_2'\right)+j\right]\left[k_{i,z}\left(z_2-z_1\right)+j\right]e^{-j\left[k_{m,z}\left(z_2'+2d_m-d_{m-1}\right)+k_{i,z}\left(z_1+d_i\right)\right]}$$

$$c_{10} = -A_1 A_3\left[jk_{i,z}\left(z_1-z_2\right)-1\right]e^{j\left[k_{m,z}\left(z_1'+d_{m-1}\right)+k_{i,z}\left(z_1+2d_{i-1}-d_i\right)\right]}$$

$$c_{11} = A_2 A_3\left[k_{m,z}\left(z_1'-z_2'\right)+j\right]\left[k_{i,z}\left(z_1-z_2\right)+j\right]e^{-j\left[k_{m,z}\left(z_2'+2d_m-d_{m-1}\right)-k_{i,z}\left(z_1+2d_{i-1}-d_i\right)\right]}$$

$$c_{12} = A_1\left[k_{m,z}\left(z_2'-z_1'\right)+j\right]\left[k_{i,z}\left(z_2-z_1\right)+j\right]e^{j\left[k_{m,z}\left(z_2'+d_{m-1}\right)-k_{i,z}\left(z_1+d_i\right)\right]}$$

$$c_{13} = -A_2\left[jk_{i,z}\left(z_2-z_1\right)-1\right]e^{-j\left[k_{m,z}\left(z_1'+2d_m-d_{m-1}\right)+k_{i,z}\left(z_1+d_i\right)\right]}$$

(B.83)

$$c_{14} = -A_2 A_3\left[jk_{i,z}\left(z_1-z_2\right)-1\right]e^{-j\left[k_{m,z}\left(z_1'+2d_m-d_{m-1}\right)-k_{i,z}\left(z_1+2d_{i-1}-d_i\right)\right]}$$

$$c_{15} = A_1 A_3\left[k_{m,z}\left(z_2'-z_1'\right)+j\right]\left[k_{i,z}\left(z_1-z_2\right)+j\right]e^{j\left[k_{m,z}\left(z_2'+d_{m-1}\right)+k_{i,z}\left(z_1+2d_{i-1}-d_i\right)\right]}$$

$$c_{16} = -A_1\left[jk_{i,z}\left(z_2-z_1\right)-1\right]e^{j\left[k_{m,z}\left(z_1'+d_{m-1}\right)-k_{i,z}\left(z_1+d_i\right)\right]}$$

$$c_1 = B_1 B_3 \left[k_{m,z} \left(z_1' - z_2' \right) + j \right] \left[k_{i,z} \left(z_2 - z_1 \right) + j \right] e^{-j\left[k_{m,z} \left(z_2' + d_m \right) + k_{i,z} \left(z_1 + 2d_i - d_{i-1} \right) \right]}$$

$$c_2 = -B_2 B_3 \left[k_{m,z} \left(z_1' - z_2' \right) - j \right] \left[k_{i,z} \left(z_2 - z_1 \right) + j \right] e^{j\left[k_{m,z} \left(z_2' + 2d_{m-1} - d_m \right) + k_{i,z} \left(z_1 + 2d_i - d_{i-1} \right) \right]}$$

$$c_3 = -B_1 \left[k_{m,z} \left(z_1' - z_2' \right) + j \right] \left[k_{i,z} \left(z_2 - z_1 \right) - j \right] e^{-j\left[k_{m,z} \left(z_2' + d_m \right) - k_{i,z} \left(z_1 + d_{i-1} \right) \right]}$$

$$c_4 = -B_1 B_3 \left[j k_{i,z} \left(z_2 - z_1 \right) - 1 \right] e^{-j\left[k_{m,z} \left(z_1' + d_m \right) + k_{i,z} \left(z_1 + 2d_i - d_{i-1} \right) \right]}$$

$$c_5 = B_2 \left[k_{m,z} \left(z_1' - z_2' \right) - j \right] \left[k_{i,z} \left(z_2 - z_1 \right) - j \right] e^{j\left[k_{m,z} \left(z_2' + 2d_{m-1} - d_m \right) + k_{i,z} \left(z_1 + d_{i-1} \right) \right]}$$

$$c_6 = -B_2 B_3 \left[j k_{i,z} \left(z_2 - z_1 \right) - 1 \right] e^{j\left[k_{m,z} \left(z_1' + 2d_{m-1} - d_m \right) + k_{i,z} \left(z_1 + 2d_i - d_{i-1} \right) \right]}$$

$$c_7 = B_2 \left[j k_{i,z} \left(z_2 - z_1 \right) + 1 \right] e^{j\left[k_{m,z} \left(z_1' + 2d_{m-1} - d_m \right) + k_{i,z} \left(z_1 + d_{i-1} \right) \right]}$$

$$c_8 = B_1 \left[j k_{i,z} \left(z_2 - z_1 \right) + 1 \right] e^{-j\left[k_{m,z} \left(z_1' + d_m \right) - k_{i,z} \left(z_1 + d_{i-1} \right) \right]}$$

$$c_9 = -B_1 B_3 e^{-j\left[k_{m,z} \left(z_1' + d_m \right) + k_{i,z} \left(z_2 + 2d_i - d_{i-1} \right) \right]}$$

$$c_{10} = -B_1 e^{-j\left[k_{m,z} \left(z_1' + d_m \right) + k_{i,z} \left(z_2 + d_{i-1} \right) \right]}$$

$$c_{11} = -B_2 e^{j\left[k_{m,z} \left(z_1' + 2d_{m-1} - d_m \right) + k_{i,z} \left(z_2 + d_{i-1} \right) \right]}$$

$$c_{12} = B_2 \left[j k_{m,z} \left(z_1' - z_2' \right) + 1 \right] e^{j\left[k_{m,z} \left(z_2' + 2d_{m-1} - d_m \right) + k_{i,z} \left(z_2 + d_{i-1} \right) \right]}$$

$$c_{13} = -B_2 B_3 e^{j\left[k_{m,z} \left(z_1' + 2d_{m-1} - d_m \right) + k_{i,z} \left(z_2 + 2d_i - d_{i-1} \right) \right]} \tag{B.84}$$

$$c_{14} = -B_1 \left[j k_{m,z} \left(z_1' - z_2' \right) - 1 \right] e^{-j\left[k_{m,z} \left(z_2' + d_m \right) - k_{i,z} \left(z_2 + d_{i-1} \right) \right]}$$

$$c_{15} = B_2 B_3 \left[j k_{m,z} \left(z_1' - z_2' \right) + 1 \right] e^{j\left[k_{m,z} \left(z_2' + 2d_{m-1} - d_m \right) + k_{i,z} \left(z_2 + 2d_i - d_{i-1} \right) \right]}$$

$$c_{16} = -B_1 B_3 \left[j k_{m,z} \left(z_1' - z_2' \right) - 1 \right] e^{-j\left[k_{m,z} \left(z_2' + d_m \right) + k_{i,z} \left(z_2 + 2d_i - d_{i-1} \right) \right]}$$

Closed-form formulation (2):

$$\int_{z_1}^{z_2} \int_{z_1'}^{z_2'} \left(z - z_1 \right) \tilde{G}_{zz} \left(k_r, z, z' \right) \left(z' - z_2' \right) dz' dz = \frac{\sum_{i=1}^{16} C_i}{k_{m,z}^2 k_{i,z}^2} \tag{B.85}$$

The analytical form of (B.85) for the cases of $\left(i < m \right)$ and $\left(i > m \right)$ are derived, respectively, as:

$$c_1 = -jA_1A_3\left[k_{m,z}\left(z_1^{'}-z_2^{'}\right)+j\right]e^{j\left[k_{m,z}\left(z_1^{'}+d_{m-1}\right)+k_{i,z}\left(z_1+2d_{i-1}-d_i\right)\right]}$$

$$c_2 = -jA_2\left[k_{m,z}\left(z_2^{'}-z_1^{'}\right)+j\right]e^{-j\left[k_{m,z}\left(z_1^{'}+2d_m-d_{m-1}\right)+k_{i,z}\left(z_1+d_i\right)\right]}$$

$$c_3 = -A_2A_3e^{-j\left[k_{m,z}\left(z_2^{'}+2d_m-d_{m-1}\right)-k_{i,z}\left(z_1+2d_{i-1}-d_i\right)\right]}$$

$$c_4 = -A_1A_3e^{j\left[k_{m,z}\left(z_2^{'}+d_{m-1}\right)+k_{i,z}\left(z_1+2d_{i-1}-d_i\right)\right]}$$

$$c_5 = -jA_2A_3\left[k_{m,z}\left(z_2^{'}-z_1^{'}\right)+j\right]e^{-j\left[k_{m,z}\left(z_1^{'}+2d_m-d_{m-1}\right)-k_{i,z}\left(z_1+2d_{i-1}-d_i\right)\right]}$$

$$c_6 = -jA_1\left[k_{m,z}\left(z_1^{'}-z_2^{'}\right)+j\right]e^{j\left[k_{m,z}\left(z_1^{'}+d_{m-1}\right)-k_{i,z}\left(z_1+d_i\right)\right]}$$

$$c_7 = -A_2e^{-j\left[k_{m,z}\left(z_2^{'}+2d_m-d_{m-1}\right)+k_{i,z}\left(z_1+d_i\right)\right]}$$

$$c_8 = -A_1e^{j\left[k_{m,z}\left(z_2^{'}+d_{m-1}\right)-k_{i,z}\left(z_1+d_i\right)\right]}$$

$$c_9 = A_1\left[k_{m,z}\left(z_1^{'}-z_2^{'}\right)+j\right]\left[k_{i,z}\left(z_1-z_2\right)+j\right]e^{j\left[k_{m,z}\left(z_1^{'}+d_{m-1}\right)-k_{i,z}\left(z_2+d_i\right)\right]}$$

$$c_{10} = A_2\left[k_{m,z}\left(z_2^{'}-z_1^{'}\right)+j\right]\left[k_{i,z}\left(z_1-z_2\right)+j\right]e^{-j\left[k_{m,z}\left(z_1^{'}+2d_m-d_{m-1}\right)+k_{i,z}\left(z_2+d_i\right)\right]}$$

$$c_{11} = A_2A_3\left[k_{m,z}\left(z_2^{'}-z_1^{'}\right)+j\right]\left[k_{i,z}\left(z_2-z_1\right)+j\right]e^{-j\left[k_{m,z}\left(z_1^{'}+2d_m-d_{m-1}\right)-k_{i,z}\left(z_2+2d_{i-1}-d_i\right)\right]}$$

$$c_{12} = A_1A_3\left[k_{m,z}\left(z_1^{'}-z_2^{'}\right)+j\right]\left[k_{i,z}\left(z_2-z_1\right)+j\right]e^{j\left[k_{m,z}\left(z_1^{'}+d_{m-1}\right)+k_{i,z}\left(z_2+2d_{i-1}-d_i\right)\right]}$$

$$c_{13} = -jA_1\left[k_{i,z}\left(z_1-z_2\right)+j\right]e^{j\left[k_{m,z}\left(z_2^{'}+d_{m-1}\right)-k_{i,z}\left(z_2+d_i\right)\right]} \tag{B.86}$$

$$c_{14} = -jA_2\left[k_{i,z}\left(z_1-z_2\right)+j\right]e^{-j\left[k_{m,z}\left(z_2^{'}+2d_m-d_{m-1}\right)+k_{i,z}\left(z_2+d_i\right)\right]}$$

$$c_{15} = -jA_1A_3\left[k_{i,z}\left(z_2-z_1\right)+j\right]e^{j\left[k_{m,z}\left(z_2^{'}+d_{m-1}\right)+k_{i,z}\left(z_2+2d_{i-1}-d_i\right)\right]}$$

$$c_{16} = -jA_2A_3\left[k_{i,z}\left(z_2-z_1\right)+j\right]e^{-j\left[k_{m,z}\left(z_2^{'}+2d_m-d_{m-1}\right)-k_{i,z}\left(z_2+2d_{i-1}-d_i\right)\right]}$$

$$c_1 = B_2 B_3 \left[k_{m,z} \left(z_1' - z_2' \right) + j \right] \left[k_{i,z} \left(z_1 - z_2 \right) + j \right] e^{j \left[k_{m,z} \left(z_1' + 2 d_{m-1} - d_m \right) - k_{i,z} \left(z_2 + 2 d_i - d_{i-1} \right) \right]}$$

$$c_2 = B_2 \left[k_{m,z} \left(z_1' - z_2' \right) + j \right] \left[k_{i,z} \left(z_2 - z_1 \right) + j \right] e^{j \left[k_{m,z} \left(z_1' + 2 d_{m-1} - d_m \right) + k_{i,z} \left(z_2 + d_{i-1} \right) \right]}$$

$$c_3 = B_1 B_3 \left[k_{m,z} \left(z_2' - z_1' \right) + j \right] \left[k_{i,z} \left(z_1 - z_2 \right) + j \right] e^{-j \left[k_{m,z} \left(z_1' + d_m \right) + k_{i,z} \left(z_2 + d_i - d_{i-1} \right) \right]}$$

$$c_4 = B_1 \left[k_{m,z} \left(z_2' - z_1' \right) + j \right] \left[k_{i,z} \left(z_2 - z_1 \right) + j \right] e^{-j \left[k_{m,z} \left(z_1' + d_m \right) - k_{i,z} \left(z_2 + d_{i-1} \right) \right]}$$

$$c_5 = -j B_1 \left[k_{i,z} \left(z_2 - z_1 \right) + j \right] e^{-j \left[k_{m,z} \left(z_2' + d_m \right) - k_{i,z} \left(z_2 + d_{i-1} \right) \right]}$$

$$c_6 = -j B_1 B_3 \left[k_{i,z} \left(z_1 - z_2 \right) + j \right] e^{-j \left[k_{m,z} \left(z_2' + d_m \right) + k_{i,z} \left(z_2 + 2 d_i - d_{i-1} \right) \right]}$$

$$c_7 = -j B_2 \left[k_{i,z} \left(z_2 - z_1 \right) + j \right] e^{j \left[k_{m,z} \left(z_2' + 2 d_{m-1} - d_m \right) - k_{i,z} \left(z_2 + d_{i-1} \right) \right]}$$

$$c_8 = -j B_2 B_3 \left[k_{i,z} \left(z_1 - z_2 \right) + j \right] e^{j \left[k_{m,z} \left(z_2' + 2 d_{m-1} - d_m \right) - k_{i,z} \left(z_2 + 2 d_i - d_{i-1} \right) \right]}$$

$$c_9 = -B_1 B_3 e^{-j \left[k_{m,z} \left(z_2' + d_m \right) + k_{i,z} \left(z_1 + 2 d_i - d_{i-1} \right) \right]}$$

$$c_{10} = -j B_2 B_3 \left[k_{m,z} \left(z_1' - z_2' \right) + j \right] e^{j \left[k_{m,z} \left(z_1' + 2 d_{m-1} - d_m \right) - k_{i,z} \left(z_1 + 2 d_i - d_{i-1} \right) \right]}$$

$$c_{11} = -B_2 e^{j \left[k_{m,z} \left(z_2' + 2 d_{m-1} - d \right) + k_{i,z} \left(z_1 + d_{i-1} \right) \right]}$$

$$c_{12} = -j B_1 \left[k_{m,z} \left(z_2' - z_1' \right) + j \right] e^{-j \left[k_{m,z} \left(z_1' + d_m \right) - k_{i,z} \left(z_1 + d_{i-1} \right) \right]}$$

$$c_{13} = -j B_2 \left[k_{m,z} \left(z_1' - z_2' \right) + j \right] e^{j \left[k_{m,z} \left(z_1' + 2 d_{m-1} - d_m \right) + k_{i,z} \left(z_1 + d_{i-1} \right) \right]} \tag{B.87}$$

$$c_{14} = -B_1 e^{-j \left[k_{m,z} \left(z_2' + d_m \right) - k_{i,z} \left(z_1 + d_{i-1} \right) \right]}$$

$$c_{15} = -B_2 B_3 e^{j \left[k_{m,z} \left(z_2' + 2 d_{m-1} - d_m \right) - k_{i,z} \left(z_1 + 2 d_i - d_{i-1} \right) \right]}$$

$$c_{16} = -j B_1 B_3 \left[k_{m,z} \left(z_2' - z_1' \right) + j \right] e^{-j \left[k_{m,z} \left(z_1' + d_m \right) + k_{i,z} \left(z_1 + 2 d_i - d_{i-1} \right) \right]}$$

Closed-form formulation (3):

$$\int_{z_1}^{z_2} \int_{z_1'}^{z_2'} \left(z - z_1 \right) \tilde{G}_{zz} \left(k_r, z, z' \right) \left(z' - z_1' \right) dz' dz = \frac{-\sum_{i=1}^{16} C_i}{k_{m,z}^2 k_{i,z}^2} \tag{B.88}$$

The analytical form of (B.88) for the cases of $\left(i < m \right)$ and $\left(i > m \right)$ are derived, respectively, as:

$$c_1 = -jA_1\left[k_{m,z}\left(z_2' - z_1'\right) + j\right]e^{j\left[k_{m,z}\left(z_2' + d_{m-1}\right) - k_{i,z}\left(z_1 + d_i\right)\right]}$$

$$c_2 = -jA_1A_3\left[k_{m,z}\left(z_2' - z_1'\right) + j\right]e^{j\left[k_{m,z}\left(z_2' + d_{m-1}\right) + k_{i,z}\left(z_1 + 2d_{i-1} - d_i\right)\right]}$$

$$c_3 = jA_2\left[k_{m,z}\left(z_2' - z_1'\right) - j\right]e^{-j\left[k_{m,z}\left(z_2' + 2d_m - d_{m-1}\right) + k_{i,z}\left(z_1 + d_i\right)\right]}$$

$$c_4 = -A_2A_3e^{-j\left[k_{m,z}\left(z_1' + 2d_m - d_{m-1}\right) - k_{i,z}\left(z_1 + 2d_{i-1} - d_i\right)\right]}$$

$$c_5 = -A_1A_3e^{j\left[k_{m,z}\left(z_1' + d_{m-1}\right) + k_{i,z}\left(z_1 + 2d_{i-1} - d_i\right)\right]}$$

$$c_6 = jA_2A_3\left[k_{m,z}\left(z_2' - z_1'\right) - j\right]e^{-j\left[k_{m,z}\left(z_2' + 2d_m - d_{m-1}\right) - k_{i,z}\left(z_1 + 2d_{i-1} - d_i\right)\right]}$$

$$c_7 = -A_2e^{-j\left[k_{m,z}\left(z_1' + 2d_m - d_{m-1}\right) + k_{i,z}\left(z_1 + d_i\right)\right]}$$

$$c_8 = -A_1e^{j\left[k_{m,z}\left(z_1' + d_{m-1}\right) - k_{i,z}\left(z_1 + d_i\right)\right]}$$

$$c_9 = A_1\left[k_{m,z}\left(z_2' - z_1'\right) + j\right]\left[k_{i,z}\left(z_1 - z_2\right) + j\right]e^{j\left[k_{m,z}\left(z_2' + d_{m-1}\right) - k_{i,z}\left(z_2 + d_i\right)\right]}$$

$$c_{10} = -jA_2\left[k_{i,z}\left(z_1 - z_2\right) + j\right]e^{-j\left[k_{m,z}\left(z_1' + 2d_m - d_{m-1}\right) + k_{i,z}\left(z_2 + d_i\right)\right]}$$

$$c_{11} = -A_2\left[k_{m,z}\left(z_2' - z_1'\right) - j\right]\left[k_{i,z}\left(z_1 - z_2\right) + j\right]e^{-j\left[k_{m,z}\left(z_2' + 2d_m - d_{m-1}\right) + k_{i,z}\left(z_2 + d_i\right)\right]}$$

$$c_{12} = -jA_1A_3\left[k_{i,z}\left(z_2 - z_1\right) + j\right]e^{j\left[k_{m,z}\left(z_1' + d_{m-1}\right) + k_{i,z}\left(z_2 + 2d_{i-1} - d_i\right)\right]}$$

$$c_{13} = A_1A_3\left[k_{m,z}\left(z_2' - z_1'\right) + j\right]\left[k_{i,z}\left(z_2 - z_1\right) + j\right]e^{j\left[k_{m,z}\left(z_2' + d_{m-1}\right) + k_{i,z}\left(z_2 + 2d_{i-1} - d_i\right)\right]} \qquad \text{(B.89)}$$

$$c_{14} = -A_2A_3\left[k_{m,z}\left(z_2' - z_1'\right) - j\right]\left[k_{i,z}\left(z_2 - z_1\right) + j\right]e^{-j\left[k_{m,z}\left(z_2' + 2d_m - d_{m-1}\right) - k_{i,z}\left(z_2 + 2d_{i-1} - d_i\right)\right]}$$

$$c_{15} = -jA_2A_3\left[k_{i,z}\left(z_2 - z_1\right) + j\right]e^{-j\left[k_{m,z}\left(z_1' + 2d_m - d_{m-1}\right) - k_{i,z}\left(z_2 + 2d_{i-1} - d_i\right)\right]}$$

$$c_{16} = -jA_1\left[k_{i,z}\left(z_1 - z_2\right) + j\right]e^{j\left[k_{m,z}\left(z_1' + d_{m-1}\right) - k_{i,z}\left(z_2 + d_i\right)\right]}$$

$$c_1 = -jB_2B_3\left[k_{i,z}(z_1 - z_2) + j\right]e^{j\left[k_{m,z}\left(z_1' + 2d_{m-1} - d_m\right) - k_{i,z}(z_2 + 2d_i - d_{i-1})\right]}$$

$$c_2 = jB_1\left[k_{i,z}(z_1 - z_2) - j\right]e^{-j\left[k_{m,z}\left(z_1' + d_m\right) - k_{i,z}(z_2 + d_{i-1})\right]}$$

$$c_3 = B_2B_3\left[k_{i,z}(z_1 - z_2) + j\right]\left[k_{m,z}(z_2' - z_1') + j\right]e^{j\left[k_{m,z}\left(z_2' + 2d_{m-1} - d_m\right) - k_{i,z}(z_2 + 2d_i - d_{i-1})\right]}$$

$$c_4 = B_3B_1\left[k_{m,z}(z_1' - z_2') + j\right]\left[k_{i,z}(z_1 - z_2) + j\right]e^{-j\left[k_{m,z}\left(z_2' + d_m\right) + k_{i,z}(z_2 + 2di - d_{i-1})\right]}$$

$$c_5 = -B_2\left[k_{m,z}(z_2' - z_1') + j\right]\left[k_{i,z}(z_1 - z_2) - j\right]e^{j\left[k_{m,z}\left(z_2' + 2d_{m-1} - d_m\right) + k_{i,z}(z_2 + d_{i-1})\right]}$$

$$c_6 = -jB_1B_3\left[k_{i,z}(z_1 - z_2) + j\right]e^{-j\left[k_{m,z}\left(z_1' + d_m\right) + k_{i,z}(z_2 + 2d_i - d_{i-1})\right]}$$

$$c_7 = -B_1\left[k_{m,z}(z_1' - z_2') + j\right]\left[k_{i,z}(z_1 - z_2) - j\right]e^{-j\left[k_{m,z}\left(z_2' + d_m\right) - k_{i,z}(z_2 + d_{i-1})\right]}$$

$$c_8 = -jB_1\left[k_{m,z}(z_1' - z_2') + j\right]e^{-j\left[k_{m,z}\left(z_2' + d_m\right) - k_{i,z}(z_1 + d_{i-1})\right]}$$

$$c_9 = -jB_1B_3\left[k_{m,z}(z_1' - z_2') + j\right]e^{-j\left[k_{m,z}\left(z_2' + d_m\right) + k_{i,z}(z_1 + 2d_i - d_{i-1})\right]}$$

$$c_{10} = -B_2B_3 e^{j\left[k_{m,z}\left(z_1' + 2d_{m-1} - d_m\right) - k_{i,z}(z_1 + 2d_i - d_{i-1})\right]}$$

$$c_{11} = -jB_2\left[k_{m,z}(z_2' - z_1') + j\right]e^{j\left[k_{m,z}\left(z_2' + 2d_{m-1} - d_m\right) + k_{i,z}(z_1 + d_{i-1})\right]}$$

$$c_{12} = -B_1B_3 e^{-j\left[k_{m,z}\left(z_1' + d_m\right) + k_{i,z}(z_1 + 2d_i - d_{i-1})\right]}$$

$$c_{13} = -B_2 e^{j\left[k_{m,z}\left(z_1' + 2d_{m-1} - d_m\right) + k_{i,z}(z_1 + d_{i-1})\right]} \tag{B.90}$$

$$c_{14} = -B_1 e^{-j\left[k_{m,z}\left(z_1' + d_m\right) - k_{i,z}(z_1 + d_{i-1})\right]}$$

$$c_{15} = -jB_2B_3\left[k_{m,z}(z_2' - z_1') + j\right]e^{j\left[k_{m,z}\left(z_2' + 2d_{m-1} - d_m\right) + k_{i,z}(z_1 + 2d_i - d_{i-1})\right]}$$

$$c_{16} = jB_2\left[k_{i,z}(z_1 - z_2) - j\right]e^{j\left[k_{m,z}\left(z_1' + 2d_{m-1} - d_m\right) + k_{i,z}(z_2 + d_{i-1})\right]}$$

Closed-form formulation (4):

$$\int_{z_1}^{z_2}\int_{z_1'}^{z_2'}(z - z_2)\,\tilde{G}_{zz}\left(k_r, z, z'\right)\left(z' - z_2'\right)dz'dz = \frac{-\sum_{i=1}^{16}C_i}{k_{m,z}^2 k_{i,z}^2} \tag{B.91}$$

The analytical form of (B.91) for the cases of $(i < m)$ and $(i > m)$ are derived, respectively, as:

$$c_1 = jA_2A_3\left[k_{m,z}\left(z_2^{'}-z_1^{'}\right)+j\right]e^{-j\left[k_{m,z}\left(z_1^{'}+2d_m-d_{m-1}\right)-k_{i,z}\left(z_2+2d_{i-1}-d_i\right)\right]}$$

$$c_2 = -jA_1\left[k_{m,z}\left(z_2^{'}-z_1^{'}\right)-j\right]e^{j\left[k_{m,z}\left(z_1^{'}+d_{m-1}\right)-k_{i,z}\left(z_2+d_i\right)\right]}$$

$$c_3 = A_2A_3e^{-j\left[k_{m,z}\left(z_2^{'}+2d_m-d_{m-1}\right)-k_{i,z}\left(z_2+2d_{i-1}-d_i\right)\right]}$$

$$c_4 = A_1e^{j\left[k_{m,z}\left(z_2^{'}+d_{m-1}\right)-k_{i,z}\left(z_2+d_i\right)\right]}$$

$$c_5 = A_2e^{-j\left[k_{m,z}\left(z_2^{'}+2d_m-d_{m-1}\right)+k_{i,z}\left(z_2+d_i\right)\right]}$$

$$c_6 = A_1A_3e^{j\left[k_{m,z}\left(z_2^{'}+d_{m-1}\right)+k_{i,z}\left(z_2+2d_{i-1}-d_i\right)\right]}$$

$$c_7 = -jA_1A_3\left[k_{m,z}\left(z_2^{'}-z_1^{'}\right)-j\right]e^{j\left[k_{m,z}\left(z_1^{'}+d_{m-1}\right)+k_{i,z}\left(z_2+2d_{i-1}-d_i\right)\right]}$$

$$c_8 = jA_2\left[k_{m,z}\left(z_2^{'}-z_1^{'}\right)+j\right]e^{-j\left[k_{m,z}\left(z_1^{'}+2d_m-d_{m-1}\right)+k_{i,z}\left(z_2+d_i\right)\right]}$$

$$c_9 = -jA_1A_3\left[k_{i,z}\left(z_2-z_1\right)-j\right]e^{j\left[k_{m,z}\left(z_2^{'}+d_{m-1}\right)+k_{i,z}\left(z_2+2d_{i-1}-d_i\right)\right]}$$

$$c_{10} = -jA_2A_3\left[k_{i,z}\left(z_2-z_1\right)-j\right]e^{-j\left[k_{m,z}\left(z_2^{'}+2d_m-d_{m-1}\right)-k_{i,z}\left(z_2+2d_{i-1}-d_i\right)\right]}$$

$$c_{11} = jA_2\left[k_{i,z}\left(z_2-z_1\right)+j\right]e^{-j\left[k_{m,z}\left(z_2^{'}+2d_m-d_{m-1}\right)+k_{i,z}\left(z_1+d_i\right)\right]}$$

$$c_{12} = jA_1\left[k_{i,z}\left(z_2-z_1\right)+j\right]e^{j\left[k_{m,z}\left(z_2^{'}+d_{m-1}\right)-k_{i,z}\left(z_1+d_i\right)\right]}$$

$$c_{13} = -A_2\left[k_{m,z}\left(z_2^{'}-z_1^{'}\right)+j\right]\left[k_{i,z}\left(z_2-z_1\right)+j\right]e^{-j\left[k_{m,z}\left(z_1^{'}+2d_m-d_{m-1}\right)+k_{i,z}\left(z_1+d_i\right)\right]}$$

$$c_{14} = A_2A_3\left[k_{m,z}\left(z_2^{'}-z_1^{'}\right)+j\right]\left[k_{i,z}\left(z_2-z_1\right)-j\right]e^{-j\left[k_{m,z}\left(z_1^{'}+2d_m-d_{m-1}\right)-k_{i,z}\left(z_2+2d_{i-1}-d_i\right)\right]}$$

$$c_{15} = -A_1A_3\left[k_{m,z}\left(z_2^{'}-z_1^{'}\right)-j\right]\left[k_{i,z}\left(z_2-z_1\right)-j\right]e^{j\left[k_{m,z}\left(z_1^{'}+d_{m-1}\right)+k_{i,z}\left(z_2+2d_{i-1}-d_i\right)\right]}$$

$$c_{16} = A_1\left[k_{m,z}\left(z_2^{'}-z_1^{'}\right)-j\right]\left[k_{i,z}\left(z_2-z_1\right)+j\right]e^{j\left[k_{m,z}\left(z_1^{'}+d_{m-1}\right)-k_{i,z}\left(z_1+d_i\right)\right]}$$

(B.92)

$$c_1 = B_2 \left[jk_{i,z} \left(z_2 - z_1 \right) + 1 \right] e^{j\left[k_{m,z} \left(z_2' + 2d_{m-1} - d_m \right) + k_{i,z} \left(z_1 + d_{i-1} \right) \right]}$$

$$c_2 = B_1 B_3 \left[k_{m,z} \left(z_2' - z_1' \right) + j \right] \left[k_{i,z} \left(z_2 - z_1 \right) + j \right] e^{-j\left[k_{m,z} \left(z_1' + d_m \right) + k_{i,z} \left(z_1 + d_i - d_{i-1} \right) \right]}$$

$$c_3 = B_1 \left[jk_{i,z} \left(z_2 - z_1 \right) + 1 \right] e^{-j\left[k_{m,z} \left(z_2' + d_m \right) - k_{i,z} \left(z_1 + d_{i-1} \right) \right]}$$

$$c_4 = -B_1 \left[k_{m,z} \left(z_2' - z_1' \right) + j \right] \left[k_{i,z} \left(z_2 - z_1 \right) - j \right] e^{-j\left[k_{m,z} \left(z_1' + d_m \right) - k_{i,z} \left(z_1 + d_{i-1} \right) \right]}$$

$$c_5 = -B_2 B_3 \left[k_{m,z} \left(z_2' - z_1' \right) - j \right] \left[k_{i,z} \left(z_2 - z_1 \right) + j \right] e^{j\left[k_{m,z} \left(z_1' + 2d_{m-1} - d_m \right) + k_{i,z} \left(z_1 + 2d_i - d_{i-1} \right) \right]}$$

$$c_6 = B_2 \left[k_{m,z} \left(z_2' - z_1' \right) - j \right] \left[k_{i,z} \left(z_2 - z_1 \right) - j \right] e^{j\left[k_{m,z} \left(z_1' + 2d_{m-1} - d_m \right) + k_{i,z} \left(z_1 + d_{i-1} \right) \right]}$$

$$c_7 = -jB_1 B_3 \left[k_{i,z} \left(z_2 - z_1 \right) + j \right] e^{-j\left[k_{m,z} \left(z_2' + d_m \right) + k_{i,z} \left(z_1 + 2d_i - d_{i-1} \right) \right]}$$

$$c_8 = -jB_2 B_3 \left[k_{i,z} \left(z_2 - z_1 \right) + j \right] e^{j\left[k_{m,z} \left(z_2' + 2d_{m-1} - d_m \right) + k_{i,z} \left(z_1 + 2d_i - d_{i-1} \right) \right]}$$

$$c_9 = -B_2 B_3 e^{j\left[k_{m,z} \left(z_2' + 2d_{m-1} - d_m \right) - k_{i,z} \left(z_2 + 2d_i - d_{i-1} \right) \right]}$$

$$c_{10} = jB_2 B_3 \left[k_{m,z} \left(z_2' - z_1' \right) - j \right] e^{j\left[k_{m,z} \left(z_1' + 2d_{m-1} - d_m \right) - k_{i,z} \left(z_2 + 2d_i - d_{i-1} \right) \right]}$$

$$c_{11} = jB_2 \left[k_{m,z} \left(z_2' - z_1' \right) - j \right] e^{j\left[k_{m,z} \left(z_1' + 2d_{m-1} - d_m \right) + k_{i,z} \left(z_2 + d_{i-1} \right) \right]}$$

$$c_{12} = -B_1 e^{-j\left[k_{m,z} \left(z_2' + d_m \right) - k_{i,z} \left(z_2 + d_{i-1} \right) \right]}$$

$$c_{13} = -jB_1 B_3 \left[k_{m,z} \left(z_2' - z_1' \right) + j \right] e^{-j\left[k_{m,z} \left(z_1' + d_m \right) + k_{i,z} \left(z_2 + 2d_i - d_{i-1} \right) \right]}$$

$$c_{14} = -jB_1 \left[k_{m,z} \left(z_2' - z_1' \right) + j \right] e^{-j\left[k_{m,z} \left(z_1' + d_m \right) - k_{i,z} \left(z_2 + d_{i-1} \right) \right]}$$

$$c_{15} = -B_1 B_3 e^{-j\left[k_{m,z} \left(z_2' + d_m \right) + k_{i,z} \left(z_2 + 2d_i - d_{i-1} \right) \right]}$$

$$c_{16} = -B_2 e^{j\left[k_{m,z} \left(z_2' + 2d_{m-1} - d_m \right) - k_{i,z} \left(z_2 + d_{i-1} \right) \right]}$$

(B.93)

Closed-form formulation (5):

$$\int_{z_1}^{z_2} \int_{z_1'}^{z_2'} \tilde{G}_{xx} \left(k_r, z, z' \right) dz' dz = \frac{\sum_{i=1}^{4} C_i}{k_{m,z} k_{i,z}}$$

(B.94)

in which the layered media Green's function $\tilde{G}_{xx}$ is due to an x-directed field and an x-directed source projection. The Fresnel reflection coefficients of $\tilde{G}_{xx}$ (A.148) in layered media can be expressed as:

$$\tilde{G}_{xx} = \begin{cases} \left[A_1 e^{jk_{m,z}\left(d_{m-1}+z'\right)} + A_2 e^{-jk_{m,z}\left(2d_m - d_{m-1}+z'\right)} \right] \left[e^{-jk_{i,z}\left(d_i+z\right)} + A_3 e^{jk_{i,z}\left(2d_{i-1}-d_i+z\right)} \right] & for\left(i<m\right) \\ \left[B_1 e^{-jk_{m,z}\left(d_m+z'\right)} + B_2 e^{jk_{m,z}\left(2d_{m-1}-d_m+z'\right)} \right] \left[e^{jk_{i,z}\left(d_{i-1}+z\right)} + B_3 e^{-jk_{i,z}\left(2d_i -d_{i-1}+z\right)} \right] & for\left(i>m\right) \end{cases}$$

$$A_1 = \tilde{T}_{m,i}^{TE<} \tilde{M}_m^{TE} \qquad\qquad B_1 = \tilde{T}_{m,i}^{TE>} \tilde{M}_m^{TE}$$

$$A_2 = \tilde{T}_{m,i}^{TE<} \tilde{M}_m^{TE} \tilde{R}_{m,m+1}^{TE} \qquad B_2 = \tilde{T}_{m,i}^{TE>} \tilde{M}_m^{TE} \tilde{R}_{m,m-1}^{TE}$$

$$A_3 = \tilde{R}_{i,i-1}^{TE} \qquad\qquad\qquad B_3 = \tilde{R}_{i,i+1}^{TE}$$

(B.95)

and the analytical form of (B.95) for the cases of $\left(i<m\right)$ and $\left(i>m\right)$ are derived, respectively, as:

$$c_1 = A_1 \begin{Bmatrix} -e^{j\left[k_{m,z}\left(z_1'+d_{m-1}\right)-k_{i,z}\left(z_2+d_i\right)\right]} + e^{j\left[k_{m,z}\left(z_2'+d_{m-1}\right)-k_{i,z}\left(z_2+d_i\right)\right]} \\ -e^{j\left[k_{m,z}\left(z_2'+d_{m-1}\right)-k_{i,z}\left(z_1+d_i\right)\right]} + e^{j\left[k_{m,z}\left(z_1'+d_{m-1}\right)-k_{i,z}\left(z_1+d_i\right)\right]} \end{Bmatrix}$$

$$c_2 = A_1 A_3 \begin{Bmatrix} e^{j\left[k_{m,z}\left(z_1'+d_{m-1}\right)+k_{i,z}\left(z_2+2d_{i-1}-d_i\right)\right]} - e^{j\left[k_{m,z}\left(z_2'+d_{m-1}\right)+k_{i,z}\left(z_2+2d_{i-1}-d_i\right)\right]} \\ +e^{j\left[k_{m,z}\left(z_2'+d_{m-1}\right)+k_{i,z}\left(z_1+2d_{i-1}-d_i\right)\right]} - e^{j\left[k_{m,z}\left(z_1'+d_{m-1}\right)+k_{i,z}\left(z_1+2d_{i-1}-d_i\right)\right]} \end{Bmatrix}$$

(B.96)

$$c_3 = A_2 \begin{Bmatrix} e^{-j\left[k_{m,z}\left(z_1'+2d_m-d_{m-1}\right)+k_{i,z}\left(z_2+d_i\right)\right]} - e^{-j\left[k_{m,z}\left(z_2'+2d_m-d_{m-1}\right)+k_{i,z}\left(z_2+d_i\right)\right]} \\ +e^{-j\left[k_{m,z}\left(z_2'+2d_m-d_{m-1}\right)+k_{i,z}\left(z_1+d_i\right)\right]} - e^{-j\left[k_{m,z}\left(z_1'+2d_m-d_{m-1}\right)+k_{i,z}\left(z_1+d_i\right)\right]} \end{Bmatrix}$$

$$c_4 = A_2 A_3 \begin{Bmatrix} -e^{-j\left[k_{m,z}\left(z_1'+2d_m-d_{m-1}\right)-k_{i,z}\left(z_2+2d_{i-1}-d_i\right)\right]} + e^{-j\left[k_{m,z}\left(z_2'+2d_m-d_{m-1}\right)-k_{i,z}\left(z_2+2d_{i-1}-d_i\right)\right]} \\ -e^{-j\left[k_{m,z}\left(z_2'+2d_m-d_{m-1}\right)-k_{i,z}\left(z_1+2d_{i-1}-d_i\right)\right]} + e^{-j\left[k_{m,z}\left(z_1'+2d_m-d_{m-1}\right)-k_{i,z}\left(z_1+2d_{i-1}-d_i\right)\right]} \end{Bmatrix}$$

$$c_1 = B_1 \begin{Bmatrix} e^{-j\left[k_{m,z}\left(z_1'+d_m\right)-k_{i,z}\left(z_1+d_{i-1}\right)\right]} - e^{-j\left[k_{m,z}\left(z_2'+d_m\right)-k_{i,z}\left(z_1+d_{i-1}\right)\right]} \\ -e^{-j\left[k_{m,z}\left(z_1'+d_m\right)-k_{i,z}\left(z_2+d_{i-1}\right)\right]} + e^{-j\left[k_{m,z}\left(z_2'+d_m\right)-k_{i,z}\left(z_2+d_{i-1}\right)\right]} \end{Bmatrix}$$

$$c_2 = B_1 B_3 \begin{Bmatrix} -e^{-j\left[k_{m,z}\left(z_1'+d_m\right)+k_{i,z}\left(z_1+2d_i-d_{i-1}\right)\right]} + e^{-j\left[k_{m,z}\left(z_2'+d_m\right)+k_{i,z}\left(z_1+2d_i-d_{i-1}\right)\right]} \\ +e^{-j\left[k_{m,z}\left(z_1'+d_m\right)+k_{i,z}\left(z_2+2d_i-d_{i-1}\right)\right]} - e^{-j\left[k_{m,z}\left(z_2'+d_m\right)+k_{i,z}\left(z_2+2d_i-d_{i-1}\right)\right]} \end{Bmatrix}$$

(B.97)

$$c_3 = B_2 \begin{Bmatrix} -e^{j\left[k_{m,z}\left(z_1'+2d_{m-1}-d_m\right)+k_{i,z}\left(z_1+d_{i-1}\right)\right]} + e^{j\left[k_{m,z}\left(z_2'+2d_{m-1}-d_m\right)+k_{i,z}\left(z_1+d_{i-1}\right)\right]} \\ +e^{j\left[k_{m,z}\left(z_1'+2d_{m-1}-d_m\right)+k_{i,z}\left(z_2+d_{i-1}\right)\right]} - e^{j\left[k_{m,z}\left(z_2'+2d_{m-1}-d_m\right)+k_{i,z}\left(z_2+d_{i-1}\right)\right]} \end{Bmatrix}$$

$$c_4 = B_2 B_3 \begin{Bmatrix} e^{j\left[k_{m,z}\left(z_1'+2d_{m-1}-d_m\right)-k_{i,z}\left(z_1+2d_i-d_{i-1}\right)\right]} - e^{j\left[k_{m,z}\left(z_2'+2d_{m-1}-d_m\right)-k_{i,z}\left(z_1+2d_i-d_{i-1}\right)\right]} \\ -e^{j\left[k_{m,z}\left(z_1'+2d_{m-1}-d_m\right)-k_{i,z}\left(z_2+2d_i-d_{i-1}\right)\right]} + e^{j\left[k_{m,z}\left(z_2'+2d_{m-1}-d_m\right)-k_{i,z}\left(z_2+2d_i-d_{i-1}\right)\right]} \end{Bmatrix}$$

Closed-form formulation (6):

$$\int_{z_1}^{z_2}\int_{z_1'}^{z_2'}\tilde{G}_{vz}\left(k_r, z, z'\right)dzdz' = \frac{\sum_{i=1}^{4}C_i}{k_{m,z}k_{i,z}}$$ (B.98)

in which the layered media Green's function $\tilde{G}_{vz}$ (A.99) is the scalar potential of the MPIE. For this case, the horizontal current is supported by a vertical patch, and the field basis is supported by a vertical patch. The analytical form of (B.98) for $(i < m)$ and $(i > m)$ are derived, respectively, as:

$$c_1 = A_1\left\{\begin{matrix} e^{j\left[k_{m,z}\left(z_1'+d_{m-1}\right)-k_{i,z}(z_1+d_i)\right]} - e^{j\left[k_{m,z}\left(z_1'+d_{m-1}\right)+k_{i,z}(z_2+d_i)\right]} \\ e^{j\left[k_{m,z}\left(z_2'+d_{m-1}\right)-k_{i,z}(z_2+d_i)\right]} - e^{j\left[k_{m,z}\left(z_2'+d_{m-1}\right)-k_{i,z}(z_1+d_i)\right]} \end{matrix}\right\}$$

$$c_2 = A_1A_3\left\{\begin{matrix} e^{j\left[k_{m,z}\left(z_1'+d_{m-1}\right)+k_{i,z}\left(z_1+2d_{i-1}-d_i\right)\right]} - e^{j\left[k_{m,z}\left(z_1'+d_{m-1}\right)+k_{i,z}\left(z_2+2d_{i-1}-d_i\right)\right]} \\ +e^{j\left[k_{m,z}\left(z_2'+d_{m-1}\right)+k_{i,z}\left(z_2+2d_{i-1}-d_i\right)\right]} - e^{j\left[k_{m,z}\left(z_2'+d_{m-1}\right)+k_{i,z}\left(z_1+2d_{i-1}-d_i\right)\right]} \end{matrix}\right\}$$

$$c_3 = A_2\left\{\begin{matrix} -e^{-j\left[k_{m,z}\left(z_1'+2d_m-d_{m-1}\right)+k_{i,z}(z_1+d_i)\right]} - e^{-j\left[k_{m,z}\left(z_1'+2d_m-d_{m-1}\right)+k_{i,z}(z_2+d_i)\right]} \\ +e^{-j\left[k_{m,z}\left(z_2'+2d_m-d_{m-1}\right)+k_{i,z}(z_2+d_i)\right]} - e^{-j\left[k_{m,z}\left(z_2'+2d_m-d_{m-1}\right)+k_{i,z}(z_1+d_i)\right]} \end{matrix}\right\}$$ (B.100)

$$c_4 = A_2A_3\left\{\begin{matrix} e^{-j\left[k_{m,z}\left(z_1'+2d_m-d_{m-1}\right)-k_{i,z}\left(z_1+2d_{i-1}-d_i\right)\right]} - e^{-j\left[k_{m,z}\left(z_1'+2d_m-d_{m-1}\right)-k_{i,z}\left(z_2+2d_{i-1}-d_i\right)\right]} \\ e^{-j\left[k_{m,z}\left(z_2'+2d_m-d_{m-1}\right)-k_{i,z}\left(z_2+2d_{i-1}-d_i\right)\right]} - e^{-j\left[k_{m,z}\left(z_2'+2d_m-d_{m-1}\right)-k_{i,z}\left(z_1+2d_{i-1}-d_i\right)\right]} \end{matrix}\right\}$$

$$c_1 = B_1\left\{\begin{matrix} e^{-j\left[k_{m,z}\left(z_1'+d_m\right)-k_{i,z}(z_1+d_{i-1})\right]} - e^{-j\left[k_{m,z}\left(z_2'+d_m\right)-k_{i,z}(z_1+d_{i-1})\right]} \\ +e^{-j\left[k_{m,z}\left(z_2'+d_m\right)-k_{i,z}(z_2+d_{i-1})\right]} - e^{-j\left[k_{m,z}\left(z_1'+d_m\right)-k_{i,z}(z_2+d_{i-1})\right]} \end{matrix}\right\}$$

$$c_2 = B_1B_3\left\{\begin{matrix} e^{-j\left[k_{m,z}\left(z_1'+d_m\right)+k_{i,z}\left(z_1+2d_i-d_{i-1}\right)\right]} - e^{-j\left[k_{m,z}\left(z_2'+d_m\right)+k_{i,z}\left(z_1+2d_i-d_{i-1}\right)\right]} \\ -e^{-j\left[k_{m,z}\left(z_1'+d_m\right)+k_{i,z}\left(z_2+2d_i-d_{i-1}\right)\right]} + e^{-j\left[k_{m,z}\left(z_2'+d_m\right)+k_{i,z}\left(z_2+2d_i-d_{i-1}\right)\right]} \end{matrix}\right\}$$

$$c_3 = B_2\left\{\begin{matrix} e^{j\left[k_{m,z}\left(z_1'+2d_{m-1}-d_m\right)+k_{i,z}(z_1+d_{i-1})\right]} - e^{j\left[k_{m,z}\left(z_2'+2d_{m-1}-d_m\right)+k_{i,z}(z_1+d_{i-1})\right]} \\ -e^{j\left[k_{m,z}\left(z_1'+2d_{m-1}-d_m\right)+k_{i,z}(z_2+d_{i-1})\right]} + e^{j\left[k_{m,z}\left(z_2'+2d_{m-1}-d_m\right)+k_{i,z}(z_2+d_{i-1})\right]} \end{matrix}\right\}$$ (B.101)

$$c_4 = B_2B_3\left\{\begin{matrix} e^{j\left[k_{m,z}\left(z_1'+2d_{m-1}-d_m\right)-k_{i,z}\left(z_1+2d_i-d_{i-1}\right)\right]} - e^{j\left[k_{m,z}\left(z_2'+2d_{m-1}-d_m\right)-k_{i,z}\left(z_1+2d_i-d_{i-1}\right)\right]} \\ -e^{j\left[k_{m,z}\left(z_1'+2d_{m-1}-d_m\right)-k_{i,z}\left(z_2+2d_i-d_{i-1}\right)\right]} + e^{j\left[k_{m,z}\left(z_2'+2d_{m-1}-d_m\right)-k_{i,z}\left(z_2+2d_i-d_{i-1}\right)\right]} \end{matrix}\right\}$$

where the Fresnel reflection coefficients B_1, B_2 and B_3 are defined in (B.82) for the TM$_z$-polarization.

Closed-form formulation (7):

149

$$\int_{z_1}^{z_2}\int_{z_1'}^{z_2'} \tilde{G}_{vt} dz dz' = \frac{\sum_{i=1}^{4} c_i}{k_{m,z} k_{i,z}}$$

(B.102)

where the layered media Green's function $\tilde{G}_{vt}$ (A.103) is the scalar potential of the MPIE for $(i < m)$ and $(i > m)$ are defined, respectively, as:

$$\tilde{G}_{vt}^{i<m} = \left\{ \begin{array}{l} (A_1 - B_1) e^{j\left[k_{m,z}\left(d_{m-1} + z'\right) + k_{i,z}\left(\ell_i + z\right)\right]} + (A_1 A_3 + B_1 B_3) e^{j\left[k_{m,z}\left(d_{m-1} + z'\right) + k_{i,z}\left(2d_{i-1} - d_i + z\right)\right]} \\ + (A_2 + B_2) e^{-j\left[k_{m,z}\left(2d_m - d_{m-1} + z'\right) + k_{i,z}\left(\ell_i + z\right)\right]} + (A_2 A_3 - B_2 B_3) e^{-j\left[k_{m,z}\left(2d_m - d_{m-1} + z'\right) - k_{i,z}\left(2d_{i-1} - d_i + z\right)\right]} \end{array} \right\} \text{ for } (i < m)$$

(B.104)

where

$$\begin{array}{ll} A_1 = k_0 e_{r_i} m_{r_m} \tilde{T}_{m,i}^{TE^<} \tilde{M}_m^{TE} & B_1 = k_{i,z} k_{m,z} \tilde{T}_{m,i}^{TM^<} \tilde{M}_m^{TM} \\ A_2 = A_1 \tilde{R}_{m,m+1}^{TE} & B_2 = B_1 \tilde{R}_{m,m+1}^{TM} \\ A_3 = \tilde{R}_{i,i-1}^{TE} & B_3 = \tilde{R}_{i,i-1}^{TM} \end{array}$$

(B.105)

$$\tilde{G}_{vt}^{i>m} = \left\{ \begin{array}{l} (A_1 - B_1) e^{-j\left[k_{m,z}\left(d_m + z'\right) - k_{i,z}\left(d_{i-1} + z\right)\right]} + (A_1 A_3 + B_1 B_3) e^{-j\left[k_{m,z}\left(d_m + z'\right) + k_{i,z}\left(2d_i - d_{i-1} + z\right)\right]} \\ + (A_2 + B_2) e^{j\left[k_{m,z}\left(2d_{m-1} - d_m + z'\right) + k_{i,z}\left(d_{i-1} + z\right)\right]} + (A_2 A_3 - B_2 B_3) e^{j\left[k_{m,z}\left(2d_{m-1} - d_m + z'\right) - k_{i,z}\left(2d_i - d_{i-1} + z\right)\right]} \end{array} \right\} \text{ for } (i > m)$$

(B.106)

where

$$\begin{array}{ll} A_1 = k_0^2 e_{r_i} m_{r_m} \tilde{T}_{m,i}^{TE^>} \tilde{M}_m^{TE} & B_1 = k_{i,z} k_{m,z} \tilde{T}_{m,i}^{TM^>} \tilde{M}_m^{TM} \\ A_2 = A_1 \tilde{R}_{m,m-1}^{TE} & B_2 = B_1 \tilde{R}_{m,m-1}^{TM} \\ A_3 = \tilde{R}_{i,i+1}^{TE} & B_3 = \tilde{R}_{i,i+1}^{TM} \end{array}$$

(B.107)

For this case, it is assumed that the horizontal current is supported by a vertical patch, and the field basis is supported by a vertical patch. The analytical form of (B.102) for $(i < m)$ and $(i > m)$ are derived, respectively, as:

$$c_1 = \left(B_1 - A_1\right)\left\{ \begin{array}{c} e^{j\left[k_{m,z}\left(z_2' + d_{m-1}\right) - k_{i,z}\left(z_1 + d_i\right)\right]} + e^{j\left[k_{m,z}\left(z_1' + d_{m-1}\right) - k_{i,z}\left(z_2 + d_i\right)\right]} \\ -e^{j\left[k_{m,z}\left(z_1' + d_{m-1}\right) - k_{i,z}\left(z_1 + d_i\right)\right]} - e^{j\left[k_{m,z}\left(z_2' + d_{m-1}\right) - k_{i,z}\left(z_2 + d_i\right)\right]} \end{array} \right\}$$

$$c_2 = \left(A_2 + B_2\right)\left\{ \begin{array}{c} e^{-j\left[k_{m,z}\left(z_2' + 2d_m - d_{m-1}\right) + k_{i,z}\left(z_1 + d_i\right)\right]} + e^{-j\left[k_{m,z}\left(z_1' + 2d_m - d_{m-1}\right) + k_{i,z}\left(z_2 + d_i\right)\right]} \\ -e^{-j\left[k_{m,z}\left(z_1' + 2d_m - d_{m-1}\right) + k_{i,z}\left(z_1 + d_i\right)\right]} - e^{-j\left[k_{m,z}\left(z_2' + 2d_m - d_{m-1}\right) + k_{i,z}\left(z_2 + d_i\right)\right]} \end{array} \right\}$$

$$c_3 = \left(B_3 B_1 + A_3 A_1\right)\left\{ \begin{array}{c} e^{j\left[k_{m,z}\left(z_1' + d_{m-1}\right) + k_{i,z}\left(z_2 + 2d_{i-1} - d_i\right)\right]} + e^{j\left[k_{m,z}\left(z_2' + d_{m-1}\right) + k_{i,z}\left(z_1 + 2d_{i-1} - d_i\right)\right]} \\ -e^{j\left[k_{m,z}\left(z_2' + d_{m-1}\right) + k_{i,z}\left(z_2 + 2d_{i-1} - d_i\right)\right]} - e^{j\left[k_{m,z}\left(z_1' + d_{m-1}\right) + k_{i,z}\left(z_1 + 2d_{i-1} - d_i\right)\right]} \end{array} \right\}$$

$$c_4 = \left(A_3 A_2 - B_3 B_2\right)\left\{ \begin{array}{c} e^{-j\left[k_{m,z}\left(z_2' + 2d_m - d_{m-1}\right) - k_{i,z}\left(z_2 + 2d_{i-1} - d_i\right)\right]} + e^{-j\left[k_{m,z}\left(z_1' + 2d_m - d_{m-1}\right) - k_{i,z}\left(z_1 + 2d_{i-1} - d_i\right)\right]} \\ -e^{-j\left[k_{m,z}\left(z_1' + 2d_m - d_{m-1}\right) - k_{i,z}\left(z_2 + 2d_{i-1} - d_i\right)\right]} - e^{-j\left[k_{m,z}\left(z_2' + 2d_m - d_{m-1}\right) - k_{i,z}\left(z_1 + 2d_{i-1} - d_i\right)\right]} \end{array} \right\}$$

.(B.108)

$$c_1 = \left(B_1 - A_1\right)\left\{ \begin{array}{c} e^{-j\left[k_{m,z}\left(z_2' + d_m\right) + k_{i,z}\left(z_2 + d_{i-1}\right)\right]} + e^{-j\left[k_{m,z}\left(z_1' + d_m\right) - k_{i,z}\left(z_1 + d_{i-1}\right)\right]} \\ -e^{-j\left[k_{m,z}\left(z_2' + d_m\right) - k_{i,z}\left(z_1 + d_{i-1}\right)\right]} - e^{-j\left[k_{m,z}\left(z_1' + d_m\right) - k_{i,z}\left(z_2 + d_{i-1}\right)\right]} \end{array} \right\}$$

$$c_2 = \left(A_2 + B_2\right)\left\{ \begin{array}{c} e^{j\left[k_{m,z}\left(z_1' + 2d_{m-1} - d_m\right) + k_{i,z}\left(z_1 + d_{i-1}\right)\right]} + e^{j\left[k_{m,z}\left(z_2' + 2d_{m-1} - d_m\right) + k_{i,z}\left(z_2 + d_{i-1}\right)\right]} \\ -e^{j\left[k_{m,z}\left(z_1' + 2d_{m-1} - d_m\right) + k_{i,z}\left(z_2 + d_{i-1}\right)\right]} - e^{j\left[k_{m,z}\left(z_2' + 2d_{m-1} - d_m\right) + k_{i,z}\left(z_1 + d_{i-1}\right)\right]} \end{array} \right\}$$

$$c_3 = \left(B_1 B_3 + A_1 A_3\right)\left\{ \begin{array}{c} e^{-j\left[k_{m,z}\left(z_1' + d_m\right) + k_{i,z}\left(z_1 + 2d_i - d_{i-1}\right)\right]} + e^{-j\left[k_{m,z}\left(z_2' + d_m\right) + k_{i,z}\left(z_2 + 2d_i - d_{i-1}\right)\right]} \\ -e^{-j\left[k_{m,z}\left(z_2' + d_m\right) + k_{i,z}\left(z_1 + 2d_i - d_{i-1}\right)\right]} - e^{-j\left[k_{m,z}\left(z_1' + d_m\right) + k_{i,z}\left(z_2 + 2d_i - d_{i-1}\right)\right]} \end{array} \right\}$$

$$c_4 = \left(A_2 A_3 - B_2 B_3\right)\left\{ \begin{array}{c} e^{j\left[k_{m,z}\left(z_1' + 2d_{m-1} - d_m\right) - k_{i,z}\left(z_2 + 2d_i - d_{i-1}\right)\right]} + e^{j\left[k_{m,z}\left(z_2' + 2d_{m-1} - d_m\right) - k_{i,z}\left(z_1 + 2d_i - d_{i-1}\right)\right]} \\ -e^{j\left[k_{m,z}\left(z_2' + 2d_{m-1} - d_m\right) - k_{i,z}\left(z_2 + 2d_i - d_{i-1}\right)\right]} - e^{j\left[k_{m,z}\left(z_1' + 2d_{m-1} - d_m\right) - k_{i,z}\left(z_1 + 2d_i - d_{i-1}\right)\right]} \end{array} \right\}$$

(B.109)

Closed-form formulation (8):

$$\int_{z_1}^{z_2}\int_{z_1'}^{z_2'} \left(z - z_1\right)\tilde{G}_{zt}\, dz' dz = \frac{\displaystyle\sum_{i=1}^{16} c_i}{k_{m,z}\, k_{i,z}^2} \tag{B.110}$$

for the reaction of a horizontal source basis with a vertical field basis where the layered media Green's function $\tilde{G}_{zt}$ (A.151) is the scalar potential of the MPIE for $(i < m)$ and $(i > m)$ are defined, respectively, as:

$$\tilde{G}_{zt}^{i<m} = \begin{cases} (B_1 - A_1)e^{j\left[k_{m,z}\left(d_{m-1}+z'\right)-k_{i,z}\left(d_i+z\right)\right]} + (A_1A_3 + B_1B_3)e^{j\left[k_{m,z}\left(d_{m-1}+z'\right)+k_{i,z}\left(2d_{i-1}-d_i+z\right)\right]} \\ -(A_2 + B_2)e^{-j\left[k_{m,z}\left(2d_m-d_{m-1}+z'\right)+k_{i,z}\left(d_i+z\right)\right]} + (A_2A_3 - B_2B_3)e^{-j\left[k_{m,z}\left(2d_m-d_{m-1}+z'\right)-k_{i,z}\left(2d_{i-1}-d_i+z\right)\right]} \end{cases} for\,(i<m)$$

(B.111)

where

$$A_1 = \tilde{T}_{m,i}^{TE^<}\tilde{M}_m^{TE}\frac{k_{i,z}\mathbf{m}_m}{k_{m,z}\mathbf{m}_i} \qquad B_1 = \tilde{T}_{m,i}^{TM^<}\tilde{M}_m^{TM}$$

$$A_2 = A_1\tilde{R}_{m,m+1}^{TE} \qquad\qquad B_2 = B_1\tilde{R}_{m,m+1}^{TM} \qquad\qquad (B.112)$$

$$A_3 = \tilde{R}_{i,i-1}^{TE} \qquad\qquad B_3 = \tilde{R}_{i,i-1}^{TM}$$

and

$$\tilde{G}_{zt}^{i>m} = \begin{cases} (A_1 - B_1)e^{-j\left[k_{m,z}\left(d_m+z'\right)-k_{i,z}\left(d_{i-1}+z\right)\right]} - (B_1B_3 + A_1A_3)e^{-\left[k_{m,z}\left(d_m+z'\right)+k_{i,z}\left(2d_i-d_{i-1}+z\right)\right]} \\ +(A_2 + B_2)e^{j\left[k_{m,z}\left(2d_{m-1}-d_m+z'\right)+k_{i,z}\left(d_{i-1}+z\right)\right]} - (A_2A_3 - B_2B_3)e^{j\left[k_{m,z}\left(2d_{m-1}-d_m+z'\right)-k_{i,z}\left(2d_i-d_{i-1}+z\right)\right]} \end{cases} for\,(i>m)$$

(B.113)

where

$$A_1 = \tilde{T}_{m,i}^{TE^>}\tilde{M}_m^{TE}\frac{k_{i,z}\mathbf{m}_m}{k_{m,z}\mathbf{m}_i} \qquad B_1 = \tilde{T}_{m,i}^{TM^>}\tilde{M}_m^{TM}$$

$$A_2 = A_1\tilde{R}_{m,m-1}^{TE} \qquad\qquad B_2 = B_1\tilde{R}_{m,m-1}^{TM} \qquad\qquad (B.114)$$

$$A_3 = \tilde{R}_{i,i+1}^{TE} \qquad\qquad B_3 = \tilde{R}_{i,i+1}^{TM}$$

For this case, it is assumed that the horizontal source basis is supported by a vertical patch. The analytical form of (B.110) for $(i<m)$ and $(i>m)$ are derived, respectively, as:

$$c_1 = j\left(A_2 + B_2\right)\left[jk_{i,z}\left(z_2 - z_1\right) + 1\right]e^{-j\left[k_{m,z}\left(z_1' + 2d_m - d_{m-1}\right) + k_{i,z}\left(z_2 + d_i\right)\right]}$$

$$c_2 = -j\left(A_2 + B_2\right)\left[jk_{i,z}\left(z_2 - z_1\right) + 1\right]e^{-j\left[k_{m,z}\left(z_2' + 2d_m - d_{m-1}\right) + k_{i,z}\left(z_2 + d_i\right)\right]}$$

$$c_3 = j\left(A_1 A_3 + B_1 B_3\right)\left[jk_{i,z}\left(z_1 - z_2\right) + 1\right]e^{j\left[k_{m,z}\left(z_1' + d_{m-1}\right) + k_{i,z}\left(z_2 + 2d_{i-1} - d_i\right)\right]}$$

$$c_4 = j\left(A_1 - B_1\right)\left[jk_{i,z}\left(z_2 - z_1\right) + 1\right]e^{j\left[k_{m,z}\left(z_2' + d_{m-1}\right) - k_{i,z}\left(z_2 + d_i\right)\right]}$$

$$c_5 = j\left(B_2 B_3 - A_2 A_3\right)\left[jk_{i,z}\left(z_2 - z_1\right) - 1\right]e^{-j\left[k_{m,z}\left(z_2' + 2d_m - d_{m-1}\right) - k_{i,z}\left(z_2 + 2d_{i-1} - d_i\right)\right]}$$

$$c_6 = -j\left(B_2 B_3 - A_2 A_3\right)\left[jk_{i,z}\left(z_2 - z_1\right) - 1\right]e^{-j\left[k_{m,z}\left(z_1' + 2d_m - d_{m-1}\right) - k_{i,z}\left(z_2 + 2d_{i-1} - d_i\right)\right]}$$

$$c_7 = j\left(B_1 - A_1\right)\left[jk_{i,z}\left(z_2 - z_1\right) + 1\right]e^{j\left[k_{m,z}\left(z_1' + d_{m-1}\right) - k_{i,z}\left(z_2 + d_i\right)\right]}$$

$$c_8 = -j\left(A_1 A_3 + B_1 B_3\right)\left[jk_{i,z}\left(z_1 - z_2\right) + 1\right]e^{j\left[k_{m,z}\left(z_2' + d_{m-1}\right) + k_{i,z}\left(z_2 + 2d_{i-1} - d_i\right)\right]}$$

$$c_9 = j\left(A_1 - B_1\right)e^{j\left[k_{m,z}\left(z_1' + d_{m-1}\right) - k_{i,z}\left(z_1 + d_i\right)\right]}$$

$$c_{10} = j\left(A_2 + B_2\right)e^{-j\left[k_{m,z}\left(z_2' + 2d_m - d_{m-1}\right) + k_{i,z}\left(z_1 + d_i\right)\right]}$$

$$c_{11} = j\left(B_1 - A_1\right)e^{j\left[k_{m,z}\left(z_2' + d_{m-1}\right) - k_{i,z}\left(z_1 + d_i\right)\right]}$$

$$c_{12} = -j\left(A_2 + B_2\right)e^{-j\left[k_{m,z}\left(z_1' + 2d_m - d_{m-1}\right) + k_{i,z}\left(z_1 + d_i\right)\right]}$$

$$c_{13} = -j\left(A_1 A_3 + B_1 B_3\right)e^{j\left[k_{m,z}\left(z_1' + d_{m-1}\right) + k_{i,z}\left(z_1 + 2d_{i-1} - d_i\right)\right]} \tag{B.115}$$

$$c_{14} = j\left(B_2 B_3 - A_2 A_3\right)e^{-j\left[k_{m,z}\left(z_2' + 2d_m - d_{m-1}\right) - k_{i,z}\left(z_1 + 2d_{i-1} - d_i\right)\right]}$$

$$c_{15} = j\left(A_2 A_3 - B_2 B_3\right)e^{-j\left[k_{m,z}\left(z_1' + 2d_m - d_{m-1}\right) - k_{i,z}\left(z_1 + 2d_{i-1} - d_i\right)\right]}$$

$$c_{16} = j\left(A_1 A_3 + B_1 B_3\right)e^{j\left[k_{m,z}\left(z_2' + d_{m-1}\right) + k_{i,z}\left(z_1 + 2d_{i-1} - d_i\right)\right]}$$

$$c_1 = j\left(B_2 B_3 - A_2 A_3\right) e^{j\left[k_{m,z}\left(z_1' + 2d_{m-1} - d_m\right) - k_{i,z}\left(z_1 + 2d_i - d_{i-1}\right)\right]}$$

$$c_2 = j\left(A_1 - B_1\right) e^{-j\left[k_{m,z}\left(z_2' + d_m\right) - k_{i,z}\left(z_1 + d_{i-1}\right)\right]}$$

$$c_3 = j\left(B_1 - A_1\right) e^{-j\left[k_{m,z}\left(z_1' + d_m\right) - k_{i,z}\left(z_1 + d_{i-1}\right)\right]}$$

$$c_4 = j\left(A_1 A_3 + B_1 B_3\right) e^{-j\left[k_{m,z}\left(z_1' + d_m\right) + k_{i,z}\left(z_1 + 2d_i - d_{i-1}\right)\right]}$$

$$c_5 = -j\left(A_2 + B_2\right) e^{j\left[k_{m,z}\left(z_2' + 2d_{m-1} - d_m\right) + k_{i,z}\left(z_1 + d_{i-1}\right)\right]}$$

$$c_6 = j\left(A_2 A_3 - B_2 B_3\right) e^{j\left[k_{m,z}\left(z_2' + 2d_{m-1} - d_m\right) - k_{i,z}\left(z_1 + 2d_i - d_{i-1}\right)\right]}$$

$$c_7 = j\left(A_2 + B_2\right) e^{j\left[k_{m,z}\left(z_1' + 2d_{m-1} - d_m\right) + k_{i,z}\left(z_1 + d_{i-1}\right)\right]}$$

$$c_8 = -j\left(A_1 A_3 + B_1 B_3\right) e^{-j\left[k_{m,z}\left(z_2' + d_m\right) + k_{i,z}\left(z_1 + 2d_i - d_{i-1}\right)\right]}$$

$$c_9 = j\left(A_1 A_3 + B_1 B_3\right)\left[jk_{i,z}\left(z_2 - z_1\right) + 1\right] e^{-j\left[k_{m,z}\left(z_2' + d_m\right) + k_{i,z}\left(z_2 + 2d_i - d_{i-1}\right)\right]}$$

$$c_{10} = -j\left(B_2 B_3 - A_2 A_3\right)\left[jk_{i,z}\left(z_2 - z_1\right) + 1\right] e^{j\left[k_{m,z}\left(z_1' + 2d_{m-1} - d_m\right) - k_{i,z}\left(z_2 + 2d_i - d_{i-1}\right)\right]}$$

$$c_{11} = j\left(A_2 + B_2\right)\left[jk_{i,z}\left(z_2 - z_1\right) - 1\right] e^{j\left[k_{m,z}\left(z_1' + 2d_{m-1} - d_m\right) + k_{i,z}\left(z_2 + d_{i-1}\right)\right]}$$

$$c_{12} = j\left(B_2 B_3 - A_2 A_3\right)\left[jk_{i,z}\left(z_2 - z_1\right) + 1\right] e^{j\left[k_{m,z}\left(z_2' + 2d_{m-1} - d_m\right) - k_{i,z}\left(z_2 + 2d_i - d_{i-1}\right)\right]}$$

$$c_{13} = j\left(B_1 - A_1\right)\left[jk_{i,z}\left(z_2 - z_1\right) - 1\right] e^{-j\left[k_{m,z}\left(z_1' + d_m\right) - k_{i,z}\left(z_2 + d_{i-1}\right)\right]}$$

$$c_{14} = -j\left(A_1 + B_1\right)\left[jk_{i,z}\left(z_2 - z_1\right) - 1\right] e^{-j\left[k_{m,z}\left(z_2' + d_m\right) - k_{i,z}\left(z_2 + d_{i-1}\right)\right]}$$

$$c_{15} = -j\left(A_2 + B_2\right)\left[jk_{i,z}\left(z_2 - z_1\right) - 1\right] e^{j\left[k_{m,z}\left(z_2' + 2d_{m-1} - d_m\right) + k_{i,z}\left(z_2 + d_{i-1}\right)\right]}$$

$$c_{16} = -j\left(A_1 A_3 + B_1 B_3\right)\left[jk_{i,z}\left(z_2 - z_1\right) + 1\right] e^{-j\left[k_{m,z}\left(z_1' + d_m\right) + k_{i,z}\left(z_2 + 2d_i - d_{i-1}\right)\right]}$$

(B.116)

Closed-form formulation (9):

$$\int_{z_1}^{z_2}\int_{z_1'}^{z_2'}\left(z - z_2\right)\tilde{G}_{zz}dz'dz = \frac{\sum_{i=1}^{16} c_i}{k_{m,z}k_{i,z}^2}$$

(B.117)

where the analytical form for $\left(i < m\right)$ and $\left(i > m\right)$ are derived, respectively, as:

$$c_1 = j\left(A_2 + B_2\right)\left[jk_{i,z}\left(z_1 - z_2\right) + 1\right]e^{-j\left[k_{m,z}\left(z_1 + 2d_m - d_{m-1}\right) + k_{i,z}\left(z_1 + d_i\right)\right]}$$

$$c_2 = -j\left(A_1A_3 + B_1B_3\right)\left[jk_{i,z}\left(z_1 - z_2\right) - 1\right]e^{j\left[k_{m,z}\left(z_1 + d_{m-1}\right) + k_{i,z}\left(z_1 + 2d_{i-1} - d_i\right)\right]}$$

$$c_3 = j\left(B_2B_3 - A_2A_3\right)\left[jk_{i,z}\left(z_1 - z_2\right) - 1\right]e^{-j\left[k_{m,z}\left(z_2 + 2d_m - d_{m-1}\right) - k_{i,z}\left(z_1 + 2d_{i-1} - d_i\right)\right]}$$

$$c_4 = -j\left(A_2 + B_2\right)\left[jk_{i,z}\left(z_1 - z_2\right) + 1\right]e^{-j\left[k_{m,z}\left(z_2 + 2d_m - d_{m-1}\right) + k_{i,z}\left(z_1 + d_i\right)\right]}$$

$$c_5 = -j\left(B_1 - A_1\right)\left[jk_{i,z}\left(z_1 - z_2\right) + 1\right]e^{j\left[k_{m,z}\left(z_2 + d_{m-1}\right) - k_{i,z}\left(z_1 + d_i\right)\right]}$$

$$c_6 = -j\left(B_2B_3 - A_2A_3\right)\left[jk_{i,z}\left(z_1 - z_2\right) - 1\right]e^{-j\left[k_{m,z}\left(z_1 + 2d_m - d_{m-1}\right) - k_{i,z}\left(z_1 + 2d_{i-1} - d_i\right)\right]}$$

$$c_7 = j\left(B_1 - A_1\right)\left[jk_{i,z}\left(z_1 - z_2\right) + 1\right]e^{j\left[k_{m,z}\left(z_1 + d_{m-1}\right) - k_{i,z}\left(z_1 + d_i\right)\right]}$$

$$c_8 = j\left(B_1B_3 + A_1A_3\right)\left[jk_{i,z}\left(z_1 - z_2\right) - 1\right]e^{j\left[k_{m,z}\left(z_2 + d_{m-1}\right) + k_{i,z}\left(z_1 + 2d_{i-1} - d_i\right)\right]}$$

$$c_9 = -j\left(A_1A_3 + B_1B_3\right)e^{j\left[k_{m,z}\left(z_1 + d_{m-1}\right) + k_{i,z}\left(z_2 + 2d_{i-1} - d_i\right)\right]}$$

$$c_{10} = j\left(B_2B_3 - A_2A_3\right)e^{-j\left[k_{m,z}\left(z_2 + 2d_m - d_{m-1}\right) - k_{i,z}\left(z_2 + 2d_{i-1} - d_i\right)\right]}$$

$$c_{11} = j\left(B_1 - A_1\right)e^{j\left[k_{m,z}\left(z_2 + d_{m-1}\right) + k_{i,z}\left(z_2 + d_i\right)\right]}$$

$$c_{12} = -j\left(A_2 + B_2\right)e^{-j\left[k_{m,z}\left(z_1 + 2d_m - d_{m-1}\right) + k_{i,z}\left(z_2 + d_i\right)\right]}$$

$$c_{13} = j\left(A_2 + B_2\right)e^{-j\left[k_{m,z}\left(z_2 + 2d_m - d_{m-1}\right) + k_{i,z}\left(z_2 + d_i\right)\right]} \tag{B.118}$$

$$c_{14} = j\left(A_1 - B_1\right)e^{j\left[k_{m,z}\left(z_1 + d_{m-1}\right) - k_{i,z}\left(z_2 + d_i\right)\right]}$$

$$c_{15} = j\left(A_1A_3 + B_1B_3\right)e^{j\left[k_{m,z}\left(z_2 + d_{m-1}\right) + k_{i,z}\left(z_2 + 2d_{i-1} - d_i\right)\right]}$$

$$c_{16} = j\left(A_2A_3 - B_2B_3\right)e^{-j\left[k_{m,z}\left(z_1 + 2d_m - d_{m-1}\right) - k_{i,z}\left(z_2 + 2d_{i-1} - d_i\right)\right]}$$

$$c_1 = j\left(A_2 A_3 - B_2 B_3\right)e^{j\left[k_{m,z}\left(z_2' + 2d_{m-1} - d_m\right) - k_{i,z}\left(z_2 + 2d_i - d_{i-1}\right)\right]}$$

$$c_2 = j\left(A_1 - B_1\right)e^{-j\left[k_{m,z}\left(z_2' + d_m\right) - k_{i,z}\left(z_2 + d_{i-1}\right)\right]}$$

$$c_3 = j\left(A_1 A_3 + B_1 B_3\right)e^{-j\left[k_{m,z}\left(z_2' + d_m\right) + k_{i,z}\left(z_2 + 2d_i - d_{i-1}\right)\right]}$$

$$c_4 = j\left(B_1 - A_1\right)e^{-j\left[k_{m,z}\left(z_1' + d_m\right) - k_{i,z}\left(z_2 + d_{i-1}\right)\right]}$$

$$c_5 = j\left(B_2 B_3 - A_2 A_3\right)e^{j\left[k_{m,z}\left(z_1' + 2d_{m-1} - d_m\right) - k_{i,z}\left(z_2 + 2d_i - d_{i-1}\right)\right]}$$

$$c_6 = j\left(A_2 + B_2\right)e^{j\left[k_{m,z}\left(z_1' + 2d_{m-1} - d_m\right) + k_{i,z}\left(z_2 + d_{i-1}\right)\right]}$$

$$c_7 = -j\left(A_1 A_3 + B_1 B_3\right)\left[jk_{i,z}\left(z_1 - z_2\right) + 1\right]e^{-j\left[k_{m,z}\left(z_1' + d_m\right) - k_{i,z}\left(z_1 + 2d_i - d_{i-1}\right)\right]}$$

$$c_8 = -j\left(A_2 A_3 + B_2 B_3\right)\left[jk_{i,z}\left(z_1 - z_2\right) + 1\right]e^{j\left[k_{m,z}\left(z_1' + 2d_{m-1} - d_m\right) - k_{i,z}\left(z_1 + 2d_i - d_{i-1}\right)\right]}$$

$$c_9 = -j\left(A_2 + B_2\right)\left[jk_{i,z}\left(z_2 - z_1\right) + 1\right]e^{j\left[k_{m,z}\left(z_1' + 2d_{m-1} - d_m\right) + k_{i,z}\left(z_1 + d_{i-1}\right)\right]}$$

$$c_{10} = -j\left(A_1 - B_1\right)\left[jk_{i,z}\left(z_2 - z_1\right) + 1\right]e^{-j\left[k_{m,z}\left(z_2' + d_m\right) - k_{i,z}\left(z_1 + d_{i-1}\right)\right]}$$

$$c_{11} = j\left(A_1 - B_1\right)\left[jk_{i,z}\left(z_2 - z_1\right) + 1\right]e^{-j\left[k_{m,z}\left(z_1' + d_m\right) - k_{i,z}\left(z_1 + d_{i-1}\right)\right]}$$

$$c_{12} = j\left(A_1 A_3 + B_1 B_3\right)\left[jk_{i,z}\left(z_1 - z_2\right) + 1\right]e^{-j\left[k_{m,z}\left(z_2' + d_m\right) + k_{i,z}\left(z_1 + 2d_i - d_{i-1}\right)\right]}$$

$$c_{13} = j\left(A_2 + B_2\right)\left[jk_{i,z}\left(z_2 - z_1\right) + 1\right]e^{j\left[k_{m,z}\left(z_2' + 2d_{m-1} - d_m\right) + k_{i,z}\left(z_1 + d_{i-1}\right)\right]}$$

$$c_{14} = j\left(B_2 B_3 - A_2 A_3\right)\left[jk_{i,z}\left(z_1 - z_2\right) + 1\right]e^{j\left[k_{m,z}\left(z_2' + 2d_{m-1} - d_m\right) - k_{i,z}\left(z_1 + 2d_i - d_{i-1}\right)\right]}$$

$$c_{15} = -j\left(A_1 A_3 + B_1 B_3\right)e^{-j\left[k_{m,z}\left(z_1' + d_m\right) + k_{i,z}\left(z_2 + 2d_i - d_{i-1}\right)\right]}$$

$$c_{16} = -j\left(A_2 + B_2\right)e^{j\left[k_{m,z}\left(z_2' + 2d_{m-1} - d_m\right) + k_{i,z}\left(z_2 + d_{i-1}\right)\right]}$$

(B.119)

Closed-form formulation (10):

$$\int_{z_1}^{z_2}\left(z - z_1\right)\tilde{G}_{zt}\,dz = \frac{\sum_{i=1}^{8}c_i}{k_{i,z}^2} \tag{B.120}$$

where the analytical form for $\left(i < m\right)$ and $\left(i > m\right)$ are derived, respectively, as:

$$c_1 = -\left(A_2 + B_2\right)e^{-j\left[k_{m,z}\left(z' + 2d_m - d_{m-1}\right) + k_{i,z}\left(z_1 + d_i\right)\right]}$$

$$c_2 = -\left(A_2 + B_2\right)\left[jk_{i,z}\left(z_1 - z_2\right) - 1\right]e^{-j\left[k_{m,z}\left(z' + 2d_m - d_{m-1}\right) + k_{i,z}\left(z_2 + d_i\right)\right]}$$

$$c_3 = \left(B_1 - A_1\right)e^{j\left[k_{m,z}\left(z' + d_{m-1}\right) - k_{i,z}\left(z_1 + d_i\right)\right]}$$

$$c_4 = \left(A_2 A_3 - B_2 B_3\right)e^{-j\left[k_{m,z}\left(z' + 2d_m - d_{m-1}\right) - k_{i,z}\left(z_1 + 2d_{i-1} - d_i\right)\right]}$$

$$c_5 = \left(A_1 A_3 + B_1 B_3\right)e^{j\left[k_{m,z}\left(z' + d_{m-1}\right) + k_{i,z}\left(z_1 + 2d_{i-1} - d_i\right)\right]}$$ (B.121)

$$c_6 = \left(B_2 B_3 - A_2 A_3\right)\left[jk_{i,z}\left(z_1 - z_2\right) + 1\right]e^{-j\left[k_{m,z}\left(z' + 2d_m - d_{m-1}\right) - k_{i,z}\left(z_2 + 2d_{i-1} - d_i\right)\right]}$$

$$c_7 = \left(B_1 - A_1\right)\left[jk_{i,z}\left(z_1 - z_2\right) - 1\right]e^{j\left[k_{m,z}\left(z' + d_{m-1}\right) - k_{i,z}\left(z_2 + d_i\right)\right]}$$

$$c_8 = -\left(A_1 A_3 + B_1 B_3\right)\left[jk_{i,z}\left(z_1 - z_2\right) + 1\right]e^{j\left[k_{m,z}\left(z' + d_{m-1}\right) + k_{i,z}\left(z_2 + 2d_{i-1} - d_i\right)\right]}$$

and

$$c_1 = \left(B_2 B_3 - A_2 A_3\right)\left[jk_{i,z}\left(z_1 - z_2\right) - 1\right]e^{j\left[k_{m,z}\left(z' + 2d_{m-1} - d_m\right) - k_{i,z}\left(z_2 + 2d_i - d_{i-1}\right)\right]}$$

$$c_2 = -\left(A_2 + B_2\right)\left[jk_{i,z}\left(z_1 - z_2\right) + 1\right]e^{j\left[k_{m,z}\left(z' + 2d_{m-1} - d_m\right) + k_{i,z}\left(z_2 + d_{i-1}\right)\right]}$$

$$c_3 = \left(B_1 - A_1\right)\left[jk_{i,z}\left(z_1 - z_2\right) + 1\right]e^{-j\left[k_{m,z}\left(z' + d_m\right) - k_{i,z}\left(z_2 + d_{i-1}\right)\right]}$$

$$c_4 = -\left(A_1 A_3 + B_1 B_3\right)\left[jk_{i,z}\left(z_1 - z_2\right) - 1\right]e^{-j\left[k_{m,z}\left(z' + d_m\right) + k_{i,z}\left(z_2 + 2d_i - d_{i-1}\right)\right]}$$ (B.122)

$$c_5 = \left(A_1 - B_1\right)e^{-j\left[k_{m,z}\left(z' + d_m\right) - k_{i,z}\left(z_1 + d_{i-1}\right)\right]}$$

$$c_6 = \left(A_2 + B_2\right)e^{j\left[k_{m,z}\left(z' + 2d_{m-1} - d_m\right) + k_{i,z}\left(z_1 + d_{i-1}\right)\right]}$$

$$c_7 = \left(B_2 B_3 - A_2 A_3\right)e^{j\left[k_{m,z}\left(z' + 2d_{m-1} - d_m\right) - k_{i,z}\left(z_1 + 2d_i - d_{i-1}\right)\right]}$$

$$c_8 = -\left(A_1 A_3 + B_1 B_3\right)e^{-j\left[k_{m,z}\left(z' + d_m\right) + k_{i,z}\left(z_1 + 2d_i - d_{i-1}\right)\right]}$$

Closed-form formulation (11):

$$\int_{z_1}^{z_2}\left(z - z_2\right)\tilde{G}_{z1}\,dz = \frac{\sum_{i=1}^{8} c_i}{k_{i,z}^2}$$ (B.123)

where the analytical form for $\left(i < m\right)$ and $\left(i > m\right)$ are derived, respectively, as:

$$c_1 = \left(B_1 B_3 + A_1 A_3\right)\left[\, jk_{i,z}\left(z_2 - z_1\right)+1\right]e^{\, j\left[k_{m,z}\left(z'+d_{m-1}\right)+k_{i,z}\left(z_1+2\,d_{i-1}-d_i\right)\right]}$$

$$c_2 = \left(A_2 A_3 - B_2 B_3\right)\left[\, jk_{i,z}\left(z_2 - z_1\right)+1\right]e^{\, -j\left[k_{m,z}\left(z'+2d_m-d_{m-1}\right)-k_{i,z}\left(z_1+2\,d_{i-1}-d_i\right)\right]}$$

$$c_3 = \left(A_1 - B_1\right)\left[\, jk_{i,z}\left(z_2 - z_1\right)-1\right]e^{\, j\left[k_{m,z}\left(z'+d_{m-1}\right)-k_{i,z}\left(z_1+d_i\right)\right]}$$

$$c_4 = \left(A_2 + B_2\right)\left[\, jk_{i,z}\left(z_2 - z_1\right)-1\right]e^{\, -j\left[k_{m,z}\left(z'+2d_m-d_{m-1}\right)+k_{i,z}\left(z_1+d_i\right)\right]}$$

$$c_5 = \left(A_2 + B_2\right)e^{\, -j\left[k_{m,z}\left(z'+2d_m-d_{m-1}\right)+k_{i,z}\left(z_2+d_i\right)\right]}$$

$$c_6 = \left(A_1 - B_1\right)e^{\, j\left[k_{m,z}\left(z'+d_{m-1}\right)-k_{i,z}\left(z_2+d_i\right)\right]}$$

$$c_7 = \left(B_2 B_3 - A_2 A_3\right)e^{\, -j\left[k_{m,z}\left(z'+2d_m-d_{m-1}\right)-k_{i,z}\left(z_2+2\,d_{i-1}-d_i\right)\right]}$$

$$c_8 = -\left(B_1 B_3 + A_1 A_3\right)e^{\, j\left[k_{m,z}\left(z'+d_{m-1}\right)+k_{i,z}\left(z_2+2\,d_{i-1}-d_i\right)\right]}$$

(B.124)

and

$$c_1 = -\left(A_1 A_3 + B_1 B_3\right)e^{\, -j\left[k_{m,z}\left(z'+d_m\right)+k_{i,z}\left(z_2+2d_i-d_{i-1}\right)\right]}$$

$$c_2 = \left(A_1 - B_1\right)e^{\, -j\left[k_{m,z}\left(z'+d_m\right)-k_{i,z}\left(z_2+d_{i-1}\right)\right]}$$

$$c_3 = \left(B_2 B_3 - A_2 A_3\right)e^{\, j\left[k_{m,z}\left(z'+2d_{m-1}-d_m\right)-k_{i,z}\left(z_2+2d_i-d_{i-1}\right)\right]}$$

$$c_4 = \left(A_2 + B_2\right)e^{\, j\left[k_{m,z}\left(z'+2d_{m-1}-d_m\right)-k_{i,z}\left(z_2+d_{i-1}\right)\right]}$$

$$c_5 = -\left(A_1 - B_1\right)\left[\, jk_{i,z}\left(z_2 - z_1\right)+1\right]e^{\, -j\left[k_{m,z}\left(z'+d_m\right)-k_{i,z}\left(z_1+d_{i-1}\right)\right]}$$

$$c_6 = -\left(A_2 + B_2\right)\left[\, jk_{i,z}\left(z_2 - z_1\right)+1\right]e^{\, j\left[k_{m,z}\left(z'+2d_{m-1}-d_m\right)+k_{i,z}\left(z_1+d_{i-1}\right)\right]}$$

$$c_7 = \left(B_2 B_3 - A_2 A_3\right)\left[\, jk_{i,z}\left(z_2 - z_1\right)-1\right]e^{\, j\left[k_{m,z}\left(z'+2d_{m-1}-d_m\right)-k_{i,z}\left(z_1+2d_i-d_{i-1}\right)\right]}$$

$$c_8 = -\left(B_1 B_3 + A_1 A_3\right)\left[\, jk_{i,z}\left(z_2 - z_1\right)-1\right]e^{\, -j\left[k_{m,z}\left(z'+d_m\right)+k_{i,z}\left(z_1+2d_i-d_{i-1}\right)\right]}$$

(B.125)

Closed-form formulation (1 2):

$$\int_{z_1}^{z_2} \tilde{G}_{xx}\left(k_r, z, z'\right)dz$$

(B.126)

for the reaction of a horizontal source with a horizontal field. In this case, the horizontal field is assumed to be supported by a vertical patch. The analytical form for $(i < m)$ and $(i > m)$ are derived, respectively, as:

$$\int_{z_1}^{z_2} \tilde{G}_{xx}\left(k_r, z, z'\right) dz$$

$$= \frac{j}{k_{i,z}} \left\{ \begin{array}{l} A_1 \left[e^{j\left[k_{m,z}\left(z'+d_{m-1}\right)-k_{i,z}\left(z_2+d_i\right)\right]} - e^{j\left[k_{m,z}\left(z'+d_{m-1}\right)-k_{i,z}\left(z_1+d_i\right)\right]} \right] \\[8pt] + A_1 A_3 \left[e^{j\left[k_{m,z}\left(z'+d_{m-1}\right)+k_{i,z}\left(z_1+2d_{i-1}-d_i\right)\right]} - e^{j\left[k_{m,z}\left(z'+d_{m-1}\right)+k_{i,z}\left(z_2+2d_{i-1}-d_i\right)\right]} \right] \\[8pt] + A_2 \left[e^{-j\left[k_{m,z}\left(z'+2d_m-d_{m-1}\right)+k_{i,z}\left(z_2+d_i\right)\right]} - e^{-j\left[k_{m,z}\left(z'+2d_m-d_{m-1}\right)+k_{i,z}\left(z_1+d_i\right)\right]} \right] \\[8pt] + A_2 A_3 \left[e^{-j\left[k_{m,z}\left(z'+2d_m-d_{m-1}\right)-k_{i,z}\left(z_1+2d_{i-1}-d_i\right)\right]} - e^{-j\left[k_{m,z}\left(z'+2d_m-d_{m-1}\right)-k_{i,z}\left(z_2+2d_{i-1}-d_i\right)\right]} \right] \end{array} \right\} \tag{B.127}$$

and

$$\int_{z_1}^{z_2} \tilde{G}_{xx}\left(k_r, z, z'\right) dz$$

$$= \frac{j}{k_{i,z}} \left\{ \begin{array}{l} B_1 \left[e^{-j\left[k_{m,z}\left(z'+d_m\right)-k_{i,z}\left(z_1+d_{i-1}\right)\right]} - e^{-j\left[k_{m,z}\left(z'+d_m\right)-k_{i,z}\left(z_2+d_{i-1}\right)\right]} \right] \\[8pt] + B_1 B_3 \left[e^{-j\left[k_{m,z}\left(z'+d_m\right)+k_{i,z}\left(z_2+2d_i-d_{i-1}\right)\right]} - e^{-j\left[k_{m,z}\left(z'+d_m\right)-k_{i,z}\left(z_1+2d_i-d_{i-1}\right)\right]} \right] \\[8pt] + B_2 \left[e^{j\left[k_{m,z}\left(z'+2d_{m-1}-d_m\right)-k_{i,z}\left(z_1+d_{i-1}\right)\right]} - e^{j\left[k_{m,z}\left(z'+2d_{m-1}-d_m\right)-k_{i,z}\left(z_2+d_{i-1}\right)\right]} \right] \\[8pt] + B_2 B_3 \left[e^{j\left[k_{m,z}\left(z'+2d_{m-1}-d_m\right)-k_{i,z}\left(z_2+2d_i-d_{i-1}\right)\right]} - e^{j\left[k_{m,z}\left(z'+2d_{m-1}-d_m\right)-k_{i,z}\left(z_1+2d_i-d_{i-1}\right)\right]} \right] \end{array} \right\} \tag{B.128}.$$

Closed-form formulation (13):

$$\int_{z_1}^{z_2} \tilde{G}_{vt} dz' = \frac{\sum_{i=1}^{4} c_i}{j k_{i,z}} \tag{B.129}$$

for the reaction through the scalar potential with a vertical source. In this case, the reaction with a source basis on a horizontal patch is considered. The analytical form for $(i < m)$ and $(i > m)$ are derived, respectively, as:

$$c_1 = \left(A_1 - B_1 \right)\left\{ e^{j\left[k_{m,z}\left(z' + d_{m-1} \right) - k_{i,z}\left(z_2 + d_i \right) \right]} - e^{j\left[k_{m,z}\left(z' + d_{m-1} \right) - k_{i,z}\left(z_1 + d_i \right) \right]} \right\}$$

$$c_2 = \left(A_1 A_3 + B_1 B_3 \right)\left\{ e^{j\left[k_{m,z}\left(z' + d_{m-1} \right) + k_{i,z}\left(z_1 + 2 d_{i-1} - d_i \right) \right]} - e^{j\left[k_{m,z}\left(z' + d_{m-1} \right) + k_{i,z}\left(z_2 + 2 d_{i-1} - d_i \right) \right]} \right\}$$

$$c_3 = \left(A_2 + B_2 \right)\left\{ e^{-j\left[k_{m,z}\left(z' + 2 d_m - d_{m-1} \right) + k_{i,z}\left(z_2 + d_i \right) \right]} - e^{-j\left[k_{m,z}\left(z' + 2 d_m - d_{m-1} \right) + k_{i,z}\left(z_1 + d_i \right) \right]} \right\}$$

$$c_4 = \left(A_2 A_3 - B_2 B_3 \right)\left\{ e^{-j\left[k_{m,z}\left(z' + 2 d_m - d_{m-1} \right) - k_{i,z}\left(z_1 + 2 d_{i-1} - d_i \right) \right]} - e^{-j\left[k_{m,z}\left(z' + 2 d_m - d_{m-1} \right) - k_{i,z}\left(z_2 + 2 d_{i-1} - d_i \right) \right]} \right\}$$

$$(B.130)$$

and

$$c_1 = \left(A_1 - B_1 \right)\left\{ e^{-j\left[k_{m,z}\left(z' + d_m \right) - k_{i,z}\left(z_2 + d_{i-1} \right) \right]} - e^{-j\left[k_{m,z}\left(z' + d_m \right) - k_{i,z}\left(z_1 + d_{i-1} \right) \right]} \right\}$$

$$c_2 = \left(A_2 + B_2 \right)\left\{ e^{j\left[k_{m,z}\left(z' + 2 d_{m-1} - d_m \right) + k_{i,z}\left(z_2 + d_{i-1} \right) \right]} - e^{j\left[k_{m,z}\left(z' + 2 d_{m-1} - d_m \right) + k_{i,z}\left(z_1 + d_{i-1} \right) \right]} \right\}$$

$$c_3 = \left(A_1 A_3 + B_1 B_3 \right)\left\{ e^{-j\left[k_{m,z}\left(z' + d_m \right) + k_{i,z}\left(z_1 + 2 d_i - d_{i-1} \right) \right]} - e^{-j\left[k_{m,z}\left(z' + d_m \right) + k_{i,z}\left(z_2 + 2 d_i - d_{i-1} \right) \right]} \right\}$$

$$c_4 = \left(A_2 A_3 - B_2 B_3 \right)\left\{ e^{j\left[k_{m,z}\left(z' + 2 d_{m-1} - d_m \right) - k_{i,z}\left(z_1 + 2 d_i - d_{i-1} \right) \right]} - e^{j\left[k_{m,z}\left(z' + 2 d_{m-1} - d_m \right) - k_{i,z}\left(z_2 + 2 d_i - d_{i-1} \right) \right]} \right\}$$

$$(B.131)$$

Closed-form formulation (14):

$$\int_{z_1'}^{z_2'} \tilde{G}_{vt} \, dz' = \frac{\sum_{i=1}^{4} c_i}{j k_{m,z}} \quad (B.132)$$

for the reaction through the scalar potential with a horizontal source. In this case, the reaction with a source basis on a horizontal patch is considered. The analytical form for $(i < m)$ and $(i > m)$ are derived, respectively, as:

$$c_1 = \left(A_1 - B_1 \right)\left\{ e^{-j\left[-k_{m,z}\left(d_{m-1} + z_2' \right) + k_{i,z}\left(d_i + z \right) \right]} - e^{-j\left[-k_{m,z}\left(d_{m-1} + z_1' \right) + k_{i,z}\left(d_i + z \right) \right]} \right\}$$

$$c_2 = \left(A_1 A_3 + B_1 B_3 \right)\left\{ e^{j\left[k_{m,z}\left(d_{m-1} + z_2' \right) + k_{i,z}\left(2 d_{i-1} - d_i + z \right) \right]} - e^{j\left[k_{m,z}\left(d_{m-1} + z_1' \right) + k_{i,z}\left(2 d_{i-1} - d_i + z \right) \right]} \right\}$$

$$c_3 = \left(A_2 + B_2 \right)\left\{ e^{-j\left[k_{m,z}\left(2 d_m - d_{m-1} + z_1' \right) + k_{i,z}\left(d_i + z \right) \right]} - e^{-j\left[k_{m,z}\left(2 d_m - d_{m-1} + z_2' \right) + k_{i,z}\left(d_i + z \right) \right]} \right\}$$

$$c_4 = \left(A_2 A_3 - B_2 B_3 \right)\left\{ e^{j\left[-k_{m,z}\left(2 d_m - d_{m-1} + z_1' \right) + k_{i,z}\left(2 d_{i-1} - d_i + z \right) \right]} - e^{j\left[-k_{m,z}\left(2 d_m - d_{m-1} + z_2' \right) + k_{i,z}\left(2 d_{i-1} - d_i + z \right) \right]} \right\}$$

$$(B.133)$$

and

$$c_1 = \left(A_1 - B_1 \right) \left\{ e^{-j\left[k_{m,z}\left(d_m + z_1' \right) - k_{i,z}\left(d_{-1} + z \right) \right]} - e^{-j\left[k_{m,z}\left(d_m + z_2' \right) - k_{i,z}\left(d_{-1} + z \right) \right]} \right\}$$

$$c_2 = \left(A_1 A_3 + B_1 B_3 \right) \left\{ e^{-j\left[k_{m,z}\left(d_m + z_1' + k_{i,z}\left(2d_i - d_{i-1} + z \right) \right) \right]} - e^{-j\left[k_{m,z}\left(d_m + z_2' \right) + k_{i,z}\left(2d_i - d_{i-1} + z \right) \right]} \right\}$$

$$c_3 = \left(A_2 + B_2 \right) \left\{ e^{j\left[k_{m,z}\left(2d_{m-1} - d_m + z_2' \right) + k_{i,z}\left(d_{-1} + z \right) \right]} - e^{j\left[k_{m,z}\left(2d_{m-1} - d_m + z_1' \right) + k_{i,z}\left(d_{-1} + z \right) \right]} \right\}$$

$$c_4 = \left(A_2 A_3 - B_2 B_3 \right) \left\{ e^{j\left[k_{m,z}\left(2d_{m-1} - d_m + z_2' \right) - k_{i,z}\left(2d_i - d_{i-1} + z \right) \right]} - e^{j\left[k_{m,z}\left(2d_{m-1} - d_m + z_1' \right) - k_{i,z}\left(2d_i - d_{i-1} + z \right) \right]} \right\}$$

(B.134)

Closed-form formulation (15):

$$\int_{z_1'}^{z_2'} \tilde{G}_{vz}\left(k_r, z, z' \right) dz' \quad \text{(B.135)}$$

for the reaction through the scalar potential with a vertical source. In this case, the reaction with a source basis on a vertical patch is considered. The analytical form for $(i < m)$ and $(i > m)$ are derived, respectively, as:

$$
\int_{z_1'}^{z_2'} \tilde{G}_{vz}\left(k_r, z, z' \right) dz'
$$

$$
= \frac{jk_{i,z}}{k_{m,z}^2} \left\{
\begin{array}{l}
A_1 \left[e^{j\left[k_{m,z}\left(z_1' + d_{m-1} \right) - k_{i,z}\left(z + d_i \right) \right]} - e^{j\left[k_{m,z}\left(z_2' + d_{m-1} \right) - k_{i,z}\left(z + d_i \right) \right]} \right] \\[6pt]
+ A_1 A_3 \left[e^{j\left[k_{m,z}\left(z_2' + d_{m-1} \right) + k_{i,z}\left(z + 2d_{-1} - d_i \right) \right]} - e^{j\left[k_{m,z}\left(z_1' + d_{m-1} \right) + k_{i,z}\left(z + 2d_{-1} - d_i \right) \right]} \right] \\[6pt]
+ A_2 \left[e^{-j\left[k_{m,z}\left(z_1' + 2d_m - d_{m-1} \right) + k_{i,z}\left(z + d_i \right) \right]} - e^{-j\left[k_{m,z}\left(z_2' + 2d_m - d_{m-1} \right) + k_{i,z}\left(z + d_i \right) \right]} \right] \\[6pt]
+ A_2 A_3 \left[e^{-j\left[k_{m,z}\left(z_2' + 2d_m - d_{m-1} \right) - k_{i,z}\left(z + 2d_{-1} - d_i \right) \right]} - e^{-j\left[k_{m,z}\left(z_1' + 2d_m - d_{m-1} \right) - k_{i,z}\left(z + 2d_{-1} - d_i \right) \right]} \right]
\end{array}
\right\}
$$

(B.136)

and

$$\int_{z_1^{'}}^{z_2^{'}} \tilde{G}_{vz}\left(k_r, z, z^{'}\right)dz^{'}$$

$$= \frac{jk_{i,z}}{k_{m,z}^2}\left\{\begin{matrix} B_1\left[e^{-j\left[k_{m,z}\left(z_2^{'}+d_m\right)-k_{i,z}(z+d_{i-1})\right]} - e^{-j\left[k_{m,z}\left(z_1^{'}+d_m\right)-k_{i,z}(z+d_{i-1})\right]}\right] \\ +B_1B_3\left[e^{-j\left[k_{m,z}\left(z_1^{'}+d_m\right)+k_{i,z}\left(z+2d_i-d_{i-1}\right)\right]} - e^{-j\left[k_{m,z}\left(z_2^{'}+d_m\right)+k_{i,z}\left(z+2d_i-d_{i-1}\right)\right]}\right] \\ +B_2\left[e^{j\left[k_{m,z}\left(z_2^{'}+2d_{m-1}-d_m\right)+k_{i,z}(z+d_{i-1})\right]} - e^{j\left[k_{m,z}\left(z_1^{'}+2d_{m-1}-d_m\right)+k_{i,z}(z+d_{i-1})\right]}\right] \\ +B_2B_3\left[e^{j\left[k_{m,z}\left(z_1^{'}+2d_{m-1}-d_m\right)-k_{i,z}\left(z+2d_i-d_{i-1}\right)\right]} - e^{j\left[k_{m,z}\left(z_2^{'}+2d_{m-1}-d_m\right)-k_{i,z}\left(z+2d_i-d_{i-1}\right)\right]}\right] \end{matrix}\right\} \qquad \text{(B.137)}$$

where the exception of Fresnel reflection coefficients B_1, B_2 and B_3 are defined in (B.82) for the TM$_z$-polarization.

Closed-form formulation (16):

$$\int_{z_1^{'}}^{z_2^{'}} \tilde{G}_{xx}\left(k_r, z, z^{'}\right)dz^{'} \qquad \text{(B.138)}$$

for the reaction of a horizontal source with a vertical field. In this case, the horizontal source is assumed to be supported by a vertical patch and the horizontal field is assumed to be supported by a horizontal patch. The analytical form for $(i < m)$ and $(i > m)$ are derived, respectively, as:

$$\int_{z_1^{'}}^{z_2^{'}} \tilde{G}_{xx}\left(k_r, z, z^{'}\right)dz^{'}$$

$$= \frac{j}{k_{m,z}}\left\{\begin{matrix} A_1\left[e^{j\left[k_{m,z}\left(z_1^{'}+d_{m-1}\right)-k_{i,z}(z+d_i)\right]} - e^{j\left[k_{m,z}\left(z_2^{'}+d_{m-1}\right)-k_{i,z}(z+d_i)\right]}\right] \\ +A_1A_3\left[e^{j\left[k_{m,z}\left(z_1^{'}+d_{m-1}\right)+k_{i,z}\left(z+2d_{i-1}-d_i\right)\right]} - e^{j\left[k_{m,z}\left(z_2^{'}+d_{m-1}\right)+k_{i,z}\left(z+2d_{i-1}-d_i\right)\right]}\right] \\ +A_2\left[e^{-j\left[k_{m,z}\left(z_2^{'}+2d_m-d_{m-1}\right)+k_{i,z}(z+d_i)\right]} - e^{-j\left[k_{m,z}\left(z_1^{'}+2d_m-d_{m-1}\right)+k_{i,z}(z+d_i)\right]}\right] \\ +A_2A_3\left[e^{-j\left[k_{m,z}\left(z_2^{'}+2d_m-d_{m-1}\right)-k_{i,z}\left(z+2d_{i-1}-d_i\right)\right]} - e^{-j\left[k_{m,z}\left(z_1^{'}+2d_m-d_{m-1}\right)-k_{i,z}\left(z+2d_{i-1}-d_i\right)\right]}\right] \end{matrix}\right\} \qquad \text{(B.139)}$$

and

$$\int\limits_{z_1'}^{z_2'} \tilde{G}_{xx}\left(k_r, z, z'\right) dz'$$

$$= \frac{-j}{k_{m,z}} \left\{ \begin{array}{l} B_1 \left[e^{-j\left[k_{m,z}\left(z_1'+d_m\right)-k_{i,z}\left(z+d_{i-1}\right)\right]} - e^{-j\left[k_{m,z}\left(z_2'+d_m\right)-k_{i,z}\left(z+d_{i-1}\right)\right]} \right] \\[2mm] + B_1 B_3 \left[e^{-j\left[k_{m,z}\left(z_1'+d_m\right)+k_{i,z}\left(z+2d_i-d_{i-1}\right)\right]} - e^{-j\left[k_{m,z}\left(z_2'+d_m\right)+k_{i,z}\left(z+2d_i-d_{i-1}\right)\right]} \right] \\[2mm] + B_2 \left[e^{j\left[k_{m,z}\left(z_2'+2d_{m-1}-d_m\right)+k_{i,z}\left(z+d_{i-1}\right)\right]} - e^{j\left[k_{m,z}\left(z_1'+2d_{m-1}-d_m\right)+k_{i,z}\left(z+d_{i-1}\right)\right]} \right] \\[2mm] + B_2 B_3 \left[e^{j\left[k_{m,z}\left(z_2'+2d_{m-1}-d_m\right)-k_{i,z}\left(z+2d_i-d_{i-1}\right)\right]} - e^{j\left[k_{m,z}\left(z_1'+2d_{m-1}-d_m\right)-k_{i,z}\left(z+2d_i-d_{i-1}\right)\right]} \right] \end{array} \right\}$$

(B.140)

B.8 Asymptotic extraction for the free-space Green's function

The Two-level DCIM would not work well the zero-arguments complex functions as presented in the Chapter four. This can be avoided by extracting the terms analytically in the spectral domain before applying the DCIM, and adding back in the spatial domain. For example in (B.78) when the observation point z equals z_2', the argument of the exponential term $-jA_1 e^{jk_{m,z}\left(z+z_2'+2d_{m-1}\right)}$ is zero. This term must be extracted asymptotically in the spectral domain as:

$$\frac{-jA_1^\infty}{k_{m,z}} \quad where$$

$$A_1^\infty = R_{m,m-1}^{TM^\infty} = \frac{e_{m-1}-e_m}{e_{m-1}+e_m}$$

(B.141)

where $R_{m,m-1}^{TM^\infty}$ is the asymptotic reflection coefficient when $k_r \to \infty$. Next we add the term back in closed-form at the spatial domain after applying the DCIM. The closed-form term can be obtained via the Residue Theorem:

$$\int\limits_0^\infty J_0\left(k_r \boldsymbol{r}\right) \frac{k_r}{k_{m,z}} \left(\frac{-jA_1^\infty}{k_{m,z}} \right) dk_r$$
$$= \frac{A_1^\infty \boldsymbol{p} H_0^{(2)}\left(k_m \boldsymbol{r}\right)}{2}.$$

(B.142)

Similarly for $z = z_1'$ we need to extract the term $-jA_1 e^{jk_{m,z}\left(z+z_2'+2d_{m-1}\right)}$ for zero argument in the exponential. The asymptotic term in the spectral domain and the closed-form term in spatial domain can be expressed, respectively, as:

$$\frac{-jA_3^\infty}{k_{m,z}} \quad where$$

$$A_3^\infty = R_{m,m+1}^{TM^\infty} = \frac{\boldsymbol{e}_{m+1} - \boldsymbol{e}_m}{\boldsymbol{e}_{m+1} + \boldsymbol{e}_m} \tag{B.143}$$

and

$$\int_0^\infty J_0\left(k_r \boldsymbol{r}\right) \frac{k_r}{k_{m,z}} \left(\frac{-jA_3^\infty}{k_{m,z}}\right) dk_r$$

$$= \frac{A_3^\infty \boldsymbol{p} H_0^{(2)}\left(k_m \boldsymbol{r}\right)}{2} \tag{B.144}.$$

Similarly, all the asymptotic terms of the closed-form z-integrations in Table B.1 can be extracted by applying the same procedure.

B.9 Asymptotic extraction for layered media Green's function

The asymptotic extraction for the Two-level DCIM in multi-layered media case is presented in this section. Consider the scalar potential term in (B.73), the extracted terms are:

$$\tilde{I}\left(k_r\right) = \begin{cases} \dfrac{-j\left(A_5^\infty k_{m,z}^2 + A_6^\infty k_m^2\right)}{k_{m,z} k_r^2} & if \ z' + z_1 = -2dm \\[4mm] \dfrac{-j\left(A_3^\infty k_{m,z}^2 + A_1^\infty k_m^2\right)}{k_{m,z} k_r^2} & if \ z' + z_2 = -2d_{m-1} \end{cases} \tag{B.145}$$

where the asymptotic expressions of $A_1^\infty, A_3^\infty, A_5^\infty, A_6^\infty$ in (B.74) can be expressed as:

$$A_1^\infty = \frac{m_{m-1} - m_m}{m_{m-1} + m_m} = 0$$

$$A_6^\infty = \frac{m_{m+1} - m_m}{m_{m+1} + m_m} = 0$$

$$A_3^\infty = R_{m,m-1}^{TM\infty} = \frac{e_{m-1} - e_m}{e_{m-1} + e_m}$$

$$A_5^\infty = R_{m,m+1}^{TM\infty} = \frac{e_{m+1} - e_m}{e_{m+1} + e_m}$$

$$(B.146).$$

After applying the DCIM, the extracted terms are added back analytically in the spatial domain:

$$I(\mathbf{r}) = \begin{cases} \dfrac{-p}{2} R_{m,m+1}^{TM\infty} H_0^{(2)}(k_m \mathbf{r}) & \text{if } z' + z_1 = -2d_m \\[3mm] \dfrac{-p}{2} R_{m,m-1}^{TM\infty} H_0^{(2)}(k_m \mathbf{r}) & \text{if } z' + z_2 = -2d_{m-1} \end{cases}$$

$$(B.147).$$

Similarly for the closed-form z-integrations in (B.133), the zero argument terms $(z_2' + d_{m-1}$ and $z + d_m)$ of the exponentials are extracted out in the spectral domain and are added back in closed-form in the spatial domain. The closed-form can be expressed as:

$$j \int_0^\infty \frac{\left(A_1^\infty - B_1^\infty\right) J_0(k_r \mathbf{r})}{k_{m,z}^2 k_r} dk_r$$

$$= j T_{m,m-1}^{TM\infty} \int_0^\infty \frac{k_r J_0(k_r \mathbf{r})}{k_{m,z}^2} dk_r$$

$$= \frac{-p}{2} \left(\frac{2e_{r_{m-1}}}{e_{r_{m-1}} + e_{r_m}} \right) H_0^{(2)}(k_m \mathbf{r})$$

$$(B.148)$$

The asymptotic extraction for the Fresnel transmission coefficient for $i < m$ in (B.139) is derived as:

$$\tilde{T}_{m,i}^{TE^<} = \prod_{\substack{j=m \\ (i<m)}}^{i+1} S_{j,j-1}^{TE^<} \Theta_j$$

$$S_{j,j-1}^{TE^<} = \frac{T_{j,j-1}^{TE}}{1 + R_{j,j-1}^{TE} \tilde{R}_{j-1,j-2}^{TE} e^{-2jk_{j-1,z}\left(d_{j-1}-d_{j-2}\right)}} \tag{B.149}$$

$$\Theta_j = \begin{cases} 1 & , j = m \\ e^{jk_{j,z}\left(d_{j-1}-d_j\right)} & , j \neq m \end{cases}$$

and the asymptotic approximation for (B.149) is:

$$\tilde{T}_{m,i}^{TE^{<\infty}} = \prod_{\substack{j=m \\ (i<m)}}^{i+1} S_{j,j-1}^{TE^{<\infty}}$$

$$= \prod_{\substack{j=m \\ (i<m)}}^{i+1} \left(1 - R_{j,j-1}^{TE^\infty}\right) = 1 \tag{B.150).}$$

Finally, some useful integral identities for the asymptotic terms are summarized:

$$\int_0^\infty \frac{J_0\left(k_r \boldsymbol{r}\right)k_r}{k_{m,z}^2} dk_{\boldsymbol{r}} = \int_0^\infty \frac{J_0\left(k_r \boldsymbol{r}\right)k_r}{k_m^2 - k_{\boldsymbol{r}}^2} dk_{\boldsymbol{r}} = \frac{\boldsymbol{p}\,j}{2} H_0^{(2)}\left(k_m \boldsymbol{r}\right) = -K_0\left(\frac{\boldsymbol{r}}{\sqrt{\frac{-1}{k_m^2}}}\right) \tag{B.151}$$

$$\int_0^\infty \frac{J_0\left(k_r \boldsymbol{r}\right)k_r}{k_m^2 + k_{\boldsymbol{r}}^2} dk_{\boldsymbol{r}} = \frac{\boldsymbol{p}\,j}{2} H_0^{(2)}\left(-jk_m \boldsymbol{r}\right) \tag{B.152}$$

$$\int_0^\infty \frac{J_0\left(k_r \boldsymbol{r}\right)k_r}{k_{m,z}^3} dk_{\boldsymbol{r}} = -\frac{e^{\frac{-\boldsymbol{r}}{\sqrt{\frac{-1}{k_m^2}}}}}{k_m} \tag{B.153}$$

$$\int_0^\infty \frac{J_0\left(k_r \boldsymbol{r}\right)k_r}{k_{m,z}^4} dk_{\boldsymbol{r}} = -\frac{\boldsymbol{r} K_1\left(\frac{\boldsymbol{r}}{\sqrt{\frac{-1}{k_m^2}}}\right)}{2k_m^2 \sqrt{\frac{-1}{k_m^2}}} \tag{B.154}$$

$$\int_0^\infty \frac{J_0(k_r r)k_r}{k_{m,z}^5} dk_r = \frac{e^{\frac{-r}{\sqrt{\frac{-1}{k_m^2}}}}\left(rk_m^2\sqrt{\frac{-1}{k_m^2}}-1\right)}{3k_m^3} \tag{B.155}$$

$$\int_0^\infty \frac{J_1(k_r r)}{k_{m,z}^2} dk_r = \frac{1}{k_m^2 r} + K_1\left(\frac{rd(r)}{\sqrt{\frac{-1}{k_m^2}}}\right)d(r)\sqrt{\frac{-1}{k_m^2}}$$

$$\mathrm{Im}(r)=0 \qquad and \qquad \arg\left(k_m^2\right)\neq 0 \tag{B.156}$$

$$d(r)=\begin{cases} -1 & if & r<0 \\ 0 & if & r=0 \\ 1 & if & r>0 \end{cases}$$

where K_1 is the modified Bessel function of first-order.

References

[1]   R. F. Harrington, *Field Computation by Moment Methods*. New York: Macmillan, 1968.

[2]   K. A. Michalski and D. L. Zheng, "Electromagnetic scattering and radiation by surfaces of arbitrary shape in layered media.II. Implementation and Results for Contigious Half-Space," *IEEE Trans. on Antennas and Propagation*, vol. 38, pp. 345-352, 1990.

[3]   K. A. Michalski and D. L. Zheng, "Electromagnetic scattering and radiation by surfaces of arbitrary shape in layered media.I. Theory," *IEEE Trans. on Antennas and Propagation*, vol. 38, pp. 335-344, 1990.

[4]   K. A. Michalski and J. R. Mosig, "Multilayered Media Green's Functions in Integral Equation Formulations," *IEEE Trans. on Antennas and Propagation*, vol. 45, pp. 508-519, Mar. 1997.

[5]   F. E. G. J.R. Mosig, "General integral equation formulation for microstrip antennas and scatterers," *Inst. Elec. Eng. Proc.*, vol. 132, Dec. 1985.

[6]   F. E. G. J.R. Mosig, "A dynamical Radiation Model for," *Advances in Electronics and Electron Physics*, vol. 59, pp. 139-237, 1982.

[7]   W. A. Johnson, "Analysis of vertical, tubular cylinder which penetrates an air-dielectric interface and which is excited by an azimuthally symmetric source," *Radio Science*, vol. 18, pp. 1273-1281, Dec 1983.

[8]   L. Feng, Kalyan Donepudi, Jian_ming Jin, "Higher Order Full-wave Analysis of Multilayer Microstrip Structures," *Microwave and Optical Technical Letters*, vol. 25, pp. 141-145, Nov. 1999.

[9]   C. H. C. R.A. Kipp, "Complex image method for sources in bounded regions of multilayer structures," *IEEE Trans. on Microwave Theory and Tech.*, vol. 42, pp. 860-865, May 1994.

[10]   J. D.G Fang, J Yang, G.Y. Delisle, "Discrete image theory for horizontal electric dipole in a multilayer medium," *Proc. Inst. Elect. Eng.*, vol. 135, pp. 297-303, Oct. 1988.

[11]   M. I. Aksun, "A Robust Approach for the Derivation of Closed-form Green's Functions," *IEEE Trans. on Microwave Theory and Tech.*, vol. 44, pp. 651-658, May 1996.

[12]   G. Dural and M. I. Aksun, "Closed-Form Green's Functions for General Sources and Stratified Media," *IEEE Trans. on Microwave Theory and Tech.*, vol. 4, pp. 1545-1552, July 1995.

[13]   D. R. Wilton, S. M. Rao, and A. W. Glisson, "Potential integrals for uniform and linear source distributions on polygonal and polyhedral domains," *IEEE Trans. on Antennas and Propagation*, vol. 32, pp. 276-281, Mar. 1984.

[14]   M. G. Duffy, "Quadrature over a pyramid or cube of integrands with a singularity at a vertex," *SIAM J. Num. Analysis*, vol. 19, pp. 1260-1262, 1982.

[15]   M. Khayat and D. R. Wilton, "Revisiting the Evaluation of Potential Integrals," *ICEAA*, 2003.

[16]   Zeland, "Full-wave EM analysis IE3D," 9.3 ed. California: Zeland, 1999.

[17]   P. W. Hawkes, "Advances in Electronics and Electron Physics," in *A dynamical radiation model for microstrip structures*, vol. 59, J. R. Mosig and F. E. Gardiol, Eds. New York: Academic, 1982, pp. 139-237.

[18]   K. A. Michalski, "The mixed-potential electric field integral equation for objects in layered media," *Arch. Elek. Ubertragung.*, vol. 39, pp. 317-322, Oct. 1985.

[19]   L. S. Canino, J. J. Ottusch, M. A. Stalzer, J. L. Visher, and S. Wandzura, "Numerical solution of the Helmholtz equation in 2D and 3D using a high-order Nystrom discretization," *J. Comput. Phys.*, vol. 146, pp. 627-633, 1998.

[20]   K. Donepudi, G. Kang, J. M. Song, J. M. Jin, and W. C. Chew, "Higher-order MoM implementation to solve integral equations," presented at IEEE AP-S Int. Symp, FL, July 11-16, 1999.

[21]   R. D. Graglia, D. R. Wilton, and A. F. Peterson, "Higher-Order Interpolatory Vector bases for Computational Electromagnetics," *IEEE Trans. on Antennas and Propagation*, vol. 45, pp. 329-342, Mar. 1997.

[22]   S. M. Rao, D. R. Wilton, and A. W. Glisson, "Electromagnetic scattering by surfaces of arbitrary shape," *IEEE Trans. on Antennas and Propagation*, vol. 30, pp. 409-418, May 1982.

[23]   G.Liu and S. D. Gedney, "High-order moment method solution for the scattering analysis ofpenetrable bodies," *Electromagnetics*, vol. 23, pp. 331-345, 2003.

[24]   S. D. Gedney, "High-order method-of-moment solution of the scattering by three-dimensional PEC bodies using quadrature-based point matching," *Microwave Opt. Tech. Letter*, vol. 29, pp. 303-309, 2001.

[25]   S. D. Gedney, "De-Embedding Scheme in 3d_ho_gal," University of Kentucky, Lexington, KY, USA., Technical Report March 17 2003.

[26]   S. D. Gedney, "On deriving a locally corrected Nyström scheme from a quadrature sampled moment method," *IEEE Trans. on Antennas and Propagation*, vol. 51, pp. 2402-2412, 2003.

[27]   A. H. Stroud and D. Secrest, *Gaussian Quadrature Formulas.* Englewood Cliffs, NJ: Prentice-Hall, 1966.

[28]   E. G. Ladopoulos, *Singular Integral Equations: Linear and Non-Linear Theory and its Applications in Science and Engineering*. Berlin, Germany: Springer-Verlag, 2000.

[29]   K. A. Michalski, "Extrapolation Methods for Sommerfeld Integral Tails," *IEEE Trans. on Antennas and Propagation*, vol. 46, pp. 1405-1418, Oct. 1998.

[30]   W. C. Chew, J. S. Zhao, and T. J. Cui, "The Layered medium green's function – A new look," *Microwave and Optical Technical Letters*, vol. 31, pp. 252255, Nov. 2001.

[31]   T. J. Bromwich, *An introduction to the theory of infinite series.* New York: Macmillan, 1965.

[32]   A. Alaylioglu, G. A. Evans, and J. Hyslop, "The evaluation of oscillatory integrals with infinite limits," *Journal of Computational Physics*, vol. 13, pp. 433-438, 1973.

[33]   C. Brezinski, "A general extrapolation algorithm," *Numerical Mathematics*, vol. 35, pp. 175-180, 1980.

[34]   T. Havie, "Generalized Neville type extrapolation scheme," *BIT*, vol. 19, pp. 204-213, 1979.

[35]   C. Schneider, "Vereinfachte Rekursionen zur Richardson-extrapolation in Spezialfallen," *Numerical Mathematics*, vol. 24, pp. 177-184, 1975.

[36]   D. Shanks, "Nonlinear transformations of divergent slowly convergent sequences," *J. Math. Phys.*, vol. 34, pp. 1-42, 1955.

[37]   D. Levin, "Development of nonlinear transformations for improving convergence of sequences," *Int. J. Comput. Math. Section B*, vol. 3, pp. 371-388, 1973.

[38]   J. R. Mosig, "Integral Equation Technique," in *Numerical Techniques for Microwave and Millimeter-Wave Passive Structures*, T. Itoh, Ed. New York: Wiley, 1989, pp. 133-213.

[39]   M. Abramowitz and I. A. Stegun, *Handbook of Mathematical Functions*. New York: Dover, 1965.

[40]   T. K. Sarkar and e. al, "Sub-optimal Approximation/Identification of Transient Waveforms from Electromagnetic System by Pencil-of-function Method," *IEEE Trans. on Antennas and Propagation*, vol. 28, pp. 928-933, Nov. 1980.

[41]   G. Dural and M. I. Aksun, "Closed-Form Green's Functions for General Sources and Stratified Media," *IEEE Trans. on Microwave Theory and Tech.*, vol. 4, pp. 1545-1552, 1995.

[42]   M. I. Aksun, "A Robust Approach for the Derivation of Closed-form Green's Functions," *IEEE Trans. on Microwave Theory and Tech.*, vol. 44, pp. 651-658, 1996.

[43]   F. Ling and J.-M. Jin, "Full-wave Analysis of Multilayer Microstrip Problems," in *Fast and Efficient Algorithms in Computational Electromagnetics*, J. M. J. W.C. Chew, E. Michielssen, J. Song, Ed. Boston: Artech House, 2001, pp. 729-780.

[44]   Y. L. Chow, J. J. Yang, D. G. Fang, and G. E. Delisle, "A closed-form spatial Green's function for the thick microstrip substrate," *IEEE Trans. on Microwave Theory and Tech.*, vol. 39, pp. 588-592, March 1991.

[45]   A. Erdelyi, *Tables of Integral Transforms, Bateman Manuscript Project*, vol. 2. New York: McGraw-Hill Book Company, Inc., 1954.

[46]   T. K. Sarkar and Pereira, "Using the Matrix Pencil Method to Estimate the Parameters of a Sum of Complex Exponentials," *IEEE Antennas Propagation Magzine*, vol. 37, pp. 48-55, Feb. 1995.

[47]   Y. Hua and T. K. Sarkar, "Generalized Pencil-of-Function Method for Extracting Poles of an EM System from Its Transient Response," *IEEE Trans. on Antennas and Propagation*, vol. 37, pp. 229-234, Feb. 1989.

[48]   I. S. Gradshteyn and I. M. Ryzhik, *Tables of Integrals, Series and Products*. New York: Academic Press, 1980.

[49]   N. V. Shuley, R. R. Boix, F. Medina, and M. Horno, "On the Fast Approximation of Green's Functions in MPIE Formulations for Planar Layered Media," *IEEE Trans. on Antennas and Propagation*, vol. 50, pp. 2185-2192, Sept. 2002.

[50]   N. Yuan, T. S. yeo, X.-C. Nie, and L. W. Li, "A Fast Analysis of scattering and radiation of Large microstrip antenna arrays," *IEEE Antennas Propagation Magzine*, vol. 51, pp. 2218-2226, Sept. 2003.

[51]   L. Feng and J.-M. Jin, "Discrete Complex Image Method for Green's Functions of General Multilayer Media," *IEEE Microwave and Guided Wave Letters*, vol. 10, pp. 400-402, Oct. 2000.

[52]   C. H. Chan and R. A. Kipp, "Application of the complex image method to multilevel, multiconductor microstrip lines," *Int. J. Microwave Milimeter Wave Computer Aided Eng.*, vol. 7, pp. 368-379, 1997.

[53]   C. H. Chan and R. A. Kipp, "Application of the complex image method to characterization of microstrip vias," *Int. J. Microwave Milimeter Wave Computer Aided Eng.*, vol. 7, 1997.

[54] A. Alaa and A. Mohsen, "An Accurate Computation of Green's Functions for Multilayer Media," *Microwave and Optical Technical Letters*, vol. 29, pp. 130-131, April 2001.

[55] M. I. Aksun, M. E. Yavuz, and G. Dural, "Comments on the problems in DCIM," presented at IEEE AP-S, San Diego, CA, July 2003.

[56] B. Hu and W. C. Chew, "Fast inhomogeneous plane wave algorithm for electromagnetic solutions in layered medium structures-2D case," *Radio Science*, vol. 35, Jan 2000.

[57] L. Feng and J.-M. Jin, "Discrete Complex Image Method for Green's Functions of General Multilayer Media," *IEEE Microwave and Guided Wave Letters*, vol. 10, pp. 400-402, 2000.

[58] L. Alatan, M. I. Aksun, K. Mahadevan, and M. T. Birand, "Analytical evaluation of the MoM matrix elements," *IEEE Trans. on Microwave Theory and Tech.*, vol. 44, pp. 519-525, April 1996.

[59] P. P. Silvester and R. L. Ferrari, *Finite Elements for electrical engineers*. Cambridge: Cambridge University Press, 1986.

[60] D. C. Chang and J. X. Zhang, "Electromagnetic modeling of passive circuit elements in MMIC," *IEEE Trans. on Microwave Theory and Tech.*, vol. 40, pp. 1741-1747, Sept. 1992.

[61] J. C. Rautio, "A de-embedding algorithm for electromagnetics," *Int. J. Microwave Milimeter Wave Computer Aided Eng.*, vol. 11, pp. 282-287, 1991.

[62] J. S. Hong and M. J. Lancaster, *Microstrip filters for RF/microwave applications*. New York: Wiley, 2001.

[63] F. Huang, L. Yue, and D. Gulati, "Compact copper microstrip filters with spiral resonators," *Microwave and Optical Technical Letters*, vol. 42, pp. 460-463, Sept. 2004.

[64] G. Prigent, E. Rius, F. L. Pennec, S. L. Maguer, and C. Quendo, "A novel design method for improvement of narrow bandpass planar filter response," *Microwave and Optical Technical Letters*, vol. 41, pp. 98-104, April 2004.

[65] M. Matsuo, H. Yabuki, and M. Makimoto, "Dual-mode stepped-impedance ring resonator for bandpass filter applications," *IEEE Trans. on Microwave Theory and Tech.*, vol. 49, pp. 1235-1240, July 2001.

[66] M. Matsuo and e. al, "Analysis of Resonant Characteristics for a one-wavelength ring resonator coupled with two orthogonal resonant modes," *Electronics and Communications in Japan*, vol. 82, pp. 19-27, Oct 1998.

[67] K. H. Kwon, S. Han, S. Nahm, M. Kim, and Y. Kim, "Compact hairpin-shaped duplexer using a bmt substrate with high dielectric constant," *Microwave and Optical Technical Letters*, vol. 41, pp. 251-253, May 2004.

[68] L. Zhu and K. Wu, "A Joint field/circuit model of line-to-ring coupling structures and its application to the design of microstrip dual-mode filters and ring resonator circuits," *IEEE Trans. on Microwave Theory and Tech.*, vol. 47, pp. 1938-1948, Oct 1999.

[69] C. S. Hsu and C. L. Huang, "Cross-coupled hairpin filter design using high-permittivity substrates," *Microwave and Optical Technical Letters*, vol. 41, pp. 419-423, June 2004.

[70] C. C. Chen, B. F. Hung, A. Chin, and S. P. McAlister, "High performance cpw and microstrip ring resonators on silicon substrates," *Microwave and Optical Technical Letters*, vol. 43, pp. 511-514, Sept. 2004.

[71]   S. D. Gedney, A. Zhu, and W. H. Tang, "A fast high-order quadrature sampled pre-corrected fast-fourier transform for electromagnetic scattering," *Microwave and Optical Technical Letters*, vol. 36, pp. 343-349, Mar 2003.

[72]   E. Bleszynski, M. Bleszynski, and T. Jaroszewicz, "AIM adaptive integral method for solving large-scale electromagnetic scattering and radiation problems," *Journal of Radio Science*, vol. 31, pp. 1225-1251, 1996.

[73]   J. R. Phillips and J. K. White, "A precorrected-FFTmethod for electrostatic analysis of complicated 3D structures," *IEEE Trans. on Computer-Aided Design Integrated Ciccuits Systems*, vol. 16, pp. 1059-1072, 1997.

[74]   Z. Q. Zhang and Q. H. Liu, "Three-dimensional weak-form conjugate- and biconjugate-gradient FFT methods for volume integral equations," *Microwave and Optical Technical Letters*, vol. 29, pp. 350-356, 2001.

[75]   S. Q. Li, Y. X. Yu, C. H. Chan, and L. Tsang, "A sparse matrix/canonical grid method for analyzing densely packed interconnects," *IEEE Trans. on Microwave Theory and Tech.*, vol. 49, pp. 1221-1228, 2001.

[76]   N. Engheta, W. D. Murphy, V. Rokhlin, and M. S. Vassiliou, "The fast multipole method (FMM) for electromagnetic cattering problems," *IEEE Trans. on Antennas and Propogation*, vol. 40, pp. 634-641, 1992.

[77]   V. Rokhlin, "Rapid solution of integral equations of scattering theory in two dimensions," *Journal of Computational Physics*, vol. 86, pp. 414-439, 1990.

[78]   J. M. Song and W. C. Chew, "Multilevel fast multipole algorithm for solving combined field integral equations of electrogmanetic scattering," *Microwave Opt. Tech. Letter*, vol. 10, pp. 14-19, 1995.

[79]   J. M. Song and W. C. Chew, "Multilevel fast multipole algorithm for electromagnetic scattering by complex objects," *IEEE Trans. on Antennas and Propogation*, vol. 45, pp. 1488-1493, 1997.

[80]   G. X. Fan and Q. H. Liu, "The CGFFT method with a discontinuous FFT algorithm," *Microwave and Optical Technical Letters*, vol. 29, pp. 47-49, 2001.

[81]   E. Topsakal, R. Kindt, K. Sertel, and J. Volakis, "Evaluation of the BICGSTAB(l) algorithm for the finite-element/boundary integral method," in *IEEE Antennas and Propagation*, vol. 43, Dec 2001, pp. 124-131.

[82]   L. T. Pillage and R. A. Rohrer, "Asymptotic waveform evaluation for timing analysis," *IEEE Trans. on Computer-Aided Design*, vol. 9, pp. 352-266, April 1990.

[83]   E. Chiproult and M. S. Nakhla, "Analysis of interconnect networks using complex frequency hopping," *IEEE Trans. on Computer-Aided Design*, vol. 14, pp. 186-200, Feb. 1995.

[84]   M. A. Kolbehdari, M. Srinivasan, M. S. Nakhla, Q. J. Zhang, and R.Achar, "Simulation time and frequency domain solutions of EM problems using finte element and CFH techniques," *IEEE Trans. on Computer-Aided Design*, vol. 44, pp. 1526-1534, Sept. 1996.

[85]   M. Celik and A. C. Cangellaris, "Simulation of dispersive multiconductor transmission lines by Pad?approximation via the Lanczos process," *IEEE Trans. on Computer-Aided Design*, vol. 44, pp. 2525-2535, Dec. 1996.

[86]   C. J. Reddy, M. D. Deshpande, C. R. Cockrell, and F. B. Beck, "Fast RCS computation over a frequency band using method of moments in conjunction with asymptotic waveform evulation techniques," *IEEE Trans. on Antennas and Propagation*, vol. 46, pp. 1229-1233, Aug. 1998.

[87] J. E. Bracken, D. K. Sun, and Z. J. Cendes, "S-domain methods for simultaneous time and frequenc y characterization of electromagnetic devices," *IEEE Trans. on Antennas and Propagation*, vol. 46, Sept. 1998.

[88] J. P. Zhang and M. J, Jin, "Preliminary study of AWE method for FEM analysis of scattering problems," *Microwave and Optical Technical Letters*, vol. 17, pp. 7-12, Jan 1998.

[89] L. Davis and Ed., *Genetic Algorithms and Simulated Annealing.* London, UK: Pitman, 1987.

[90] D. E. Goldberg, *Genetic Algorithm in Search, Optimization and Machine Learning*. Reading, MA: Addison-Wesley, 1989.

[91] O.Ozgun, S.Mutlu, M. I. Aksun, and L. Alatan, "Design of Dual-Frequency prob-fed microstrip antennas with genetic optimization algorithm," *IEEE Trans. on Microwave Theory and Tech.*, vol. 51, pp. 1947-1954, August 2003.

[92] L. Alatan, M.I.Aksun, K. Leblebicioglu, and M. Birand, "Use of computationally efficient method of moment in the optimization of printed antennas," *IEEE Trans. on Microwave Theory and Tech.*, vol. 47, pp. 725-732, April 1999.

[93] J. A. Kong, "Electromagnetic field due to dipole antennas over stratified anisotropic media," *Geophysics*, pp. 985-996, 1972.

[94] W. C. Chew, *Waves and fields in homogeneous media*. Piscataway, New Jersey: IEEE Press, 1995.

[95] J. M. J. W.C. Chew, E. Michielssen, J. Song, "Fast and Efficient Algorithms in Computational Electromagnetics." Boston: Artech House, 2001.

[96] W. C. Chew, *Waves and Fields in Inhomogeneous Media*. New York, 1990.

[97] N. Kinayman and M. I. Aksun, *Modern Microwave Circuits*. Boston: Artech House, February 28, 2005.

Vita

DATE OF BIRTH: September 27, 1975

PLACE OF BIRTH: Johor, Malaysia

EDUCATION

- M.sc.: University of Kentucky, Lexington KY, USA. 2000
- B.sc.: University of Kentucky, Lexington KY, USA. 1999
- Diploma in Applied Science: INTI College Malaysia, Subang Jaya, Malaysia. 1996

ACADEMIC EXPERIENCE

- Graduate Research Assistant in the department of Electrical Engineering at the University of Kentucky, KY USA. 2001-2005.
- Undergraduate Research Assistant in the department of Electrical Engineering at the University of Kentucky, KY USA. 1998-1999.
- Chemistry Laboratory Assistant in the INTI College Malaysia, Subang Jaya, Malaysia. 1994-1996.